Characterisation of Intermediate(s) in the Folding Pathway of Porcine Growth Hormone

by

Emma Jane Parkinson

B.Sc. (Hons)

Division of Biochemistry

School of Molecular and Biomedical Science

THE UNIVERSITY OF ADELAIDE
AUSTRALIA

This thesis is submitted for the degree of Doctor of Philosophy

June, 2004

TABLE OF CONTENTS

THESIS SUMMARY

The equilibrium denaturation of recombinant porcine growth hormone (pGH) demonstrated that pGH does not follow a simple two-state folding mechanism, but is consistent with the framework model of folding (Bastiras and Wallace, 1992). Stable intermediates observed were similar to other non-human growth hormones and characterised as compact and largely α-helical, yet lacked native-like tertiary structure; characteristics of the molten globule state. The detection of intermediate states along a protein's folding pathway, is crucial to understanding the principles of protein folding. To further understand the folding mechanism of pGH, this thesis describes the acid-induced denaturation and folding kinetics of recombinant pGH, 3 site-directed mutants (pGH analogues) and recombinant rat growth hormone (rGH).

The acid−induced denaturation of pGH, in the absence and presence of 4 M urea, was monitored by a variety of physicochemical techniques. Changes in tertiary structure were followed by (i) UV absorption spectroscopy (including second derivative analysis), (ii) intrinsic tryptophan fluorescence and (iii) near-UV circular dichroism. Secondary structural changes were followed by far-UV circular dichroism. Changes in the hydrodynamic radius self-association were followed by size-exclusion chromatography and analytical ultracentrifugation. The hydrophobic dye 1-anilinonapthalene-8-sulfonate (ANS) was also used to probe conformational changes upon acidification. Acidification alone (pH 8.0 to pH 2.0) of pGH resulted in changes in intrinsic fluorescence, UV absorbance, and near-UV CD, with transitions centred at pH 4.1. At pH 2.0, a red shift in the fluorescence emission maximum of approximately 3 nm and a 15% loss of the far-UV CD signal at 222 nm implied that the protein did not become extensively unfolded. Acidification in the presence

of 4 M urea resulted in similar pH-dependent transitions, however, these occurred at a more alkaline pH. At pH 2.0 + 4 M urea, an 8 nm red shift in the fluorescence emission maximum suggested that unfolding was greater than in the absence of urea. Sedimentation equilibrium experiments in the analytical ultracentrifuge showed that native pGH and partially unfolded intermediates reversibly self-associate. The model of association of the partially unfolded intermediates in the absence and presence of 4 M urea was different. These results demonstrate that acidification of pGH in the absence or presence of 4 M urea induced the formation of molten globule-like states with measurable differences in conformation.

Previous equilibrium denaturation studies of recombinant bovine growth hormone (bGH) showed that a peptide fragment corresponding to helix 3 of bGH could inhibit molecular association (Brems *et al.*, 1986). The amino acid sequence encompassing the third helix of pGH is identical in sequence to helix 3 of bGH except for a leucine to glutamine substitution at position 121. The fragment composed of residues 96-133 from native pGH was isolated by partial tryptic digestion and subsequently purified by reverse phase HPLC. The presence of this pGH fragment during the acid-induced denaturation of pGH was found to reduce the self-association of partially unfolded intermediates at pH 2.0 in the presence of 4 M urea, but had no significant effect on self-association at pH 2.0 in the absence of 4 M urea.

The acid-induced denaturation of the 3 pGH analogues and rGH was characterised. In terms of acid-mediated partial unfolding, the four proteins in this study, similar to wild-type pGH, possess folding intermediates with classic characteristics of the molten globule. Experimental evidence suggested that the mutations invoked subtle differences in

conformation between the intermediates, which were dependent on the solvent system employed.

The folding kinetics of pGH, the 3 pGH analogues and rGH were studied using stopped-flow fluorescence spectroscopy. Specifically, the intrinsic fluorescence of the single internalised tryptophan at position 86 within helix 2 (Trp86) was used to monitor the folding mechanism. Kinetic experiments employing the single-jump method were analysed. Concentration jumps from 5 M to 1.5 M Gdn–HCl and 0 M to 4 M Gdn–HCl for refolding and unfolding, respectively, were employed. For wild-type pGH refolding, two kinetic phases, accounting for the total expected amplitude were resolved. Unfolding experiments resulted in one kinetic phase representative of approximately 60% of the expected amplitude change. An un-observed phase, more commonly termed 'burst phase' accounting for the remaining amplitude, occurred within the dead-time of mixing (4 ms) of the stopped-flow instrument. The effect of protein and Gdn–HCl denaturant concentration was also examined. The folding kinetics of the pGH analogues and rGH exhibited similarities in the number of kinetic phases resolved for both refolding and unfolding, however, the rate constants differed. These results are compared to those for wild-type pGH and are interpreted in terms of the stability of folding intermediates.

Declaration

This work contains no material which has been accepted for the award of any other degree or diploma in any university or other tertiary institution and, to the best of my knowledge and belief, contains no other material previously published or written by another person, except where due reference has been made in the text.

I give consent to this copy of my thesis, when deposited in the University Library, being available for loan and photocopying.

Emma Jane Parkinson

June, 2004

This thesis is dedicated to my precious mother

Heather May Parkinson

You are the most amazing woman I have ever known and the words below are simply not enough for all the love and emotional support you have given, and still give me today.

THANK YOU

In Loving Memory of

my dad, Jeffrey Harry Parkinson

my nanna, Eileen Florence May McKenzie

and

my gran, Eva Parkinson

all who passed away during the making of this thesis

ACKNOWLEDGEMENTS

To my supervisor Professor John Wallace, thank you for all your support and encouragement throughout the past years. I also thank you for your patience and belief that I will "get it done". Thanks also goes to Dr. S. Bastiras and Dr. J. Smeaton for allowing me to work at Bresagen Ltd.

I wish to thank Dr. Pat Wallace for introducing me to the intriguing, exciting and sometimes frustrating world of science. Your friendship throughout the years has been very much appreciated. I am indebted to my present supervisor, Assoc. Professor Doug Brooks for employing me whilst completing this thesis. I am also very grateful for his unwavering encouragement and continued belief in my capability. I wish to acknowledge the late Dr. Greg Ralston, University of New South Wales, for allowing me to perform the equilibrium sedimentation and CD measurements in his laboratory. I am also grateful to Dr. Michael Morris for assisting me in the measurements. Thanks must also go to Mr. Geoff Francis at GroPep for allowing me to use the HPLC system.

To all my past and present colleagues who have helped me both technically and emotionally over the years, I thank you. I would like to especially thank the following people for their wonderful friendship; without them, I would never have reached the end of this roller coaster ride: Gary Shooter, Rod Snow, Zara and Andrew Zannettino, Julie Lake, Tim Blake, Steven Polyak, Revecca Kakavanos, Melanie Lovejoy, Carolyn Harrington, and Kristy Shaedel. I again thank my Mum who has provided me with the inspiration and motivation to reach my goals. Finally, I would like to thank my husband Shane, for his love, patience and understanding.

ABBREVIATIONS

The following abbreviations were used in addition to those abbreviations commonly accepted

A_{xxx}	absorbance at xxx nm
ACN	acetonitrile
ANS	1-anilinonapthalene-8-sulphonate
AUFS	absorbance units of full scale
bGH	recombinant bovine growth hormone
CD	circular dichroism
F_{app}	the apparent fraction of unfolded protein
FPLC	fast pressure liquid chromatography
Gdn–HCl	guanidine hydrochloride
HCl	hydrochloric acid
hGH	recombinant human growth hormone
HPLC	high performance liquid chromatography
IPTG	isopropylthio-β-D-galactopyranoside
I_{xxx}	fluorescence intensity at xxx nm
K_a	association constant
MES	2-[N-Morphilino]ethanesulfonic acid
M.R.E.	mean residue ellipticity
λ_{max}	fluorescence emission maximum
pGH	recombinant porcine growth hormone
rGH	recombinant rat growth hormone

RP HPLC	reverse phase high performance liquid chromatography
SDS	sodium dodecyl sulphate
SDS-PAGE	SDS-polyacrylamide gel electrophoresis
Tris	Tris-(hydroxymethyl)methylamine
TFA	trifluoroacetic acid

LIST OF FIGURES

LIST OF TABLES

PUBLICATIONS ARISING FROM THIS THESIS

Parkinson EJ, Morris MB, Bastiras S (2000): Acid denaturation of recombinant porcine growth hormone: formation and self-association of folding intermediates. *Biochemistry* **39**, 12345-54.

Parkinson EJ, Wallace JC and Bastiras S (1998): Folding kinetics of porcine growth hormone. *42nd Annual Australian Society for Biochemistry and Molecular Biology (ASBMB) Conference, Convention Centre, Adelaide, Australia*

Parkinson EJ, Wallace JC and Bastiras S (1996): Acid-induced denaturation of porcine growth hormone (pGH). *FASEB Summer Research Conference on "Protein Folding and Assembly in the Cell", Saxtons River, Vermont, USA.* **Invited presenter**

Parkinson EJ, Wallace JC and Bastiras S (1995): Acid-induced denaturation of porcine growth hormone (pGH). *Twentieth Annual Lorne Conference on Protein Structure and Function, Erskine House, Lorne, Victoria, Australia.*

CHAPTER 1

INTRODUCTION AND LITERATURE REVIEW

1.1 INTRODUCTION

Now that the human genome sequence is complete, it is extremely important to understand how a protein achieves its unique three dimensional and biologically active structure. Investigations into the mechanism of protein folding constitute a vast and continually expanding field. Small proteins (< 100 amino acids) can fold without populating intermediates in an apparently two-state transition. However, larger proteins (> 100 amino acids) fold by a three-state transition, populating folding intermediate(s).

This thesis examines the acid-induced denaturation and folding kinetics of pGH and analogues thereof, to investigate the formation and characteristics of the folding intermediate(s). This literature review covers several broad categories; first a brief overview of the forces that play an integral role in protein structure and stability is discussed. There have been a number of models described for the mechanism of protein folding. Advances in experimental technology combined with the development of powerful theoretical models has been responsible for major progress in unravelling the folding mechanisms of proteins and are briefly reviewed in terms of the classical and new view of folding. The detection of partially folded intermediate states along a protein's folding pathway is crucial to understanding the principles of protein folding and this review examines in detail the formation, structure and biological significance of the folding intermediates, with specific reference to the molten globule state. The role of folding intermediates *in vivo* is also briefly discussed. Chapter 1 culminates in an overview of the structure and previous work on the folding of growth hormone, and it is during this part of the review that the aims underpinning this thesis are developed. The majority of work cited in this review was published prior to or during 1998, pertaining to the general

understanding of these topics during the time that the project was undertaken. More recent studies are cited where appropriate.

1.2 FORCES THAT DICTATE PROTEIN FOLDING AND STABILITY

The stability of a protein is defined as the difference in free energy between the native and denatured states. The minimal stability of the native state over the plethora of denatured states is a consequence of the fine balance between those forces contributing primarily to the stabilisation of the native state; viz. hydrophobic interactions, hydrogen-bonding, van der Waals interactions and electrostatic interactions, and those opposing stabilisation, specifically classical charge repulsion and conformational entropy (Dill, 1990).

1.2.1 Electrostatic Interactions

Electrostatic interactions are important in determining the stability of a protein (Tanford, 1970). They also play an important role in protein folding, flexibility and function. There are two types of electrostatic interactions, classical and specific. Classical electrostatics describes the nonspecific repulsions, that arise when a protein is highly charged, for example, at extremes of pH (Tanford, 1961), and are based on the Linderstrom-Lang model (Linderstrom-Lang, 1924). Increasing the acidity or basicity of the solution increases the net charge on a native protein. The increasing charge repulsion destabilises the folded protein because the charge density on the folded protein is greater than on the unfolded molecule. No electrostatic contribution to protein stability is expected near the isoelectric point. Specific charge interactions can also affect stability. Salt bridges (ion pairing) are formed by spatially proximal pairs (< 3.5 Å) of oppositely charged residues in native protein structures. Salt bridges generally fall in the same secondary structural

element, autonomous folding unit, domain or subunit. Charged residues in protein molecules are generally located on the protein's surface (Rashin and Honig, 1984). The few that are found buried, are often catalytically or functionally important (Barlow and Thornton, 1983). The strength of electrostatic interactions is variable, depending on the location in the protein structure. Buried charged groups do not generally form ion pairs but are instead solvated by hydrogen bonds (Rashin and Honig, 1984). In recent years, evidence has accumulated that suggests a significant component of the electrostatic free energy difference between native and denatured states is due to a small number of amino acids whose pKa's are shifted anomalously in the native protein (Pace *et al.*, 1990; Yang and Honig, 1992, Yang and Honig, 1993).

Electrostatic interactions play an important role in stabilising α-helices. The peptide bond has a substantial dipole moment and in the α-helix the peptide dipole moments add end to end across the hydrogen bonds generating a macrodipole. The macrodipole is orientated such that a partial positive charge is located near the N-terminus and a partial negative charge near the C-terminus (Wada, 1976). Many proteins fold with their α-helices aligned in an antiparallel fashion, which results in the favourable alignment of the dipoles (Ohlendorf *et al.*, 1987). Statistical analysis shows that negatively charged residues are strongly preferred in the first turn of helices in proteins (Richardson and Richardson, 1988). In contrast, there is only a marginal trend towards positively charged residues near the C terminus. It is unclear whether charge-helix dipole interactions at the carboxyl ends of helices are of similar importance as at the N-terminal regions for the stability of folded proteins (Walter *et al.*, 1995).

1.2.2 Hydrogen Bonding

A hydrogen bond occurs when a hydrogen atom is shared between two electronegative atoms. The role of hydrogen bonds in the formation and stability of the α-helix and beta sheet is unquestionable. All groups that are capable of hydrogen bonding are in fact, hydrogen bonded either to other protein groups or to water. Water molecules are released to interact with each other, and specific water binding sites are formed on the protein (Alber, 1989). The strength of a hydrogen bond depends on the electronegativity and orientation of the bonding atoms i.e. geometric arrangement of bond angles. However, the distribution of hydrogen bond angles in proteins is similar to that observed in small-molecule compounds (Baker and Hubbard, 1984).

A central question in protein chemistry asks to what extent does the formation of intrachain hydrogen bonds contribute to the stability of the folded state. In early studies the hydrogen bond was suggested to be the most important force that contributed to the stability of the native state (Mirsky and Pauling, 1936). However, resolving the question has been unsuccessful due to the difficulty in assessing the energetics of solute-solute hydrogen bonds relative to those of solvent hydrogen bonds (Dill, 1990).

1.2.3 van der Waals forces

Van der Waals forces arise from interactions among fixed or induced dipoles. These forces are only significant at close atomic distances. If atoms get too close, the electron charge clouds overlap appreciably and electron repulsion dominates. The interiors of proteins are tightly packed, with approximately 75% of adjacent atoms in van der Waals contact (Richards, 1977). This compares to 70-78% observed in crystals of small organic molecules and 58% in liquids such as water (Bello, 1978). The total number of van der

Waals contacts in the denatured state at any point in time would be expected to be lower than that in the folded state because of the transient nature of the peptide-water interactions. The additional stabilisation of the folded state provided by hydrogen bonds and the hydrophobic effect would maintain the proximity of adjacent atoms necessary for van der Waals contact. Van der Waals forces contribute very little to the stabilisation of the folded state. However, due to their ubiquitous nature and reliance on tight packing, they may play a crucial role in stabilisation of the folded state. They may also be important in stabilisation of the compact denatured state observed in the early stages of refolding (Kuwajima, 1989).

1.2.4 Disulphide Bonds

Disulphide bonds make large contributions to the stability of some globular proteins by reducing the conformational entropy of the folded state (Anfinsen and Scheraga, 1975). The greatest stabilisation is expected by connecting residues that are distantly located in the amino acid sequence (Pace, 1986). Disulphide bonds have been genetically engineered into many proteins, including T4 lysozyme (Wetzel *et al.*, 1988; Jacobson *et al.*, 1992) subtilisin (Mitchinson and Wells, 1989) and dihydrofolate reductase (Villafranca *et al.*, 1987), to increase the stability of the native state. Disulphide bonds have also been proposed to provide the required stabilisation for the formation of secondary structure in early folding intermediates. For example, comparison of reduced and non-reduced hen egg white lysozyme showed that within 4 ms the non-reduced possessed significant structure whereas the reduced form was structureless (Goldberg and Guillou, 1994).

1.2.5 The Hydrophobic Effect

The hydrophobic effect is generally viewed as the major driving force in protein folding. In globular protein structures, non-polar side chains are sequestered into a core, thus avoiding contact with water. Moreover, polar side-chains tend to be located on or near the surface of the protein.

Site-directed mutagenesis, combined with thermal- and denaturant-induced denaturation measurements, has been used to determine the contributions of individual amino acids to the hydrophobic effect. The $\Delta(\Delta G)$ values for hydrophobic mutants increase with the amount of non-polar surface area buried, with a range of values for a given type of hydrophobic mutation (Pace *et al.*, 1996). The range of values has been attributed to the cavity volume with the removal of a specific group, for example a methyl (CH_2) group. The polarity of the environment surrounding the mutation also affects $\Delta(\Delta G)$ (Pace *et al*, 1996).

While hydrophobic interactions play a major role in stabilizing the folded state of proteins, they are also important in stabilizing the unfolded state, particularly in disulphide-bonded proteins, where non-polar exposure to the solvent is decreased. Hydrophobic interactions are instrumental in forcing the collapse of the unfolded state in the early stages of folding, resulting in the non-specific formation of local secondary structure elements. For example, in the kinetic folding of many proteins, burst-phase intermediates (molten globules formed within the dead time of the instrument, discussed later) possess secondary structure with the formation of a loose hydrophobic core (Ptitsyn, 1995). Interestingly, in the folding of Barstar, the polypeptide chain rapidly collapses within 4 ms to a compact structure that has a solvent-inaccessible hydrophobic core, yet lacks secondary and tertiary structure. This

globular structure precedes the molten globule-like intermediate on the folding pathway (Agashe *et al.*, 1995). The formation of a hydrophobic core with some specific native-like packing interactions is important in stabilising the highly fluctuating molten globule (Wu and Kim, 1998).

1.2.6 Conformational Entropy

Entropy is a measure of the freedom of a system to explore its available conformational space. Thus, a reduction in conformational entropy is synonymous with the folding of a protein. As a protein folds, there is a loss of entropy. To overcome this unavoidable loss of entropy, specific and favourable intramolecular or intermolecular interactions such as hydrogen bond formation, salt bridge formation, hydrophobic contacts and disulphide bonds must be formed.

Disulphide links stabilise proteins by reducing the conformational entropy of the unfolded state i.e.; the number of possible conformations is decreased by the constraint of the covalent link. Site-directed mutagenesis has been used to examine the entropy associated with the freedom of the polypeptide backbone ("local entropy"). The introduction of an ala → pro mutation destabilised the unfolded state of T4 lysozyme by 1.4 kcal/mol (Matthews *et al.*, 1987). Restricting the rotation around the polypeptide backbone lowers the entropy of the unfolded state.

Shortle and co workers have suggested that single site mutations can exert their dominant effects on protein stability by changing the entropy of folding. Using a model for protein-folding equilibrium ($N \leftrightarrow D_0$, where D_0 is the denatured state under folding conditions) based on short self-avoiding chains of hydrophobic/polar copolymers on a

two-dimensional square lattice (Lau and Dill, 1990), they suggest that a single mutation can have a large effect on the stability of a protein by controlling how may highly compact denatured conformations (D_0) are available. The entropy of the denatured state under strong folding conditions is therefore highly sequence dependent (Shortle *et al.*, 1992).

At acid pH, interleukin 4 (IL-4) retains a highly ordered hydrophobic core in which most but not all of the secondary structure is preserved. That such a core is stable is likely to be associated with the preservation of hydrophobic interactions in the partly unfolded molecule, and compensation for the loss of some of these interactions in the disordered regions by an increase in chain entropy (Redfield *et al.*, 1994).

The loss of side-chain configurational entropy also makes a significant contribution to the total free energy balance. Based on the entropy changes that accompany the freezing of hydrocarbons, the side chain entropy corresponding to a methyl group (CH_2) is approximately 0.45 kcal/mol (Nicholls *et al.*, 1991). Freezing of motion however leads to an increase in van der Waals interactions and when taken into account, the effect of close packing is estimated as 0.15 kcal/mol, favouring the folded state. Aromatic residues can closely pack with far less reduction in side-chain entropy, leading to a larger estimate for the net contribution of close packing, thus being an essential element of a folded protein (Honig and Yang, 1995).

1.3 MECHANISMS OF PROTEIN FOLDING

If a protein was to attain its native three-dimensional (3D) structure through a random and unbiased search of all possible conformations, such a mechanism would take an infinite amount of time (Levinthal, 1969). Levinthal proposed that proteins must fold by specific

"folding pathways". Since the experiments performed by Anfinsen (1973), it is been largely accepted that the 3D structure of a protein is determined by its sequence of amino acids - but how?

Early models describing the mechanism of protein folding predicted that protein folding follows a specific folding pathway with an emphasis on specific structures. One of the first proposed mechanisms of folding took the form of nucleation-growth, a variant of hierarchical condensation (Wetlaufer, 1973). This mechanism proposed that the tertiary structure of a protein rapidly propagates from an initial nucleus of local secondary structure. In the early eighties, based on experimental evidence from several small proteins, which possessed stable equilibrium intermediates, Kim and Baldwin (1982) proposed that protein folding is a sequential process beginning with the rapid formation of secondary structure followed by the collapse to a compact native-like state, before the tertiary structure is locked into place. This proposal was aptly named the framework model of protein folding. Indeed, many proteins (including growth hormone) have been described as folding via this mechanism. A similar mechanism named the hydrophobic collapse model was also introduced, whereby the hydrophobic side chains of a protein became buried away from the solvent exterior, forming a collapsed intermediate or molten globule species, from which the native state develops. These early models have been described as the classical view of protein folding (Baldwin, 1995).

In terms of kinetics, the classical view is based on simple phenomenological kinetic models (Dill and Chan, 1997). Two-state kinetics describes a single exponential time decay monitored by an optical probe in both folding and unfolding conditions where only the native (N) and denatured (D) states are observed. The resolution of multiple exponential

functions describes a more complicated system, which requires additional symbols to fit the raw data. The additional symbols represent intermediate (X) conformations. The three most important classical models are:

(1) off-pathway model;

$$X \leftrightarrow U \leftrightarrow N$$

(2) on-pathway model;

$$U \leftrightarrow X \leftrightarrow N$$

(3) sequential model;

$$U \leftrightarrow X_1 \leftrightarrow X_2 \leftrightarrow \bullet\bullet\bullet \leftrightarrow N,$$

where U represents the fully unfolded or denatured state, N the native state and X the intermediate states (Dill and Chan, 1997). The model is chosen based on which returns the best fit of with the experimental data. However, experiments performed to elucidate these models only probe the average behaviour of the protein, as they are unable to resolve much atomic detail.

While the classical view describes folding as a specific pathway, statistical mechanical modelling describes these specific states as distributions or ensembles of individual chain conformations and is known as the new view of protein folding (Dill and Chan, 1997). This view replaces the pathway concept of sequential events with the funnel concept of parallel events; a parallel microscopic multipathway diffusion-like process. A multi-dimensional energy landscape or folding funnel best describes the folding process. In this model there are many routes to the native state, and which pathways are populated are dependent on the system being studied (Radford, 2000). This new view does present

problems for monitoring transitions between ensembles that are populated simultaneously, but it is anticipated that some pathways are likely to predominate (Lazaridis and Karplus, 1997).

1.4 FOLDING INTERMEDIATE(S): THE MOLTEN GLOBULE

In the late 1960's there was evidence to suggest that under certain conditions protein molecules could possess properties that were intermediate between the rigid native state and fully unfolded state (Aune *et al.*, 1967; Brandts and Hunt, 1967). The concept of such an intermediate in protein folding was suggested as early as 1973 (Ptitsyn, 1973). In 1981, Dolgikh and co-workers (Dolgikh *et al.*, 1981) showed that the acid forms of bovine and human α-lactalbumins were almost as compact as their native state with native-like secondary structure. However, there was no rigid tertiary structure, a lack of cooperative temperature melting and an enhanced intramolecular mobility when compared to the native state. Due to its physical properties, Ohgushi and Wada (1983), first labelled this intermediate, the "molten globule state. (N. B. In the literature the molten globule state has also been referred to as a "compact denatured state" and "compact intermediate", however, in this review I will keep with the term "molten globule").

1.4.1 Formation of a Molten Globule

In equilibrium denaturation experiments, the molten globule is observed under conditions that disrupt the native structure of the protein in a relatively mild way. Such conditions include low pH and elevated temperature in the absence of strong denaturants, or low to moderate concentrations of urea or Gdn-HCl, generally, at neutral pH. The removal of ligands, lack of cofactors such as metal ions or heme groups, disruption of disulfide bonds

or mutations can also result in the destabilisation of the native state and formation of the molten globule.

Acid-induced denaturation of proteins has proved to be an invaluable tool in gaining insight into the physical properties of intermediate states. The use of chemical denaturing agents such as Gdn-HCl and urea, often lead to mixtures of native, intermediate and unfolded protein states, thus making the study of intermediates difficult. The transformation of some proteins at low pH to an intermediate state with properties similar to those of the Gdn-HCl induced intermediate has allowed us to gain an understanding into the physical properties of the molten globule. The acid-induced compact denatured states in proteins have also been referred to as "A states" in the literature.

In acid-denaturation, intramolecular charge repulsion is the driving force for protein unfolding. The formation of denatured states that are less unfolded than those obtained at high concentrations of Gdn-HCl or urea are attributed to the failure of electrostatic repulsion to overcome the favourable folding interactions, such as hydrophobic forces, disulfide bonds, salt bridges, and metal ion-protein interactions (Fink *et al.*, 1994). While several proteins at low pH, which include α-lactalbumin, bovine carbonic anhydrase B and bovine growth hormone form a molten globule, other proteins such as β-lactamase, cytochrome *c* and apomyoglobin require a high concentration of salt to stabilise the molten globule (A state) (Goto *et al.*, 1990a,b). For these proteins, the protonation of carboxyl groups at low pH results in intramolecular repulsion, leading to a relatively extended conformation. The addition of anions, either as salts or by the further addition of acid (for example the addition of HCl supplies the chloride ion) diminishes the electrostatic repulsion, resulting in the preferential formation of the A state.

A systematic investigation of 20 monomeric proteins has shown that acidification results in three different types of conformation, which is apparently dependent on the protein (Fink *et al.*, 1994). The first conformational state describes proteins that initially unfold (the degree of which varies) and then refold into a compact or expanded molten globule conformation. Within this first state, three subclasses have been further defined, based on the compactness of the A state. Cytochrome *c* and β-lactamase undergo a cooperative transition from pH 4.0 to pH 2.0, with a loss of both secondary structure and tertiary structure equivalent to that observed at 6 M Gdn-HCl. Further addition of HCl induces the formation of secondary structure which is comparable to that found in the native state but there is no apparent native-like tertiary structure (Goto *et al.*, 1990a,b). Apomyoglobin behaves similarly to that of the above proteins, however, the A state is less compact with a radius approximately 50% that of the native state. The degree of secondary structure is reduced when compared to the native state and there is negligible tertiary structure. This protein was labelled as a Type IB state. Acidification with trifluoroacteic acid rather than HCl produced an A state for apomyoglobin with similar characteristics to those described for cytochrome c and β-lactamase. The third subclass describes proteins that convert from the native state to a collapsed, unfolded state with significant residual secondary structure, for example ribonuclease A. Further acidification results in the formation of additional secondary structure consistent with the formation of the A state. For all type I proteins, acidification in the presence of salts can lead directly from the native state to the A state.

The second conformational state describes proteins that undergo a transition directly from the native state to a molten globule at low pH and in the absence of salts. These proteins are characterised by a minimal transition when monitored by far UV CD but a pH-induced

transition when monitored by near UV-CD. The archetypal case is that of α-lactalbumin (discussed later).

The third conformational state describes proteins that maintain native like far- and near-UV CD upon acid titration. Such proteins include T4 lysozyme, chicken lysozyme, ubiquitin and human growth hormone. A subsequent transition at low pH can be seen upon the addition of denaturant (e.g. urea)

1.4.2 Detection Techniques

The key to de-convoluting a folding mechanism is to combine the results from different techniques so that different aspects of folding can be probed and the results combined into a common picture of the folding process (Dobson *et al.*, 1994). Therefore, it is of interest to briefly describe the techniques used today. Intrinsic fluorescence and near-UV circular dichroism provide information about the extent of a protein's tertiary structure, whereas far-UV CD provides information with respect to secondary structure formation. Stopped flow methods using these optical probes can access folding events on the millisecond timescale. More recently, the development of technologies, which include ultra-rapid mixing, temperature and pressure jump, in combination with the optical probes described above can access folding events on the nanosecond to microsecond time scale. Fluorescence of non-polar dyes such as 1-anilinonapthalene-8-sulphonate (ANS) provides information on the exposure of hydrophobic surface area. Small-angle X-ray scattering determines the dimension and shape of the protein. Information at the level of individual residues is obtained using hydrogen exchange and protein engineering. Hydrogen exchange coupled with detection by multi dimensional NMR can be used to determine the location and stability of hydrogen bonds at different stages of folding, although the exact

identity of the hydrogen bond acceptor can only be inferred. Protein engineering allows us to determine site-specific information about the role of the individual chains, for example, the effect of an individual amino acid residue on protein stability and the role of individual residues in stabilising intermediates and transition states.

The development of theoretical models to simulate protein folding is also advancing our understanding of the mechanism of protein folding. Molecular dynamics can be used to monitor protein unfolding at the atomic level and the folding of small proteins using the computer power now available. Also used are Lattice simulations that rely on very simple models for proteins based on polymer beads. These have the advantage of being able to exhaustively search the conformational space.

1.4.3 Structure of the Molten Globule

The molten globule state has been described for a number of globular proteins, with the molten globule of α-lactalbumin, cytochrome c, apomyoglobin, ribonuclease HI, β lactoglobulin and staphylococcal nuclease are by far the best characterised. The molten globule of α-lactalbumin has been suggested to be the archetypical or "classical" molten globule (Kuwajima, 1989).

The molten globule state of many proteins has been shown to have some common structural characteristics. The molten globule shares a similar compactness to the native state protein. In general, the radius of gyration of the molten globule is increased by approximately 10–30% when compared to the native state; the core of the protein is loosely packed whilst the peripheral structure is more expanded (Ptitsyn, 1995). Far-UV CD measurements have shown the molten globule to retain a relatively high content of secondary structure, similar to that of the native state. Two-dimensional (2D) NMR studies

have been used to establish the presence of elements of hydrogen bonded secondary structure in which amide protons are protected from hydrogen exchange. The molten globule of α-lactalbumin was shown to retain the native helices B and C corresponding to the α domain (Baum *et al.*, 1989, Dobson, 1991). The cytochrome c molten globule has been shown to retain structure in the three main native α helices (Jeng *et al.*, 1990) and the molten globule of apomyoglobin retains secondary structure associated with the A, G and H helices (Hughson *et al.*, 1990). The near UV-CD spectra have a significantly reduced signal in comparison to the native state, suggesting the absence of rigid tertiary structure. ^{1}NMR spectra of the molten globule are substantially simpler than the native state and resemble spectra seen for the unfolded protein (Kuwajima *et al.*, 1986; Dobson, 1991). The molten globule has an increased mobility. Studies of the carbonic anhydrase molten globule have shown that small and symmetric aliphatic groups possess a mobility similar to that of the unfolded state whereas aromatic residues remain substantially hindered (Ptitsyn, 1992). Shaknovich and Finkelstein (1989) first predicted the important difference between the mobilities. A large increase in the rate of hydrogen exchange in ^{1}NMR studies is consistent with large scale fluctuations of the molten globule structure, which makes internal parts of the molecule accessible to solvent (Baum *et al.*, 1989). Human α-lactalbumin can adopt a molten globule conformation when one of its four disulphide bonds is reduced. However, in this state the disulphide bonds rearrange spontaneously, but the isomers formed maintain a molten globule like conformation (Ewbank and Creighton, 1991), confirming the looseness of the packing of secondary structure and the lack of tertiary interactions. The increased flexibility of the molten globule permits the exposure of some nonpolar groups to become exposed to solvent. As a consequence of increased hydrophobicity, nonpolar probes, typically ANS, bind the molten globule more strongly than the native state. Indeed, the binding of ANS is commonly used as a convenient test for

the molten globule as its binding leads to a large increase in its fluorescence. A second consequence of increased hydrophobicity is the tendency for molten globules to aggregate. The molten globule also exhibits a less cooperative unfolding transition compared to that of the native state. However, this can vary depending on the amount of structure present in the intermediate (Ptitsyn, 1995). For example, the A-state of cytochrome c, which has been described as a molten globule, does undergo a cooperative thermal unfolding transition accompanied by substantial changes in enthalpy and heat capacity, suggesting that the molten globule is more native-like than others (Kuroda *et al.*, 1992)

The archetypical molten globule is apparently highly disordered and is similar to the intermediate observed in the early stages of folding (discussed below). A "highly ordered " molten globule has been described for the 4 α-helical bundle protein interleukin-4 (IL-4) at acid pH (pH 2.8). Structurally, this intermediate is more similar to the native state compared to that of the classical molten globule. While the characteristics of the near UV spectra and ANS fluorescence are consistent with a classical molten globule, very little change in both the chemical shifts and NOE's in NMR spectra for the majority of residues are not consistent with a substantial global loss of tertiary structure. Examination of the N-H order parameters determined from ^{15}N relaxation measurements showed the existence of a well defined core with the local unfolding in the N-terminal of helix C. Highly ordered molten globules have also been described for Staphylococcus nuclease (Carra *et al.*, 1994) and apocytochromes (Feng *et al.*, 1994). This type of intermediate has been suggested to serve as a late intermediate in the folding process. However, the highly ordered molten globule has yet to be observed in proteins that have the "classical" molten globule and probably reflects that molten globules differ between proteins (Ptitsyn, 1995).

The term pre-molten globule has also been used to describe a second equilibrium intermediate between the native and unfolded state for β-lactamase (Uversky *et al.*, 1994) and carbonic anhydrase (Ptitsyn *et al.*, 1995). For both proteins, at low temperature, three stages of Gdn-HCl induced unfolding were observed. In comparison to the molten globule, this intermediate is more expanded, has substantial secondary structure, albeit less than that seen in the molten globule, and binds to ANS but to a lesser extent.

The retention of substantial secondary structure in the molten globule gave rise to the very important question of whether the molten globule possesses a native-like tertiary fold or is it compact but structureless. A single chain recombinant model of the α helical domain (α domain) of α-lactalbumin was constructed and exhibited characteristics of a molten globule: substantial helical structure (CD and NMR) and a diffuse thermal transition consistent with the inability of this domain to form rigid tertiary structure (Peng and Kim, 1994). A disulphide exchange reaction of the α domain produced predominantly native disulphide bonds clearly indicating that the α domain has a native-like tertiary fold. Ordered structure has also been shown within the loop moiety of the 6-120 disulphide bond of bovine α lactalbumin (Ikeguchi *et al.*, 1992). In a study of the structural specificity of disulphide bonds in the molten globule state it was shown that the local region surrounding the 28-111 disulphide bond has a high preference for adopting a native-like structure in the molten state (Peng *et al.*, 1995). This data, together with the NMR data provides evidence for the formation of a native-like tertiary fold in the molten globule rather than a non-specific collapsed conformation.

How does a native-like fold in a molten globule form in the apparent absence of extensive specific tertiary interactions? The intrinsic stability of individual helices may stabilise the

molten globule intermediate. Studies on *de novo* protein design show that a constructed amphiphilic helix in some cases is sufficient to produce four-helix bundle proteins (Kamtekar *et al.*, 1993). Protein stability is invoked only by the removal of the hydrophobic surface form the solvent exterior, as tight close-chain packing observed in the native state protein, is not present. Specific side-chain packing is an important factor in stabilising the molten globule. Packing of the N- and C-terminal helices plays a critical role in the kinetics of folding of cytochrome c (Cólon *et al.*, 1996). The apomyoglobin molten globule is characterised by the retention of helices A, G and H that form a compact subdomain in the native myoglobin molecule (Hughson *et al.*, 1990). The mutation of residues that result in a decrease in the side chain hydrophobicity or introduce a charged group into the AGH hydrophobic interface destabilised the intermediate. However, the effect observed by the introduction of a bulky hydrophobic side was negligible. Urea-induced denaturation of the mutants showed significant effects on the stability of the intermediate, suggesting that the residues make energetically important packing interactions. The α-lactalbumin molten globule is a highly fluctuating structure and it is interesting that specific native-like packing and a native-like fold can exist. The hydrophobic core formed by the A, B and C terminal 3_{10} helices, play a dominant role in stabilising the molten globule. Both non-native and native-like side-chain packing interactions formed by hydrophobic residues are important for stabilising the molten globule state of α-lactalbumin (Wu and Kim, 1998). Hydrophobic sequence minimisation of the α-lactalbumin molten globule suggests that non-specific hydrophobic interactions as opposed to specific packing interactions are sufficient for the formation of a native-like topology. In addition, substitution of amino acids in the core of the α-lactalbumin molten globule may increase the stability suggesting that hydrophobic interactions distinct from native-like packing may play a role in stabilising the molten globule. These two things are

not mutually exclusive. Non-specific hydrophobic interactions may help establish the overall fold while specific core interactions may help stabilise the nascent structure. The existence of specific chain packing does not exclude the importance of non-specific hydrophobic interactions.

It has been suggested that the molten globule is a common or general intermediate in all protein folding pathways (Ptitsyn *et al.*, 1990). For the molten globule to be a general intermediate, the intermediates formed from different proteins would have to be similar in structure. With the description of a "highly ordered molten globule" and a "pre-molten globule" this generalisation has been questioned. The refolding of acid-unfolded apomyoglobin and staphylococcal nuclease as a function of anion concentration further challenges the idea that the molten globule is the general intermediate in protein folding (Fink *et al.*, 1998, Uversky *et al.*, 1998). For both proteins, three distinct states have been detected as a function of anion strength (A_1 induced by chloride, A_2 induced by TFA and A_3 induced by TCA). For both proteins, each state differs in the amount of structure, with A_1 having the least structured conformation and A_3 the most. The stability toward urea denaturation positively correlated with the amount of structure and importantly the urea induced unfolding studies showed that each state was separated from each other and from the unfolded state, by significant free energy barriers, suggesting that they are distinct conformational states. For apomyoglobin, the three states obtained as a function of anion strength have been proposed to be very similar to the three kinetic states observed by NMR (Jennings and Wright, 1993). Similarly, the A_1 and A_3 states of staphylococcal nuclease have been likened to the early (burst) kinetic intermediate and the native-like transient intermediate (Kalnin and Kuwajima, 1995, Wallenhorst *et al.*, 1997). From this data the authors propose that at least some proteins fold via a hierarchical path in which additional

structural units coalesce to an initially formed core with native-like structure and that the nature of the intermediates will be specific to a given protein. It is interesting to note that the A_1 discrete intermediate for apomyoglobin has been likened to the early kinetic intermediate which has been described as a molten globule and similarly the A_1 discrete intermediate of staphylococcal nuclease has been ascribed to the burst intermediate, also suggested to be a molten globule.

1.4.4 The Molten Globule as a Kinetic Intermediate

Folding intermediates have been detected on the kinetic folding pathway of many proteins (Matthews, 1993; Evans and Radford, 1994). Measurements in the peptide absorption region by UV CD have shown the formation of secondary structure to occur within the dead time of the stopped-flow instrument, giving rise to a burst phase (missing amplitude). In contrast, near UV CD and NMR chemical shift dispersion, characteristic of the formation of tertiary structure are maximal at later stages of folding. The formation of secondary structure prior to the formation of tertiary structure is the basis for the framework model of folding and implies the existence of folding intermediates along the folding pathway of a protein (Kuwajima, 1989).

Evidence of kinetic intermediates has also been shown from the effect of denaturants. A plot of the logarithm of the observed rates of folding and unfolding is typically V-shaped for a simple two-state mechanism. A deviation from linearity in the unfolding transition at low denaturant concentrations where the observed rate plateaus has been attributed to the presence of an intermediate (Matouschek *et al.*, 1990). Detailed quantitative 3-state analysis has also shown that a linear three-state mechanism provides a self-consistent

description for the unfolding and unfolding rates as well as the kinetic amplitudes for the burst phase as a function of denaturant concentrations (Khorasanizadeh *et al.*, 1996).

Studies of the kinetic intermediates have predominantly focussed on the early (burst) intermediate, with particular emphasis on the physical properties of the intermediates. Using a combination of stopped flow far-UV CD, hydrogen exchange coupled to 2D NMR, intrinsic fluorescence probes, binding of ANS, near UV CD and NMR chemical-shift dispersion, the early kinetic intermediate has been described as a molten globule. Indeed, comparison of the physical properties of the kinetic intermediate with the equilibrium molten globule intermediate of apomyoglobin (Hughson *et al.*, 1990, Jennings and Wright, 1993), α-lactalbumin (Arai and Kuwajima, 1996) and RNAse H (Yamaski *et al.*, 1995, Dabora *et al.*, 1996; Raschke and Marqusee, 1997), have shown them to be the same. Thus characterising the nature of the equilibrium intermediate can provide insights into the nature of the kinetic intermediate and the folding pathway of individual proteins

There is substantial evidence to suggest that the formation of intermediates is an obligatory step in protein folding and that intermediates are productive species that play a key role in the search for the native state (Khorasanizadeh *et al.*, 1996). However, the observation that some small proteins fold rapidly without populating intermediates (Jackson, 1998), and the observation that some intermediates are kinetically trapped, for example by non-native heme ligands (Sosnick *et al.*, 1994, Kiefhaber, 1995) has questioned the role of the intermediate. Capaldi and co workers (2001) have provided evidence that the early kinetic intermediate is indeed productive. They state that the problem arises from the difficulty in determining the role of the kinetic intermediate experimentally. In summary, for the vast majority of proteins, both equilibrium and kinetic data can be described equally well by

either a productive or partially folded state (on-pathway) or, a misfolded state that must unfold before the native state can form:

$$\begin{array}{ccccc} & K_{ui} & & K_{in} & \\ U & \longleftrightarrow & I & \longleftrightarrow & N \text{ (on-pathway)} \\ & K_{iu} & & K_{ni} & \end{array}$$

$$\begin{array}{ccccc} & K_{iu} & & K_{un} & \\ I & \longleftrightarrow & U & \longleftrightarrow & N \text{ (off-pathway)} \\ & K_{ui} & & K_{nu} & \end{array}$$

where U, I and N are the unfolded ensemble, the intermediate ensemble and the native state, respectively and K_{iu}, K_{un}, K_{ui} and K_{nu} are the microscopic rate constants. As the kinetic intermediate is generally formed within the dead time of measuring their formation must be considered a pre-equilibrium step and the above schemes become indistinguishable. Using a micro-capillary mixing apparatus, with a time resolution of approximately 150 μs, and quantitative kinetic analysis, the formation of an intermediate in the folding of the four-helix protein, Im7 was been examined (Capaldi *et al.*, 2001). A single exponential phase of kinetic folding (corresponding to the burst phase with conventional equipment) was followed by a second single exponential phase seen in the stopped flow experiments. While the refolding and unfolding data obtained by conventional methods fitted both the on-pathway and off-pathway models of folding equally well, the data on the submillisecond time scale did not. This data provided evidence that burst phase intermediates are a well populated ensemble and productive on the submillisecond time scale.

1.4.5 Physiological Role of The Molten Globule

The possible biological significance of the molten globule state of proteins is now recognised (Ptitsyn, 1995). The native-like overall fold of a molten globule, together with its enhanced flexibility, could facilitate the insertion into and translocation across

membranes, chaperone mediated protein folding in vivo, cell fusion and protein-receptor interactions (Ptitsyn, 1995). There is direct evidence for complex formation between proteins in their molten globule state and molecular chaperones (van der Vies *et al.*, 1992; Hayer-Hartl, *et al.*, 1994). It has been suggested that the molecular chaperone smooths the energy landscape for protein folding, thereby minimising the number of potential traps (Radford, 2000). Glucosyltransferase (Gt) glucosylates misfolded or partly folded glycoproteins, which are then retained by the endoplasmic reticulum and eventually degraded in proteosomes. In a recent study, using a family of chemically glucosylated proteins derived from chymotrypsin inhibitor-2 as Gt substrates, Gt was shown to recognize solvent accessible hydrophobic patches in molten globule-like conformers that mimicked intermediate folding stages of nascent glycoproteins. (Caramelo *et al.*, 2003).

The cytokine Interleukin 6 (IL-6) plays a major role in the pathogenesis of inflammation (van Snick, 1990). The environment is acidic with a pH of approximately 3.6 near the surface of activated macrophages and contains a variety of proteolytic enzymes released by the macrophages. The A-state of IL-6 possesses characteristics of a molten globule and is quite resistant to proteolysis. It is suggested that the molten globule of IL-6 plays a role in the cytokine's biological activity, which can exert its activity also at mildly acidic pH, as in inflammation sites (De Filippis *et al.*, 1996).

The role of the molten globule in the progression of disease has been of great interest (Dobson, 1995; Bychkova and Ptitsyn, 1995). For example, the two naturally occurring human lysozyme variants (Ile56Thr and Asp67His) are amyloidogenic and form molten globule-like structures similar to that of α-lactalbumin, with persistent structure in the α domain but lack stable, native-like structure in the β domain (Booth *et al.*, 1997). The

authors propose a model for lysozyme fibrillogenesis in which the association of the partly folded forms of the variants occurs through the unstable β domain. The development of stable β structure through intermolecular association acts as a template for the progressive recruitment of polypeptide chain into the nascent fibril. Indeed, mutations responsible for amyloid formation in immunoglobulin light chain (Hurle *et al.*, 1994), transthyretin variants (McCutchen *et al.*, 1995) and prion protein PrP(121-231) (Riek *et al.*, 1996) affect protein stability, maintenance of the hydrophobic core and tendency to aggregate. Moreover, recent biophysical studies of beta2microglobulin, a protein responsible for amyloid deposition in patients undergoing renal dialysis have shown that the molten globule is an amyloidogenic precursor (McParland *et al.*, 2000; McParland *et al.*, 2002).

1.5 GROWTH HORMONE STRUCTURE

The three dimensional structure of a recombinant methionyl-pGH has been determined by X-ray crystallography (Abdel-Meguid *et al.*, 1987). The structure comprises four antiparallel α-helices arranged in a tightly packed left-twisted helical bundle connected by largely unstructured loop regions (Chapter 3, Fig 3.1). Unlike the up-down-up-down helix connectivity for approximately 80-90% of four α-helix bundles, pGH has an up-up-down-down connectivity. This unusual helix connectivity for pGH does not affect the alignment of the helix macro-dipoles; helices 1 and 4 and helices 2 and 3 are arranged in pairs with their macro-dipoles aligned favourably. This contributes to the stability of the helix bundle. The X-ray structure of hGH has also been determined (de Vos *et al.*, 1992); the structure, not surprisingly is very similar to that of pGH. The only minor difference is an extra short helix in the segment between helices 2 and 3, which has an omega loop conformation in pGH. Determination of both structures confirms that the GHs all have a similar three-dimensional structure.

The arrangement of the four α-helix bundle in pGH results in a tightly packed globular structure. The amphipathic helices have their hydrophobic faces orientated inwards to form the hydrophobic core of the molecule. The central portion of helix 2, mostly buried within the core of the protein is almost completely made up of hydrophobic residues. A single conserved tryptophan residue, located halfway along this helix, forms part of the core of the molecule (Carlacci *et al.*, 1991). The UV absorption and fluorescence properties of this residue make it useful as an intrinsic probe for monitoring the unfolding of the protein. In hGH, the core is mostly made up of hydrophobic residues with the exceptions of Ser79 and Asp169 (de Vos *et al.,* 1992). Theses residues have their side chain oxygen hydrogen bonded to nearby residues in the core. Other hydrophobic clusters in the hGH structure can be found between the four-helix bundle and connecting loops.

The obvious feature of the GH's is their high α helix content. The amphipathic nature of the helices suggests that the hydrophobic effect would be instrumental in stabilising the tightly packed conformation. The connecting loops would also be important in stabilising the bundle, via hydrogen bonding with the side-chains of the helices or as seen in hGH, via hydrophobic interactions. The greater sequence divergence with the connecting loops may explain the difference in stability between the GH species. The disulphide bonds, in particular the Cys55 and Cys164 link which connects helix 4 to the long unstructured loop between helices 1 and 2, stabilise the structure by decreasing the conformational entropy of the unfolded state. In addition, the Cys53-Cys164 bond promotes the favourable interaction between the long connecting loop and helix 4. The favourable electrostatic alignment of the helix macrodipoles also contributes, albeit minimally, to the stability of the folded state. The small species sequence variation in the helical regions, results in

different intrinsic helix stabilities, which in turn may affect the stability of the whole molecule. It is the variation in the amino acid sequence, which determines the overall stability and folding behaviour of the various GH species.

1.6 FOLDING INTERMEDIATES OF BOVINE AND HUMAN GROWTH HORMONE

Bovine growth hormone (bGH) The equilibrium denaturation of bGH is a multistate process in which at least four species are involved: native, a monomeric intermediate, an associated form of the monomeric intermediate and the unfolded protein (Brems *et al.*, 1986; Havel *et al.*, 1986; Havel *et al.*, 1988) The monomeric intermediate has characteristics of a molten globule: largely α-helical, with a compact hydrodynamic radius similar to the native state, yet possessing a tertiary structure similar to the unfolded state (Brems and Havel, 1989). At elevated protein concentrations, the molten globule-like intermediate associates, and is characterised by a unique signal at 300 nm in the near-UV CD spectrum. The molten globule intermediate has also been detected in kinetic refolding studies (Brems *et al.*, 1987a). At dilute protein concentrations the refolding rate detected by far UV CD is faster than the rate detected by UV absorbance, indicating the existence of a kinetic folding intermediate with appreciable amounts of α-helix. At elevated concentrations, the kinetic intermediate self-associates and is characterised by the same unique near-UV CD spectrum as seen for the equilibrium intermediate, suggesting that the equilibrium and kinetic intermediates are the same.

At pH 2.0, bGH exhibits characteristics similar to the molten globule; little or no tertiary structure and a 50% loss of secondary structure compared to the native state (Burger *et al.*, 1966; Kauffman *et al.*, 1989; Holzman *et al.*, 1990).

Human growth hormone (hGH) At moderate concentrations of Gdn-HCl and elevated protein concentrations, hGH forms a stable folding intermediate, which has a significantly high propensity to self-associate (DeFelippis *et al.*, 1993). Although the monomer cannot be detected, it is presumed to form due to self-association and has been suggested to be a molten globule. In kinetic folding studies, a multiple number of phases have been resolved however, there is very little structural characterisation (Youngman *et al.*, 1995). An intermediate has also been detected at pH 2.0 (DeFelippis *et al.*, 1995). In contrast to bGH, the intermediate conformation maintains close secondary and tertiary structural similarity to that of the native state, consistent with a highly ordered molten globule. When subjected to Gdn–HCl-induced denaturation at pH 2.0, hGH forms stabilised equilibrium intermediates with characteristics of the molten globule. Similar state(s) have been observed in the thermal denaturation of the intermediate at pH 2.0 (Kasimova *et al.*, 1998).

1.7 AIMS OF THIS STUDY

A molten globule state of bGH and hGH has been observed under different experimental conditions; an equilibrium intermediate in the denaturant–induced unfolding transition, an acid-induced partially unfolded state and a transient folding intermediate in the kinetic folding reaction. The intermediates of bGH and hGH, however, do differ structurally, particularly at low pH. At the time of commencing my PhD, an equilibrium folding intermediate with properties characteristic of a molten globule had been detected in the denaturant-induced unfolding transition of pGH (Bastiras and Wallace, 1992). With the apparently important role of the molten globule in protein folding and the variability in structure of the folding intermediates for bGH and hGH the overall aims of this thesis were:

i) characterise the acid induced equilibrium denaturation of pGH using a variety of spectroscopic and hydrodynamic probes.

ii) characterise the folding kinetics of pGH using stopped-flow technology.

iii) characterise the acid-induced denaturation and folding kinetics of selected pGH analogues, the major emphasis being the effect of site-directed mutants on the intermediate state of pGH.

CHAPTER 2

MATERIALS AND METHODS

2.1 MATERIALS

Water was purified by a Milli-Q apparatus (Millipore, Sydney, Australia). FPLC apparatus, Mono-Q HR5/5 and Superose-12 HR10/30 columns, Q-Sepharose Fast Flow, Sephadex G-25, and Bioprocess columns were purchased from Pharmacia Biotechnology, Uppsala, Sweden. Cartridge prefilters were from Pall Process Filtration Ltd., Portsmouth, England. Delta Prep 4000 Preparative Chromatography System, 486 Tunable Absorbance Detector, Preparative LC System controller and C4 (47 mm i.d. x 300 mm; 500 ml column volume) were all purchased from Waters, Division of Millipore, Milford, MA., USA. HPLC apparatus was from Beckman, Beckman Instruments Inc., San Ramon, CA., USA. C4 (10 mm i.d. x 30 mm) and Aquapore, Butyl, Silica Prep 10 (20 mm i.d. x 30 mm) reverse-phase HPLC columns were obtained from Brownlee laboratories, Santa Clara, CA., USA. "Ultrapure" urea was from Merck, Darmstadt, F. R. G. Ampicillin, chloramphenicol, isopropylthio-β-D-galactopyranoside (IPTG), acrylamide, bisacrylamide, protein molecular weight standards for size exclusion chromatography, 2-[N-Morpholino]ethanesulfonic acid (MES) and 1-anilinonapthalene-8-sulphonate (ANS) were all supplied by Sigma Chemical Company, St. Louis, MO., USA. Low molecular weight protein markers for SDS polyacrylamide gel electrophoresis (SDS-PAGE), were purchased from Pharmacia Biotechnology, Uppsala, Sweden. HPLC grade acetonitrile was obtained from BDH Laboratory Supplies, Poole, England. Sequence-modified trypsin (trypsin cross-linked to a hydrophilic polymer to prevent autocatalysis) was from Boehringer Mannheim, Mannheim, Germany. TPCK-treated trypsin was from Worthington Biochemical Corporation, Freehold, New Jersey, USA. Ultrapure Tris-(hydroxymethyl)methylamine (Tris) was purchased from ICN Biomedicals, Uarona, Ohio. Pre-Filters, Type SS filters and 0.2 μm filters were obtained from Millipore, Milford, MA., USA. All other chemicals were of analytical reagent grade.

2.2 SOLUTIONS AND BUFFERS

C1 medium 1.61 g/L NH_4Cl, 1.22 g/L K_2SO_4, 2.65 g/L KH_2PO_4, 4.33 g/L Na_2HPO_4, 0.63 g/L $MgSO_4.7H_2O$, 20 g/L dextrose.H_2O, 0.004% (v/v) antifoam, 0.004% (w/v) thiamine solution, and trace metals: 20 mg/L $FeSO_4$, 5.1 mg/L $MnSO_4$, 8.6 mg/L $ZnSO_4$, 0.75 mg/L $CuSO_4$, 44 mg/L Na_3 citrate.

Combination buffer 20 mM each of sodium acetate, sodium bicarbonate, MES and Tris-HCl, pH 2.0-pH 8.0

Digestion buffer 100 mM Tris-HCl, pH 8.0

2.3 METHODS

2.3.1 Growth Hormone Production and Purification

The production and purification procedures used for generating pGH, pGH analogues and rGH is schematically represented in Figure 2.1. and were carried out by methods previously implemented for the large scale production of growth hormones at BresaGen Ltd.

2.3.1.1 Fermentation and Inclusion Body Harvesting

E.coli JM101 transfected with constructs encoding pGH, rGH or pGH analogues were maintained on minimal agar plates containing 100 μg/ml ampicillin. A single colony was used to inoculate 20 ml of C1 medium containing 100 μg/ml ampicillin, and grown at 37°C overnight with vigorous shaking. The 20 ml overnight culture was then used to inoculate a 15 litre fermenter containing C1 medium. The freshly inoculated culture had a starting optical density at 600 nm (OD_{600}) of 0.001. Induction with IPTG (0.25 mM final concentration) was performed at an OD_{600} of 50 which was reached after overnight incubation at 37°C. The fermentation was allowed to proceed for 5 hours post induction,

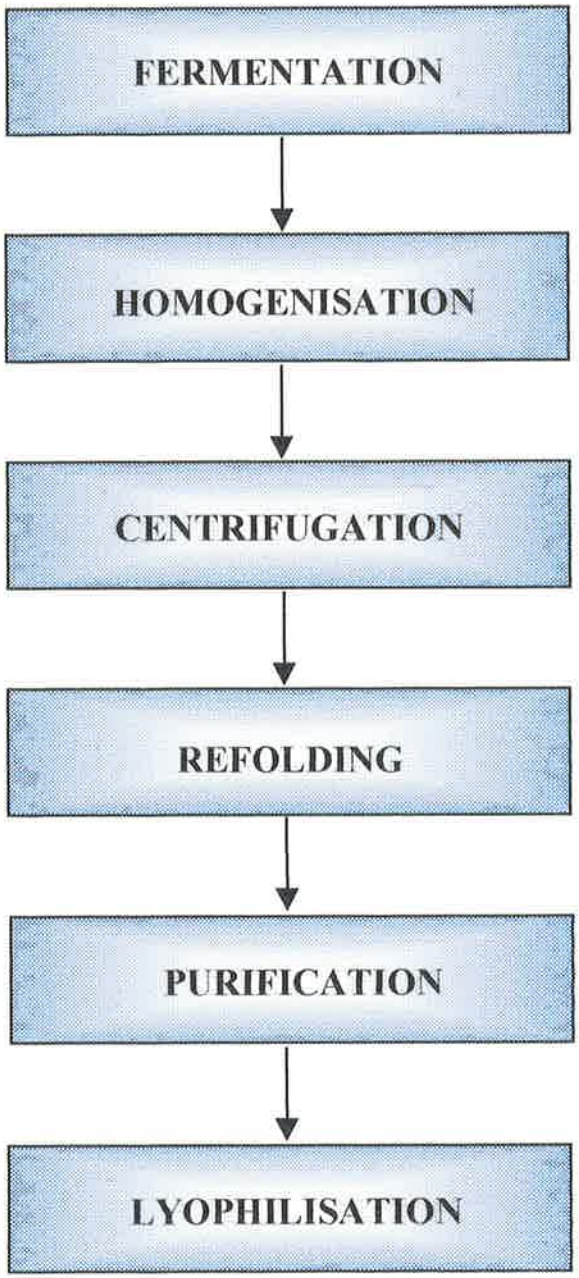

FIGURE 2.1 SCHEMATIC REPRESENTATION OF THE PRODUCTION PROCEDURES USED FOR GENERATING pGH, pGH ANALOGUES AND rGH.

then terminated by reducing the oxygen supply and temperature, before storage overnight at 4 °C.

The inclusion bodies were isolated from the cells by 3 passes through an APV CD30 homogeniser (APV Gaulin Inc., MA, U. S. A.) at 15,000 psi. The homogenate was then passed through a continuous flow Verenosi centrifuge at 9,000 rpm and a flow rate of:

$$\left[\frac{\text{inclusion body diameter } (\mu m)}{0.4}\right]^2 \times 400 = \text{ml/min.}$$

where inclusion body diameter was determined by Joyce Loebl.

The harvested inclusion bodies were diluted in 30 mM NaCl, 10 mM KH_2PO_4 and recentrifuged at a flow rate of:

$$\left[\frac{\text{inclusion body diameter } (\mu m)}{0.4}\right]^2 \times 900 = \text{ml/min.}$$

The resulting concentrated paste was collected and used for subsequent refolding and purification of protein.

2.3.1.2 Refolding and Purification

Inclusion bodies were solubilised in unbuffered 3.75 M urea, pH 11.5, at a final protein concentration of approximately 1.5 g/L. Refolding was allowed to proceed for 5 hours followed by dilution with 3 volumes of 33 mM sodium borate, pH 9.1. The final pH was adjusted to pH 9.1 with 1 M HCl. Separation of correctly folded, monomeric protein from

aggregate was achieved by anion-exchange chromatography. The solution was loaded onto a Q-Sepharose (113 mm i.d. x 44 mm) column, equilibrated with 25 mM sodium borate (Buffer A), pH 9.1 at a flow rate of 80 ml/min. At the completion of sample loading, the column was washed with Buffer A until the A_{280} trace stabilised. The protein was eluted with 150 mM NaCl in Buffer A at 50 ml/min and fractions containing correctly folded monomeric growth hormone were pooled. The pooled fractions were desalted on a 113 mm i.d. x 300 mm column packed with Sephadex G-25M, equilibrated with 20 mM ammonium bicarbonate, pH 9.1 at a flow rate of 50 ml/min. Fractions were collected and analysed by size-exclusion chromatography on a Superose 12 column (Figure 2.2), SDS-PAGE (Figure 2.2, Insert) and by UV absorbance spectroscopy. Pure fractions were pooled and lyophilised. The identity of each protein was confirmed by mass spectrometry and N-terminal sequence analysis.

2.3.2 Acid–Induced Denaturation

The protocols below describe the procedures used to analyse pGH, pGH analogues and rGH.

2.3.2.1 Titrations

Solutions were prepared by dissolving lyophilised pGH at pH 8.0 in either the combination buffer or 100 mM sodium phosphate, pH 8.0, with or without 4 M urea. Titrations were typically carried out by the addition of small aliquots (20 to 100 µl) of 1 M HCl with continual mixing. Following adjustment to pH values within the pH range 8.0-2.0, the pGH samples were incubated for a minimum of 1 hour (no longer than 5 hours) at room temperature (25°C) and then centrifuged (12,000 x g, 10 min, 25°C) prior to analysis. Following the 1 hour incubation, the pH of each sample was re-evaluated and there was no

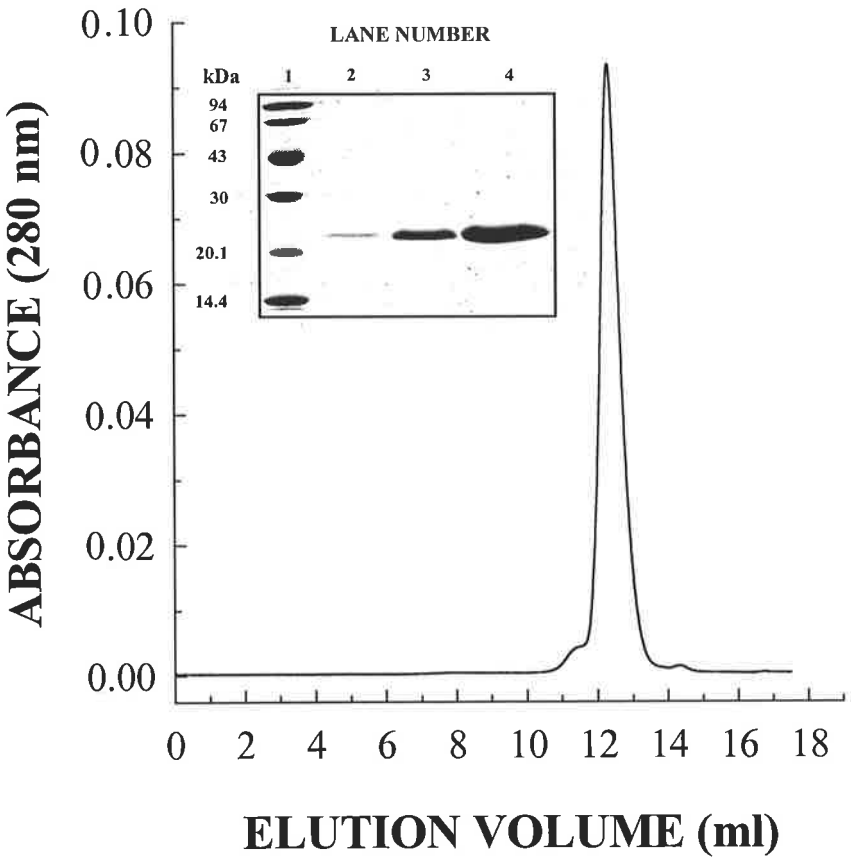

FIGURE 2.2 SIZE EXCLUSION CHROMATOGRAPHY AND SDS-PAGE GEL OF CORRECTLY FOLDED, MONOMERIC pGH. Fractions from the G-25 M column were pooled and an aliquot applied to a Superose 12 column. The single peak (10–13.5 ml as shown above) was collected, lyophilised and analysed by SDS-PAGE (12.5% acrylamide) under reducing conditions.
Inset: increasing concentrations of purified pGH electrophoresed and stained with Coomassie-Blue (Lane 1: low molecular weight protein markers; Lane 2: 1 μg, Lane 3: 5 μg, Lane 4: 20 μg).

measurable change within the incubation time limits. All pH measurements during titrations were conducted at 25 ± 0.5°C using an Activon Model 209 pH meter.

To determine the reversibility of acid titrations, solutions were prepared by dissolving lyophilised pGH at pH 2.0 in either the combination buffer or 100 mM sodium phosphate. The pH was altered to pH values within the pH range 2.0–8.0 by the careful addition of small aliquots of 1 M NaOH with continual mixing, and treated as described above. Transition apparent midpoints were determined by non-linear regression analysis using either:

Equation 1

$$y = \frac{n_0 e^{kx}}{1-\beta n_0(1-e^{kx})}$$

where n_0 determines the "lag" of the transition, k determines the rate of increase of the climb and β determines the amplitude of the rise (Bailey and Ollis, 1986).

Equation 2

$$y = \frac{(a_N+b_N pH) + (a_D+b_D pH)10^{-Meq(pH-MPeq)}}{1+10^{-Meq(pH-MPeq)}}$$

where a_N,b_N and a_D,b_D defined I_N (fluorescence intensity of the native state) and I_D (fluorescence intensity of the denatured state), respectively. MPeq was the pH at the transition midpoint and Meq the number of protons taken up in the unfolding transition (Oliveberg *et al.*, 1994). All non-linear regression analysis was performed using the data analysis program SigmaPlot (Jandel Scientific).

2.3.2.2 Fluorescence-Monitored Denaturation

Intrinsic fluorescence measurements were recorded at 25°C on an Aminco Bowman AB-2 Luminescence Spectrometer. All fluorescence data were obtained using an excitation wavelength of 295 nm, to selectively excite the single tryptophan residue present in pGH. Emission spectra were acquired in the range 310 to 400 nm at a scan rate of 60 nm/min and with slit widths of 4 nm for both the excitation and emission monochromators. The emission spectra were corrected for the Raman peak by subtracting a buffer only spectrum from each sample spectrum. The fluorescence emission intensity at 340 nm (I_{340}) and maximum emission wavelengths (λ_{max}) were read directly from the corrected emission spectra at each pH. The concentrations of pGH used were 0.05, 0.22 and 0.5 mg/ml. A concentration of 0.22 mg/ml was used for the reversibility experiments.

2.3.2.3 UV Absorbance-Monitored Denaturation

UV Absorbance measurements were recorded at 25°C on a dual-beam Cary 3 spectrophotometer. Spectra were acquired in the range 250 to 310 nm, with a spectral bandwidth of 2 nm, signal averaging time of 0.1 seconds, wavelength interval of 0.05 nm and a scan rate of 30 nm/min. Using the software supplied (Varian), a buffer control was converted into the automatic baseline. This was subsequently used to correct for background absorbance in all spectra. Absorbances at 290 nm and 278 nm were read directly from the corrected spectra. pGH concentrations were determined by measuring the absorbance at 278 nm using an extinction coefficient of 15714 $M^{-1}cm^{-1}$ (Bastiras and Wallace, 1992). The change in extinction at 290 nm (ε_{290}) was determined using the Beer-Lambert Law :

$$\mathbf{A} = C\, l\, \varepsilon$$

where A was the absorbance at 290 nm, *l* was the path length in cm and *C* was the concentration in moles/litre (M).

2.3.2.4 Second Derivative Spectroscopy

UV absorbance spectra were acquired in the range 250 to 310 nm, with a spectral bandwidth of 2 nm, signal averaging time of 0.2 seconds, wavelength interval of 0.05 nm and a scan rate of 15 nm/min. Spectra were corrected for background absorbance by scanning a buffer blank and automated baseline correction by the supplied software. The second-derivative spectra were derived from the UV absorbance spectra using an in-house computer program written by Dr. Mark Snoswell based on a method by Savitzky and Golay (1964).

2.3.2.5 Size-Exclusion Chromatography

Hydrodynamic radii were determined using a Superose 12 HR10/30 column (10 mm i.d. x 300 mm) with a Pharmacia FPLC system. A stock solution of pGH (10 mg/ml) in 5 mM sodium bicarbonate pH 8.0, was diluted to final concentrations of 0.22 mg/ml and 0.1 mg/ml in 100 mM sodium phosphate, 4 M urea, pH 8.0 and pH 2.0. Following incubation for a minimum of 1 hour at room temperature, the samples were centrifuged at 12,000 x g for 10 minutes. A 100 µl sample was injected onto the Superose 12 column pre-equilibrated in 100 mM sodium phosphate at the same pH and urea concentration as the sample. Protein elution was followed by the absorbance at 280 nm at a flow rate of 0.5 ml/min. Protein molecular weight calibration curves for the Superose 12 column were determined in 6 M Gdn–HCl and utilized to calculate the Stokes radii of pGH at each pH (Corbett and Roche, 1984).

2.3.2.6 Circular Dichroism-Monitored Denaturation

CD spectra were recorded using a Jasco Model J-720 spectropolarimeter. Stock solutions of pGH (8.8 and 2.2 mg/ml) in 5 mM sodium bicarbonate, pH 7.5, were diluted 10-fold with either 25 mM sodium phosphate, 20 mM sodium acetate ± 4M urea or 100 mM sodium phosphate, 20 mM sodium acetate ± 4M urea, which had been adjusted to various pH values. The final protein concentrations (approximately 0.88 mg/ml and 0.22 mg/ml) were determined by reading the absorbance at 278 nm (corrected for light scattering at 350 nm) and using an extinction coefficient of 15,714 $M^{-1}cm^{-1}$ (Bastiras and Wallace, 1992). The absorbance at 350 nm was always ≤5% of the absorbance at 278 nm. The pH of each diluted protein sample was checked using a narrow-bore pH probe (Amicon). Samples were kept at 25°C using a water-jacketed cell holder connected to a Neslab RT-111 waterbath.

Far-UV CD spectra were acquired in the range 180 to 260 nm with a resolution of 0.5 nm, bandwidth of 1.0 nm, signal averaging time of 1 second, sensitivity of 100 mdeg and a pathlength of 1 mm. Six accumulations were recorded. Each spectrum was corrected for background signal by the subtraction of a buffer blank. The raw data in millidegrees was converted to mean residue ellipticity $[\theta]_{MRE}$ (deg. cm^2. $dmol^{-1}$), using a mean residue weight of 114.5 calculated from the amino acid sequence. The mean residue ellipticity was calculated by the equation:

$$[\theta]_{\lambda\ nm} = \frac{[100 \times \Psi_\lambda]}{lC}$$

where $[\theta]_{\lambda\ nm}$ was the mean residue ellipticity at wavelength λ, Ψ_λ was the ellipticity at wavelength λ in degrees, l was the optical pathlength (cm) and C denotes the concentration

per residue, calculated by dividing the concentration of protein (g/L) by the mean residue molecular weight of its constituent amino acids.

Near-UV CD spectra were acquired in the range 250 to 320 nm with a resolution of 0.5 nm, bandwidth of 1.0 nm, signal averaging time of 1 second, sensitivity of 100 mdeg and a pathlength of 10 mm. Each spectrum was corrected for background signal by the subtraction of a buffer blank. The mean residue ellipticity at 285 nm, $[\theta]_{285}$ and 300 nm, $[\theta]_{300}$ was determined as described above.

2.3.2.7 Sedimentation Equilibrium Using Analytical Ultracentrifugation

Sedimentation equilibrium experiments were performed using a Beckman XL-A analytical ultracentrifuge set at 25°C. The ultracentrifuge cells were fitted with Yphantis–style 6-channel centrepieces. In each separate experiment three different concentrations of pGH (typically, 2.0 1.0 and 0.50 mg/ml) of sample (125 µl) were loaded parallel to the solvent channels containing buffer alone (130 µl). Samples were prepared by diluting a stock solution of pGH (10 mg/ml, 5 mM sodium bicarbonate, pH 8.0) into a buffer with final concentrations of 20 mM sodium phosphate, 20 mM sodium acetate ± 4M urea, pH 2.0. Following dilution, the samples were incubated for 1 hour at room temperature (25°C) and then centrifuged (12,000 x g, 10 min) prior to analysis.

Samples were centrifuged to sedimentation equilibrium at speeds of 9000-27000 rpm. Scans were collected in continuous scan mode (0.01-cm steps, 13 acquisitions/step) at 2–4 h intervals using wavelengths of 280–300 nm and 350 nm. The sedimentation equilibrium was judged to have been reached when the difference in concentration distribution between

two consecutive scans was zero. Baseline deviations were corrected by subtracting the scans collected at 350 nm from those collected at 280–300 nm.

2.3.2.8 Sedimentation Equilibrium data treatment and model fitting

Apparent point-average weight-average molecular weight values ($M_{w,app}$) were calculated from plots of ln[$c(r)$] *versus* r^2 plots (Teller, 1973), where $c(r)$ was the concentration of protein (g/L) at radial position r. Plots of $M_{w,app}$ versus concentration are qualitatively useful in assessing the self-association of a solute but substantial error is introduced into $M_{w,app}$ values through a numerical differentiation step. Therefore, as a means of assessing the quality of the sedimentation data, and for the purposes of fitting self-association models, the data was replotted in terms of the Omega function $\Omega(r)$ (Milthorpe *et al.*, 1975):

$$\Omega(r) = \frac{c(r)\exp[\phi_1 M_1(r_F^2 - r^2)]}{c(r_F)}$$

$$= \frac{a_1(r_F)c(r)}{a_1(r)c(r_F)}$$

where $\phi_1 = (1-\bar{\upsilon}\rho)\omega^2/2RT$, $\bar{\upsilon}$ was the partial specific volume of the protomer in g/mL, ρ the density of the solvent in g/mL, and ω the angular velocity in radians per second. M_1 was the molar mass of the protomer (the smallest species participating in the self-association of the protein), $c(r_F)$ was the total concentration of protein at the radial reference position r_F, and a_1 was the thermodynamic activity of the protomer. A value of 0.737 mL/g was used for υ calculated from the sequence (Abdel-Meguid *et al.*, 1987) using the method of Cohn and Edsall (Cohn and Edsall, 1943). The value of ρ was calculated from the density of the

buffer components and water using the program SEDNTERP v1.03 (Amgen). In some cases, the value of M_1 used was that of the pGH monomer (21860), while in others, no detectable monomer was present and the value of M_1 used was that of the dimer (43720).

Plots of $\Omega(r)$ *versus* $c(r)$ for the three loading concentrations of protein at sedimentation equilibrium were calculated using a common value of $c(r_F)$. Overlap of the data over the common concentration range is a very sensitive indicator that both chemical and sedimentation equilibrium have been attained (Milthorpe *et al.*, 1975; Ralston and Morris, 1992), i.e., overlap indicates that pGH was pure and that all pGH molecules were able to participate in the self-association and no irreversible aggregates were formed.

The Omega data were fitted with models of discrete (e.g., monomer-dimer) and indefinite (e.g., SEK1; Adams *et al.*, 1978) self association. For each model, the concentration of the protomer, $c_1(r)$, was written as an explicit or implicit function of $c(r)$. The SEK 1 model describes the squential addition of protomers, P, where the addition of each protomer is described by a single molar equilibrium constant, K:

$$P \overset{K}{\leftrightarrow} P_2 \overset{K}{\leftrightarrow} P_3 \overset{K}{\leftrightarrow} P_4 \ldots \overset{K}{\leftrightarrow} \ldots P_n$$

$$c(r) = c_1(r)/(1-kc_1(r)^2 \qquad \text{if } kc_1(r)<1$$

where $k = K/M_1$

For all models, the Adams-Fujita approximation (Adams and Fujita, 1963) was used to relate the thermodynamic activity of the protomer, $a_1(r)$, to the concentration of the protomer $c_1(r)$:

$$a_1(r) = c_1(r)\exp[BM_1c(r)]$$

where *B*, the second virial coefficient, is a measure of the nonideality of the solute which principally arises from the size and shape of the solute and its effective charge in the buffer conditions employed. With this approximation, a single value of *B* is sufficient to describe all species in the self-association so that, for example, the nonideality of the solute monomer would equal *B*, that of the dimer would equal 2*B*, etc.

The models were fitted to the Omega function data by nonlinear regression (Ralston & Morris, 1992; Morris & Ralston, 1985). Values of the thermodynamic parameters, *K* and *B*, ± SE, were returned where SE is the approximate (asymptotic) standard error of the variable parameter calculated from the inverse matrix set up from partial derivative equations of the fitting function (Cleland, 1967). Models which appropriately described the data resulted in random distribution of residuals as determined by the runs test at the 5% level.

2.3.2.9 ANS Fluorescence

Fluorescence measurements were recorded at 25°C on an Aminco Bowman AB-2 Luminescence Spectrometer. Fluorescence data were obtained using an excitation wavelength of 380 nm. Emission spectra were acquired in the range 400 to 600 nm at a scan rate of 60 nm/min, with slit widths of 4 nm for both the excitation and emission monochromators. The emission spectra were corrected for the Raman peak and background ANS fluorescence by subtracting a buffer only spectrum from each sample spectrum. Samples were prepared by diluting a stock solution of pGH, (1 mg/ml, 5 mM sodium bicarbonate, pH 8.0) into the combination buffer ± 4 M urea at pH 8.0 and pH 2.0 to obtain a final protein concentration of 0.05 mg/ml. Samples were incubated for a minimum of 1 hour (no longer than 5 hours) at 25°C, followed by the addition of 10 µl of

100 mM ANS (final concentration 100 μM). Samples were incubated for a further 30 minutes then centrifuged (12,000 x g, 10 min, 25 °C) prior to analysis.

2.3.3 Isolation and Purification of pGH(96–133)

2.3.3.1 Preliminary Isolation and Purification of pGH(96–133)

A stock solution of 100 μM pGH (2.2 mg/ml in digestion buffer) was diluted to 22.7 μM (0.5 mg/ml) in the same buffer to a final volume of 2 ml. Digestion of duplicate samples was initiated by the addition of 2 μg of sequence-modified trypsin (Boehringer Mannheim) in 2 μl of 10 mM acetic acid (1:500 trypsin:protein, w/w). The mixtures were incubated at 25°C for 1 hour. The reaction was stopped by the addition of 100 μl of glacial acetic acid. The purification of peptides produced from the partial digestion of pGH was performed by reverse phase HPLC (RP HPLC). Specifically, 3 μl of 10% TFA was added (0.1% TFA final) to a 300 μl aliquot of the digest. The samples were then filtered (0.2 μm) and 150 μl was added to glass tubes for programmed injection. One hundred microlitres was loaded onto a C4 RP HPLC cartridge (10 mm i.d. x 30 mm), pre-equilibrated with 0.1% TFA at a flow rate of 0.5 ml/min. The digestion products were separated at 34°C by applying a linear gradient of acetonitrile from 0% to 70% (v/v) acetonitrile in 0.1% (v/v) TFA at a flow rate of 0.5 ml/min over a period of 70 minutes. Protein elution was monitored by the absorbance at 214 nm (A_{214}) and peptide peaks collected and lyophilised. The above protocol was also implemented for the preliminary digest with unmodified trypsin. However, the subsequent purification of these digest products was achieved by RP HPLC, applying a linear gradient from 30% to 60% (v/v) acetonitrile in 0.1% (v/v) TFA at a flow rate of 0.5 ml/min over a period of 30 minutes. The presence of protein degradation and self-digestion products of trypsin were determined in control incubations of protein and trypsin in digestion buffer alone, under the same conditions.

2.3.3.2 Optimisation of Partial Tryptic Digests

A stock solution of 100 μM pGH (2.2 mg/ml in digestion buffer) was diluted, in duplicate, to 22.7 μM (0.5 mg/ml) in the same buffer to a final volume of 2 ml. Digestion was initiated by the addition of either 2 μg of trypsin in 2 μl of 10 mM acetic acid (1:500 trypsin:protein, w/w) or 5 μg of trypsin in 5.0 μl of 10 mM acetic acid (1:200 trypsin:protein, w/w). The mixtures were incubated at 25°C for a total of 3 hours. A 300 μl aliquot was taken from each reaction mixture after 30 minutes and the reaction stopped by the addition of 20 μl of glacial acetic acid. Subsequent aliquots were taken and acidified at hourly intervals after the addition of trypsin. The presence of protein degradation and self-digestion products of trypsin were determined in control incubations of protein and trypsin in digestion buffer alone, under the same conditions. Three microlitres of 10% TFA was added (0.1% TFA final) to the 300 μl digestion aliquots. The samples were then filtered (0.2 μm) and 150 μl was added to glass tubes for programmed injection. One hundred microlitres was loaded onto a C4 RP HPLC cartridge (10 mm i.d. x 30 mm), pre-equilibrated with 30 % (v/v) acetonitrile in 0.1% (v/v) TFA at a flow rate of 0.5 ml/min. Peptides were eluted by applying a linear gradient from 30% to 60% acetonitrile in 0.1% (v/v) TFA at a flow rate of 0.5 ml/min over a period of 30 minutes.

Protein quantitation was determined by the integrated peak area, based on the method described by Buck *et al.*, 1989. Briefly, a standard curve was formulated to determine the integrated peak area for 1 μg of undigested pGH (Figure 2.3). The peak area is dependent on the number of amino acid residues and other moieties (eg. peptide bonds) that absorb at 214 nm (i.e. the extinction coefficient). The extinction coefficient of peptide 96–133 was determined at 214 nm and expressed as a function of native pGH:

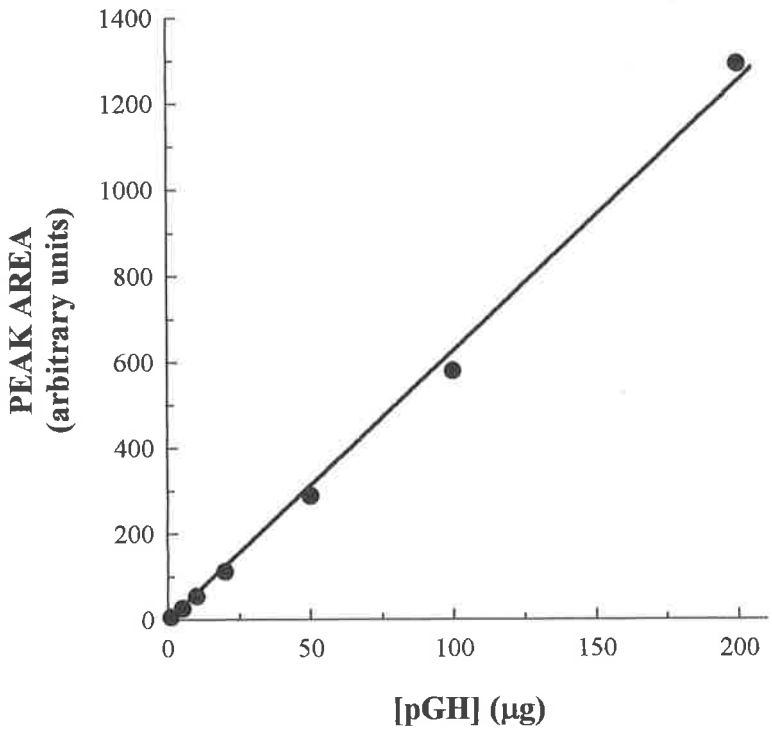

FIGURE 2.3 STANDARD CURVE OF THE INTEGRATED PEAK AREA OBTAINED AT VARIOUS pGH CONCENTRATIONS. Samples were prepared such that a 100 μl aliquot contained each of the following amounts of pGH; 1, 5, 10, 50, 100 or 200 μg. Each 100 μl sample was injected onto a C4 RP HPLC column, pre-equilibrated with 30% (v/v) acetonitrile in 0.1% TFA. Protein was eluted by applying a linear gradient from 30% to 60% acetonitrile in 0.1% (v/v) TFA at a flow rate of 0.5 ml/min over a period of 30 minutes. The integrated peak area as determined by the supplied software (Gold, Beckman) was plotted as a function of the quantity of protein. The integrated peak area for 1 μg was then determined from each protein quantity, the final value being the average of the above.

AMINO ACID RESIDUE	EXTINCTION COEFFICIENT	TOTAL EXTINCTION NATIVE pGH	TOTAL EXTINCTION pGH(96–133)
Tryptophan	22735	22735	–
Tyrosine	5755	40285	5755
Histidine	6309	18927	–
Phenylalanine	7208	93704	14416
Peptide Bonds	2846	540740	105302
TOTAL		**716391**	**105302**

TABLE 2.1 EXTINCTION COEFFICIENT OF NATIVE pGH AND pGH(96–133) AT 214 nm.

The quantity of peptide was determined:

$$\textbf{Quantity of peptide (µg):} \quad \frac{\textbf{area of peptide}}{\textbf{area of 1 µg of native pGH}} \quad \textbf{x extinction of peptide}$$

2.3.3.3 Identification of Digest Products

Electrospray mass spectrometry of purified digest products was carried out on a Perkin-Elmer SCI-EX API100 mass spectrometer by Dr. Mark Van Der Hoek, Hanson Centre for Cancer Research, Adelaide, South Australia. The identity of peptide 96–133 was verified by N-terminal sequence analysis on an Applied Biosystems Model 470A Protein Sequencer by Dr Neil Shirley at the Waite Campus, University of Adelaide.

2.3.3.4 Preparative Isolation and Purification of pGH(96–133)

The isolation and purification procedure used for generating pGH(96–133) is schematically represented in Figure 2.4. Five hundred milligrams of lyophilised pGH was dissolved in one litre of digestion buffer. Digestion was initiated by the addition of 1 mg of trypsin in 900 µl of 10 mM acetic acid (1:500 trypsin:protein, w/w). The mixture was incubated at 25°C in an air chamber with slow oscillation for 30 minutes. The reaction was stopped by acidification to pH 2.0 with 100% TFA (2 ml). A 300 µl test aliquot was analysed as described above (see 2.2.3.2) to confirm that the digestion had produced sufficient amounts of pGH(96–133).

Prior to preparative RP HPLC separation, the acidified digest solution (1 L) was filtered using a Millipore pre-filter (AP) preceding a Millipore type SS filter (3.0 µm). The digestion products were separated using a Waters Delta Prep 4000 preparative chromatography system. The 1 L sample was divided into 2 x 500 ml samples which were loaded separately onto a C4 RP HPLC column (47 mm i.d. x 300 mm), pre-equilibrated with 0.1% trifluoroacetic acid at 25 ml/min. Peptides were separated by applying a step-wise acetonitrile gradient from 0% to 30% (v/v) over 20 min, 30% to 60% (v/v) over 120 min, 60 to 80% (v/v) over 2 min, and then held at 80 % (v/v) for 20 min in 0.1% TFA at a flow rate of 25 ml/min. Elution of protein was monitored by the absorbance at 280 nm (A_{280}). The eluate was collected in 25 ml fractions.

Fractions were assayed for the presence of the desired peptide as follows: A 250 µl aliquot was lyophilised (Speed-Vac) and resuspended in 150 µl of 0.1% TFA. One hundred microlitres was loaded onto a C4 RP HPLC cartridge (10 mm i.d. x 30 mm), pre-equilibrated with 30 % (v/v) acetonitrile in 0.1% (v/v) TFA at a flow rate of 0.5 ml/min.

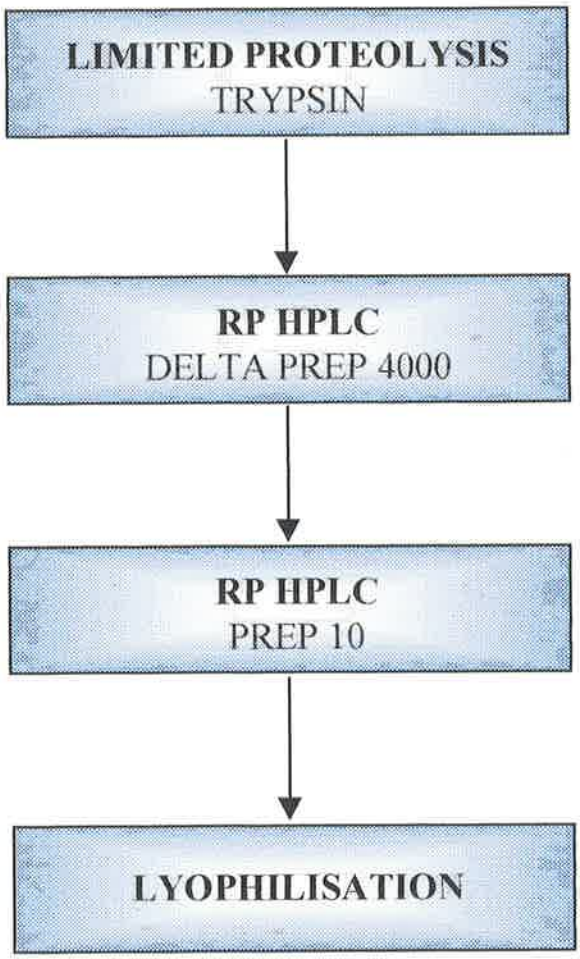

FIGURE 2.4 SCHEMATIC REPRESENTATION OF THE PREPARATIVE ISOLATION AND PURIFICATION PROCEDURES USED FOR GENERATING pGH(96–133).

Peptides were eluted by applying a linear gradient from 30% to 60% acetonitrile in 0.1% (v/v) TFA at a flow rate of 0.5 ml/min for 30 minutes. Fractions containing peptide were pooled (approximately 100 mg of peptide), 700 mg of mannitol added (mannitol:peptide ratio, 7:1), and then lyophilised under vacuum in a Lab-Conco freeze-dryer. Mannitol was added at the lyophilisation stage to increase the bulk of the sample, making it easier for further manipulations.

Approximately 50 mg of lyophilised material from the first RP HPLC step was dissolved in 1.5 ml of 10% (v/v) acetonitrile in 0.1% (v/v) TFA. The solution was filtered (0.2 μm) and loaded (2 x 100 μl injections per run) on to a C4 reverse phase Prep 10 (10 mm i.d. x 100 mm) column pre-equilibrated with 30% acetonitrile (v/v) in 0.1% TFA at a flow rate of 2 ml/min. Subsequent peptide separations were carried out at 34°C with a linear gradient of acetonitrile from 30 to 60% (v/v) in 0.1% TFA at a flow rate of 2.0 ml/min for 30 minutes. Protein elution was monitored at A_{214} and the desired peptide collected, as determined by the retention time. The peptide samples from each run were pooled and lyophilised under vacuum. The lyophilised material was redissolved in 25 ml of 10% acetonitrile (v/v), 10 mM sodium chloride before again being lyophilised. The above step was repeated twice, using 25 ml Milli-Q water only, to ensure that all residual TFA had been removed, as determined by pH measurement. The amount of material was quantified using the integrated area of the A_{214} absorbance peak standardised with accurately quantified pGH (*2.3.3.2*) and by UV absorbance spectroscopy using an extinction coefficient at 278 nm (ε_{278}) of 1280 $M^{-1}cm^{-1}$.

2.3.4 Two Step Precipitation Assay

Growth hormone was incubated at an initial protein concentration of 90 μM (2 mg/ml) in a series of buffers containing 20 mM sodium phosphate pH 2.0 and increasing concentrations of urea (0, 0.5, 1.0, 2.0, 3.0, 3.5, 4.0, 4.25, 4.5, 4.75, 5, 5.25, 5.5, 5.75, 6, 6.5, 7, 7.5, 8 and 9 M). Following a 30 minute incubation at ambient temperature, each sample was rapidly diluted into 100 mM sodium phosphate pH 8.0 to achieve a final protein concentration of 8.2 μM (0.18 mg/ml, 93 mM sodium phosphate) and 1 M urea. After a further 45 min incubation, the samples were centrifuged (12,000 x g) for 10 minutes and the absorbance of the supernatant measured at 278 nm against a 1 M urea reference with the same buffer solution.

2.3.5 Two Step Precipitation Assay in the Presence of pGH(96−133)

Growth hormone was incubated at an initial protein concentration of 90 μM (2 mg/ml) with the addition of pGH(96–133) in a 10–fold molar excess (900 μM), in buffers as described in 2.3.4. As the single tyrosine residue present in helix 3 absorbs at 280 nm, its contribution to final A_{278} readings was determined in a control incubation of helix 3 in buffer alone, under the same conditions. Subsequent dilutions were performed as described in 2.3.4. The absorbance of the supernatant was measured at 278 nm against a 1 M urea reference and corrected for the contribution due to helix 3.

2.3.6 Stopped-Flow Kinetics Monitored by Fluorescence

2.3.6.1 Stopped-Flow Instrumentation and Methodology

Fluorescence detection of the folding kinetics of pGH, pGH analogues and rGH was achieved using an Aminco Bowman AB-2 Luminescence Spectrometer fitted with an Aminco Bowman FP-120 MilliFlow Stopped Flow Reactor (Spectronic Instruments,

Rochester N.Y.). An in-built quartz condensing lens (2 mm pathlength, 32 µl volume) was used for fluorescence measurements. An excitation wavelength of 295 nm was used to selectively excite the tryptophan residue(s), with fluorescence emission recorded at a wavelength of 350 nm. Excitation and emission bandwidths of 4 and 8 nm, respectively were employed. The temperature in the stopped-flow unit was maintained at 20°C using a thermostatted circulating water bath.

Briefly, the delivery of reactants from two drive syringes was facilitated by the air-operated pneumatic activation of a drive block, expelling a controlled quantity of reactants through a mixing chamber, into the observation cell and finally into a stop syringe. The piston of the stop syringe moved until, its motion was stopped by an adjustable stop block. Once in contact with the stop block, an electrical contact triggered a signal to initiate data acquisition. The line pressure was maintained at 400 kpa.

2.3.6.2 Dead-Time and Flow-Rate Determination

The dead-time was determined based on the method described in the MilliFlow Stopped Flow Reactor Operator's manual. A solution of 20 µM pyranine (Sigma) in 150 mM ammonium bicarbonate was diluted 1:2 (v/v) with a series of solutions containing 50 mM potassium phosphate and various concentrations of carbonic anhydrase (500 units/ml, 1000 units/ml and 1500 units/ml). The reaction was followed for 200 ms, using a sampling time of 1 ms. The excitation and emission wavelengths were 454 and 512 nm with bandpasses of 4 and 8 nm respectively. The data was corrected for the blank, converted to ASCII format and downloaded to an IBM compatible computer running Excel, where the log of ($|F-F_8|$) vs time was plotted. The linear portion of each curve was extrapolated to zero at

the intercept. The dead time was calculated as the time from the intercept to the point where the log plots plateau.

The flow-rate was determined using the equation:

$$\mathbf{Td\ (sec)} = \frac{\mathbf{V\ (ml)}}{\mathbf{U\ (ml/sec)}}$$

where Td was the dead time, V (ml) was the volume contained between the points of mixing and observation (0.02 ml) and U (ml/sec) was the velocity. The dead time of the instrument equated to 4 ms with a flow rate of 5 ml/sec.

2.3.6.3 Solution Preparation for Stopped-Flow Measurements

Stock solutions of pGH and analogues thereof, were prepared by dissolving protein in degassed 20 mM sodium borate, pH 9.1, or degassed 20 mM sodium borate containing 5 M Gdn–HCl, pH 9.1. The solutions were then filtered through 0.2 μm filters (Millipore). Protein concentrations were determined by UV absorption using an extinction coefficient of 15714 $M^{-1}cm^{-1}$ (Bastiras & Wallace, 1992). The Gdn–HCl concentrations were determined by refractometry (Nozaki, 1972).

2.3.6.3.1 Protein Concentration Dependence Experiments

The initial protein concentration ranges were 0.35 to 3.5 mg/ml. The stopped flow was fitted with syringes such that concentration jumps from 5 M to 1.43 M Gdn–HCl (a 3.5-fold dilution) for refolding and from 0 M to 4 M Gdn–HCl (a 3.5-fold dilution) for unfolding experiments.

2.3.6.3.2 Gdn–HCl Concentration Dependence Experiments

The initial protein concentration for experiments was 0.5 mg/ml in 20 mM sodium borate, pH 9.1 for unfolding and 20 mM sodium borate in 5 M Gdn–HCl, pH 9.1 for refolding. These solutions were diluted (3.5-fold) to achieve the desired final Gdn–HCl concentration whilst maintaining a constant concentration of protein at 0.15 mg/ml. For each desired final Gdn–HCl concentration, buffers were prepared allowing for the 3.5 dilution. For all proteins analysed the concentrations of Gdn–HCl were the same. Typically, refolding vs [Gdn–HCl] was examined between 1.5 M and 2.7 M Gdn–HCl (midpoint of Gdn–HCl equilibrium denaturation of wild-type pGH, Bastiras and Wallace, 1992) and unfolding vs [Gdn–HCl] was examined between 2.7 M and 4 M Gdn–HCl.

2.3.6.4 Data Collection and Analysis

Typically, for each experiment 8 successive kinetic traces were averaged, the raw data converted to ASCII format and downloaded on to an IBM compatible computer. The raw data was smoothed using the fourier domain editing option in the statistical computer software package, TableCurve (Jandel Scientific). The data was then analysed by non-linear regression analysis using the statistical software package, SigmaPlot (Jandel Scientific) using the equation:

$$A(t) = \sum_{i-1}^{\eta} A_i \exp(-t/\tau_i) + A_\infty$$

where $A(t)$ was the total amplitude at time t, A_∞ was the amplitude registered at the end of the reaction, A_i is the amplitude of the individual phases, i, and τ was the associated time constant. To determine the number of kinetic phases, the data were evaluated containing 1-3 time constants. The function providing the best fit, based on the statistical output from the fitting algorithm was used to determine estimates of the time constants and amplitudes.

CHAPTER 3

ACID-INDUCED DENATURATION OF RECOMBINANT PORCINE GROWTH HORMONE

3.1 INTRODUCTION

Porcine growth hormone (pGH) is a single-chain polypeptide of 191 amino acids arranged in an antiparallel four α-helix bundle (Abdel-Meguid *et al.*, 1987). An energy minimised model of pGH (Rowlinson *et al.*, 1994) based on the hGH/hGH receptor crystal structure (de Vos *et al.*, 1992) is shown in Figure 3.1. The X-ray coordinates for pGH have not been released so the model in Figure 3.1 cannot be confirmed. Several structural features of pGH are conserved amongst the growth hormones; the primary structure contains two disulphide bridges, the first of these connects the loop between helix 1 and helix 2 to helix 4, and the second forms a small loop at the C-terminus. A single conserved tryptophan residue in helix 2 at position 86 (Trp86) occupies a hydrophobic core formed by the hydrophobic faces of the α-helix bundle (Figure 3.2). The location, absorption and fluorescence properties of Trp86 make it useful as an intrinsic probe for the study of pGH tertiary structure (Bastiras and Wallace, 1992). The Trp86 residue is in close proximity to Asp168 (Figure 3.2), an amino acid also conserved in the primary sequence of the growth hormones. The tertiary structures of human growth hormone (hGH) (de Vos *et al.*, 1992; Kasimova *et al.*, 2002) and bovine growth hormone (bGH) (Carlacci *et al.*, 1991) are very similar to that of pGH. This is consistent with pGH sharing 91% and 68% primary sequence identity with bGH and hGH, respectively.

The detection of partially folded intermediate states along a protein's folding pathway is crucial to understanding the principles of protein folding (Kim and Baldwin, 1982; Kuwajima, 1989; Ptitsyn, 1995). Molten globules are intermediates in the folding pathway of many proteins (Ptitsyn, 1992) and can be bound to molecular chaperones (Hayer-Hartl *et al.*, 1994). Molten globules have characteristics of both folded (or native) and unfolded proteins: (i) a significant amount of native-like secondary structure, (ii) a collapsed state

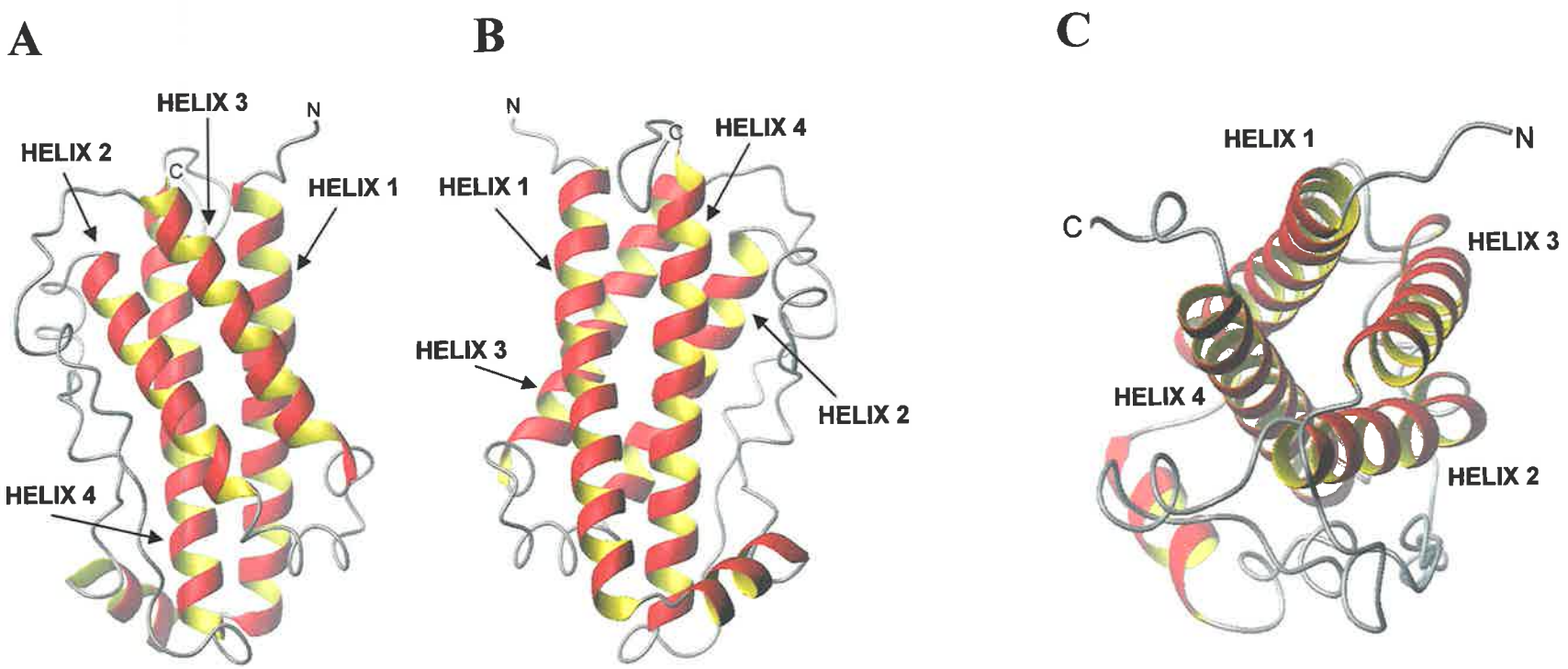

FIGURE 3.1 REPRESENTATIVE MOLECULAR MODEL OF PORCINE GROWTH HORMONE (pGH). The structure of pGH was obtained by energy minimisation (Rowlinson *et al.*, 1994), based on the hGH/hGH receptor crystal structure (de Vos *et al.*, 1992). Views A and B show each side of the molecule. View C looks down the central core of the molecule and highlights the hydrophobic core formed by the stacking of the α helices. The amino and carboxyl terminus is denoted by N and C respectively.

Figure prepared with the program MOLMOL (Koradi *et al.*, 1996)

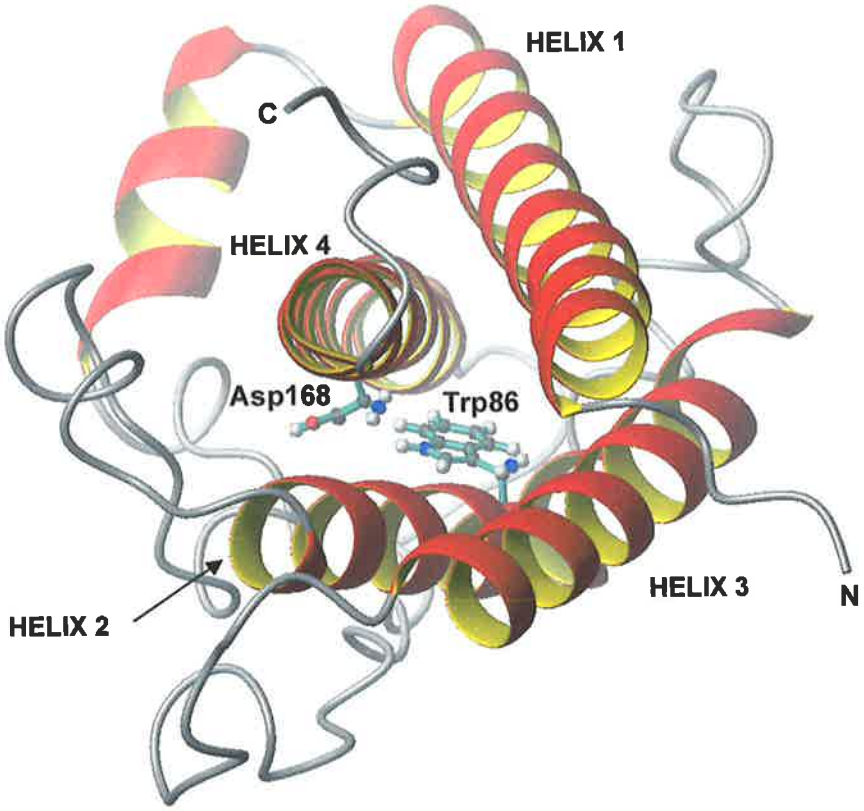

FIGURE 3.2 THE LOCATION OF TRP86 AND ASP168 IN THE MODEL OF pGH. A view looking down the central core of pGH showing the location of Trp86 and Asp168 within the hydrophobic core of the molecule. This view is similar to the one shown in Figure 1 C except that the molecule has been tilted downward slightly and rotated approximately 90° clockwise. All atoms of the amino acid residues are shown. The amino and carboxyl terminus is denoted by N and C, respectively.

Figure prepared with the program MOLMOL (Koradi *et al.*, 1996)

with hydrodynamic properties more akin to the native state, (iii) a lack of well-defined tertiary structure, (iv) enhanced solvent exposure of hydrophobic surfaces with an increased propensity to self-associate and (v) a less co-operative unfolding transition compared to that of the native state. However, it is now apparent that molten globule folding intermediates cover a broad range of conformations and degrees of unfolding, which are subject to the solvent conditions employed.

Molten globules have been observed frequently at low pH, where intramolecular charge repulsion appears to be an important driving force for partial unfolding. Acid-induced denaturation of proteins has proven to be an invaluable tool in gaining insight into the properties of intermediate states. The use of chemical denaturing agents, such as Gdn–HCl and urea, often lead to mixtures of native, intermediate and unfolded protein states, whereas a single intermediate state can be populated at low pH (Dolgikh *et al.*, 1981).

Equilibrium denaturation studies of bGH (Brems *et al.*, 1985, 1986; Havel *et al.*, 1986, 1988), hGH (DeFelippis *et al.*, 1993; Kasimova *et al.*, 1998) and pGH (Bastiras and Wallace, 1992) have detected molten globule intermediates in the folding pathway. The existence of a molten globule state of hGH at low concentrations of organic solvent has also been reported (Wicar *et al.*, 1994). Previous studies on the acid–induced unfolding of bGH (Kauffman *et al.*, 1989; Holzman *et al.*, 1990) and hGH (DeFelippis *et al.*, 1995) have shown that a partially folded intermediate(s) is formed at pH 2.0. However, the observed structural properties of these intermediates are different. At pH 2.0, bGH exhibits characteristics similar to those attributed to the molten globule, little or no tertiary structure and a 50% loss of secondary structure compared to the native state. In contrast, the conformation of hGH at pH 2.0 is predominantly native-like, with no detectable change in

secondary structure content, residual tertiary structure and a hydrodynamic radius intermediate between the native and denatured states with increased exposure of the hydrophobic core (DeFelippis *et al.*, 1995). Moreover, from a recent NMR study (Kasimova *et al.*, 2002), the conformation of recombinant hGH at approximately pH 2.7 was shown to be structurally conserved, with a dynamically more flexible helical core, surrounded by highly mobile unstructured loops.

In view of the differences observed for the acidification of bGH and hGH, the aim of this study was to characterise the acid–induced unfolding of pGH in the presence and absence of 4 M urea. The inclusion of urea was to allow a direct comparison with previous studies of bGH (Burger *et al.*, 1966; Holzman *et al.*, 1990). The acid–induced equilibrium denaturation was investigated using a range of physicochemical techniques. Intrinsic fluorescence, UV absorption spectroscopy, and near-UV circular dichroism were used to follow changes in tertiary structure, and changes in secondary structure were followed by far-UV circular dichroism. Size-exclusion chromatography and analytical ultracentrifugation were used to follow changes in the hydrodynamic radius and self-association.

3.2 RESULTS

3.2.1 Fluorescence Spectroscopy

The fluorescence emission of tryptophan is highly sensitive to the polarity of its surrounding environment (Teale, 1960; Lakowicz, 1983), thus providing a useful tool for probing conformational changes in proteins. An increase in polarity may result from a direct interaction of the tryptophan with the aqueous solvent or with a charged internal residue. An excitation wavelength of 295 nm was chosen to measure the changes in fluorescence emission of Trp86, upon acidification of pGH in both the presence and absence of 4 M urea. At lower wavelengths, for example 278 nm, both tryptophan and tyrosine residues absorb energy and can therefore contribute to the fluorescence emission spectrum. However, at a wavelength of 295 nm, the absorbance of tyrosine is negligible and therefore does not contribute any fluorescence (Wetlaufer, 1962).

The corrected emission spectra of pGH at pH 8.0 and pH 2.0, in the absence and presence of 4 M urea are shown in Figure 3.3 A. Each spectrum is characterised by two bands: (i) a broad band that varied in both the fluorescence emission intensity and the wavelength of maximum fluorescence (λ_{max}) and (ii) a less intense band, centred consistently near 380 nm irrespective of the experimental conditions employed. This second, less intense band, was believed to be a spurious signal attributable to the incomplete correction in the emission monochromator (Havel *et al.*, 1986). The acid-induced denaturation of pGH as monitored by the relative fluorescence intensity at 340 nm (I_{340}) is shown in Figure 3.3 B. In the absence of urea, I_{340} exhibited a 4-fold increase through the transition from pH 8.0 to pH 2.0. The apparent midpoint of the transition was at pH 4.1 (Figure 3.3 B; Table 3.1). A small red shift from 331 ± 1.0 nm at pH 8.0 to 334 ± 1.0 nm at pH 2.0 in the λ_{max} was also observed (Figure 3.3 C).

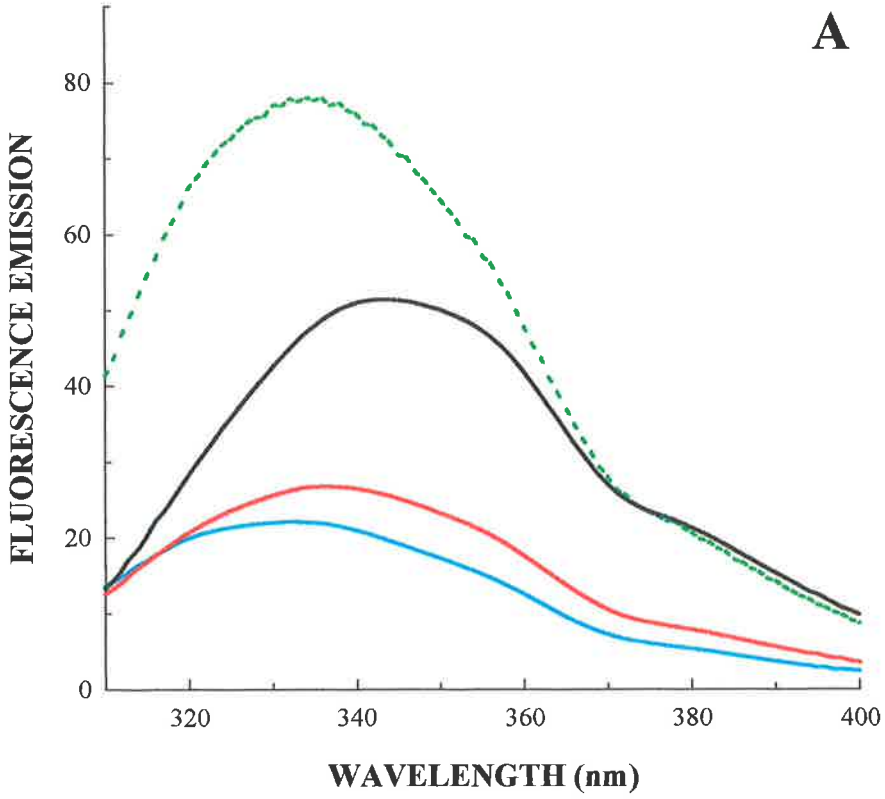

FIGURE 3.3 ACID-INDUCED DENATURATION OF pGH MONITORED BY FLUORESCENCE SPECTROSCOPY. Fluorescence emission spectra were recorded as described in 2.3.2.2. The protein concentration was 0.22 mg/ml.

A representative fluorescence emission spectra at :

pH 8.0 - urea —— pH 8.0 + urea —— pH 2.0 - urea - - - pH 2.0 + urea ——

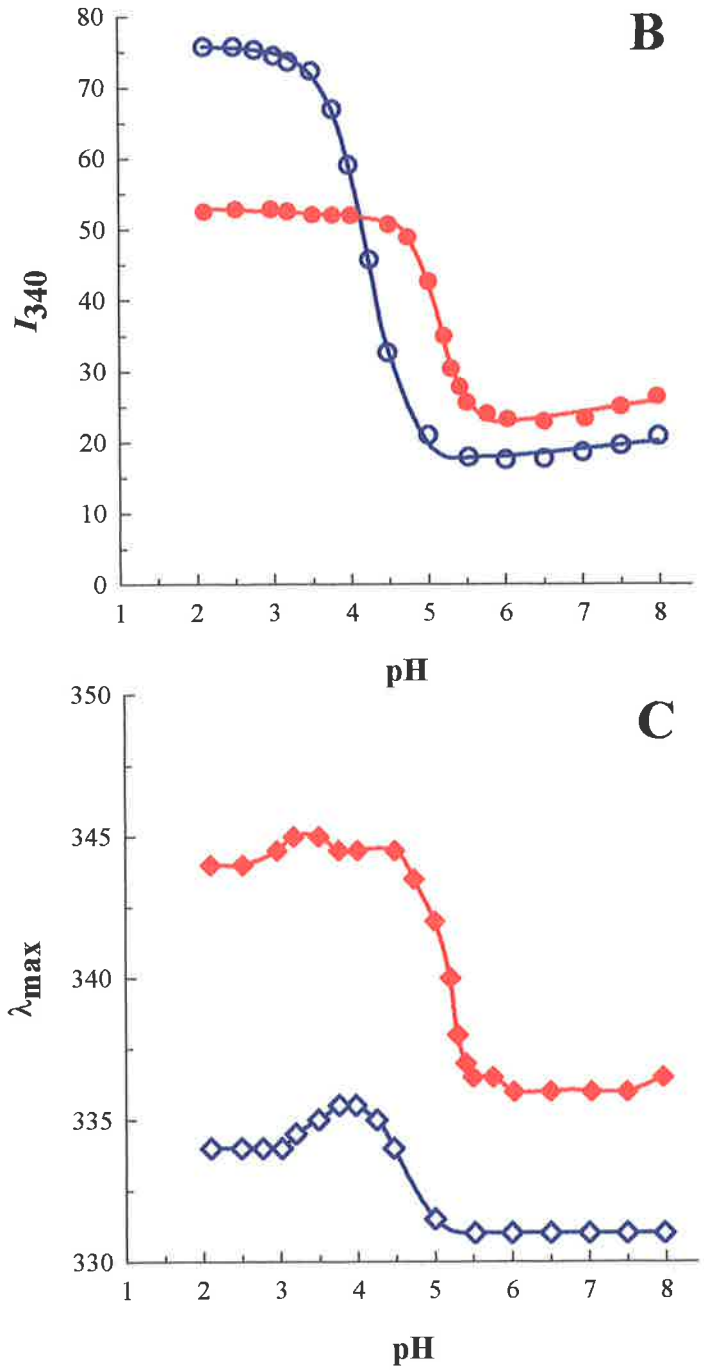

FIGURE 3.3 cont. ACID–INDUCED DENATURATION OF pGH MONITORED BY FLUORESCENCE SPECTROSCOPY. Fluorescence emission spectra were recorded as described in 2.3.2.2. The protein concentration was 0.22 mg/ml. The data are representative of n = 3 experiments.

B effect of acid on the relative fluorescence intensity (I_{340}) :

- urea ○ + urea ●

The solid lines are the calculated curves determined from non-linear regression analysis of the raw data, using Equation 2, as described in 2.3.2.1.

C effect of acid on the maximum emission wavelength (λ_{max}) :

- urea ◇— + urea —◆—

MEASUREMENT	PROTEIN CONCENTRATION (mg/ml)	MIDPOINT[a] MINUS 4 M UREA	MIDPOINT[a] PLUS 4 M UREA	NUMBER OF EXPERIMENTS (*n*)
I_{340}	0.05	4.10 ± 0.02	4.93 ± 0.04	2
I_{340}	0.22	4.08 ± 0.06	5.16 ± 0.06	3
I_{340}	0.50	4.10 ± 0.05	5.02 ± 0.03	2
ε_{290}	0.22	3.59 ± 0.03	5.11 ± 0.04	3
θ_{285}	0.22	3.94 ± 0.03	5.42 ± 0.08	1
θ_{300}	0.22	*nt*	5.24 ± 0.03	1
θ_{222}	0.22	3.89 ± 0.04	5.18 ± 0.05	1

TABLE 3.1 MIDPOINTS OF THE ACID–INDUCED TRANSITIONS OF pGH, IN THE ABSENCE AND PRESENCE OF 4 M UREA, MEASURED BY DIFFERENT SPECTROSCOPIC TECHNIQUES. [a] Data fitted by nonlinear regression using the equation described by Oliveberg *et al.*, (1994) for I_{340} or using a sigmoidal function (Bailey & Ollis, 1986). Errors represent the standard error (Cleland, 1967) returned from the nonlinear regression fit (n = 1), the range of values (n = 2), or the standard error of the mean value (n = 3).
nt = no transition

The addition of 4 M urea at pH 8.0 resulted in a red shift in the λ_{max} from 331 ± 1.0 nm to 336 ± 1.0 nm (Figure 3.3 C), and was accompanied by a 15% increase in I_{340} (Figure 3.3 B). In the presence of 4 M urea, a 2.5-fold increase in I_{340} with a concomitant increase in the λ_{max} from 336 ± 1.0 nm at pH 8.0 to 344 ± 1.0 nm at pH 2.0 was observed (Figure 3.3 B). The transition followed a smooth sigmoidal curve but was shifted to a more alkaline pH, with an apparent midpoint at pH 5.16 (Table 3.1).

The reversibility of the acid–induced denaturation of pGH was determined using fluorescence spectroscopy. Solutions of pGH at pH 8.0 and pH 2.0 were titrated with 1 M HCl and 1 M NaOH respectively, to give buffered solutions at the indicated pH (Figure 3.4). Nearly identical transitions were obtained, indicating that the acid-induced denaturation of pGH is readily reversible.

The effect of protein concentration on the acid-induced denaturation was examined at 0.05, 0.22 and 0.5 mg/ml pGH in the absence and presence of 4 M urea (Figures 3.5 A & 3.5 B). Assuming a two-state mechanism, the transitions observed at each protein concentration were compared by plotting the apparent fraction of the unfolded protein, F_{app}, versus pH, where:

$$\mathbf{F_{app} = (I_{obs} - I_{nat}) / (I_{unf} - I_{nat})}$$

I_{obs} was the observed I_{340} at a given pH and I_{nat} and I_{unf} were the observed values for the native and unfolded forms, respectively, extrapolated to each point in the transition zone (Pace, 1986). Least-squares analysis of the experimental data was used to determine I_{nat} and I_{unf} in the pre- and post-transition zones (Pace, 1986). Transitions in the absence of urea were almost superimposable with midpoints centred at pH 4.10 (Table 3.1). In the

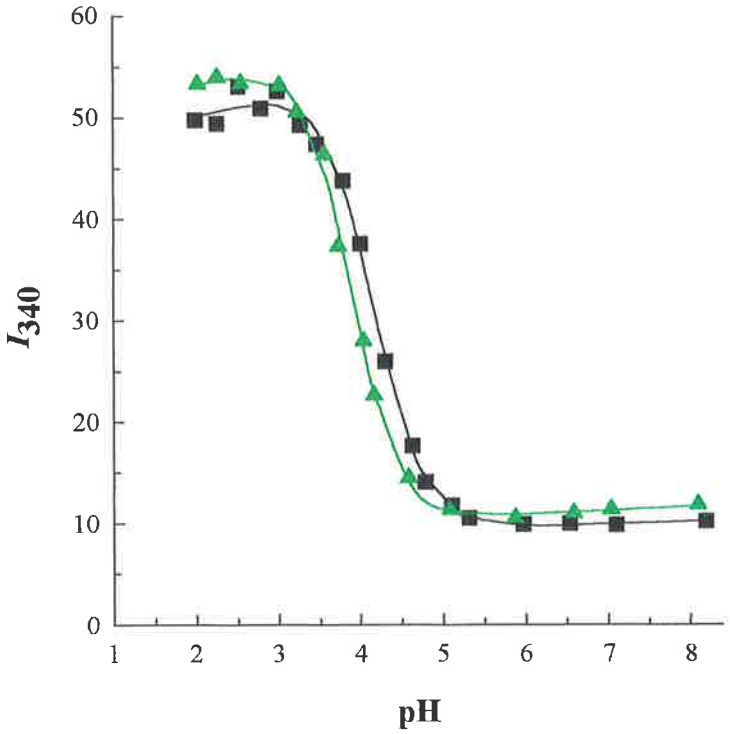

FIGURE 3.4 REVERSIBILTY OF THE ACID-INDUCED DENATURATION OF pGH. Lyophilised pGH was dissolved at pH 2.0 and titrated to pH 8.0 with 1 M NaOH. In parallel, lyophilised pGH was dissolved at pH 8.0 and titrated to pH 2.0 with 1 M HCl. Fluorescence emission spectra were recorded as described in 2.3.2.2. The protein concentration in each case was 0.22 mg/ml. The solid lines are the calculated curves determined from non-linear regression analysis of the raw data, using Equation 2, as described in 2.3.2.1.

Titrations initiated from: pH 2.0 to pH 8.0 ■ pH 8.0 to pH 2.0 ▲

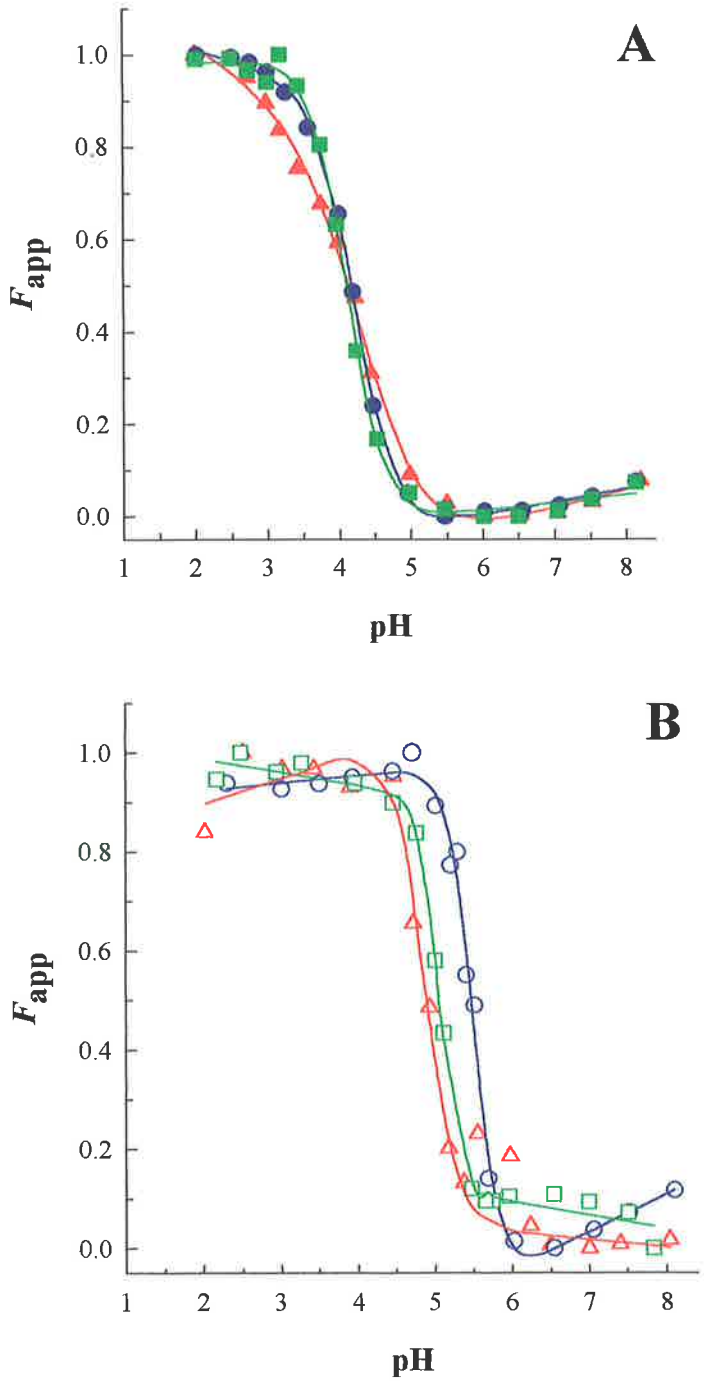

FIGURE 3.5 THE EFFECT OF PROTEIN CONCENTRATION ON THE ACID INDUCED DENATURATION OF pGH. The change in relative fluorescence intensity at 340 nm (I_{340}), in the presence and absence of 4 M urea for each protein concentration, was compared by plotting the apparent fraction of unfolded protein, F_{app}, as a function of pH, as described in 3.2.1. The solid lines are the calculated curves determined from non-linear regression analysis of the raw data, using Equation 2, as described in 2.3.2.1.

A in the absence of 4 M urea :

0.05 mg/ml ▲ 0.22 mg/ml ● 0.5 mg/ml ■

B in the presence of 4 M urea :

0.05 mg/ml △ 0.22 mg/ml ○ 0.5 mg/ml □

presence of 4 M urea the transition midpoints were centred at approximately pH 5.2 (Table 3.1) and the transitions were sharper (Figure 3.5 B).

3.2.2 UV Absorbance Spectroscopy

3.2.2.1 Zero-Order Absorbance Spectroscopy

The ultraviolet absorption spectrum of a protein can be described as a complete envelope comprised of overlapping absorption bands of the individual chromophores, cystine, phenylalanine, tyrosine and tryptophan. A change in the absorption spectrum can therefore reflect a change in the environment surrounding each of the individual chromophores.

The zero-order spectra of pGH at pH 8.0 in the absence and presence of 4 M urea display an absorption maximum at 278 ± 0.2 nm (Figure 3.6 A). The prominent shoulder centred near 290 nm is due mainly to the absorption of the single tryptophan residue buried within the hydrophobic core (Bewley and Li, 1984). The three ripples between 255 nm and 270 nm are due to phenylalanine absorption. In the absence of urea, acidification from pH 8.0 to pH 2.0 produced a general blue shift in the entire spectrum, with the absorption maximum shifted from 278 ± 0.2 nm at pH 8.0 to 276.5 ± 0.2 nm at pH 2.0 (Figure. 3.6 A). A similar blue shift in the absorption maximum to 276.2 ± 0.2 nm at pH 2.0 was observed in the presence of urea. In addition, the absorption spectrum was red shifted at wavelengths above approximately 293 nm (Figure 3.6 A).

Acidification of pGH with or without 4 M urea also produced a considerable loss in extinction (hypochromicity) near 290 nm. This can be more clearly seen in a plot of the molar extinction coefficient at 290 nm (ε_{290}) as a function of pH (Figure 3.6 B). Acidification resulted in a decrease in ε_{290} of approximately 2100 $M^{-1}cm^{-1}$ and 2500

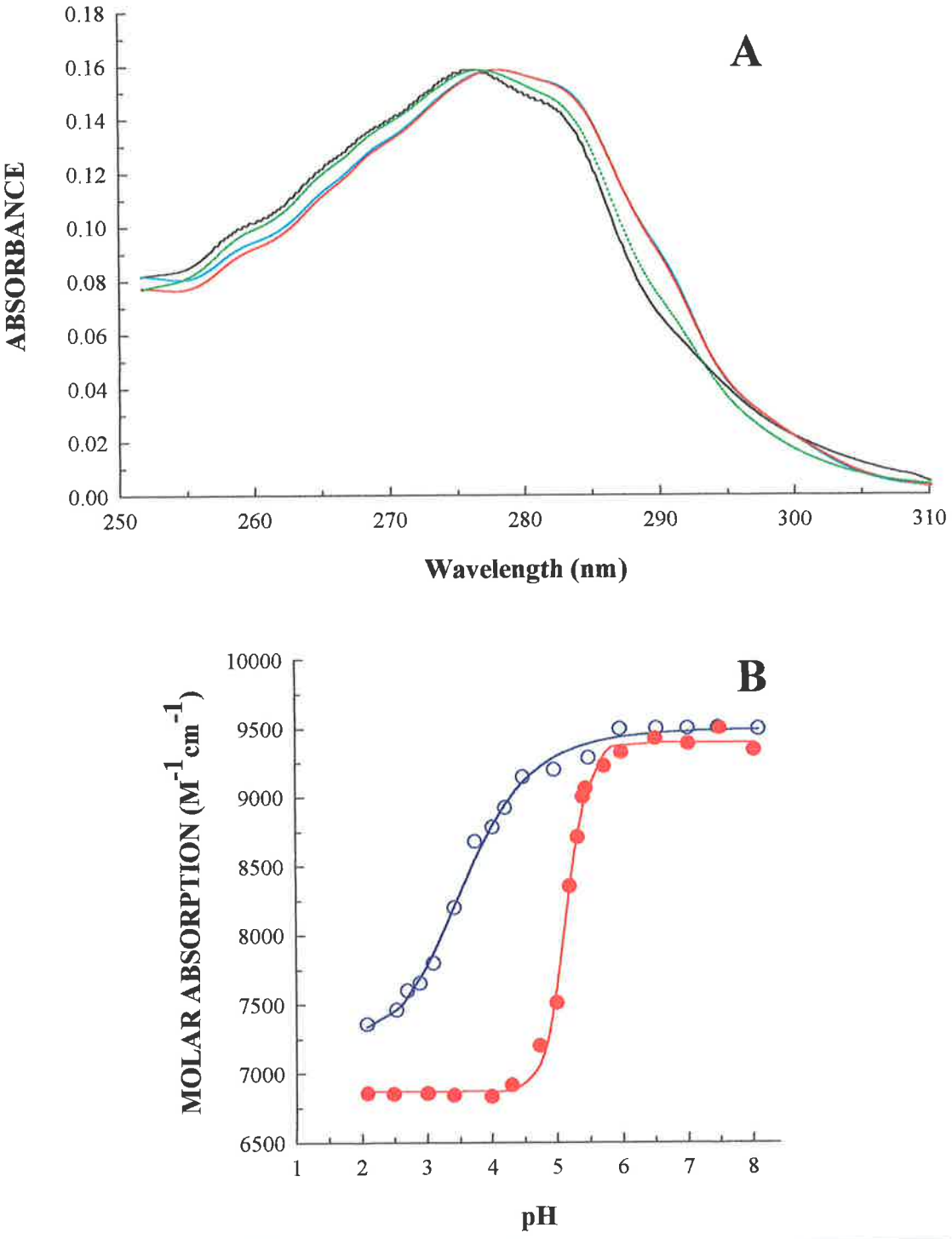

FIGURE 3.6 ACID-INDUCED DENATURATION OF pGH MONITORED BY UV-ABSORBANCE. UV-absorbance spectra were recorded as described in 2.3.2.3. The protein concentration was 0.22 mg/ml. The data are representative of n = 3 experiments.

A UV-absorbance spectra at :

pH 8.0 - urea —— pH 8.0 + urea —— pH 2.0 - urea ····· pH 2.0 + urea ——

B effect of acid on the absorbance at 290 nm (ε_{290}) :

- urea ○ + urea ●

The solid lines are the calculated curves determined from non-linear regression analysis of the raw data, using Equation 1, as described in 2.3.2.1

$M^{-1}cm^{-1}$, with midpoints at pH 3.59 and pH 5.11 (Table 3.1), in the absence and presence of 4 M urea, respectively. Interestingly, in the absence of 4 M urea the UV absorbance transition midpoint was not coincident with the midpoint obtained for the intrinsic fluorescence detected transition (Table 3.1). In contrast, in the presence of 4 M urea, the transition midpoints detected by UV absorbance and fluorescence spectroscopy were similar.

3.2.2.2 Second-Derivative Absorption Spectroscopy

Contributions from the aromatic chromophores in a protein overlap significantly in zero-order absorption spectra. Resolution can be improved and the position of individual amino acids more accurately located if the derivative of absorbance with respect to wavelength is calculated (Havel, 1996). Analysis of the second-order derivative band positions and band intensities can provide details about the microenvironment surrounding the aromatic residues, for example polarity.

An overlay of the zero-order absorbance spectrum and the calculated second derivative of the absorption spectrum for pGH at pH 8.0 is shown in Figure 3.7. This figure shows the correspondence of the minima in the second derivative of the absorption spectrum with the peaks and shoulders in the zero-order absorption spectrum. The wavelength minima were assigned based on the previous characterisation of recombinant pGH (Bastiras, 1992) and are listed in Table 3.2. The minima in the region 250 nm to 270 nm are due to the phenylalanine [0-0] transition and higher vibronic modes (Bewley and Li, 1984). Although the tyrosine and tryptophan absorption bands overlap, the minima at approximately 277 nm and 284 nm are in principle due to tyrosine and the minima at approximately 290 nm and 300 nm are due to tryptophan (Bewley and Li, 1984).

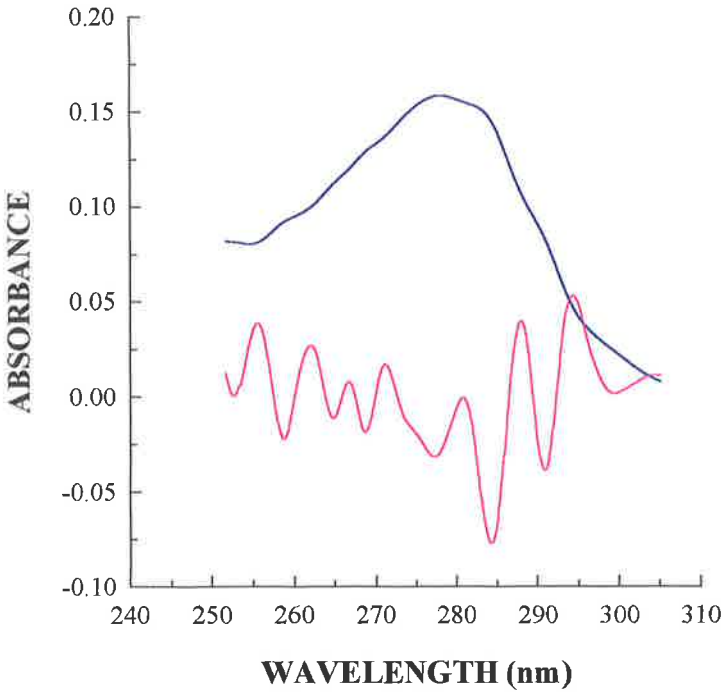

FIGURE 3.7 UV-ABSORBANCE SPECTRUM AND THE COMPUTER DERIVED SECOND DERIVATIVE SPECTRUM OF pGH AT pH 8.0 IN THE ABSENCE OF UREA. The second derivative spectra were derived from the UV-absorbance spectra using an in-house computer program based on the method by Savitzky and Golay (1964). The protein concentration was 0.22 mg/ml. The absorbance spectrum is represented by the blue line and the second derivative by the pink line.

The calculated second-order derivative of the zero-order absorption spectra for pGH at pH 8.0 and pH 2.0 in the absence and presence of 4 M urea are shown in Figure 3.8, and the wavelength minima are listed in Table 3.2.

The wavelength minima attributed to the phenylalanine chromophores in the 250-270 nm region of the spectrum (Bewley and Li, 1984) did not change in the four conditions examined, indicating no net change in the average environment of these chromophores.

The blue-shift seen in the zero-order absorption maximum on acidification (Figure 3.6 A), is also observed in the second derivative spectra minima in the 276-278 nm region (Figure 3.8; Table 3.2). This band is attributed to one of the higher vibrational modes of the Tyr^1L_b transition. There was no significant change in the wavelength of the 284 nm minimum, attributed to the Tyr^1L_b [0-0] transition (Bewley and Li, 1984).

Despite the overlap of tyrosine and tryptophan absorption bands, spectral changes in the 290–295 nm region are principally due to tryptophan. In the second-derivative spectrum, the peak to trough difference at 290 and 295 nm is a measure of the polarity of the environment surrounding tryptophan. A large difference is indicative of a non-polar tryptophan environment. At pH 2.0 in the absence and presence of 4 M urea, the peak to trough distance is reduced. The decrease in intensity of the minima at 291 nm is accompanied by a red shift from 290.9 nm at pH 8.0 (± 4 M urea) to 291.5 nm (pH 2.0) and 292.6 nm (pH 2.0 + 4 M urea) (Figure 3.8). This band is attributed to the Trp^1L_b band (Figure 3.9) and the movement of this band is responsible for the red shift above 293 nm seen in the zero-order spectrum at pH 2.0 in the presence of 4 M urea.

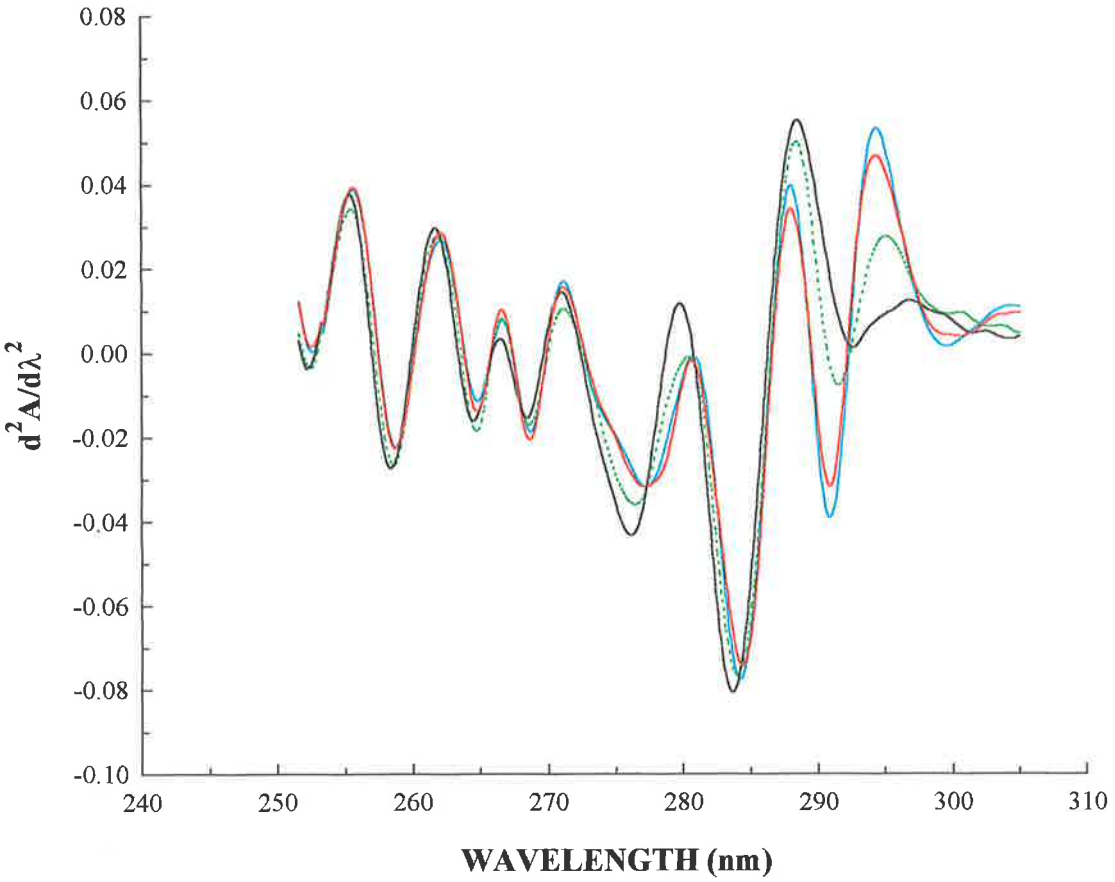

FIGURE 3.8 ACID–INDUCED DENATURATION OF pGH MONITORED BY SECOND DERIVATIVE SPECTROSCOPY. The second derivative spectra were derived from the UV absorbance spectra using an in-house computer program based on the method by Savitzky and Golay (1964). The protein concentration was 0.22 mg/ml.

pH 8 - urea —— pH 8 + urea —— pH 2 - urea ····· pH 2 + urea ——

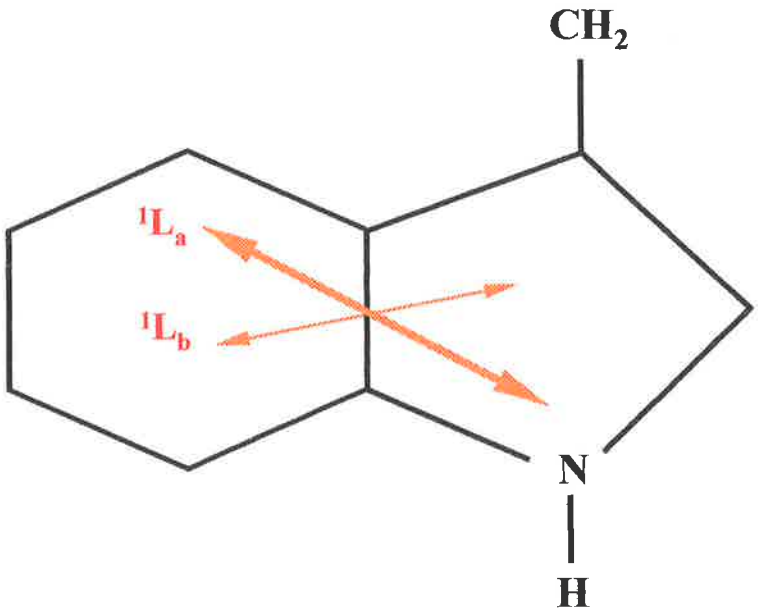

FIGURE 3.9 THE INDOLE CHROMOPHORE DEPICTING THE TRANSITION DIPOLE MOMENTS OF THE ^1L_a AND ^1L_b BANDS. The dipole moments are represented by ⟷

Adapted from Yamomoto and Tanaka, 1972

At pH 8.0, the inclusion of 4 M urea results in a decrease in intensity of the Trp^1L_a[0-0] band at 299.5 nm. In studies using hGH, Bewley and Li (1984) predicted that the extent of the red shift of this band compared to its [0-0] in water of 292 correlates with the strength and alignment of a hydrogen bond between the indole ring > NH of Trp86 and a carboxylate residue (Figure 3.9). However, for pGH at pH 2.0 with or without 4 M urea, the Trp^1L_a signal is difficult to identify possibly due to blue shifting into the intense positive band centred near 295 nm.

3.2.3 Circular Dichroism

3.2.3.1 Near-UV Circular Dichroism

Near-UV circular dichroism (CD) spectra can reflect the conformation and local environment of the aromatic and disulphide chromophores (Strickland, 1974). A decrease in the CD intensity is usually associated with a loss of tertiary structure or a localised unfolding of the protein in the vicinity of a particular aromatic group. Figure 3.10 A shows the near-UV CD spectra for pGH at pH 8.0 and pH 2.0 in the absence and presence of 4 M urea. Similar spectra were obtained at pH 8.0 (± 4 M urea), and are consistent with previous spectra for recombinant pGH produced at Bresagen Ltd. (Bastiras, 1992). The three negative bands at approximately 268 nm, 262 nm and 256 nm are due to the Phe^1L_b[0-0] transition and higher vibronic modes. Disulphide bonds also contribute to the negative dichroism in this region of the spectrum (Bewley and Li, 1970). The shoulder at approximately 278 nm is assigned to a higher vibronic mode of the Tyr[0-0] transition. The negative peak at 286 nm is comprised of the Tyr[0-0] transition and a higher vibronic mode of the Trp ^1L_b[0-0] transition. A small shoulder at 292 nm is possibly due to the Trp^1L_b[0-0] transition.

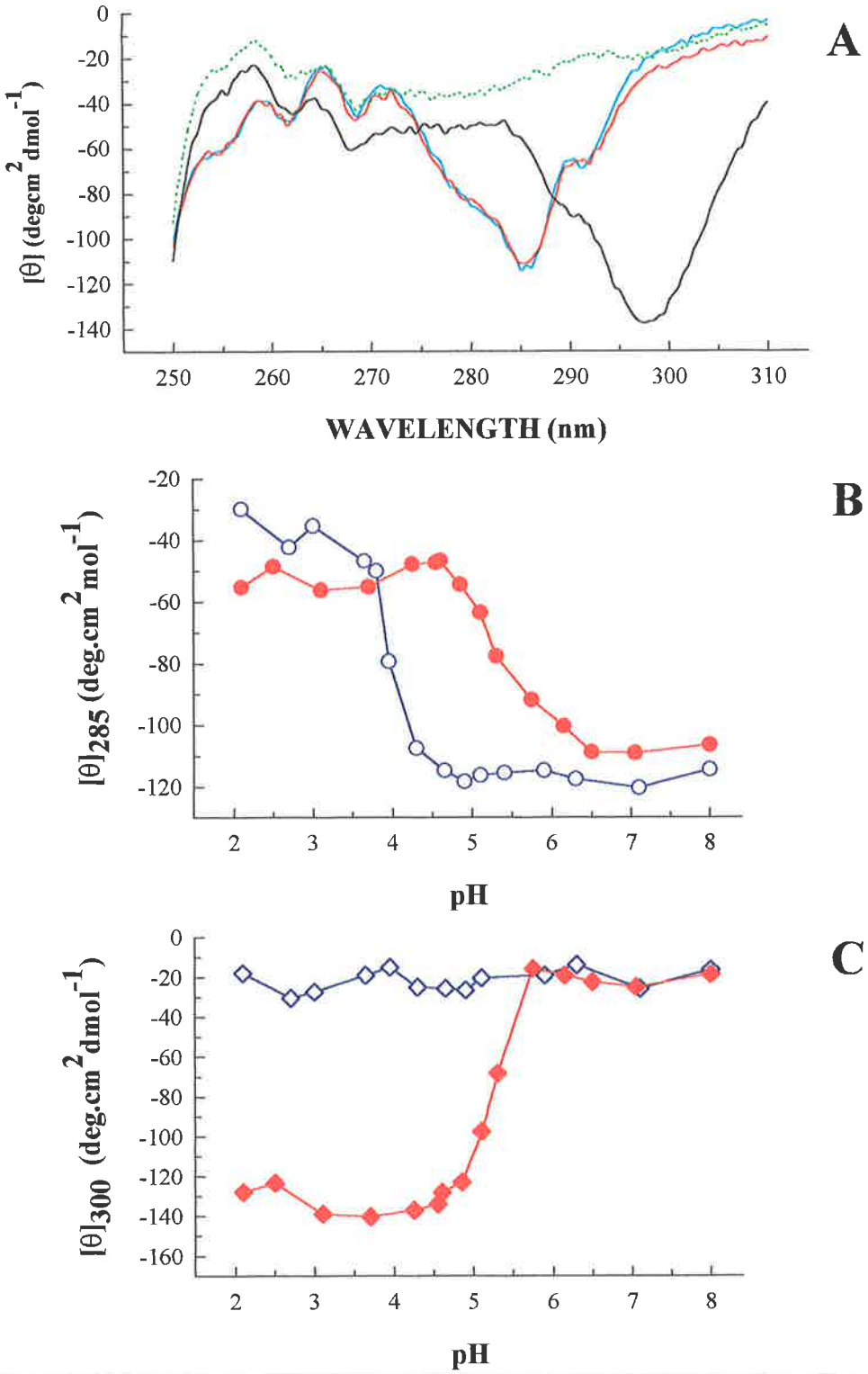

FIGURE 3.10 ACID-INDUCED DENATURATION OF pGH MONITORED BY NEAR-UV CIRCULAR DICHROISM. Near-UV CD spectra were recorded as described in 2.3.2.6. The protein concentration was 0.22 mg/ml in a 10 mm pathlength cuvette. The mean residue ellipticity, [θ], has the units deg.cm^2.dmol^{-1}.

A near-UV CD spectra at:

pH 8 - urea ——— pH 8 + urea ——— pH 2 - urea ····· pH 2 + urea ———

B the change in mean residue ellipticity at 285 nm ($[\theta]_{285}$):

- urea —○— + urea —●—

C the change in mean residue ellipticity at 300 nm ($[\theta]_{300}$):

- urea —◇— + urea —◆—

At pH 2.0 in the absence and presence of 4 M urea, the three phenylanine bands are still clearly visible but the majority of disulphide bond associated optical signal between 250 and 260 nm has been lost (Figure 3.10 A). The majority of tyrosine-attributed signal at 286 nm has also been lost. A plot of the mean residue ellipticity ($[\theta]_{MRW}$) at 285 nm, θ_{285}, as a function of pH (± 4 M urea) is shown (Figure 3.10 B). Transition midpoints were centred at pH 3.94 and pH 5.42 in the absence and presence of 4 M urea, respectively.

At pH 2.0 in the presence of 4 M urea, there is an intense negative absorption band at approximately 298 nm, whereas, in the absence of urea, this band is weak. Figure 3.10 C shows the effect of pH on the $[\theta]_{MRW}$ at 300 nm, θ_{300}, in the presence and absence of 4 M urea. In the presence of 4 M urea, a smooth sigmoidal transition is seen with a transition midpoint centred at pH 5.24 (Figure 3.10 C). There was no significant change in θ_{300} in the absence of urea.

3.2.3.2 Far-UV Circular Dichroism

Far-UV CD was used to monitor changes in the secondary structure of pGH with acidification. The far-UV CD spectra of pGH at pH 8.0 in the absence and presence of 4 M urea are shown in Figure 3.11 A. At pH 8.0, the spectra display minima at 209 nm and 221 nm, characteristic of the presence of α-helix. The addition of urea at pH 8.0 has caused a slight increase in negative ellipticity at both minima.

At pH 2.0, the two minima at 209 nm and 221 nm are still clearly present but their intensity has decreased. The loss of secondary structure (α-helix), with acidification in the absence and presence of 4 M urea, was followed by measuring $[\theta_{MRW}]$ at 222 nm, θ_{222} (Figure 3.11 B). Linear extrapolation of the post-transition region revealed an approximately 15% and

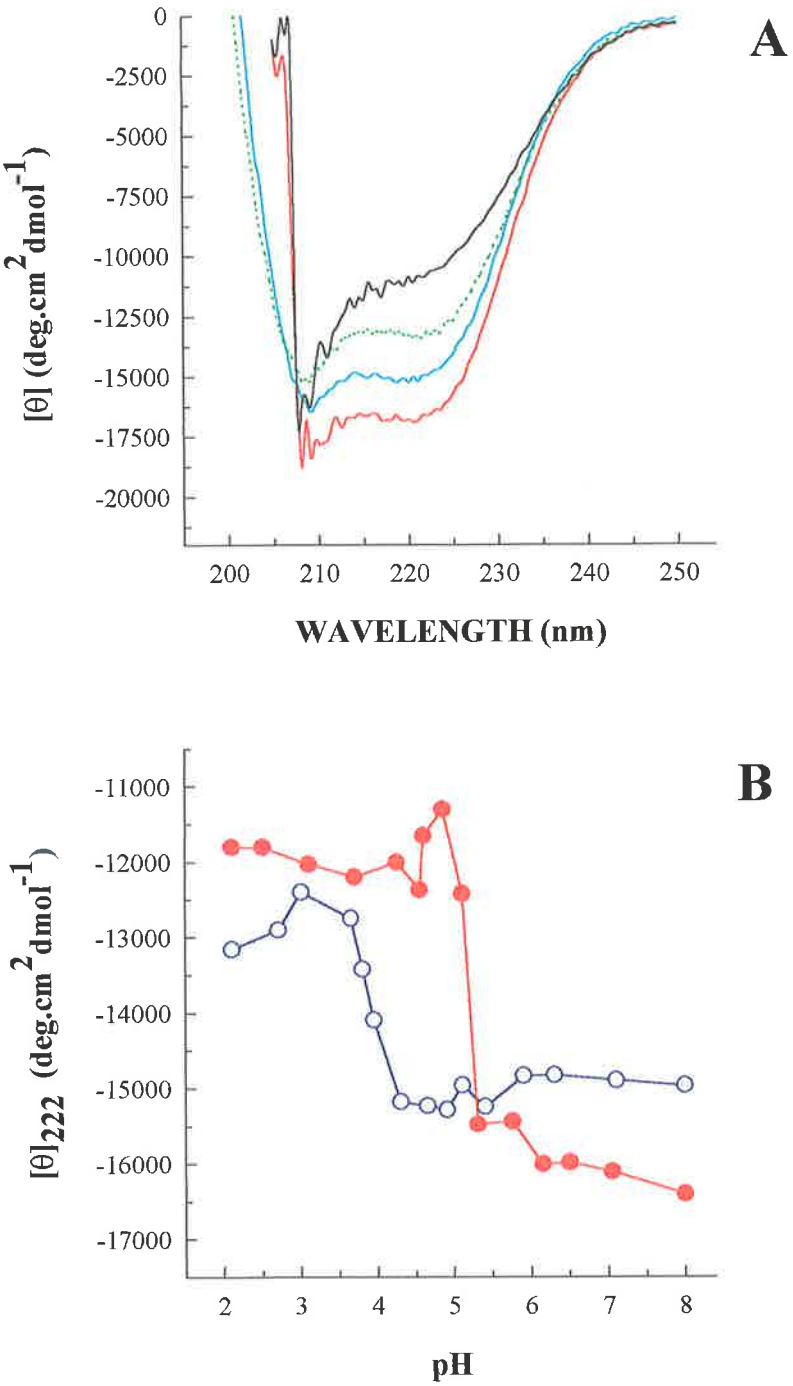

FIGURE 3.11 ACID-INDUCED DENATURATION OF pGH MONITORED BY FAR-UV CIRCULAR DICHROISM. Far-UV CD spectra were recorded as described in 2.3.2.6. The protein concentration was 0.22 mg/ml in a 1 mm path length cuvette. The mean residue ellipticity, [θ], has the units deg.cm^2.dmol^{-1}.

A far-UV CD spectra at:

pH 8 - urea ——— pH 8 + urea ——— pH 2 - urea ····· pH 2 + urea ———

B the change in mean residue ellipticity at 222 nm ($[\theta]_{222\ nm}$):

- urea —○— + urea —●—

ABSORPTION BAND	[a] pGH	pH 8.0		pH 2.0	
		minus 4 M urea	plus 4 M urea	minus 4 M urea	plus 4 M urea
*Trp^1L_a	301.4(s)	–	301.40(s)	–	301.4(s)
Trp^1L_a	299.45	299.45	299.45	299.75	–
Trp^1L_a	297.5(ws)	297.50(ws)	297.50	–	–
***Trp^1L_b**	**290.90**	**290.90**	**290.90**	**291.50**	**292.55**
*Tyr^1L_b	284.45	284.30	284.30	284.00	283.70
Tyr^1L_b	**277.70**	**277.25**	**277.00**	**276.50**	**276.20**
Trp^1L_b	273.95	274.00	274.00	–	–
*Phe^1L_b	269.15	268.70	268.70	268.55	268.50
Phe^1L_b	265.10	264.80	264.80	264.80	264.50
Phe^1L_b	258.80	258.65	258.65	258.60	258.35
Phe^1L_b	252.80	252.50	252.65	252.50	252.20

TABLE 3.2 SECOND DERIVATIVE ABSORPTION BANDS OF pGH. The wavelength positions of the second derivative minima as shown in Figure 3.8. [a] Wavelength positions assigned to pGH in 25 mM sodium acetate, pH 9.1 (Bastiras, 1992). The absorption bands which exhibit the most significant change in their wavelength positions are highlighted in red. s, shoulder; ws, weak shoulder.

25% loss of secondary structure with transition midpoints at pH 3.89 and pH 5.18 in the absence and presence of 4 M urea, respectively.

3.2.4 ANS Fluorescence

The hydrophobic probe 1-anilinonapthalene-8-sulfonate (ANS), has proved to be a useful extrinsic fluorescence reagent to probe conformational changes in protein folding. In aqueous solvent ANS has minimal fluorescence intensity with a λ_{max} at approximately 552 nm. An increase in fluorescence emission intensity and blue shift in λ_{max} is characteristic of ANS in a highly non-polar environment, or bound to hydrophobic surfaces.

The emission spectra of ANS with pGH at pH 8.0 and pH 2.0 in the absence and presence of 4 M urea are shown in Figure 3.12. At pH 8.0 (± 4 M urea) the λ_{max} of ANS has blue shifted from 552 nm to approximately 465 nm. At pH 2.0 without 4 M urea, there was an approximately 35-fold increase in fluorescence intensity. In the presence of 4 M urea, only an 8-fold increase in fluorescence was seen. A less intense band at approximately 500 nm was also seen in the spectra at pH 2.0 with or without 4 M urea. This less intense band is believed to be caused by a fluorescence artifact known as the "Woods Anomaly", which had not been completely corrected for by the software supplied with the Aminco Bowman fluorescence spectrometer.

3.2.5 Size-Exclusion Chromatography

Size-exclusion chromatography was used to examine the effect of acidification on the hydrodynamic radius (compactness) of pGH. The elution profiles of pGH in the presence of 4 M urea, at pH 8.0 and pH 2.0 are shown in Figure 3.13. In the absence of urea, no protein was recovered from the Superose 12 column between pH 5.0 and pH 2.0. Even in

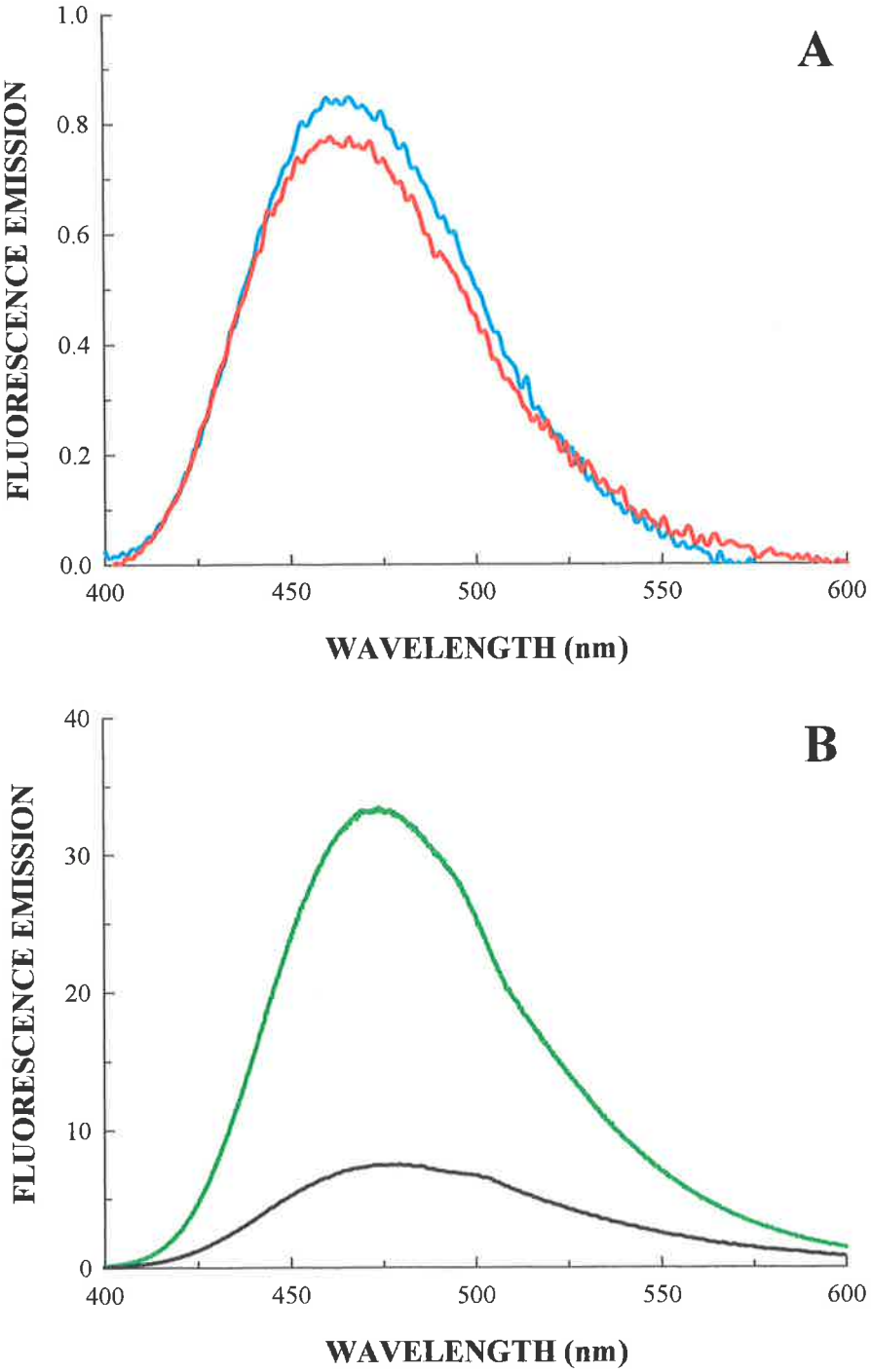

FIGURE 3.12 FLUORESCENCE EMISSION OF 1-ANILINONAPTHALENE-8-SULFONATE (ANS). Fluorescence emission spectra were recorded as described in 2.3.2.8. The ANS concentration was 100 μM and the protein concentration was 0.05 mg/ml (~ 2.5 μM).

A pH 8 - urea —— pH 8 + urea ——

B pH 2 - urea —— pH 2 + urea ——

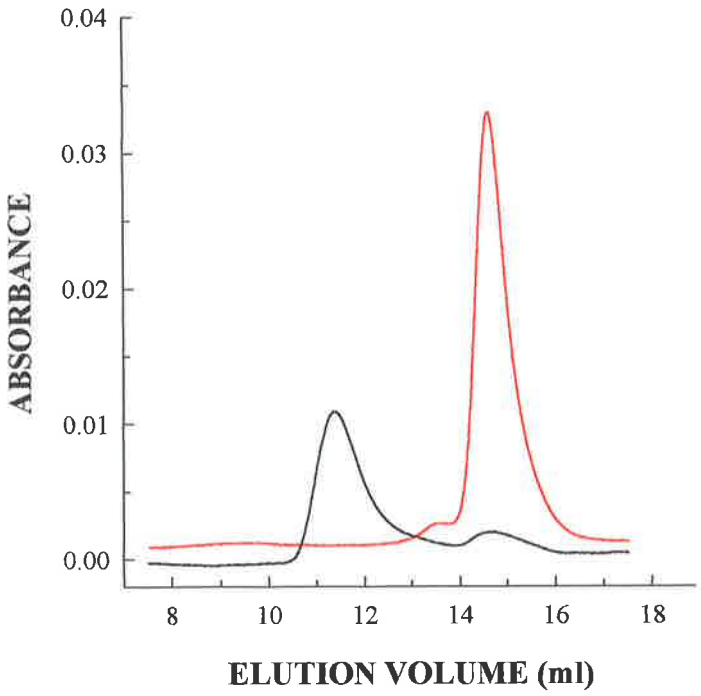

FIGURE 3.13 THE EFFECT OF ACIDIFICATION ON THE ELUTION VOLUME OF pGH. Size exclusion chromatography was performed as described in 2.3.2.5. The protein concentration was 0.22 mg/ml. Protein elution was followed by the absorbance at 280 nm. Elution profiles of pGH in the presence of 4 M urea at:

pH 8.0 ——— pH 2.0 ———

the presence of 4 M urea, no protein was recovered from the Superose 12 column at pH 5.0 and pH 4.0. At pH 8.0, a single peak with a radius of 18 Å, consistent with pGH in the folded state (Bastiras and Wallace, 1992) is observed (Figure 3.13). At pH 2.0 the majority of the protein elutes earlier, with an increase in hydrodynamic radius to 47 Å. The elution volume and increase in size at pH 2.0 are very close to that previously seen for the Gdn–HCl-induced associated form of pGH (Bastiras and Wallace, 1992) and bGH (Brems *et al.*, 1985). The associated species for both pGH and bGH is populated above 10 μM (0.22 mg/ml) in partially denaturing concentrations of Gdn–HCl. At a decreased protein concentration of 4 μM (0.1 mg/ml), the elution profile of pGH at pH 2.0 was similar to that at 10 μM (data not shown). The second, smaller peak at pH 2.0 with a radius comparable to that of the folded state of pGH at pH 8.0, may be that of the acid-denatured monomer. Although size-exclusion chromatography confirms the presence of an associated state at pH 2.0 in 4 M urea, the type of species at pH 2.0 in the absence of urea cannot be ascertained.

3.2.6 Sedimentation Equilibrium

The ability of pGH to self-associate in solution at pH 8.0 and 2.0 in the absence and presence of 4 M urea was investigated in a quantitative manner, using the thermodynamically rigorous technique of sedimentation equilibrium in the analytical ultracentrifuge. Figure 3.14 shows the apparent weight-average molecular weight ($M_{w,app}$) distributions for pGH at sedimentation equilibrium at pH 8.0 and pH 2.0 in the absence and presence of 4 M urea. Self-association takes place under all conditions and is strongly promoted by the drop in pH, and by the absence of urea at either pH. Figure 3.15 shows a typical plot of the Omega function versus radial concentration of pGH at sedimentation equilibrium for four different loading concentrations of pGH. The overlap of the data

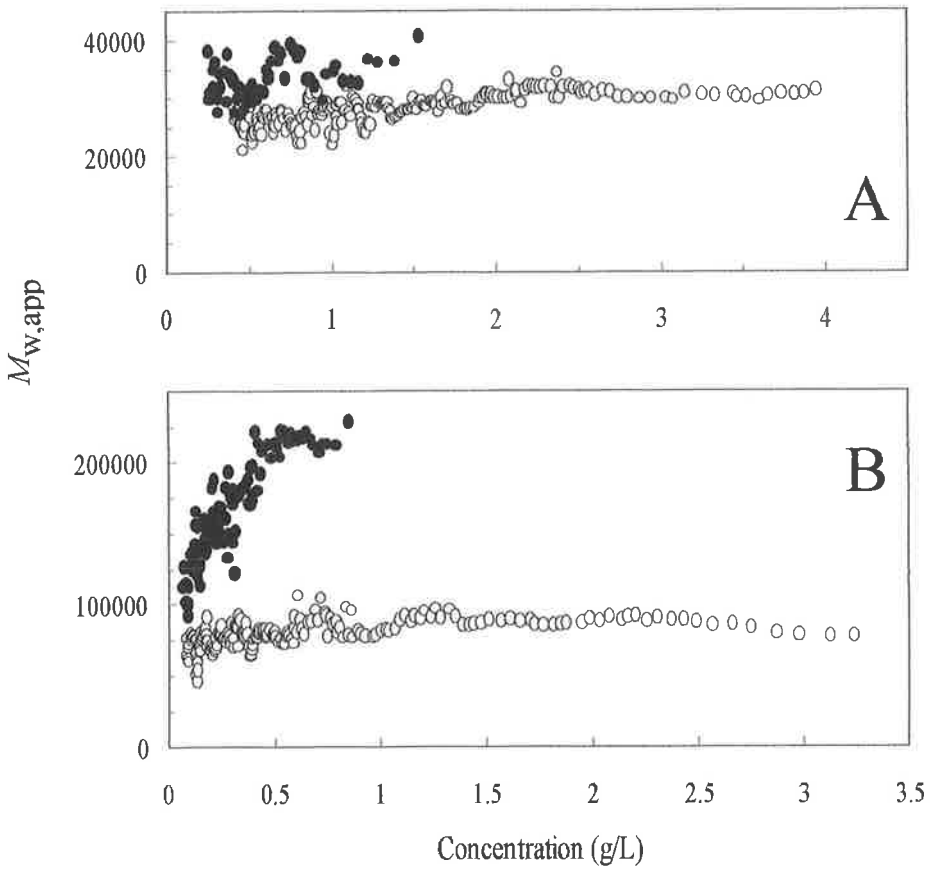

FIGURE 3.14 SELF-ASSOCIATION OF pGH AS MEASURED BY SEDIMENTATION EQUILIBRIUM IN THE ANALYTICAL ULTRACENTRIFUGE. Apparent weight-average molecular weight values ($M_{w,app}$) were calculated from absorbance values measured from the equilibrium distribution of protein in the ultracentrifuge cell. Data obtained at pH 8.0 (panel A) and pH 2.0 (panel B) in the absence (●) and presence (O) of 4 M urea.

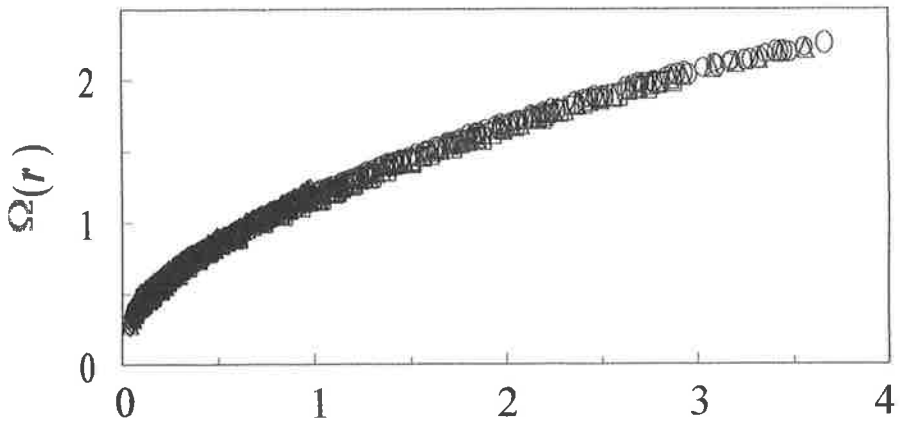

FIGURE 3.15 OMEGA FUNCTION VERSUS RADIAL POSITION OF pGH AT SEDIMENTATION EQUILIBRIUM. Four different loading concentrations of pGH (✧, 0.5 g/L; ○, 1 g/L; Δ, 1.5 g/L; □, 2 g/L) at pH 2 + 4 M urea were centrifuged at 15,000 rpm to equilibrium. The absorbance values measured from the equilibrium distribution of protein were converted to Omega values using a reference concentration [$c(r_F)$] of 0.7 g/L and a molecular weight of the protomer of 43,720 (equivalent to the dimer of pGH).

within the common concentration range indicated that the system was homogenous, showing that all pGH molecules were able to participate in the self-association and no irreversible aggregates were formed. Self-association models were fitted to the Omega plots and returned estimates of the thermodynamic parameters; the molar equilibrium constant(s), *K*, and the second virial coefficient, *B*, a measure of the nonideality of the solute (Figure 3.16, Table 3.3). Models, which appropriately described the data resulted in a random distribution of residuals (Figure 3.16) as determined by a runs test at the 5% level.

At pH 8.0 in the presence of 4 M urea, a monomer–dimer model adequately described the data over an extended concentration range (0.4–4 g/L) and the self-association, as judged by the value of *K* was very weak (Table 3.3). The returned value of *B* was $4.3 \pm 0.6 \times 10^{-7}$ L mol g^{-2}. Based on the estimated charge of pGH and a stokes radius of 2.2 nm (Ribela and Bartolini, 1988), a theoretical value of 4.5×10^{-7} L mol g^{-2} was calculated (Morris and Ralston, 1985; Johnson and Yphantis, 1978).

At pH 8.0 in the absence of urea, the Omega plot was well fitted by a monomer-dimer model but returned a negative (and therefore physically meaningless) value of *B* (data not shown). A negative value of *B* indicates that the self-association model underestimates the number and/or size of the oligomers that are present at significant concentration. On the other hand, the 'indefinite' SEK I model, in which a single value of *K* describes the sequential addition of monomers without limit (2.3.2.8) returned a value of *B* an order of magnitude larger than the theoretical value. When the value of *B* was fixed at the theoretical value, both the monomer–dimer–trimer and monomer–dimer–tetramer fit the data equally well with the value of K for the monomer-dimer step approximately five times

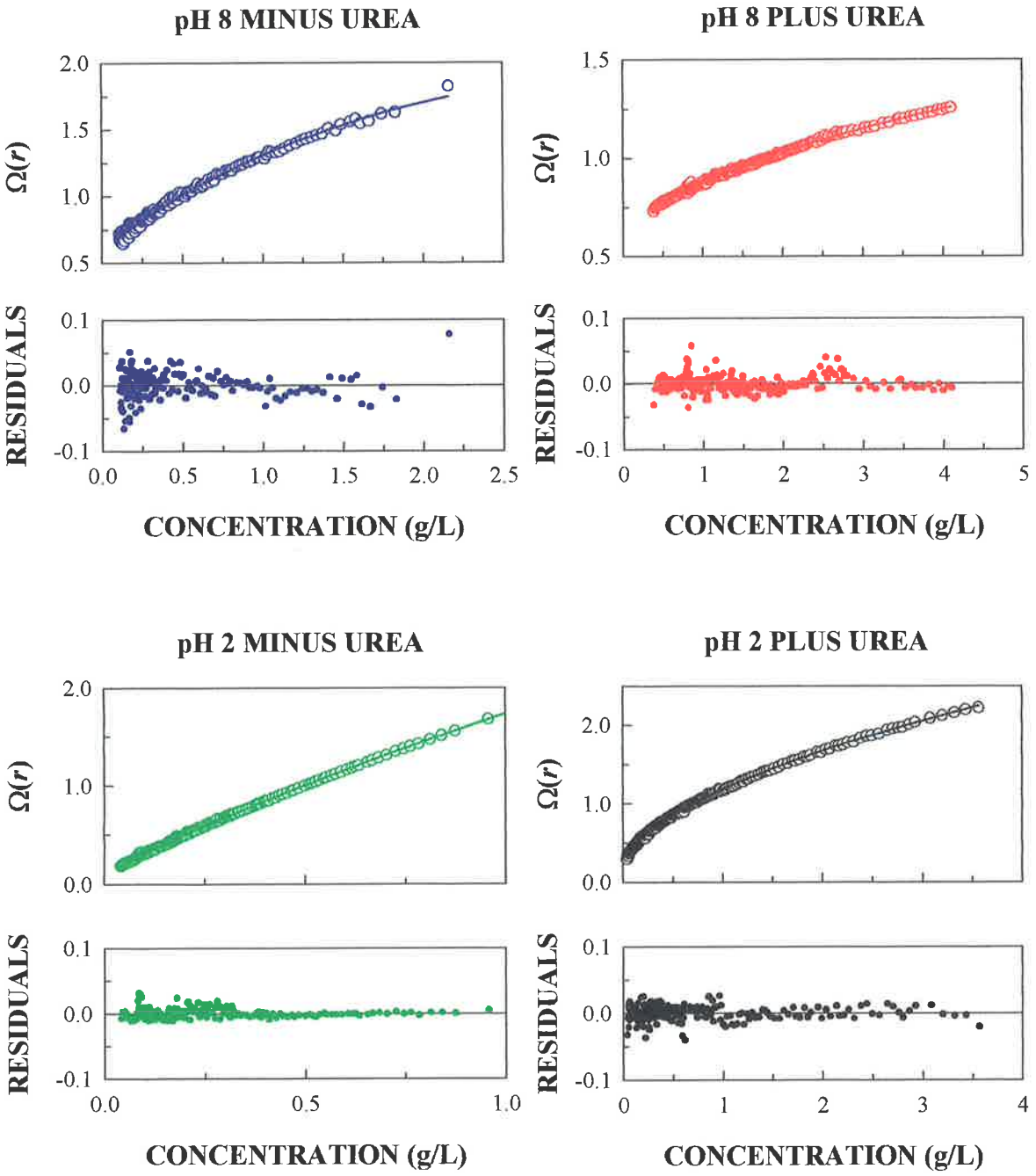

FIGURE 3.16 ANALYSIS OF SEDIMENTATION EQUILIBRIUM DATA OF pGH USING THE OMEGA FUNCTION. Four different loading concentrations of pGH (0.5 g/L, 1 g/L, 1.5 g/L and 2 g/L) at pH 8 and pH 2 in the absence and presence of 4 M urea were centrifuged to equilibrium. The absorbance values measured from the equilibrium distribution of protein were converted to Omega values using a reference concentration [$c(r_F)$] of 0.7 g/L and the molecular weight of the protomer (2.3.2.8). The data (upper panel of each set; open circles) was fitted (solid line) with a model best describing the self-association as determined by the random distribution of residuals (lower panel of each set; closed symbols).

	MODEL	K (M^{-1}) x 10^{-5}	B (L mol g^{-2}) x 10^{-7}
pH 8.0	MONOMER-DIMER-TETRAMER[a]	0.290 ± 0.03 (K_{12}) 0.025 ± 0.06 (K_{24})	4.5[c]
pH 8.0 + 4 M urea	MONOMER-DIMER	0.056 ± 0.001	4.3 ± 0.6
pH 2.0	DIMER, TETRAMER, HEXAMER,...	7.5 ± 0.02	22.3 ± 1.6
pH 2.0 + 4 M urea	DIMER-TETRAMER-OCTAMER[b]	7.3 ± 0.6 (K_{24}) 0.085 ± 0.09 (K_{48})	6.2 ± 1.1

TABLE 3.3 SEDIMENTATION EQUILIBRIUM RESULTS FOR pGH UNDER VARIOUS SOLUTION CONDITIONS. Plots of $\Omega(r)$ versus $c(r)$ were fitted with self-association models using nonlinear regression techniques. Returned values of the equilibrium constants, K, and second virial coefficient, B, are shown ± standard error.

[a] A monomer-dimer-trimer model fit the data equally well on the basis of sums of squares of the residuals and random distribution of residuals as judged by the runs test.

[b] A dimer-tetramer-hexamer model fit the data equally well on the basis of sums of squares of the residuals and random distribution of residuals as judged by the runs test.

[c] Parameter value fixed during nonlinear regression. A theoretical value for B, B_T, was calculated from the size and shape of the solute (B_E) plus a contribution from the net charge on the solute (B_C) (Morris & Ralston, 1985; Johnson & Yphantis, 1978). K_{12}, monomer-dimer equilibrium constant; K_{24}, dimer-tetramer equilibrium constant; K_{48}, tetramer-octamer equilibrium constant.

larger than that obtained in the presence of urea (Table 3.3). Thus, in the absence of urea both the strength and extent of self-association of pGH is increased. Other types of discrete self-association (e.g. monomer–trimer or monomer–tetramer) resulted in poor fits to the data as judged by the sums of squares of the residuals and a runs test performed on the distribution of the residuals.

At pH 2.0, self-association was strongly promoted (Figure 3.14), to the extent that significant concentrations of monomeric pGH could not be detected over the total concentration ranges observed. Note that the values of $M_{w,app}$ at very low concentration at pH 2.0, plus or minus urea, are larger than the monomer molecular weight of 21,860, indicating that the protomer for self-association was larger than the monomer. To confirm this, plots of the Omega function versus concentration were generated using the molecular weight of the monomer and small values (approximately 0.2 g/L) of the reference concentration, $c(r_F)$. Fits to these plots with various self-association models, using the monomer as the protomer, passed through or very close to the origin (data not shown). This showed that no detectable monomer was present at the reference concentration, and that the protomer for the self-association was the dimer or some larger species. Therefore, self-association models at pH 2.0 in which the protomer was taken to be the dimer were used.

At pH 2.0 in the absence of urea, the SEK I model (dimer, tetramer, hexamer…) fitted the data well. The returned value of K describing the sequential steps in the self-association was 1–3 orders of magnitude larger than values of K obtained at pH 8.0 plus or minus urea (Table 3.3). Extrapolation of the fit for this model to zero concentration confirmed that a

significant percentage (9%) of the protein at the reference concentration of 0.5 g/L was in the form of the dimer.

At pH 2.0 in the presence of 4 M urea, two discrete models, dimer–tetramer–hexamer and dimer–tetramer–octamer, fit the data equally well. As at pH 8.0, the presence of 4 M urea reduced both the strength and extent of self-association (Table 3.3)

3.3 DISCUSSION

In protein folding studies, the presence and concentration of intermediates is dependent upon a number of factors. These include pH, temperature, the concentrations of salts and denaturants, and importantly, the intrinsic properties of the protein employed (Fink, 1995; Ptitsyn, 1995). For acid-mediated partial unfolding, three broad classes of protein have been recognised: (i) those that unfold completely and then refold into a compact or expanded molten globule-like formation at lower pH, (ii) those that go directly to the molten globule and (iii) those that essentially remain native (Fink *et al.*, 1994). hGH falls into category iii, remaining essentially native, while bGH falls into category ii, going directly to a molten globule. This study shows that the acid-induced unfolding of pGH also falls into category ii with folding intermediates that possess many of the classic characteristics of the molten globule. These characteristics include the retention of substantial secondary structure, substantial loss of tertiary structure, maintenance of a compact shape similar in size to that of the native state, and a propensity to aggregate. However, the folding intermediates for pGH and bGH have quite distinct properties emphasising the range of structural variability of intermediates even amongst closely related proteins.

Acid-mediated unfolding in the absence of urea

Upon acidification of pGH, very little tertiary structure as detected by near-UV CD was retained. For the complete unfolding of pGH at pH 9.1 by Gdn–HCl, the λ_{max} of intrinsic fluorescence for Trp86 was shown to red shift by 14 nm to a value of 352 nm (Bastiras and Wallace, 1992). The minimal red shift of 3 nm for Trp86 upon acidification of pGH seen here indicated that Trp86 remained in a hydrophobic environment. For a two-state transition a continuous red shift in λ_{max} accompanied by fluorescence emission band

broadening would be expected, where the λ_{max} would be a function of the relative populations of native and unfolded protein. Since the red shift seen here for pGH did not coincide with the changes in I_{340} the protein must occupy an intermediate state at pH 2.0. Analogous to bGH, the native state tryptophan residue at position 86 in pGH is located close to an intramolecular quenching group, resulting in a quenched native state fluorescence. The increase in relative fluorescence intensity with minimal change in the λ_{max} suggests removal of the quenching group without a significant change in the polarity of the environment surrounding Trp86.

The reduction in molar absorption (ε_{290}) with decreasing pH (Figure 3.6) was similar to that previously seen for unfolded pGH (Bastiras and Wallace, 1992) and bGH (Brems *et al.*, 1985). In those studies, the decrease in ε_{290} was attributed to the removal of the internalised Trp86 to the polar solvent exterior. In this case, the lack of red shift in the fluorescence emission coupled with the loss of the near-UV CD signal at 285 nm ($[\theta]_{285}$, Figure 3.10), suggested that a change in the average environment of the seven tyrosine residues of pGH was responsible for a significant proportion of the ε_{290} loss. The reduction in absorbance at 290 nm produced by transfer of a tyrosine residue from the protein interior to water is approximately 600 $M^{-1}cm^{-1}$ (Donovan, 1973). In the model of pGH (Rowlinson *et al.*, 1994), tyrosine 159 is completely buried whilst tyrosines 29 and 175 are almost fully buried (Figure 3.17; Table 3.4). Exposure of these three residues to solvent is indicated by the loss of the θ_{285} signal with decreasing pH (Figure 3.10) and would be responsible for a significant proportion of the observed hypochromicity.

In the absence of 4 M urea the midpoint of the transitions obtained for the three probes of tertiary structure (θ_{285}, I_{340} and ε_{290}) are not coincident (Table 3.1). The lack of coincidence

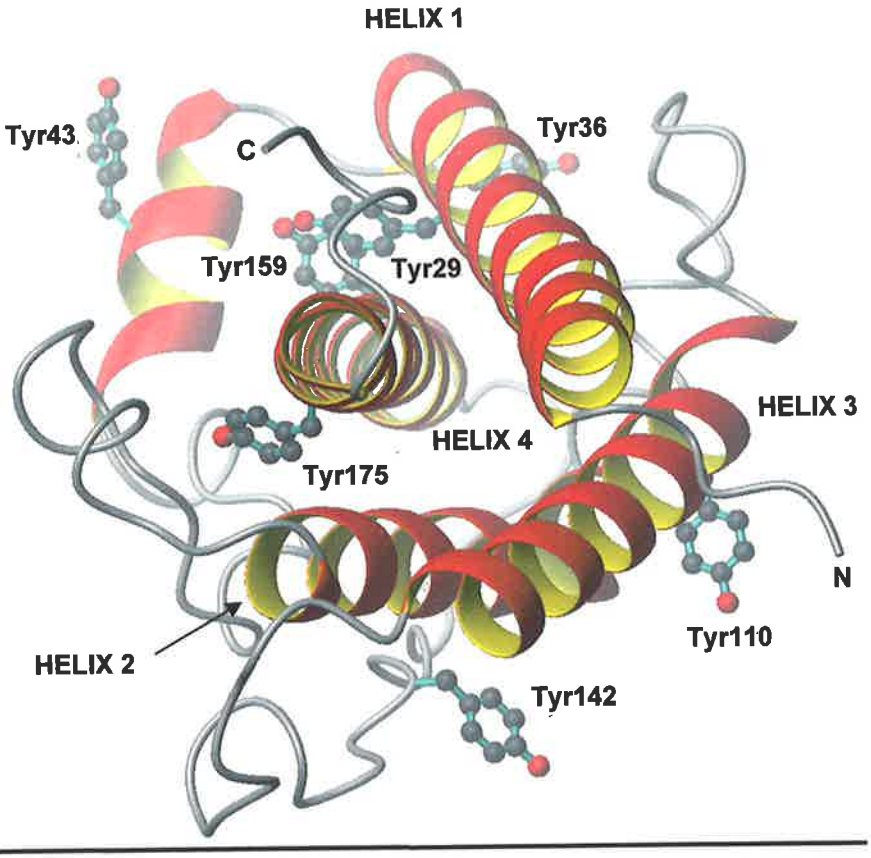

FIGURE 3.17 LOCATION OF THE SEVEN TYROSINE RESIDUES ON THE pGH MOLECULE. The location of the seven tyrosine residues is shown on the energy minimised model of pGH (Rowlinson *et al.*, 1994). The heavy atoms of the amino acid residues are highlighted. The amino and carboxyl terminus is denoted by N and C respectively. The best representation was obtained looking down the central core of the pGH molecule.

Figure prepared with the program MOLMOL (Koradi *et al.*, 1996)

RESIDUE #	SOLVENT EXPOSURE (Å^2)
29	27.1
36	86.8
43	98.9
110	81.8
142	93.4
159	00.0
175	13.7
gly-tyr-gly	148.3

TABLE 3.4 THE DEGREE OF SOLVENT EXPOSURE FOR EACH TYROSINE RESIDUE IN pGH. Values determined by the Connolly Surfaces algorithm in InsightII (Lee and Richards, 1971).

indicates that conformational changes affecting the intrinsic fluorescence of Trp86, I_{340}, (most likely to be the initial removal of the intramolecular quenching group), precede the transfer of buried or partially buried tyrosine residues to the solvent exterior (as measured by θ_{285} and ε_{290}). The pH midpoints detected by these probes suggest that the conformational change responsible for the removal of the quenching group is mediated by the titration of glutamate and/or aspartate residues. Elucidation of the residue(s) responsible for the quenching of the native state fluorescence has so far proved elusive (Kauffman *et al.*, 1989). Examination of the pGH model (Rowlinson *et al.*, 1994) shows that Trp86 is located in a hydrophobic core composed of Phe54, Ser55, Leu82, Ile83, Ser85, Leu87, Pro89, Val90, Leu93, Leu113, Leu161, Cys164, Phe165 and Asp168. At first glance, the obvious candidate appears to be Asp168 which, as seen in hGH (Bewley and Li, 1984, deVos *et al.*, 1992), is hydrogen bonded to the Nε1 of Trp86. However, all of the above residues, including Asp168, are conserved in hGH, which unlike pGH and bGH, does not have a quenched native-state fluorescence (Brems *et al.*, 1990). As suggested by Kauffman *et al.* (1989), the Cys53–Cys164 disulphide bridge cannot be ruled out as the possible Trp fluorescence quencher in native pGH and bGH, since subtle structural differences between the growth hormones could result in slightly different orientations of the disulphide bridge with respect to Trp86. Irrespective of the exact identity of the quenching group, it is not possible to determine with our data whether the increase in relative fluorescence intensity is due to either direct or indirect interaction(s) between proton-accepting group(s) and the internalised tryptophan.

The retention of a significant degree of secondary structure combined with the loss of stabilising tertiary interactions as described above, indicates that under acidic conditions pGH forms a molten globule-like structure. Previous characterisation of recombinant pGH

confirmed a helical content of 47% for the folded protein, close to previously published values (Holladay *et al.*, 1974). A decrease in θ_{222} of approximately 15% at pH 2.0 attests to the retention of a significant degree of secondary structure in pGH at pH 2.0. Previous studies have shown that small changes in helix φ and Ψ angles (≥ 5°) greatly reduces the far-UV CD intensity at 222 nm even with no change in the total number of helical residues (Manning *et al.*, 1988; Manning and Woody, 1991). Thus, the loss in CD intensity at 222 nm with decreasing pH may be due to fraying or the realignment of helices in the 4 α-helix bundle.

Acid-mediated unfolding in the presence of urea

The inclusion of urea at pH 8.0, appeared to induce a small conformational change in pGH, as detected from the fluorescence emission properties of Trp86. Note that the I_{340} for Trp86 at pH 8.0 in the presence of 4 M urea is approximately 25% larger than in the absence of 4 M urea (Figure 3.3 A and 3.3 B) and that λ_{max} is red shifted by > 5 nm (Figure 3.3 C). It is possible that a urea molecule may have diffused into the protein matrix thus altering the conformation slightly. This conformational change was not detected when monitored by UV absorbance and second-derivative spectroscopy. A possible explanation for this may be due to the different properties of absorbance and fluorescence, as shown schematically in Figure 3.18. Fluorescence is observed when an excited electron (from pre-absorbed energy) returns to its ground state energy level. On returning to the ground state, various pathways for the transition from the excited state to the ground state can be taken, which are not important in absorption studies (Brand and Witholt, 1967). These pathways are sensitive to, and can therefore detect, very small structural perturbations in proteins that are otherwise undetectable.

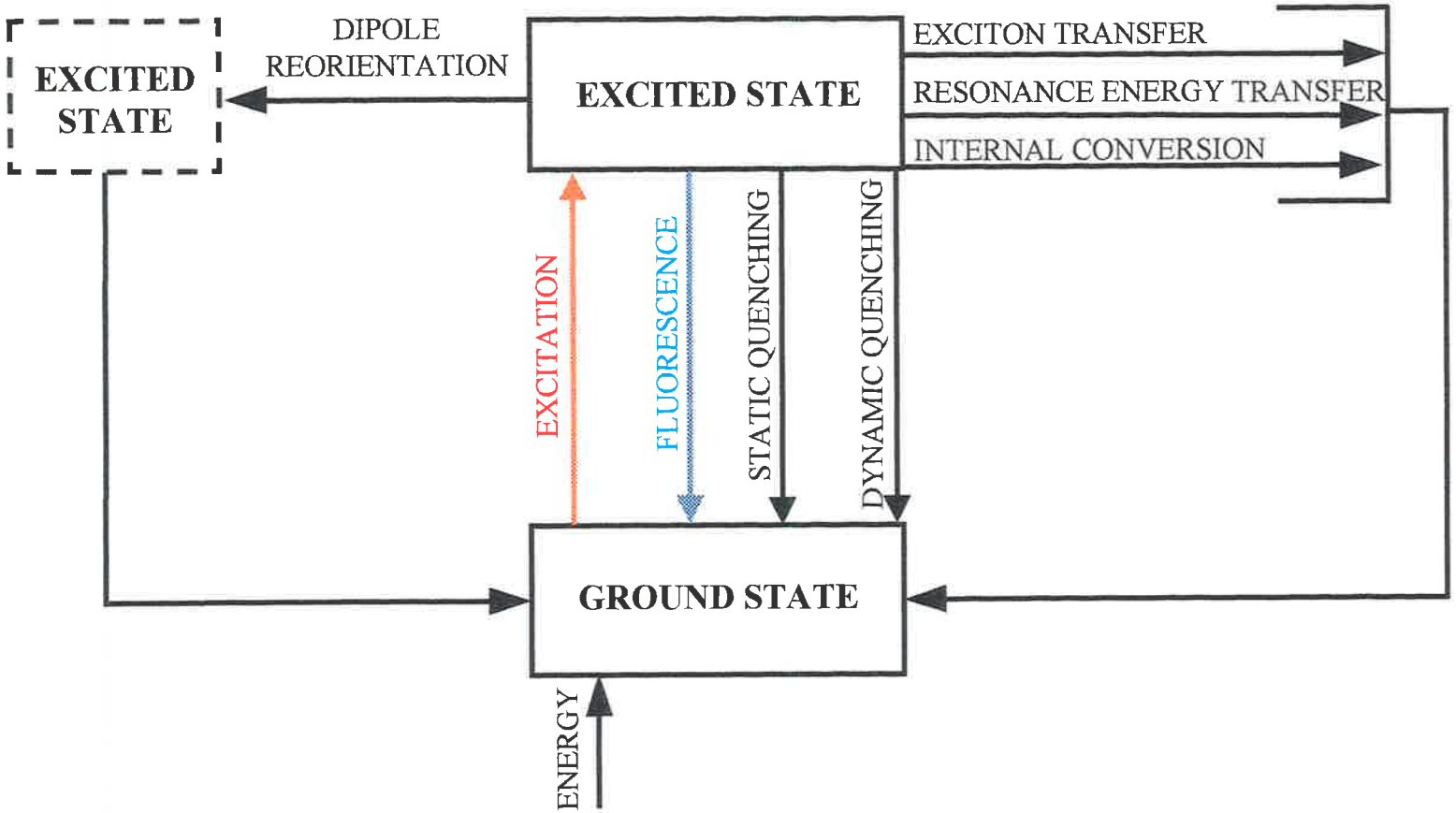

FIGURE 3.18 SCHEMATIC REPRESENTATION OF THE POSSIBLE RETURN PATHWAYS FOR AN EXCITED STATE ELECTRON.

Adapted from Brand and Witholt, 1967

The inclusion of 4 M urea in the acid-mediated unfolding resulted in a pGH population with similar loss of the asymmetrical environment of tyrosines (Figure 3.10), similar loss of α-helix (Figure 3.11) and similar hypochromicity (Figure 3.6) as that observed in the absence of urea. These properties were consistent with the formation of an intermediate of the molten globule type.

There were also clear differences in the intermediates observed at pH 2.0 in the presence and absence of urea and in the acid-induced transitions that lead to these intermediates. At pH 2.0 in the presence of 4 M urea, the λ_{max} red shifted by 8 nm (Figure 3.3 C) indicating a substantial increase but not necessarily complete exposure of Trp86 to the solvent. Although there was an increase in I_{340} it was reduced when compared to that obtained in the absence of urea. It is possible that the decrease in I_{340} resulted from an interaction with other putative quenching groups and/or the afore-mentioned quenching group responsible for the native state quenched fluorescence. An intense CD band observed near 300 nm (Figure 3.10) in conjunction with a red shift in the Trp^1L_b absorption band in the second derivative spectra (Figure 3.8), indicated that Trp86 was in a highly asymmetric environment despite its increased solvent exposure. This intermediate was also found by ANS fluorescence measurements to have reduced surface hydrophobicity (Figure 3.12).

The acid-induced folding transitions observed in the presence of urea are shifted by approximately 1 pH unit to a more alkaline pH. The shift to higher pH is unlikely to result from a shift in pK_a of titrated carboxylic acid groups. The inclusion of chemical denaturants during acid titration of proteins generally normalises the pK_a values of titratable groups to those found for the free amino acids in solution. For aspartate and glutamate residues, these values are approximately 3.9 and 4.3, respectively, well below

the apparent pH midpoint of approximately 5.2. In their study on bGH, Edelhoch and Burger (Edelhoch and Burger, 1966), also observed a shift in the midpoint of the acid transition to higher pH values in the presence of increasing urea concentrations. The authors stated that the shift in the midpoints to higher pH could not be attributed to a shift in the pK_a of carboxyl groups.

It is more likely that the shift in the pH midpoint in the presence of 4 M urea results from the titration of one or more critical histidines. A change in the pK_a for a histidyl sidechain from a value below that of the transition pH in the native state to a value higher than the transition pH in the intermediate would promote a shift in the chemical equilibrium towards the intermediate (Geierstanger *et al.*, 1998), as dictated by Le Chatalier's principle. In the model of the structure of pGH, histidine 22 and 170 are within hydrogen bonding distance of each other (< 3 Å), located in a shallow cleft which roughly divides the molecule in two (Figure 3.19) (Rowlinson *et al.*, 1994). Their interaction may produce a situation qualitatively similar to that seen for His24 and His119 in apomyoglobin (Geierstanger *et al.*, 1998). In native apomyoglobin, His24 is hydrogen bonded to His119 resulting in a very low pK_a for His24 of approximately 3. His24 is not protonated until the native state unfolds to the intermediate whereupon its pK_a is raised to approximately 6.7 (Geierstanger *et al.*, 1998). This change in pK_a largely dictates the acid-induced unfolding of apomyoglobin to its intermediate with a transition midpoint at pH 4.4 (Geierstanger *et al.*, 1998). In bGH, early NMR studies showed that either His20 or His22, located on helix-1, has a low pK_a value of 4.67 (MacKenzie *et al.*, 1989). Due to the combined effects of its partially buried location (Rowlinson *et al.*, 1994), and its interaction with His170, we speculate that it is His22 in pGH (Figure 3.19) that has the depressed value of pK_a in the native state. In the acid plus urea-induced intermediate, the pK_a of His22 would need to be

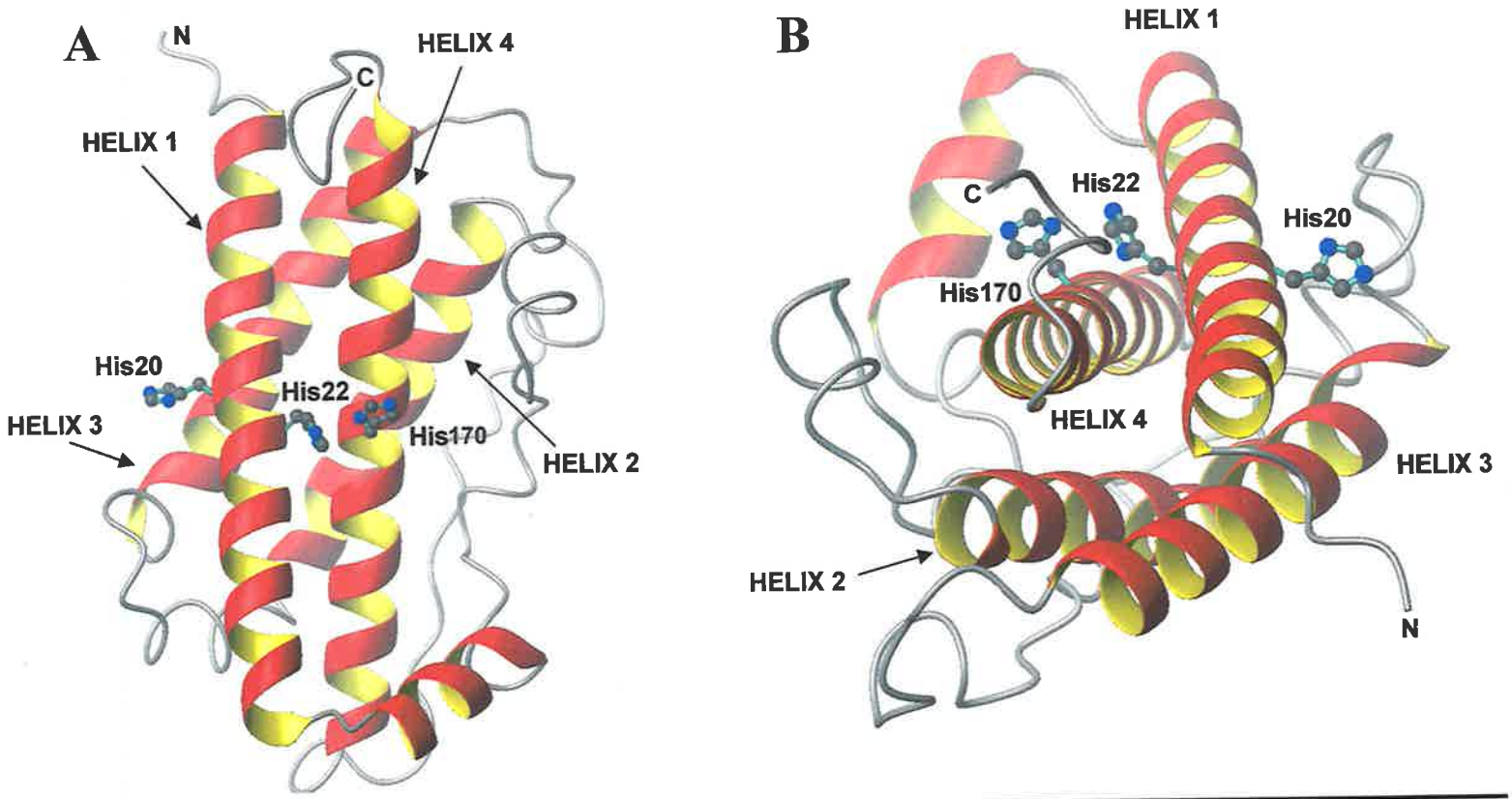

FIGURE 3.19 LOCATION OF THE THREE HISTIDINE RESIDUES ON THE pGH MOLECULE. The location of the three histidine residues is shown on the energy minimised model of pGH (Rowlinson *et al.*, 1994). The heavy atoms of the amino acid residues are highlighted. The amino and carboxyl terminus is denoted by N and C respectively. View A: a typical view of the 4 α-helix bundle. View B: looking down the central core of the molecule.

Figure prepared with the program MOLMOL (Koradi *et al.*, 1996)

raised above the transition midpoint of approximately 5.2 to serve as a driving force for the formation of the intermediate. In hGH, due to the insertion of an amino acid in the primary sequence separating the helix 1 histidines, both are located on the solvent-exposed face of the helix (de Vos *et al.*, 1992). Furthermore, the equivalent position for His170 in pGH is occupied by aspartate in hGH.

Self-association of pGH

A property of a molten globule intermediate is the propensity to self-associate. Determination of the hydrodynamic radii of pGH at pH 2.0 by SEC proved to be problematic. In the absence of 4 M urea there was no recovery of protein below pH 5.0. Even in the presence of 4 M urea, protein was unable to be eluted between pH 5.0 and pH 4.0. In previous studies, problems have also been experienced with hydrodynamic determination using SEC, presumably due to interactions with the column matrix (Fink *et al.*, 1994). A study implementing a Superose 6 column has identified that electrostatic interactions between charged patches of a protein that interact with the resin are responsible for the apparent protein retention (Edwards and Dubin, 1993). At pH 2.0 and 4 M urea the majority of protein eluted as a single broad peak with an apparent hydrodynamic radius of 47 Å (Figure 3.13). A similar peak with a radius of approximately 52 Å was resolved for the associated species of pGH at intermediate Gdn–HCl concentrations (Bastiras and Wallace, 1992). With the similarity between the chromatographic profiles, pGH at pH 2.0 and 4 M urea is an associated species.

With the problems encountered using SEC, sedimentation equilibrium was used to quantify the mode, strength and reversibility of the self-association of pGH under various solution conditions. At pH 8.0, pGH reversibly self-associates. In the absence of 4 M urea pGH

undergoes a weak but discrete self-association where the largest species appears to be the tetramer, whilst the presence of urea at pH 8.0 almost eliminates self-association, presumably by altering the interactive surface landscape (Young *et al.*, 1994; Laskowski *et al.*, 1996). At pH 2.0 in the absence and presence of 4 M urea, pGH intermediates undergo strong monomer–dimer self-association (see below). We speculate that the dimer is an off-pathway folding intermediate. The dimer is capable of further reversible self-association; the mode of self-association is different in the two solvent conditions and discussion of this is reserved for Chapter 4.

The strong monomer-dimer self association was evident even at the lowest protein concentration examined (0.1 mg/ml, ~ 4 μM). In comparison, the Gdn–HCl induced associated species of pGH and bGH were populated above 10 μM (Brems *et al.*, 1986; Bastiras, 1992). Due to the lack of detectable monomer, the monomer–dimer equilibrium could not be accurately determined. The value for the association constant, *K*, for monomer dimerisation would be $\geq 5 \times 10^6$ M^{-1}. However, based on the detection limit of the ultracentrifuge, an estimate of between $1 \times 10^8 - 1 \times 10^{10}$ may be more appropriate (Shearwin and Egan, 1996). This compares with significantly weaker equilibrium constants of 1.6×10^5 M^{-1} and 7×10^3 M^{-1} for the bGH (Brems *et al.*, 1988) and hGH (DeFelippis *et al.*, 1993) monomer-dimer equilibrium respectively. However, it must be pointed out that the equilibrium constants for bGH and hGH have been determined under different experimental conditions and methods: (i) the bGH association was determined from near-UV CD data in 0.05 M ammonium bicarbonate, 3.7 M Gdn–HCl, pH 8.5 (ii) the hGH association was determined by analytical ultracentrifugation in 0.1 M HEPES, 4.5 M Gdn–HCl, pH 7.5. In assigning the association constant for hGH, the authors point out that although the apparent weight-average molecular weight approaches that of a dimer, this

observed value may be lower than the true molecular weight. They attribute this to the observation of nonideality in the sedimentation behaviour of the protein (Munk and Cox, 1972; Van Holde, 1985) and this was taken into account when analysing the data presented for pGH. Why is the association constant so large for the monomer-dimer equilibrium of pGH at pH 2.0? The p*I* of pGH is approximately 6.9 and the p*K* of most carboxyls is ≥3. Taken together, the overall charge of pGH at pH 2.0, as with the majority of other proteins, would be positive. If two highly positively charged molecules were to come within close proximity to one another, it may be expected that the electrostatic repulsive force between the two molecules would inhibit the intermolecular association. However, it is important to consider localised charge effects and not just the global net charge of the protein. Acidic residues such as glutamic acid, are involved in hydrogen bond formation with the surrounding aqueous solvent. The addition of a positive charge upon acidification would cause the breakdown of the hydrogen bond network with solvent, in turn increasing the apparent hydrophobicity of the molecule. An increase in hydrophobicity would increase the potential for intermolecular association. For example, within helix 3 of pGH, two aspartic (Asp115 and Asp129) and five glutamic acid (Glu111, Glu117, Glu118, Glu126 and Glu128) residues are exposed to the surrounding solvent and are most probably involved in hydrogen bond formation with solvent. Protonation of these residues will increase the apparent hydrophobicity and subsequently increase the propensity of a complementary site on another monomer to associate, stabilising the conformation as a dimer.

Although self-associated intermediates exist at pH 2.0 with or without 4 M urea, quantitative differences in the intrinsic- and ANS- fluorescence (Figures 3.3 and 3.12), second derivative spectra (Figure 3.8), θ_{300} band (Figure 3.10 A) and modes of self-

association (Table 3.3), reveal that they are not structurally identical in every detail. The associated species detected in the Gdn–HCl-induced equilibrium folding pathway of bGH (Havel *et al.*, 1986) and pGH (Bastiras, 1992) is characterised by a similarly intense θ_{300} band to that seen in this study for pGH at pH 2.0 and 4 M urea. Moreover, in the second derivative spectrum (Figure 3.8), the Trp $^1L_b[0\text{-}0]$ is also significantly red shifted. Previous studies have attributed this red shift to interactions with nearby polar groups and/or a change in the polarizability of the surrounding Trp environment (Strickland *et al.*, 1969; Strickland, 1972). The similarity in these spectral properties between the Gdn–HCl self-associated intermediate(s) for bGH and pGH and the self-associated intermediate(s) for pGH at pH 2.0 in the presence of 4 M urea suggests that they may be structurally alike. The addition of a helix 3-containing peptide to an associated equilibrium folding intermediate of bGH reduces its polymerisation (Brems *et al.*, 1986). Furthermore, this reduction correlates with a loss of the prominent θ_{300} band. The association of pGH at pH 2.0 in the presence of 4 M urea may also involve helix 3, and an examination of this forms the basis of Chapter 4.

Conformational states induced by acid denaturation are governed by a fine balance between intramolecular repulsive forces, hydrophobic interactions, electrostatics and the presence of disulphide bonds and salt bridges (Fink *et al.*, 1994). Both bGH and pGH, at low pH form molten globule-like states, however, the molten globule of pGH is more structured. Acidification of hGH results in an intermediate with the majority of structure similar to the native state (DeFelippis *et al.*, 1995). hGH has significant stability, more consistent with native protein conformations, as opposed to an intermediate of the molten globule type (Abildgaard *et al.*, 1992; DeFelippis *et al.*, 1995).

In conclusion, acidification of pGH invokes the formation of molten globule-like states with measurable differences in conformation, subject to the solvent condition employed. The critical off-pathway folding intermediate for pGH may be the highly favorable formation of a dimer. The mode of self-association of this dimer then depends on its exact conformation. pGH thus provides further evidence that, within a family of proteins, folding intermediates can display a great range of structural variability and ability to polymerise.

CHAPTER 4

SELF–ASSOCIATION OF RECOMBINANT PORCINE GROWTH HORMONE

4.1 INTRODUCTION

In Chapter 3 the acid-mediated denaturation of pGH was shown to invoke the self-association of partially denatured monomeric intermediates. Quantitative differences in the physical characteristics between the intermediates at pH 2.0 in the absence and presence of 4 M urea suggested that the intermediates are not structurally identical in every detail. Moreover, the models of self-association in these two solvent conditions are different. In the absence of urea, the associated intermediate at pH 2.0 was characterised by an increased intrinsic- and ANS- fluorescence emission, with a reduced intensity and small red shift in the second derivative of the $Trp^1L_b[0\text{-}0]$ absorption band. In comparison, the associated intermediate at pH 2.0 and 4 M urea was characterised by a reduced intrinsic- and ANS- fluorescence emission, a reduced intensity but greater red shift in the second derivative of the $Trp^1L_b[0\text{-}0]$ absorption band and a prominent θ_{300} band. In the two solvent systems partially denatured monomeric pGH forms a dimer. At pH 2.0 without urea subsequent self-association of the dimer proceeded by unlimited addition of the dimer whereas the addition of urea invoked discrete self-association of the dimer with the largest species being an octamer. From this data, it is proposed that the partially denatured monomer in each solvent system has a distinct conformation and it is these conformations that determine the final oligomer stoichiometry.

Previous equilibrium denaturation studies of bGH (Havel *et al.*, 1986) and pGH (Bastiras and Wallace, 1992) at mildly alkaline pH have detected the presence of a partially denatured self-associated species at intermediate Gdn–HCl concentrations. For both bGH and pGH, the properties of this species include a reduction in intensity and red shift in the second derivative of the $Trp^1L_b[0\text{-}0]$ absorption band, a prominent θ_{300} band and a propensity to precipitate during refolding (Havel *et al.*, 1986; Brems, 1988; Bastiras and

Wallace, 1992). It has previously been shown that the addition of a peptide fragment encompassing helix 3 of bGH (residues 96–133) during the refolding of bGH, reduced both the intensity of the θ_{300} band and the precipitation that occurs during refolding, presumably by preventing the formation of the associated intermediate (Brems *et al.*, 1986; Brems, 1988; Lehrman *et al.*, 1991). An associated intermediate has also been detected in the equilibrium-folding pathway of hGH (DeFelippis *et al.*, 1993). This species did not exhibit a θ_{300} band, however, peptide fragments from the third helix of either hGH or bGH were capable of inhibiting the formation of the associated species thereby preventing precipitation during refolding (DeFelippis *et al.*, 1993).

The similarity in spectral characteristics between the Gdn–HCl-induced equilibrium associated intermediates for pGH and bGH and the associated intermediate for pGH at pH 2.0 and 4 M urea suggests that they may be structurally alike. The amino acid sequence encompassing the third helix of pGH is identical in sequence to helix 3 of bGH except for a leucine to glutamine substitution at position 121 (Figure 4.1). The helix is also amphipathic in nature and shares a high degree of sequence homology with hGH (Figure 4.1). Considering this similarity, it is possible that helix 3 of pGH is involved in the self-association of pGH at pH 2.0 and 4 M urea. In contrast, the self-associated species at pH 2.0 in the absence of 4 M urea has different characteristics, the most notable being the absence of the θ_{300} band and the different model of self-association. This suggests that helix 3 may not be involved in the formation of the associated intermediate in this solvent system. The aim of this chapter was to determine whether a peptide fragment encompassing helix 3 of pGH (residues 96–133; pGH(96–133)) was involved in the formation of the associated intermediate at pH 2.0 with or without 4 M urea.

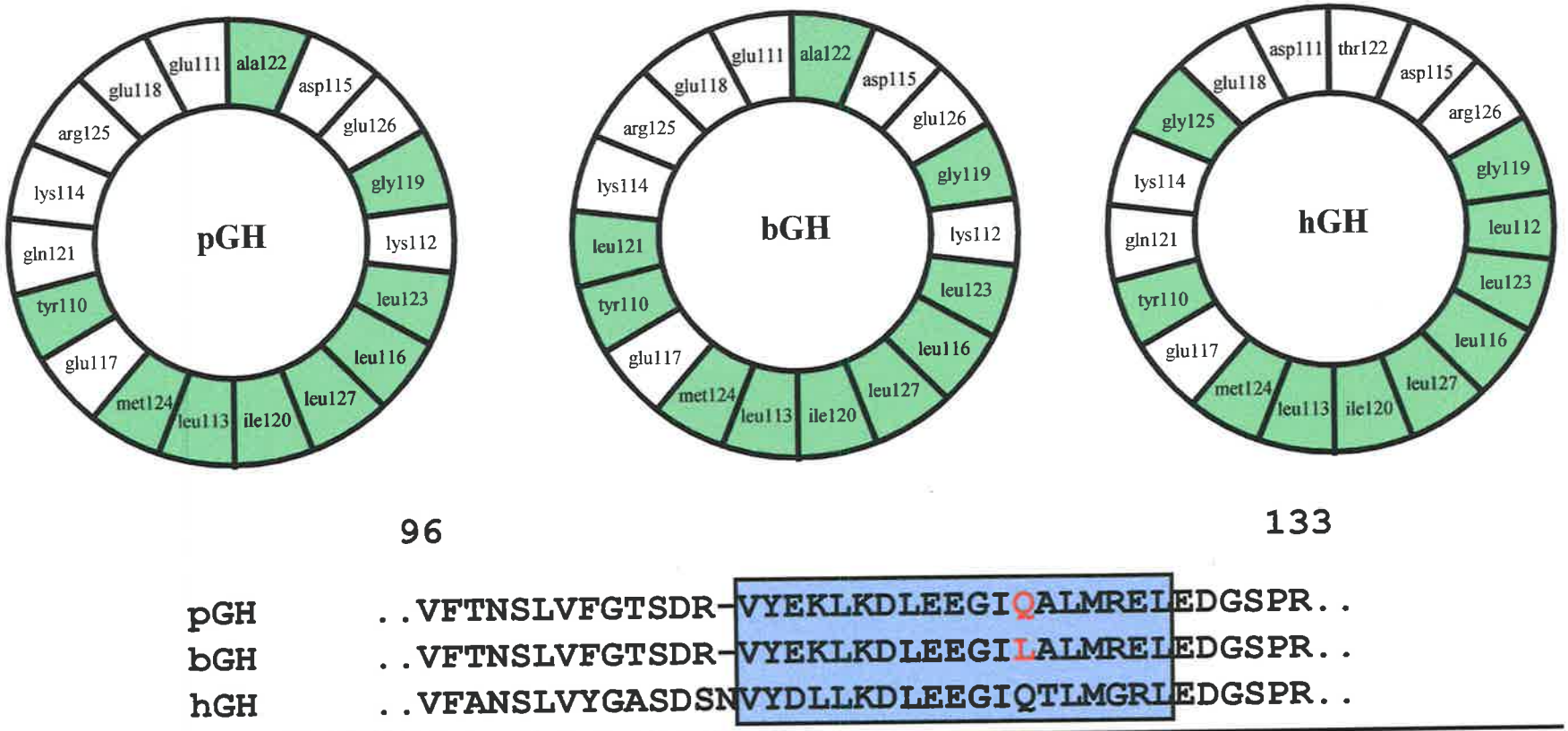

FIGURE 4.1 AXIAL PROJECTION OF THE POTENTIAL α-HELIX STRUCTURE OF RESIDUES 109-127 IN pGH, bGH and hGH. The hydrophobic amino acids are shaded in green. The amino acid sequences of peptide 96-133 for pGH, bGH and hGH are shown, with the putative amphipathic helix highlighted (boxed). The leu→gln substitution at residue 121 in pGH is highlighted in red.

Adapted from Brems *et al.*, 1986

4.2 RESULTS

4.2.1. Isolation and Purification of pGH(96–133)

4.2.1.1 Analytical Isolation and Purification of pGH(96–133)

The potential sites of trypsin cleavage in pGH are shown in Figure 4.2. Following limited proteolysis of pGH with sequence-modified trypsin (1:500 trypsin:pGH, w/w; incubated for 1 hour at 25°C), proteolytic fragments were separated by RP HPLC as described in 2.2.3. Limited proteolysis of pGH generated 4 peptides, which are identified as P1–P4 in order of elution (Figure 4.3). The digest pattern shown in Figure 4.3 was consistently reproduced in repeat experiments (n = 4). An elution profile of undigested pGH and a control incubation of trypsin alone are also shown and do not contribute to the profile of partially digested pGH (Figure 4.3). The peptides P1–P4 were collected and characterised by electrospray ionization (ESI) mass spectrometry (Table 4.1). The experimental mass of 4345 (Table 4.1) for peptide P1 agreed with the calculated theoretical mass of 4344 for intact pGH(96–133). The identity of P1 as pGH(96–133) was confirmed by partial N-terminal sequence analysis.

4.2.1.2 Optimisation of pGH Digest Conditions

For the preparative isolation and purification of peptide P1, pGH(96–133), the use of sequence-modified trypsin was inappropriate, in terms of both the quantity required and expense incurred. As a result, an unmodified enzyme was chosen to isolate pGH(96–133). To ensure that the same products as described in 4.2.1.1 were obtained, a preliminary digest with the unmodified enzyme was performed (Figure 4.4). Limited proteolysis generated 3 main peptides (Figure 4.4). Based on the % acetonitrile at which each peptide eluted, peptides P1 and P2 were assigned. Note that the elution gradient employed was

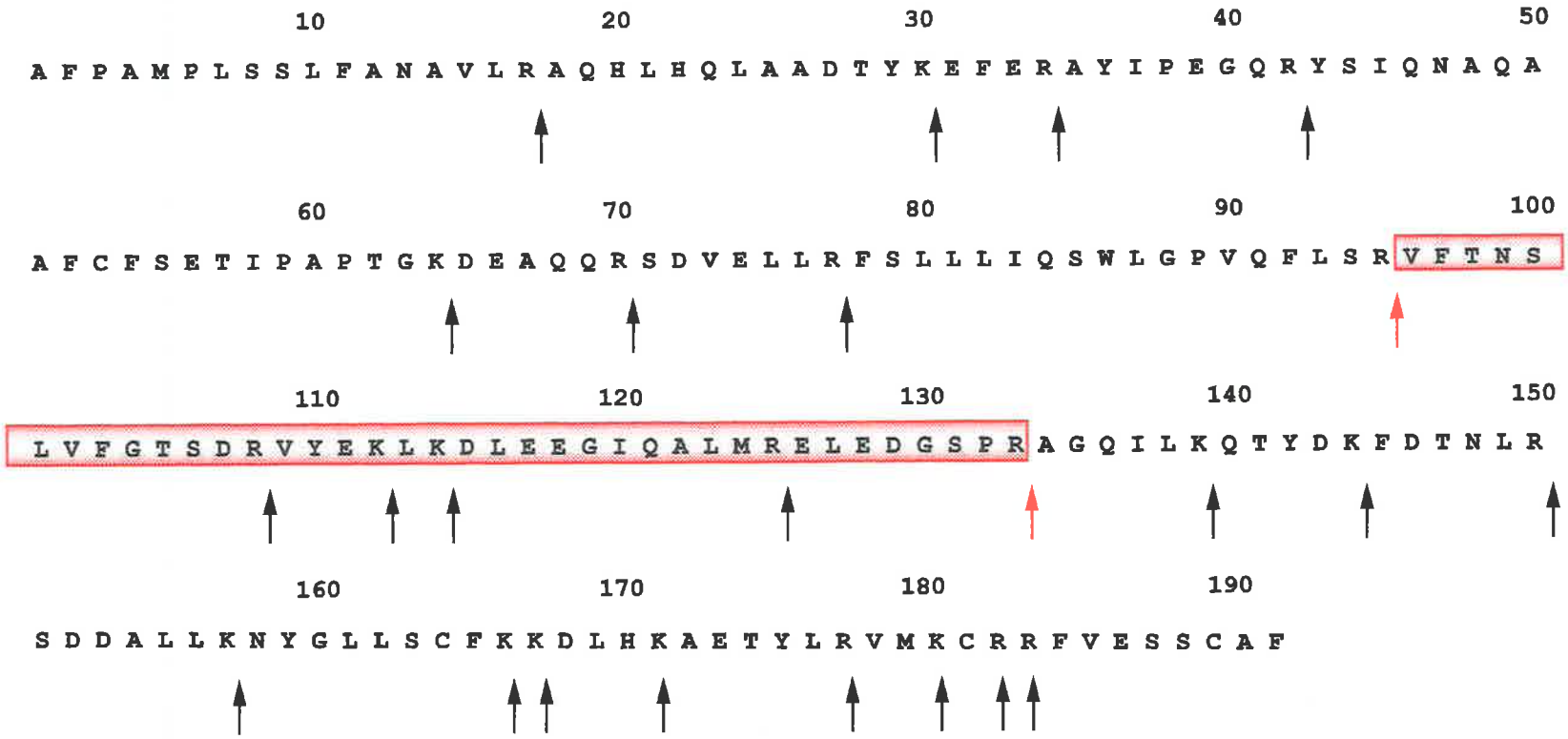

FIGURE 4.2 THE POTENTIAL SITES OF TRYPSIN CLEAVAGE IN pGH. Peptide bonds that are sensitive to Trypsin are indicated by ↑. The cleavage sites required for the release of the helix 3 containing peptide, pGH(96–133), are indicated by ↑, and the peptide is highlighted by a red box.

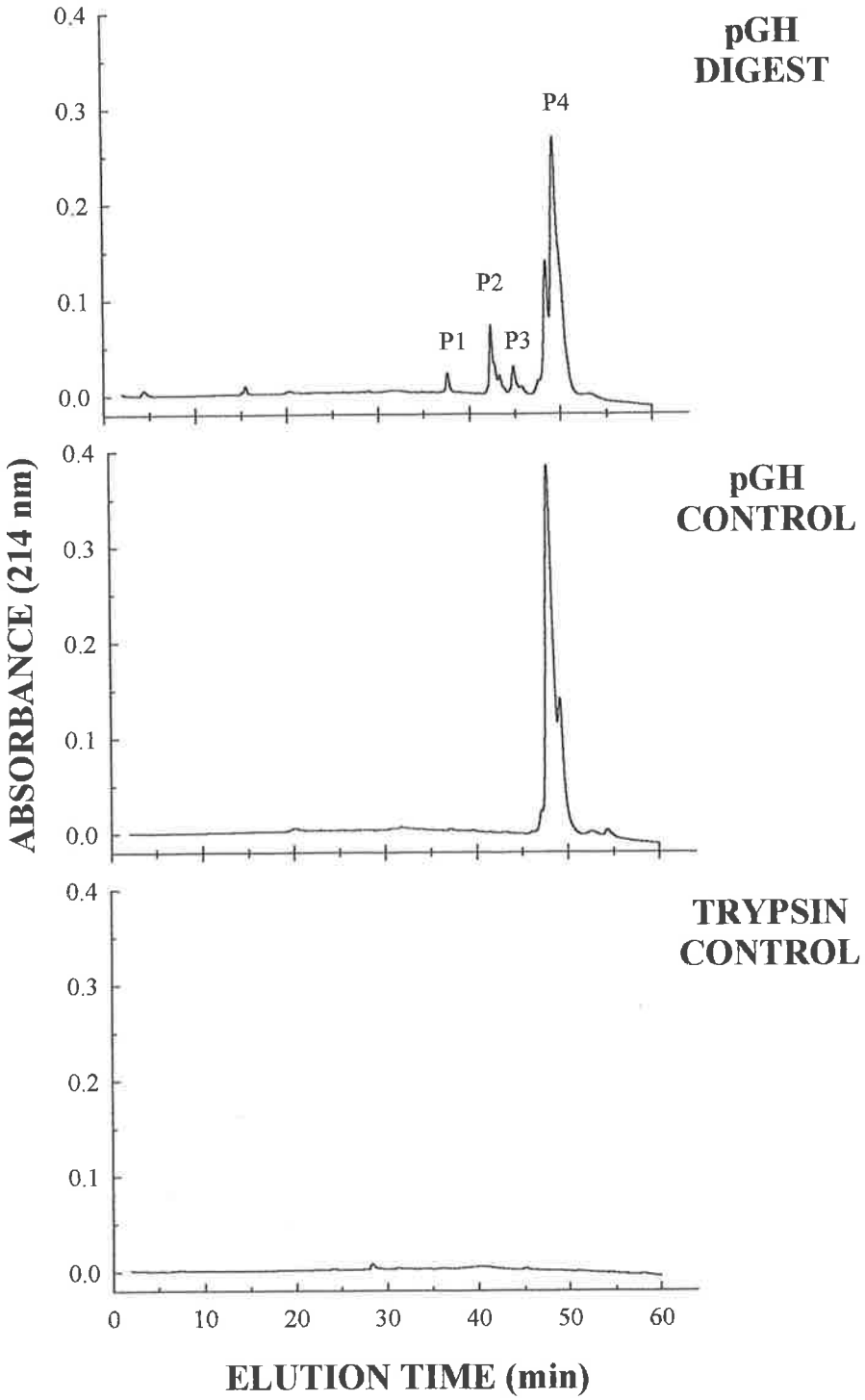

FIGURE 4.3 PARTIAL DIGEST OF pGH (sequence-modified trypsin). A 100 µl aliquot each of pGH digest, pGH control and trypsin control was analysed by RP HPLC on a C4 column (20 mm i.d. x 30 mm), pre-equilibrated in 0.1% TFA. Protein was eluted using a linear gradient of 0% to 70% (v/v) ACN in 0.1% TFA, at a flow rate of 0.5 ml/min. Protein elution was monitored at 214 nm. The digest peptides were labelled P1–P4 in order of elution.

PEPTIDE	RETENTION TIME (mins)	% ACETONITRILE	IDENTIFIED MASS
P1	37.62	42	4345
P2	42.34	47	17555
P3	44.85	49	ND
P4	49.0	54	19888, 21270, 21864, 21882

TABLE 4.1 SUMMARY OF TRYPTIC PEPTIDES (modified trypsin). Tryptic peptides were labelled P1-P4 in order of elution. The retention times and concomitant % acetonitrile of elution are shown. The mass of each peptide was determined by ESI. ND, not determined.

PEPTIDE	RETENTION TIME (mins)	% ACETONITRILE	IDENTIFIED MASS
P1	16.57	42	4345
P5	19.24	44	ND
P2	22.12	47	17555
P3	ND	–	–
P4	ND	–	–

TABLE 4.2 SUMMARY OF TRYPTIC PEPTIDES (unmodified trypsin). Tryptic peptides were labelled in accordance with the % acetonitrile and pattern of elution of the initial isolation and identification experiment (Table 4.1). P5 denotes a peptide not previously observed. ND, not determined.

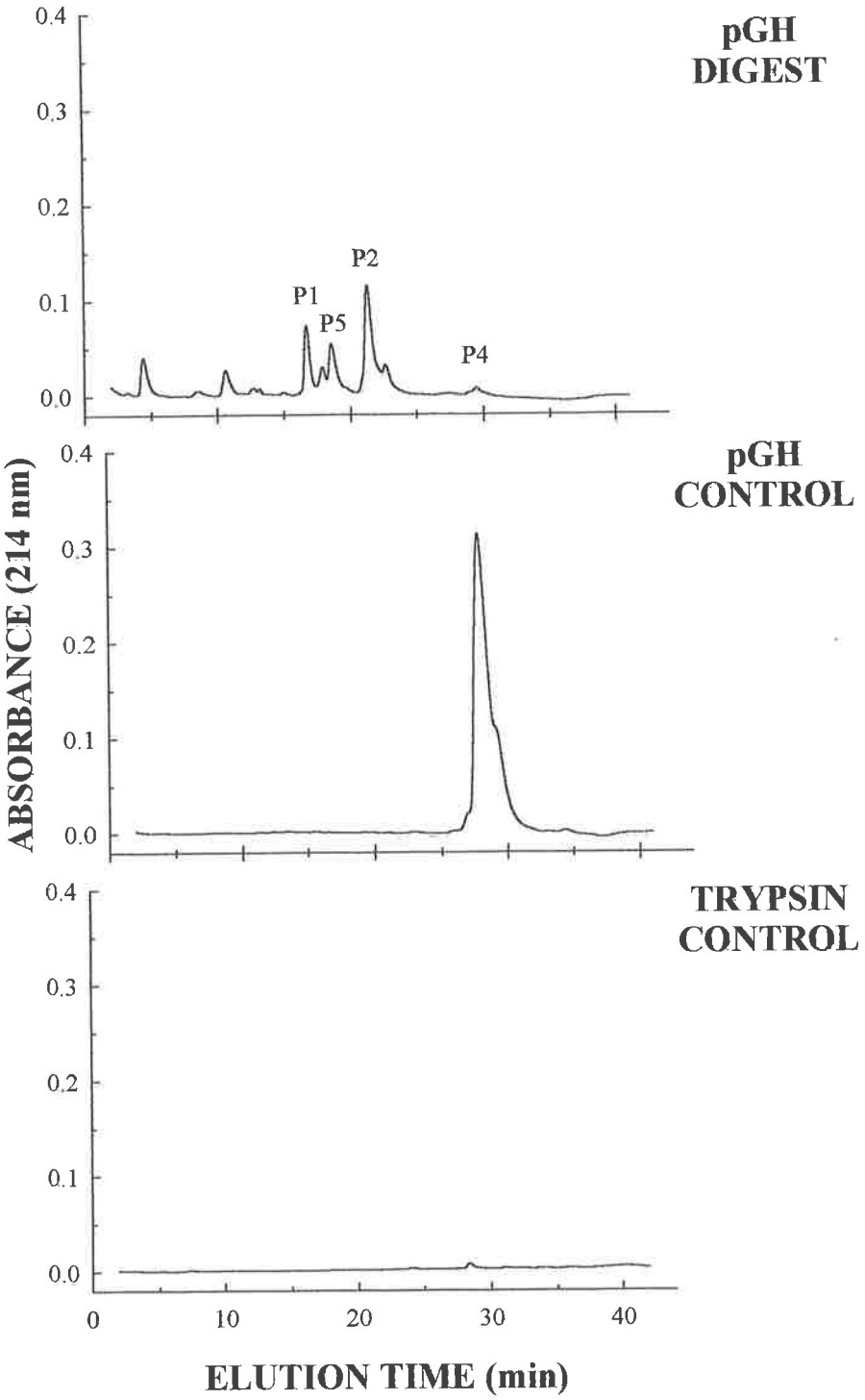

FIGURE 4.4 PARTIAL DIGEST OF pGH (unmodified trypsin). A 100 µl aliquot each of, pGH digest, pGH control and trypsin control was analysed by RP HPLC on a C4 (20 mm i.d. x 30 mm) column, pre-equilibrated in 30% (v/v) ACN/0.1% TFA. Protein was eluted using a linear 30% to 60% (v/v) ACN/0.1% TFA gradient, at a flow rate of 0.5 ml/min. Protein elution was monitored at 214 nm. The peptides P1 and P2 were labelled based on the % acetonitrile at which they eluted. A previously unobserved peptide was labelled P5.

initiated from 30% acetonitrile, resulting in different retention times to those recorded in 4.2.1.1. A previously undetected peptide was observed and denoted as P5. Very little undigested material (peptide P4, Figure 4.3) was observed, with an estimated amount of <1% remaining. This compares with approximately 40% when the sequence-modified trypsin was used. Considering the apparent extent of digestion with the unmodified trypsin, there was only a slight increase in the relative amount of peptides P1 and P2, compared to the digest using sequence-modified trypsin. The lack of undigested material using the unmodified trypsin suggested that the enzyme had an enhanced activity and an increase in the amount of P1 would have been expected. However, the negligible increase in amount of P1 suggested that some internal peptide cleavage might be occurring (Figure 4.2). In an endeavour to increase the yield of P1, a digest time course comparing two enzyme:substrate ratios was employed: pGH was digested with 1:200 (w/w) and 1:500 (w/w) trypsin, and reacted for 30 minutes, 1 hour and 2 hours (Figure 4.5). There was very little change in the amount of P1 between all time points, when using 1:500 (w/w) trypsin (Table 4.3). The amount of P1 obtained using the 1:200 (w/w) trypsin was similar to the 1:500 (w/w) digest at the 30 min and 1 hour time points but greatly reduced at 2 hours. Although the peptide P5 was present in all chromatograms (Figure 4.5), the smallest amount was seen in the 30 minute incubation using 1:500 trypsin.

4.2.1.3 Preparative Isolation and Purification of pGH(96–133)

From the above results, the preparative digest was performed using an enzyme to substrate ratio of 1:500 (w/w) and a reaction time of 30 min. An initial analysis of the digest mixture by analytical RP HPLC was performed to confirm the presence of P1, pGH(96–133), (Figure 4.6 A). The elution profile obtained was consistent with the previous profile for a reaction time of 30 minutes at 1:500 (w/w) trypsin. The elution profile from the preparative

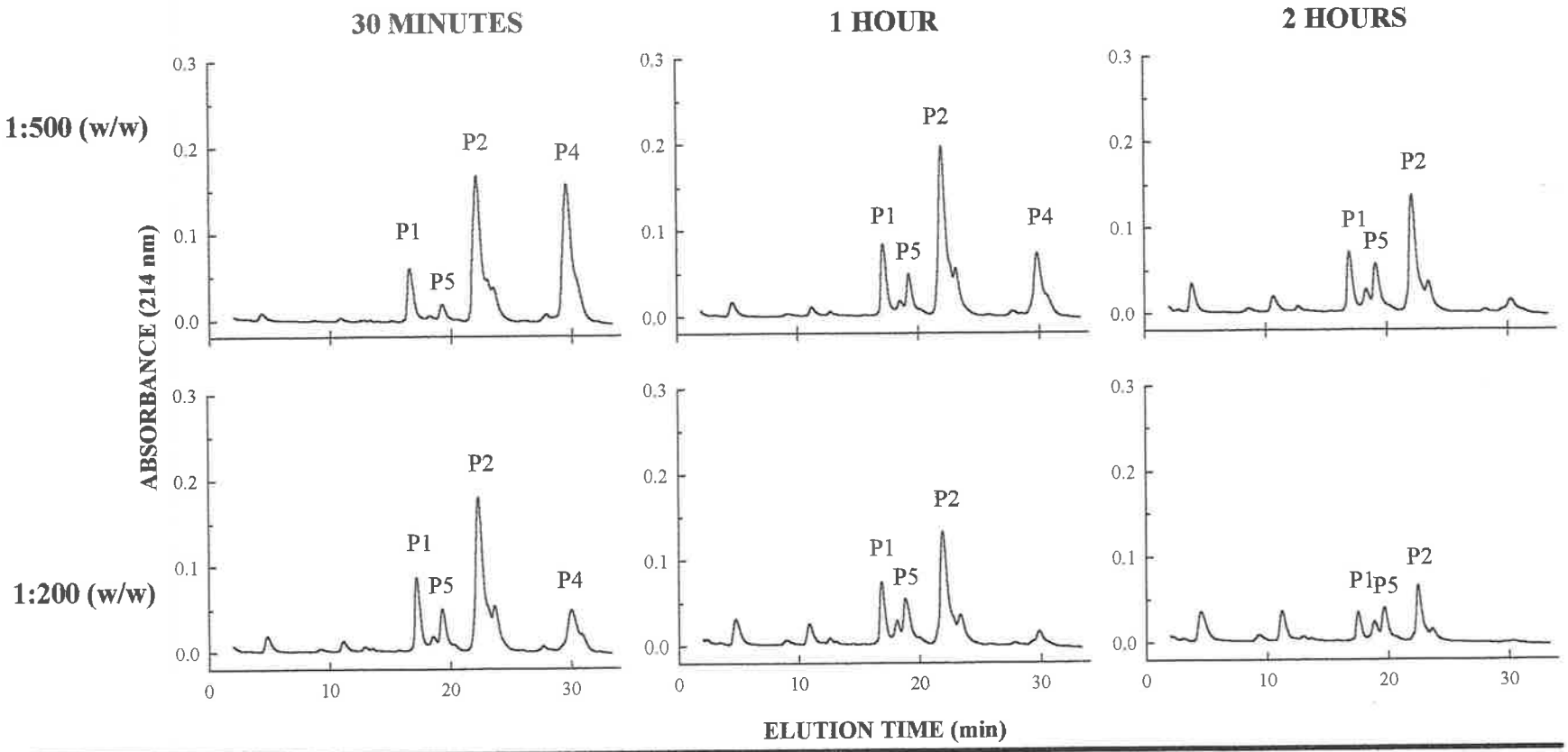

FIGURE 4.5 OPTIMISATION OF THE PARTIAL TRYPTIC DIGEST OF pGH. A 100 µl aliquot of digest reaction at each enzyme concentration and time point was analysed by RP HPLC on a C4 (20 mm i.d. x 30 mm) column, pre-equilibrated in 30% (v/v) ACN/0.1% TFA. Protein was eluted using a linear 30% (v/v) to 60% (v/v) ACN/0.1% TFA gradient, at a flow rate of 0.5 ml/min. Protein elution was monitored at 214 nm. The peptides were labeled based on the % acetonitrile at which they eluted.

[ENZYME]	QUANTITY (μg)		
	30 MINUTES	1 HOUR	2 HOURS
1:500 (w/w)	1.41	1.41	1.41
1:200 (w/w)	1.68	1.42	0.628

TABLE 4.3 QUANTITATION OF pGH 96-133. The quantity of peptide was determined as described in detail in section 2.2.3.2.

purification is shown in Figure 4.6 B. Fractions were analysed by analytical RP HPLC and P1 was detected in the back shoulder of the peak labelled b (Figure 4.6 B, highlighted in red). This purification did not afford good separation of P1, as P1 co-eluted with P2. Therefore a second RP HPLC step, using a C4 column (10 mm i.d. x 100 mm) was employed to purify P1 from P2 (see Figure 4.7 for a typical elution profile). A total of 20 runs were required to obtain sufficient material, 1 mg, for further experiments.

4.2.2 The Associated States of pGH

The associated intermediate of bGH at equilibrium is less soluble than either the native or denatured states (Brems, 1988). This was demonstrated by using an indirect two-step assay where: 1) various folding conformers, including the associated intermediate were populated at various Gdn-HCl concentrations at a protein concentration sufficient to induce the formation of the associated intermediate, 2) the various conformers were introduced, by a simple dilution, into solvent conditions that induced precipitation. Following centrifugation to remove precipitates, the remaining soluble protein was quantitated by the UV absorbance at 278 nm. The same assay has also been used to detect the presence of an associated intermediate along the equilibrium folding pathway of pGH (Bastiras, 1992) and hGH (DeFelippis *et al.*, 1993). Moreover, the assay has been used to demonstrate the ability of peptide fragments spanning the third helix of both bGH and hGH to inhibit the formation of the associated intermediate of bGH and hGH during refolding (Brems *et al.*, 1986; Brems, 1988; Lehrman *et al.*, 1991; DeFelippis *et al.*, 1993).

In this study, a similar indirect two-step assay to that described above was used to determine: 1) the relative solubility of the associated state at pH 2.0 in the absence and

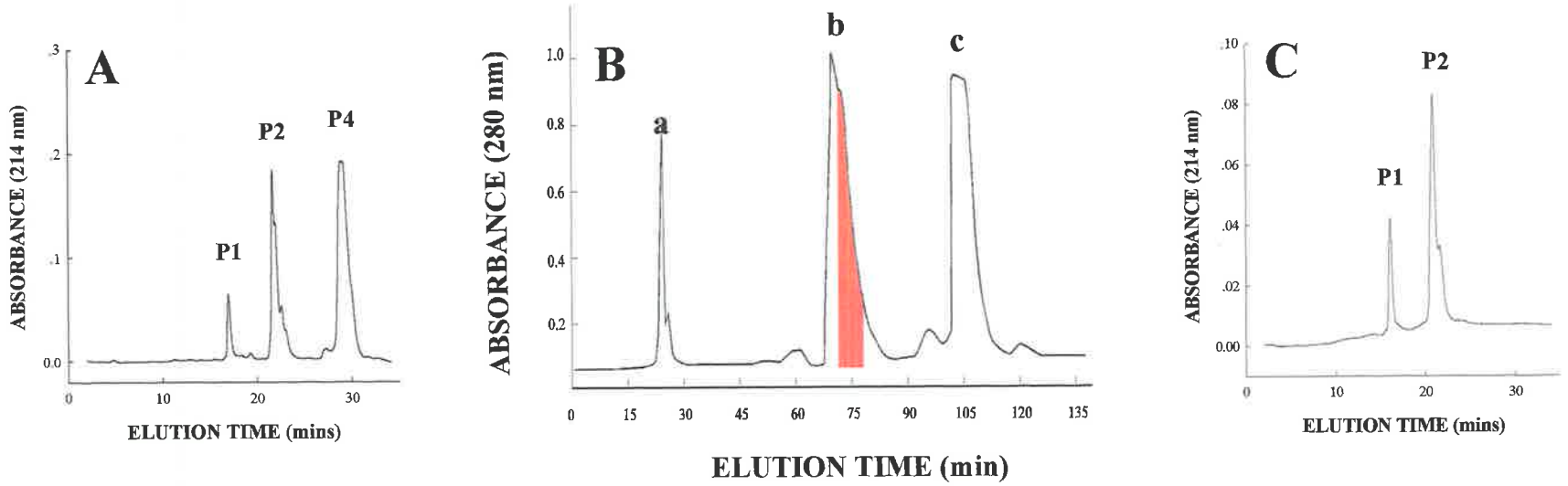

FIGURE 4.6 PREPARATIVE ISOLATION AND PURIFICATION OF pGH(96-133).

A: ANALYSIS OF THE PREPARATIVE DIGEST BY ANALYTICAL RP HPLC. A 100 µl aliquot of the preparative digest was analysed on a 20 mm i.d. x 30 mm C4 column, pre-equilibrated in 30% (v/v) ACN/0.1% TFA. Protein was eluted using a linear gradient of 30% to 60% (v/v) ACN in 0.1% TFA, at a flow rate of 0.5 ml/min. Protein elution was monitored at 214 nm.

B: PURIFICATION OF THE PREPARATIVE DIGEST BY RP HPLC. A 500 ml sample of preparative digest was loaded onto a, 47 mm i.d. x 300 mm C4 column, pre-equilibrated in 0.1% TFA at a flow rate of 25 ml/min. Protein was eluted by a step-wise ACN gradient from 0% to 30% (v/v), 30% to 60% (v/v) and 60% to 80% (v/v) in 0.1% TFA, at a flow rate of 25 ml/min. Protein elution was monitored at 280 nm.

C: ANALYSIS OF THE POOLED FRACTIONS FROM THE REGION HIGHLIGHTED IN RED IN GRAPH B USING ANALYTICAL RP HPLC. A 250 µl aliquot from each of the preparative digest fractions was lyophilised, followed by resuspension in 150 ul of 0.1% TFA. 100 µl was analysed on a 20 mm i.d. x 30 mm C4 column, pre-equilibrated in 30% (v/v) ACN/0.1% TFA. Protein was eluted using a linear gradient of 30% to 60% (v/v) ACN in 0.1% TFA, at a flow rate of 0.5 ml/min. Protein elution was monitored at 214 nm.

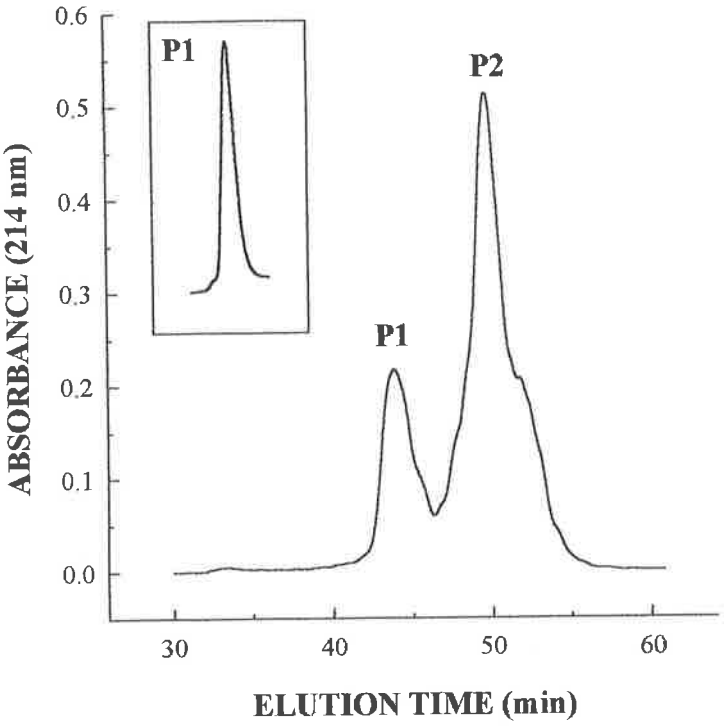

FIGURE 4.7 SECOND RP HPLC PURIFICATION STEP. Fractions collected from the preparative RP HPLC column, containing P1 and P2 were pooled together and lyophilised. The lyophilised protein was resuspended in 10% ACN and acidified before being loaded onto a C4 PREP 10 column (10 mm i.d. x 100 mm), pre-equilibrated in 30 % ACN/0.1% TFA. Protein was eluted using a linear gradient of 30% (v/v) to 60% (v/v) ACN in 0.1% TFA, at a flow rate of 2 ml/min. Protein elution was monitored at 214 nm. Inset: fractions containing P1 were collected and a 50 µl aliquot was analysed by analytical RP HPLC to confirm the homogeneity of pGH(96–133).

presence of 4 M urea, and 2) to determine if pGH(96–133) could inhibit the formation of the associated intermediate.

4.2.2.1 Solubility of the Associated States of pGH at pH 2.0

To examine the solubility characteristics of the associated states of pGH at pH 2.0, the refolding reaction was studied as a function of initial urea concentration using a protein concentration of 2 mg/ml. Refolding was initiated by dilution into a non-denaturing solution at a final concentration of 1 M urea, pH 8.0. Figure 4.8 illustrates the percentage of soluble pGH at pH 2.0, as a function of urea concentration following the precipitation step. In the absence of urea, approximately 35% of the protein precipitated when diluted to pH 8.0 and 1 M urea. At 4 M urea, as much as 85% of the protein precipitated when diluted to pH 8.0 and 1 M urea. Even at 9 M urea, 45% of the protein was found to precipitate.

4.2.2.2 The Effect of, pGH(96–133), on the Association of pGH at pH 2.0 With or Without 4 M Urea.

For this experiment, a peptide concentration of 100 μM, equating to a molar ratio of 10:1, peptide:protein was used. The ε_{278} of pGH(96–133) in comparison to pGH is negligible (there are no aromatic residues in the peptide), so any peptide remaining in solution would not contribute to the final absorbance at 278 nm. The addition of pGH(96-133) had no significant effect, within experimental error, on the extent of precipitation at pH 2.0 without urea (Figure 4.9). At pH 2.0 in the presence of 4 M urea, the addition of pGH(96-133) inhibited precipitation by approximately 25%. The change in intrinsic fluorescence and λ_{max} of pGH at pH 2.0 in the absence and presence of 4 M urea and pGH(96-133) is shown in Figure 4.10. Spectra obtained without the addition of the pGH(96-133) peptide

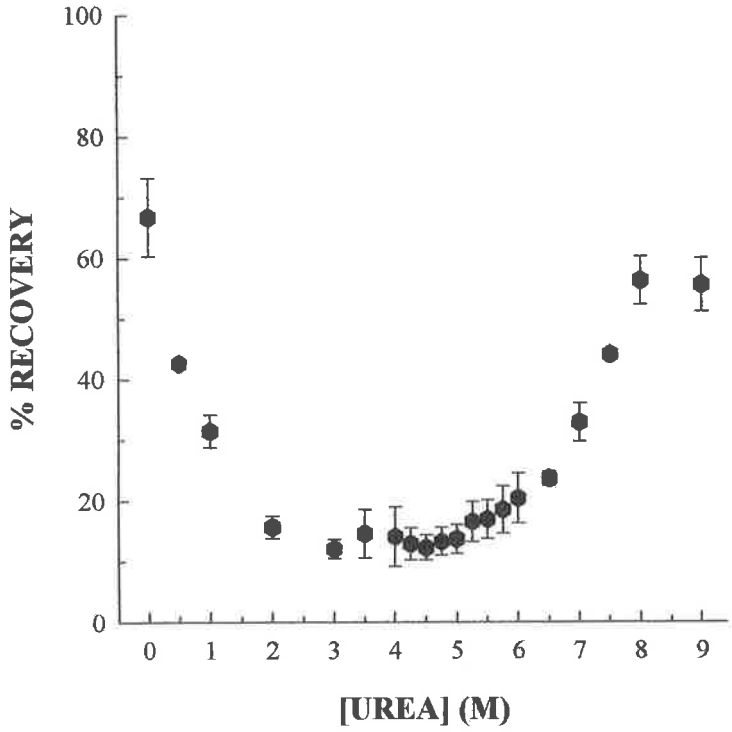

FIGURE 4.8 THE EFFECT OF UREA CONCENTRATION ON THE SOLUBILITY OF pGH at pH 2.0. Porcine growth hormone, at an initial concentration of 2 mg/ml, was incubated in varying concentrations of urea at pH 2.0. Each sample was then diluted to 1.0 M urea, pH 8.0 and 0.18 mg/ml. The amount of pGH remaining soluble was calculated from an absorbance measurement at 278 nm. The error bars represent the standard error of the mean value ($n = 3$).

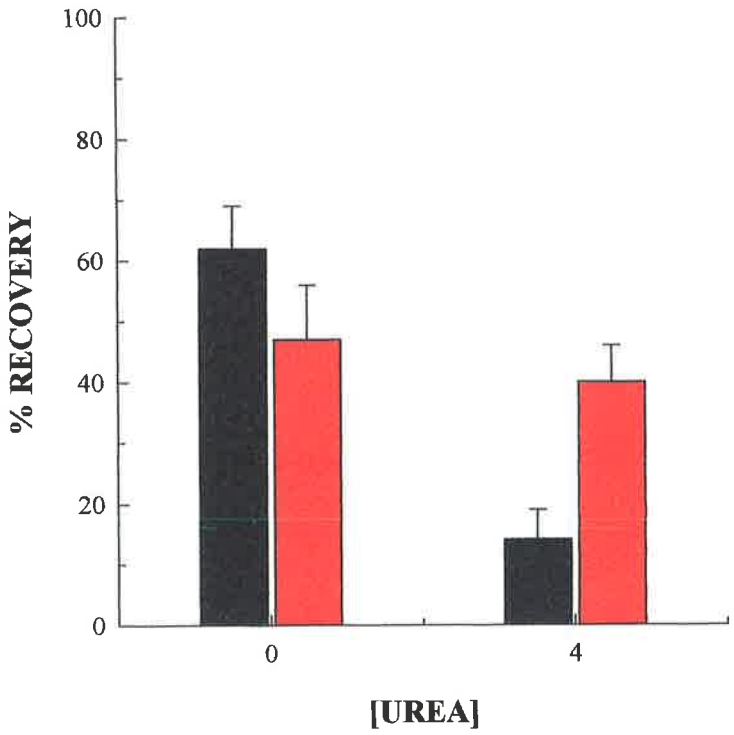

FIGURE 4.9 THE EFFECT OF pGH(96–133) ON THE SOLUBILITY OF pGH AT pH 2.0 IN THE ABSENCE AND PRESENCE OF 4 M UREA. Porcine growth hormone, at an initial concentration of 2 mg/ml, was incubated in the absence and presence of 4 M urea, with or without the addition of a 10-fold molar excess of pGH(96–133). Each sample was then diluted to a final concentration of 0.18 mg/ml pGH in 1.0 M urea, pH 8. The amount of pGH remaining soluble was calculated from an absorbance measurement at 278 nm on the supernatant after centrifugation at 12000 x g for 10 min. The error bars represent the standard error of the mean value ($n = 3$).

Black column: refolding without pGH(96–133).
Red column: refolding with pGH(96–133).

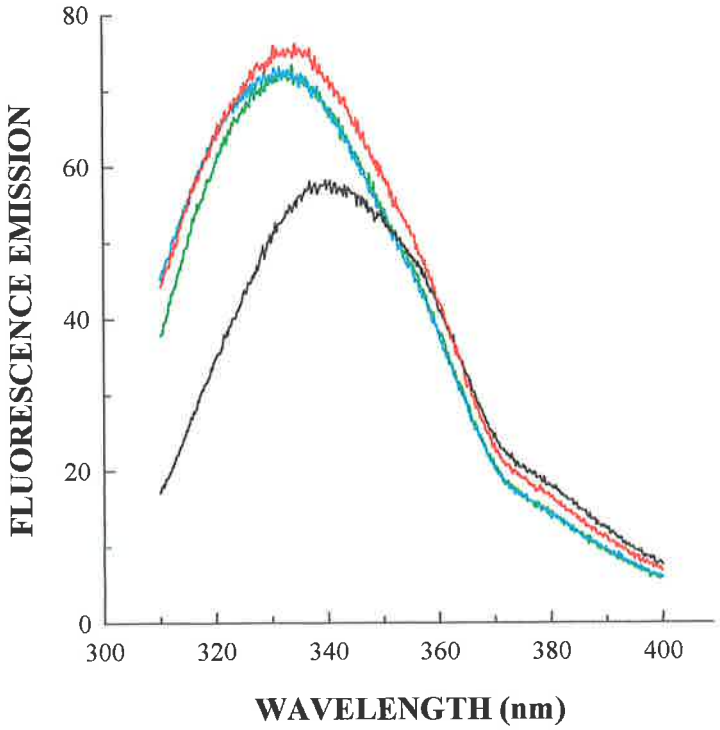

FIGURE 4.10 FLUORESCENCE EMISSION SPECTRA OF pGH AT pH 2.0, IN THE ABSENCE AND PRESENCE OF 4 M UREA AND pGH(96–133). Emission spectra were recorded as outlined in 2.2.5. The pGH concentration was 0.2 mg/ml. pGH(96–133) was at a 10-fold molar excess.

pH 2.0 - 4 M urea - pGH(96-133) — — —
pH 2.0 - 4 M urea + pGH(96-133) ——
pH 2.0 + 4 M urea - pGH(96-133) ——
pH 2.0 + 4 M urea + pGH(96-133) ——

are consistent with the spectra obtained in Chapter 3 (3.2.1). At pH 2.0 in the absence of urea, the addition of pGH(96-133) does not effect the relative fluorescence emission intensity or the λ_{max}. In contrast, when pGH(96-133) is included at pH 2.0 in the presence of 4 M urea, the relative fluorescence emission increases and is comparable to that at pH 2.0 in the absence of urea. In concert, the λ_{max} is blue-shifted from 344 ± 1.0 nm to 333 ± 1.0 nm, similar to the value of λ_{max} at pH 2.0 without urea (Chapter 3; 3.2.1).

4.3 DISCUSSION

The formation of protein aggregates from the self-association of partially denatured or misfolded proteins is a competitive off-pathway reaction in both *in vitro* and *in vivo* protein folding. Protein association, *in vitro*, is often a causative agent for technical and economical problems in the pharmaceutical and biotechnology industries. Of critical importance is the effect of protein association *in vivo*, where the pathology of a number of human diseases, for example the amyloidoses, is associated with the association and subsequent deposition of protein aggregates (Sipe, 1992). Specific interactions between hydrophobic surfaces in partially folded intermediates are believed to be responsible for association (reviewed in Fink, 1998). Importantly, the factors and conditions that invoke intermediate formation favour association, and ultimately it is the characteristics of these intermediates that are the important determinants of association.

The partial denaturation of bGH invokes the exposure of the hydrophobic surface of the third helix. If the protein concentration is sufficiently high, the hydrophobic face of one amphipathic helix will interact with complementary surfaces of adjacent molecules, resulting in the formation of the associated intermediate (Brems *et al.*, 1986). It was proposed that the hydrophobic surface of helix 3, bGH(96–133), interacted with the exposed hydrophobic surface of partially denatured bGH to prevent the self-association of bGH intermediates.

Self-association of pGH at pH 2.0 and in the absence of urea

The addition of pGH(96–133) had no significant effect on the association reaction of pGH at pH 2.0 without 4 M urea. This suggests that the hydrophobic face of helix 3 in pGH is not exposed in the partially denatured protein. Whilst there is minimal residual tertiary

structure as evidenced by the loss of signal in the near-UV CD spectra (Chapter 3, section 3.2.4.1), the majority of secondary structure is retained (Chapter 3, section 3.2.4.2). The small shift in λ_{max} is indicative of Trp86 in a hydrophobic environment; most likely remaining buried within a relatively structured hydrophobic core.

Acid is a highly specific unfolding agent that acts at a limited number of high-affinity proton binding sites (Dill, 1990). As the net charge on a native protein is increased (e.g. from acidification), there is an increase in charge repulsion, which causes a native protein to become destabilised and unfold (Dill, 1990). For pGH at pH 2.0, charge repulsion induced by an increase in the overall net charge of the protein is not strong enough to completely unfold the protein. It is more likely that acidification causes small clefts on the surface of pGH to form, exposing a hydrophobic pocket(s) that is stabilised by association with an adjacent monomer (Figure 4.11). Subsequent self-association then proceeds by unlimited addition of dimers represented as occurring in a classical 'head to tail' fashion (Chapter 3, section 3.2.7; Table 3.3; Figure 4.11).

Self-association of pGH at pH 2.0 and in the presence of urea

The addition of 4 M urea at pH 2.0 did not measurably affect the strong formation of dimer (Chapter 3, section 3.2.7; Table 3.3). However, the subsequent head to tail self-association of the dimer is replaced by a discrete self-association where the largest species is an octamer (Chapter 3, section 3.2.7; Table 3.3). This implies that the presence of urea at pH 2.0 acts to remove some binding sites from the surface of the partially folded pGH monomer and creates new self-association sites, which ultimately change the conformation and subsequent association of the dimer.

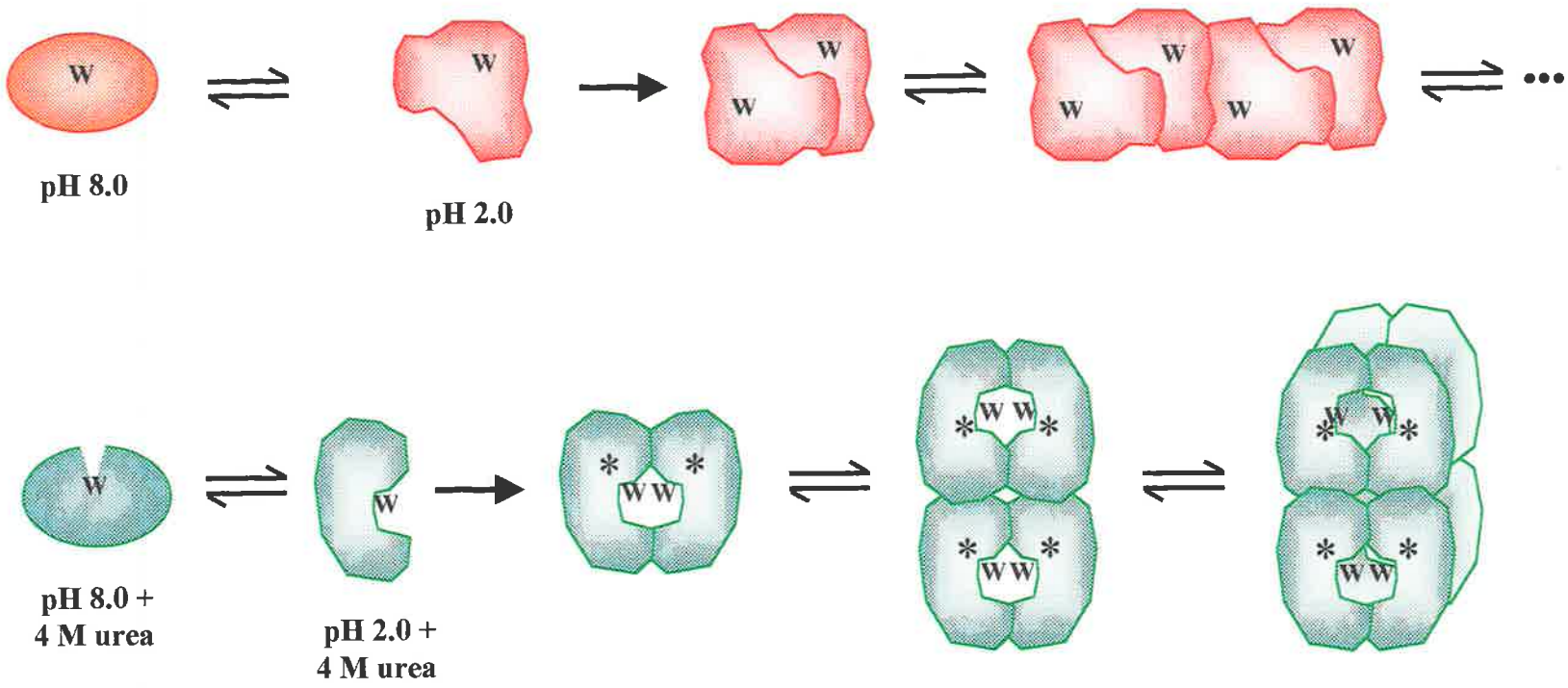

FIGURE 4.11 THEORETICAL MODELS OF pGH SELF-ASSOCIATION AT pH 2.0 IN THE ABSENCE AND PRESENCE OF 4 M UREA. The solid arrows, describing the first step at pH 2.0 and at pH 2.0 + 4 M urea, represent equilibria which could not be observed over the concentration range of pGH measured in the analytical ultracentrifuge. The association constants are estimated to be $\geq 5 \times 10^6\ M^{-1}$. All other steps are represented by equilibrium signs. "W" represents Trp86 which is partially exposed to solvent at pH 8.0 + 4 M urea and further exposed at pH 2.0 + 4 M urea but apparently still in a highly asymmetric environment (*).

The addition of pGH(96–133) reduced precipitation upon the refolding of pGH from pH 2.0 and 4 M urea, consistent with the peptide fragment preventing self-association of pGH intermediates. The inhibition of precipitation upon refolding seen in this study is similar to that observed for the refolding of bGH and hGH in the presence of the analogous fragment from each protein (Brems, 1988; DeFelippis *et al.*, 1993). This suggests that the intermediate of pGH at pH 2.0 and 4 M urea is structurally similar to the associated intermediate(s) of bGH and hGH in partially denaturing Gdn-HCl concentrations. Whilst there is no experimental evidence to show that pGH(96–133) is involved in the association of the pGH intermediate(s) in partially denaturing Gdn–HCl concentrations, the similarities in the physical characteristics with bGH and hGH would suggest that this is likely.

DeFelippis *et al.*, (1993), obtained direct evidence for the involvement of peptide fragments from the third helix of bGH and hGH in the association of partially denatured hGH. The addition of the peptide fragments increased the recovery of the monomer, which suggests that the fragment is preventing dimer formation. More recently, in a study of the conformational equilibria of hGH (Kasimova *et al.*, 1998), the hydrophobicity content of the surface in the native state and partially folded conformation was calculated at 58% and 67% respectively (Figure 4.12). The exposed hydrophobic surface in the partially folded conformation was shown to be covered to a large extent by the helix 3 containing peptide, which had been previously shown to prevent aggregation in refolding experiments (DeFelippis *et al.* 1993, Kasimova *et al.*, 1998). The fluorescence properties of pGH at pH 2.0 and 4 M urea were altered in the presence of pGH(96–133). The increase in the relative fluorescence emission intensity and concomitant blue shift in the λ_{max} are consistent with the removal of a fluorescence quenching group from the vicinity of Trp86 and concomitant formation of a more hydrophobic surrounding environment. The values for fluorescence

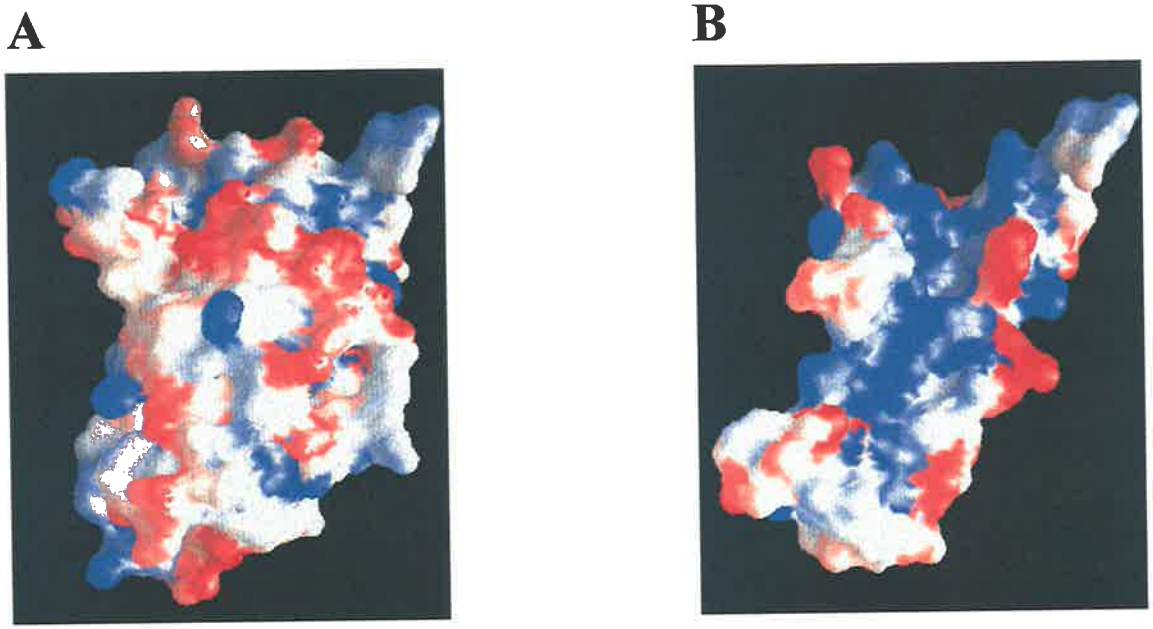

Figure 4.12 THE CALCULATED HYDROPHOBICITY CONTENT OF rhGH.

A. The calculated surface for the native state.

B. The calculated surface of the partially folded monomer.

The hydrophobic residues are coloured blue and polar residues are coloured red. The hydrophobicity surface was calculated according to the structural parameters described by Luque and Freire (1998).

Adapted from Kasimova *et al.*, 1998

emission intensity and λ_{max} are similar to those obtained for pGH at pH 2.0 and no urea. From this data it is plausible to suggest that pGH(96–133) associates with the partially denatured pGH monomer in a similar way to that described above for hGH.

It is proposed that the combination of acid and 4 M urea act to partially denatures pGH, invoking the exposure of the hydrophobic face of helix 3 and a large hydrophobic cleft formed by the other 3 helices, without gross structural perturbation. Note that at pH 2.0 and 4 M urea, 75% of the α-helix is still present. The uncompensated exposure of this surface leads to a highly unstable situation, which is satisfied by associating with a complementary surface on an adjacent monomer. In growth hormone, the protein strands connecting α-helices 1 and 2, and 3 and 4 permit separation of these α-helical pairs without the concomitant loss of protein secondary structure (Abdel-Meguid *et al.*, 1987). Interestingly, during the construction of a pGH model by Bastiras, (1992), the flexibility of helix 3 became apparent. The helix was able to easily "swing out" on a "hinge" peptide connected to helix 4 without disrupting the rest of the model. Therefore, association of partially denatured monomer may result from intermolecular packing of helix 3 from the first monomer with helices from the second monomer, stabilising the associated state via the hydrophobic effect. Electrostatic interactions may also play a role. From the model of the predicted amphipathic helix (Figure 4.1), Glu117 is located in the hydrophobic face of helix 3 and when ionised, may perturb the hydrophobic surface. Protonation of this residue would potentially relieve this, increasing the chance for intermolecular hydrophobic packing (Brems *et al.*, 1987b). If the exposed hydrophobic cleft is, as anticipated, similar to that for rhGH described above, the intermolecular packing of helix 3 from an adjacent partially denatured monomer, would re-establish a hydrophobic environment surrounding Trp86, which is consistent with the fluorescence data we observe in this study. The

association of an intact but partially folded molecule may encounter steric hindrance, particularly if intermolecular helix packing is necessary to stabilise the associated state. It is therefore proposed that in the dimer, Trp86 would be located at the dimer interface, creating a unique microenvironment that is responsible for the CD and second-derivative spectroscopy signals reported in Chapter 3 (Figure 4.11).

The addition of pGH(96-133) to pGH at pH 2.0 and 4 M urea did not completely abolish precipitation and therefore association. Similarly, the analogous peptide fragments from both bGH and hGH were not able to completely inhibit association of partially denatured bGH and hGH (Brems *et al.*, 1986; Brems, 1988; DeFelippis *et al.*, 1993). Moreover, the peptide from each species exhibited different potencies on the ability to inhibit self-association of the partially denatured proteins, which was attributed to the extent of helix structure for each peptide at a given concentration (Lehrman *et al.*, 1990; DeFelippis *et al.*, 1993). The helix content of the peptide fragment bGH(96–133) is dependent on both the pH of solution and peptide concentration, with enhanced helix stability achieved through intermolecular association (Brems *et al.*, 1987b). With the similarity between bGH(96–133) and pGH(96–133) it is likely that pGH(96–133) shares the same properties. It is proposed that the addition of 4 M urea may destabilize the helicity of pGH(96–133) thus reducing its potential to associate with partially denatured pGH. However, it is also reasonable to suggest that at the concentration of peptide used in this study (10 molar excess), self-association of the peptide fragments may be a competitive reaction, reducing the amount of peptide monomer available to associate with partially denatured pGH. Another possibility is that other partially unfolded sites may be involved in the association process. For example, formation of the monomer–pGH(96-133) complex creates new self-association sites, as schematically outlined in Figure 4.13. This "new" associated species

then precipitates upon refolding. It would be interesting to subject this system to sedimentation equilibrium experiments to resolve the mode of association. The associated intermediate(s) of partially denatured pGH at pH 2.0, 4 M urea and 3 M Gdn–HCl, pH 9.1 are structurally similar (Chapter 3 and this Chapter). It is interesting that a combination of low pH and urea has an apparently similar denaturation potential as that of 3 M Gdn–HCl at alkaline pH. Urea and Gdn–HCl are commonly used as protein denaturants but there is yet to be a well-defined molecular description of the interaction of these denaturants with proteins. For small proteins Gdn–HCl is approximately twice as effective as a denaturant as urea (Myers *et al.*, 1995). In a study examining the helix unfolding of a series of peptides as a function of Gdn–HCl, the *m*-value (defined as the slope of a linear plot of the free energy of helix formation as a function of molar concentration of Gdn–HCl), was found to be strongly dependent on the total ionic strength of the solution (Smith and Scholtz, 1996). The homologous series of peptides were also used to examine urea denaturation (Scholtz *et al.*, 1995) and comparison of the *m*-values revealed that Gdn–HCl was approximately twice as effective as a denaturant as urea, in agreement with other studies on proteins. However, when the ionic strength of Gdn–HCl was controlled with NaCl, the *m*-value for Gdn–HCl was separated into two components: one that was identical to that found for urea and a second, which was dependent on the molar concentration of the chloride ion. In this study, the pH of solution was altered using 1 M HCl, thus providing a source of chloride ions, which, in combination with 4 M urea, are apparently as effective in partially denaturing pGH as 3 M Gdn–HCl at pH 9.1.

In conclusion, acidification invoked the partial unfolding of pGH and the formation of discrete, structurally distinct intermediates with a high propensity to self-associate. The final conformation and mode of self-association was strongly dependent on the solvent

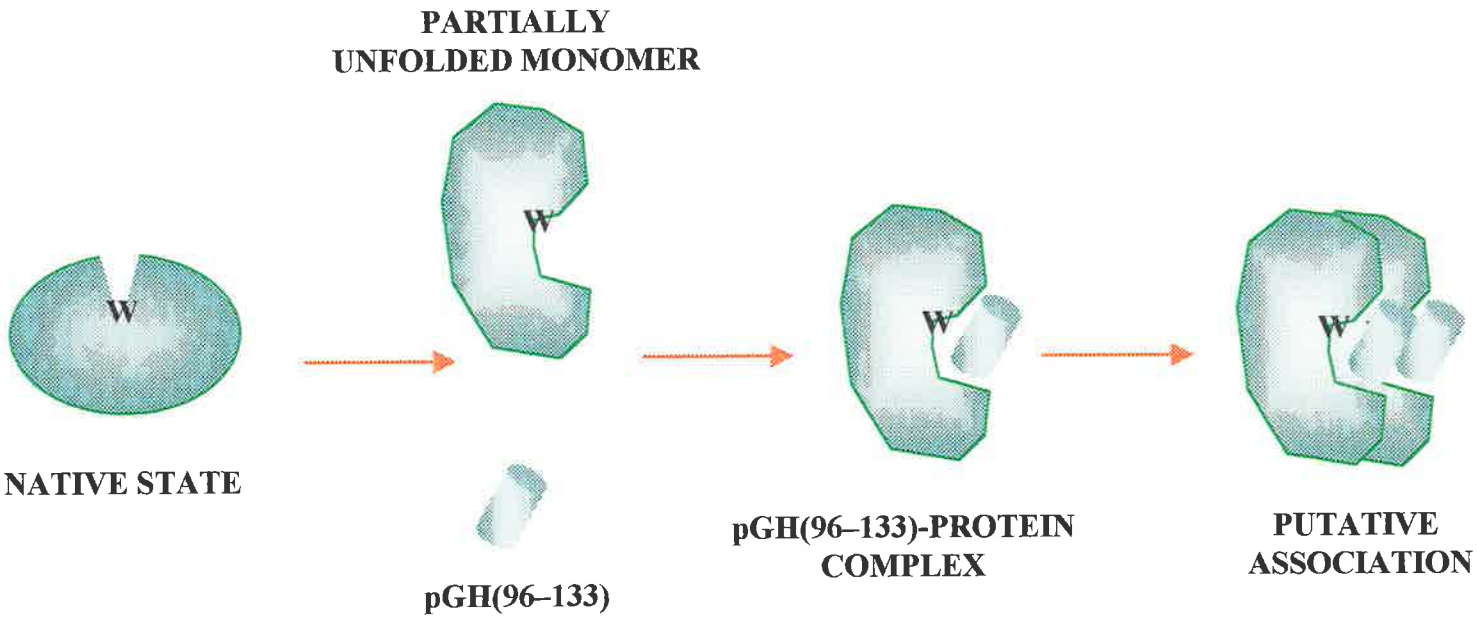

FIGURE 4.13 SCHEMATIC REPRESENTATION OF PROPOSED pGH(96–133)—PROTEIN COMPLEX AND SUBSEQUENT ASSOCIATION. "W" represents Trp86.

conditions employed. The sequence spanning helix 3 of pGH, pGH(96–133) has been shown to reduce the precipitation of pGH on refolding, thus elucidating at least one molecular association site. These findings may be important to understanding the details of protein folding and aggregation *in vivo*. Peptides which retain structure in solution, may be designed as a possible therapeutic for aggregation associated diseases, but, more than one therapeutic agent may be required.

CHAPTER 5

ACID–DENATURATION OF RECOMBINANT PORCINE GROWTH HORMONE ANALOGUES

5.1 INTRODUCTION

Protein engineering is a technique that has been used extensively to study protein folding. Whilst chemical and physical methods can characterise an overall folding mechanism, little information is provided about the actual interaction(s) involved in the folding process (Engelhard and Evans, 1996). By specifically mutating individual, or a group of amino acid residues, the quantitative roles of that residue(s) in the protein folding process may be ascertained. For example, determining the effect a mutation can have on the conformational stability of a protein can help us understand the interactive forces involved in the acquisition of the unique fold of the native state (Matthews, 1993). There are also many examples of where site directed mutagenesis has been used to study folding intermediate(s) (Brems *et al.*, 1988; Lehrman *et al.*, 1991; Sanz and Fersht, 1993).

Comparison of the acid-induced denaturation of pGH, bGH and hGH highlighted that, within a family of proteins, folding intermediates can display a great range of structural variability. At Bresagen Ltd, various analogues of pGH had been made to study ligand/receptor binding (Rowlinson *et. al.*, 1994) and the reduction of aggregation in a potential commercial refolding process. For commercial purposes rGH had also been produced. Despite not being specifically designed to study protein folding, a number of the pGH analogues have been used in the systematic evaluation of mutational effects on pGH conformational stability (Bastiras, 1992). For the focus of this chapter, three of the pGH analogues, pGH(M8), pGH(M17) and pGH(M31) and rGH were chosen for further characterisation by acid-induced denaturation, with the aim of gaining further insight into the physical properties of the intermediate state(s) of pGH (for clarity pGH will now be referred to as wild-type pGH).

The three pGH analogues used in this study are listed in Table 5.1, and the location of each mutated residue on the pGH model (Rowlinson *et al.*, 1994) is shown in Figure 5.1. The analogue pGH(M8) contains a methionine to tryptophan substitution at residue 124 in helix 3. The insertion of the tryptophan was designed to act as a fluorescence reporter group to monitor helix 3 mobility and the putative self-association reaction during refolding. Previous equilibrium denaturation studies of pGH(M8), showed that folding/unfolding was more closely approximated by a two-state mechanism, since it was observed that the population of a folding intermediate was diminished (Bastiras, 1992). It was therefore of interest to see whether a folding intermediate could be populated under acidic conditions. In pGH(M17), lysine and arginine at residues 30 and 34 respectively, located on the C terminal end of helix 1, have both been changed to glutamic acid. This double mutant was originally designed to introduce a second calcium binding site in this region (Rowlinson *et al.*, 1994). The inclusion of two glutamic acid residues results in a more acidic protein when compared to wild-type pGH. From computational analysis (DNASIS), the apparent isoelectric point (pI) of pGH(M17) is 5.36 compared to the pI of 7.1 for wild-type pGH. The pI of pGH(M17) is similar to the pI of 5.14 for hGH, which was found to remain essentially native when subjected to acid-mediated denaturation (DeFelippis *et al.*, 1995). The inclusion of pGH(M17) in this study was to determine if the more acidic protein would form a folding intermediate similar to hGH or wild-type pGH. The analogue pGH(M31) contains the hGH sequence between helix 2 and helix 3. In wild-type pGH, the short connection between helix 2 and helix 3 has an Omega loop conformation (Abdel-Meguid *et al.*, 1987), which, in hGH is a short helix. This difference in conformation was proposed to contribute to the increased stability of hGH (Bastiras, 1992). More recently Gdn–HCl equilibrium denaturation studies of pGH(M31) have shown this protein to have the same apparent conformational stability as wild-type pGH, but the stable

pGH ANALOGUE	MUTATION
pGH(M8)	Met124Trp
PGH(M17)	Lys30Glu; Arg34Glu
PGH(M31)	Thr98Ala; Phe103Tyr; Thr105Ala

TABLE 5.1 LIST OF pGH ANALOGUES USED IN THE ACID–DENATURATION AND KINETIC STUDIES. The mutation is designated as follows: the wild-type pGH amino acid residue, the residue position (Abdel Meguid *et al.*, 1987), amino acid substitute.

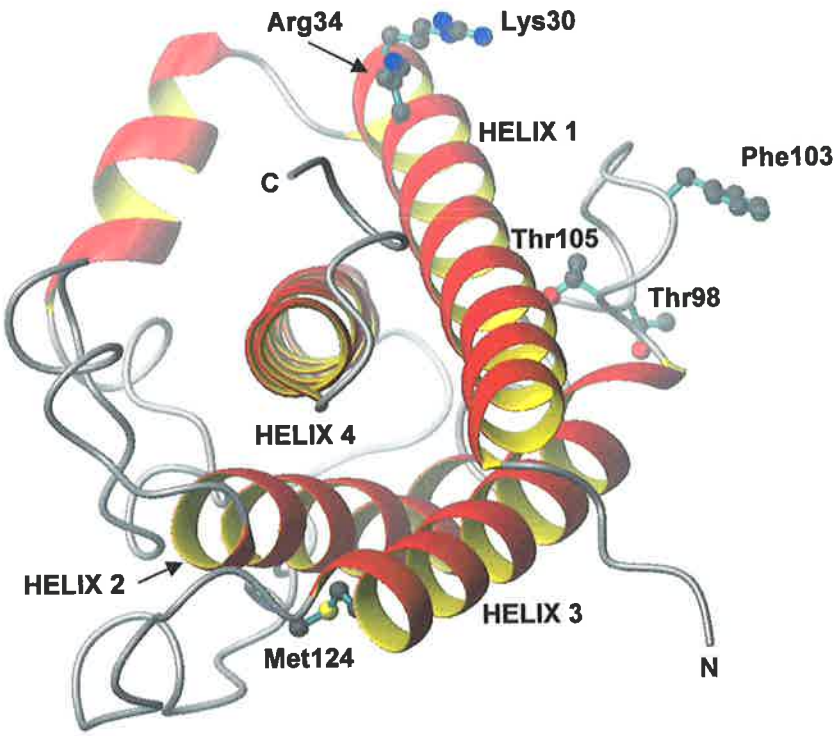

FIGURE 5.1 LOCATION OF MUTATED AMINO ACID RESIDUES ON THE pGH MOLECULE. The structure of pGH was obtained by energy minimisation (Rowlinson *et al.*, 1994). The amino and carboxyl terminus is denoted by N and C respectively. The heavy atoms of each mutated amino acid residue are highlighted. The amino acid numbering system is according to Abdel-Meguid *et al.*, (1987).

Figure prepared with the program MOLMOL (Koradi *et al.*, 1996)

folding intermediate(s) have an increased propensity to associate (S. Bastiras, personal communication). It was of interest to see the effect of this sequence change in acidic conditions. With the variability between other members of the growth hormone family, rGH was included in the study. The amino acid sequences of wild-type pGH (Seeburg *et al.*, 1983) and rGH (Page *et al.*, 1981) are shown in Figure 5.2. The location of each varied residue is shown on the model of wild-type pGH (Figure 5.3). All but one of the polymorphisms in rGH are located within the loop regions of the protein and are reasonably conservative. The amino acid substitution at position 125, where an arginine residue has been replaced with a glutamine is found within helix 3.

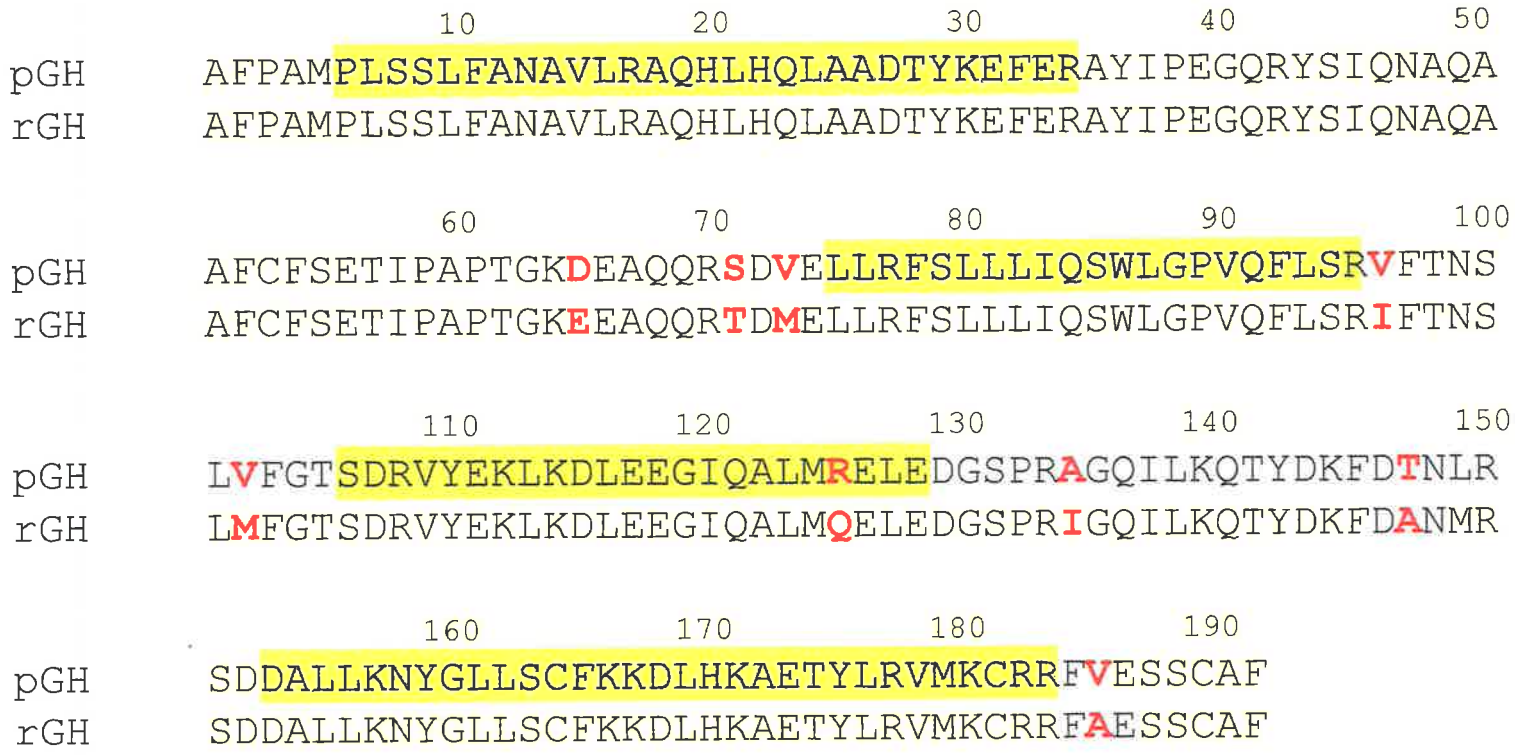

FIGURE 5.2 AMINO ACID SEQUENCES OF PORCINE GROWTH HORMONE AND RAT GROWTH HORMONE. Amino acid residue differences between pGH and rGH are highlighted in red. The positions of the four helices in pGH are highlighted by yellow boxes.

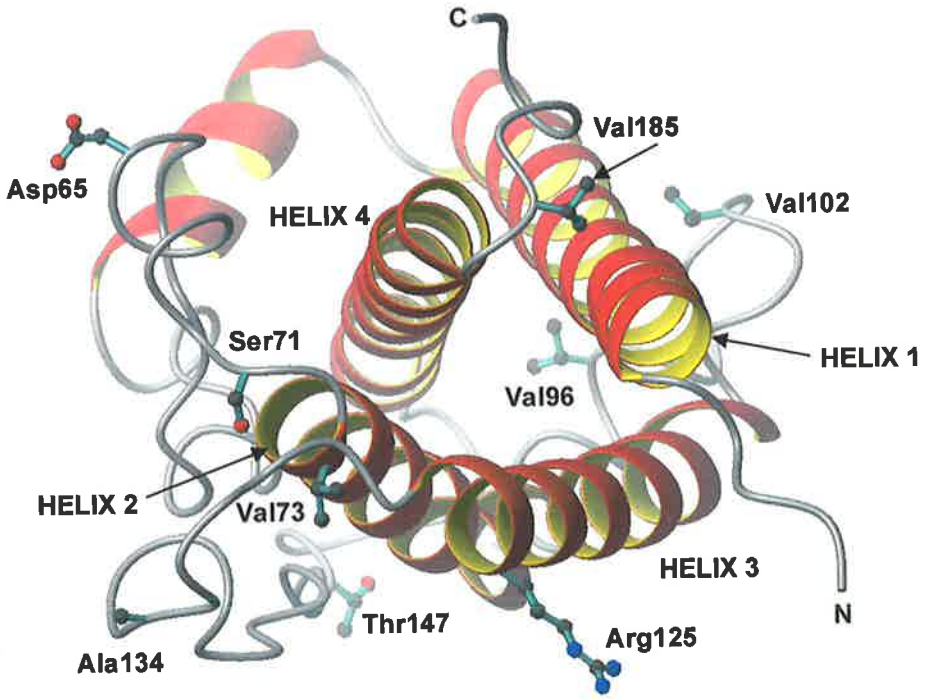

FIGURE 5.3 LOCATION OF AMINO ACID RESIDUES ON THE pGH MOLECULE THAT ARE SUBSTITUTED IN rGH. The structure of pGH was obtained by energy minimisation (Rowlinson *et al.*, 1994), based on the hGH/hGH receptor crystal structure (de Vos *et al.*, 1992). The N-terminus and C- terminus is denoted by N and C respectively. The heavy atoms of each amino acid residue are highlighted. The amino acid numbering system is according to Abdel-Meguid *et al.*, (1987).

Figure prepared with the program MOLMOL (Koradi *et al.*, 1996)

5.2 RESULTS

5.2.1 Changes in Conformation as Determined by Intrinsic Fluorescence

pGH(M8) In the absence of 4 M urea, the change in the relative fluorescence intensity (I_{340}) profile of pGH(M8) was clearly biphasic through the transition from pH 8.0 to pH 2.0 (Figure 5.4 A). I_{340} decreased between pH 8.0 and pH 5.0, reaching a minimum at pH 4.9. An increase in I_{340} was observed between pH 5.0 and 3.0 with no apparent change between pH 3.0 and pH 2.0. There was only an apparently small change in the fluorescence intensity at pH 8.0 and pH 2.0. The accompanying values of λ_{max} followed a monophasic transition (Figure 5.4 B), with an overall blue shift from 343 ± 0.5 nm at pH 8.0 to 335 ± 0.5 nm at pH 2.0.

At pH 8.0 the I_{340} was greater in the presence of 4 M urea, than in its absence (Figure 5.4 A). In contrast, there was a decrease in λ_{max} of 3 nm (Figure 5.4 B). At pH 2.0, I_{340} had decreased to a value similar to that observed at pH 2.0 in the absence of urea. Within the pH range examined, two acid–induced transitions were observed, with midpoints at approximately pH 6.3 and pH 3.9 (Figure 5.4 A; Table 5.2). A small blue shift in the λ_{max} from 340 ± 0.5 nm to 337 ± 0.5 nm at pH 8.0 and pH 2.0 accompanied the change in I_{340} (Figure 5.4 B).

pGH(M17) The acid–induced denaturation of pGH(M17) as monitored by I_{340} is shown in Figure 5.5 A. In the absence of 4 M urea, a gradual decrease in I_{340} within the pH range 8.0–5.0 was observed. In the pH range 5.0–2.0 the data followed a smooth sigmoidal curve with an approximate 3-fold increase in I_{340} and an apparent midpoint at pH 3.92 (Figure 5.5 A; Table 5.2). The change in λ_{max} was only marginal throughout the pH range

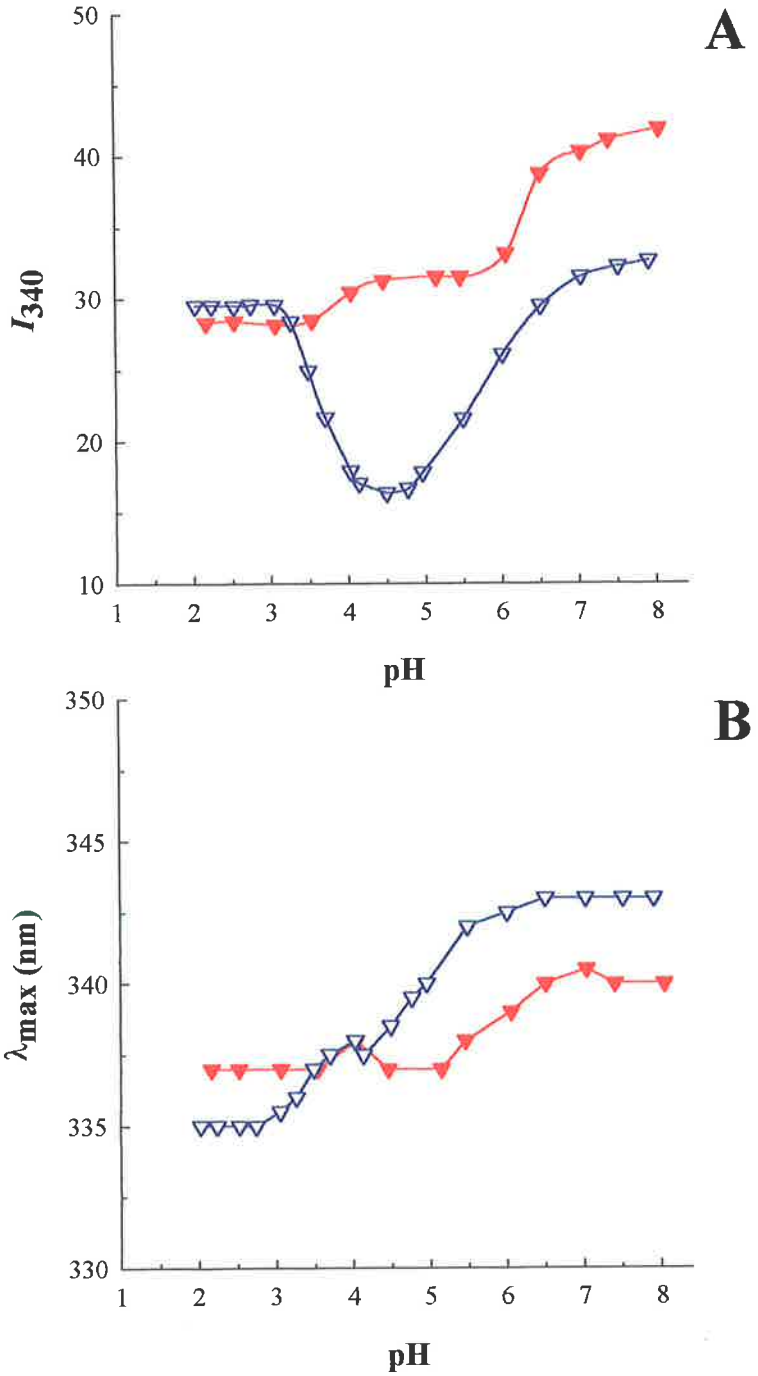

FIGURE 5.4 ACID-INDUCED DENATURATION OF pGH(M8) MONITORED BY FLUORESCENCE SPECTROSCOPY. Fluorescence emission spectra were recorded as described in 2.3.2.2. The protein concentration was 0.22 mg/ml. The data are representative of n = 5 experiments.

A relative fluorescence intensity at 340 nm (I_{340}):

- urea ▽ + urea ▼

The solid lines are the calculated curves determined from non-linear regression analysis of the raw data, using Equation 2, as described in 2.3.2.1.

B effect of acid on the maximum emission wavelength (λ_{max}):

- urea ▽ + urea ▼

pGH ANALOGUE	FLUORESCENCE MINUS UREA	FLUORESCENCE PLUS UREA	UV ABSORBANCE MINUS UREA	UV ABSORBANCE PLUS UREA
wild-type pGH	4.08 ± 0.06	5.16 ± 0.06	3.59 ± 0.03	5.11 ± 0.04
pGH(M8)	ND[a]	ND[a]	3.59 ± 0.05	4.90 ± 0.03
pGH(M17)	3.92 ± 0.06	4.39 ± 0.18	3.65 ± 0.18	5.14 ± 0.04
pGH(M31)	4.02 ± 0.06	5.50 ± 0.07	3.64 ± 0.05	5.42 ± 0.04
rGH	4.29 ± 0.03	5.44 ± 0.04	3.35 ± 0.10	4.86 ± 0.03

TABLE 5.2 SUMMARY OF MIDPOINTS FOR THE ACID-INDUCED TRANSITIONS OF WILD-TYPE pGH, pGH ANALOGUES AND rGH, IN THE PRESENCE AND ABSENCE OF 4 M UREA, MEASURED BY DIFFERENT SPECTROSCOPIC TECHNIQUES. All data were fitted by non-linear regression using the equation by Oliveberg *et. al.*, 1994 for I_{340} or using a sigmoidal function (Bailey & Ollis, 1986). The reported values are the mean and standard deviation between separate experiments (n = 5).

[a] Not Determined

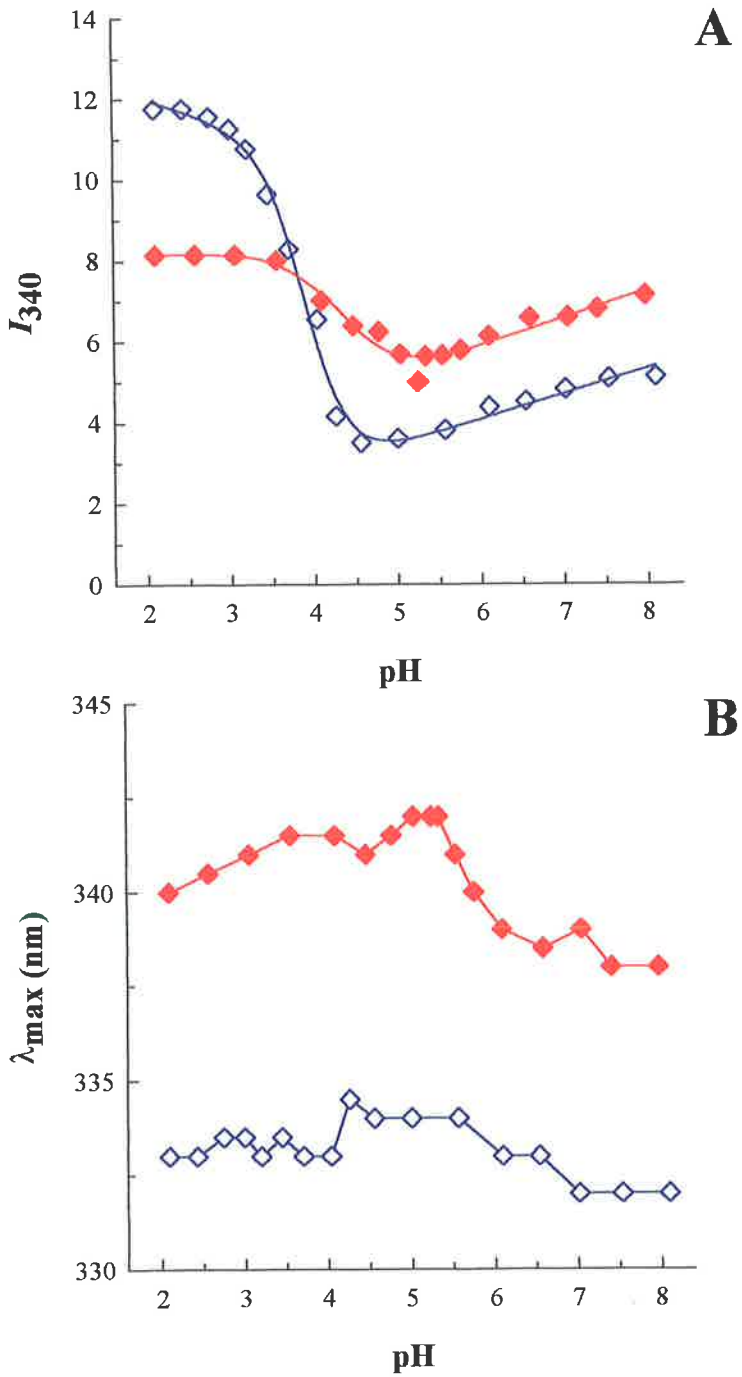

FIGURE 5.5 ACID-INDUCED DENATURATION OF pGH(M17) MONITORED BY FLUORESCENCE SPECTROSCOPY. Fluorescence emission spectra were recorded as described in 2.3.2.2. The protein concentration was 0.22 mg/ml. The data are representative of n = 5 experiments.

A relative fluorescence intensity at 340 nm (I_{340}):

- urea ◇ + urea ◆

The solid lines are the calculated curves determined from non-linear regression analysis of the raw data, using Equation 2, as described in 2.3.2.1.

B effect of acid on the maximum emission wavelength (λ_{max}):

- urea —◇— + urea —◆—

examined, with a slight red shift of 1 nm from 333 ± 0.5 nm at pH 8.0 to 334 ± 0.5 nm at pH 2.0 (Figure 5.5 B).

At pH 8.0 in the presence of 4 M urea, a 6 nm red shift in the λ_{max} to 338 ± 0.5 nm (Figure 5.5 B), was accompanied by an increase in I_{340} (Figure 5.5 A). In the pH range 8.0–5.0, a decrease in I_{340}, similar to that seen in the absence of 4 M urea was evident. In the pH range 5.0–2.0, I_{340} increased to a value only slightly above that of the folded protein at pH 8.0, with an apparent midpoint of 4.39. There was a gradual red shift in the λ_{max} to a maximum of 342.5 ± 0.5 nm. This was followed by a small blue shift back to 340 ± 0.5 nm (Figure 5.5). Interestingly, the red shift in λ_{max} occurred within the pH range 8.0–5.0, corresponding to the decrease in I_{340}.

pGH(M31) The acid–induced denaturation of pGH(M31) as monitored by I_{340} is shown in Figure 5.6 A. In the absence of 4 M urea, a gradual decrease in I_{340}, within the pH range 8.0–5.0, similar to pGH(M17) was observed. Through the pH range 5.0–2.0 I_{340} followed a smooth sigmoidal curve with an approximate 6-fold increase and an apparent midpoint at pH 4.02 (Figure 5.6 A; Table 5.2). The accompanying changes in λ_{max} are shown in Figure 5.6 B. At pH 2.0 the λ_{max} was red shifted by 4 nm from 339 ± 0.5 nm to 333 ± 0.5 nm.

At pH 8.0 and 4 M urea, the λ_{max} red shifted 7 nm to 336 ± 0.5 nm (Figure 5.6 B) and I_{340} increased (Figures 5.6 A). Through the pH range 8.0–2.0 I_{340} followed a smooth sigmoidal curve with an apparent midpoint at pH 5.5. The λ_{max} gradually increased, reaching a maximum of 345.5 ± 0.5 nm at pH 2.5 (Figure 5.6 B).

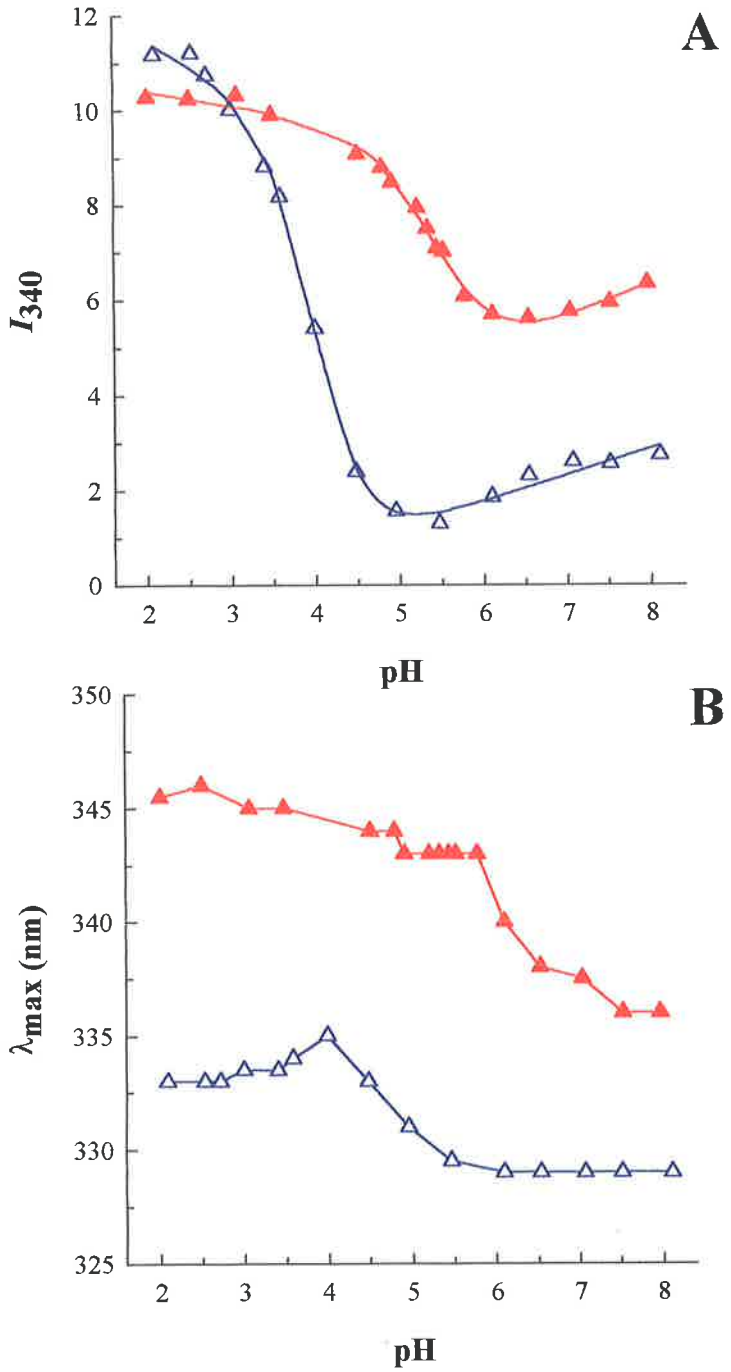

FIGURE 5.6 ACID-INDUCED DENATURATION OF pGH(M31) MONITORED BY FLUORESCENCE SPECTROSCOPY. Fluorescence emission spectra were recorded as described in 2.3.2.2. The protein concentration was 0.22 mg/ml. The data are representative of n = 5 experiments.

A relative fluorescence intensity at 340 nm (I_{340}):

- urea △ + urea ▲

The solid lines are the calculated curves determined from non-linear regression analysis of the raw data, using Equation 2, as described in 2.3.2.1.

B effect of acid on the maximum emission wavelength (λ_{max}):

- urea —△— + urea —▲—

rGH In the absence of 4 M urea, I_{340} exhibited a 5-fold increase through the transition from pH 8.0 to pH 2.0 (Figure 5.7 A). The increase followed a smooth sigmoidal curve with the apparent midpoint of transition at pH 4.29 (Figure 5.7 A; Table 5.2). The plot of λ_{max} was clearly biphasic (Figure 5.7 B). A red shift in the λ_{max} from 330 ± 0.5 nm at pH 8.0 to 336 ± 0.5 nm at pH 4.0 was observed, followed by a blue shift to 332 ± 0.5 nm at pH 2.0.

The addition of 4 M urea at pH 8.0 produced a red shift of λ_{max} to 335 ± 0.5 nm (Figure 5.7 B). This was accompanied with a slight decrease in the I_{340} (Figure 5.7 A). Lowering the pH to 2.0 invoked a 2-fold increase in I_{340}, with an apparent transition midpoint at pH 5.44 (Figure 5.7 A; Table 5.2). The λ_{max} red shifted 9 nm from 335 ± 0.5 nm at pH 8.0 to 341 ± 0.5 nm at pH 2.0 (Figure 5.7 B).

5.2.2 Changes in Conformation as Determined by UV Absorbance

Figures 5.8 A–5.11 A, show the UV absorption spectra of pGH(M8), pGH(M17), pGH(M31) and rGH at pH 8.0 and pH 2.0 in the absence and presence of 4 M urea. The absorption maxima of each protein in the four solvent conditions are summarised in Table 5.3. At pH 8.0 ± 4 M urea the absorption maxima ranged from 277 ± 0.2 nm for pGH(M17) to 278.65 ± 0.2 nm for pGH(M8), compared to 278 ± 0.1 nm for wild-type pGH. For pGH(M8), the shoulder at 290 nm, characteristic of tryptophan, was more prominent and further red shifted due to the insertion of the second tryptophan (Bastiras, 1992). The marginal difference in the absorption maxima between the other proteins was most probably caused by small alterations in conformation within the vicinity of the aromatic residues. Acidification from pH 8.0 to pH 2.0 in the absence and presence of 4 M

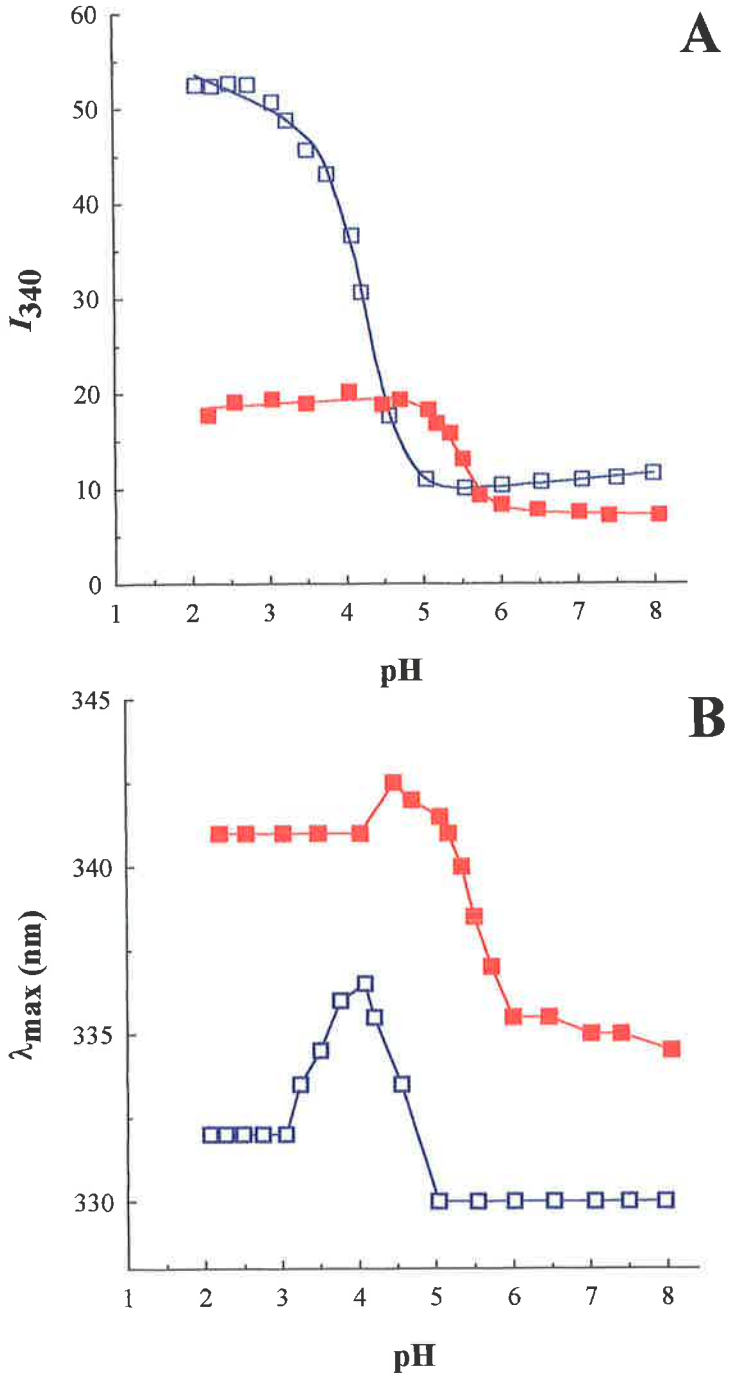

FIGURE 5.7 ACID-INDUCED DENATURATION OF rGH MONITORED BY FLUORESCENCE SPECTROSCOPY. Fluorescence emission spectra were recorded as described in 2.3.2.2. The protein concentration was 0.22 mg/ml. The data are representative of n = 5 experiments.

A relative fluorescence intensity at 340 nm (I_{340}):

- urea □ + urea ■

The solid lines are the calculated curves determined from non-linear regression analysis of the raw data, using Equation 2, as described in 2.3.2.1.

B effect of acid on the maximum emission wavelength (λ_{max}):

- urea —□— + urea —■—

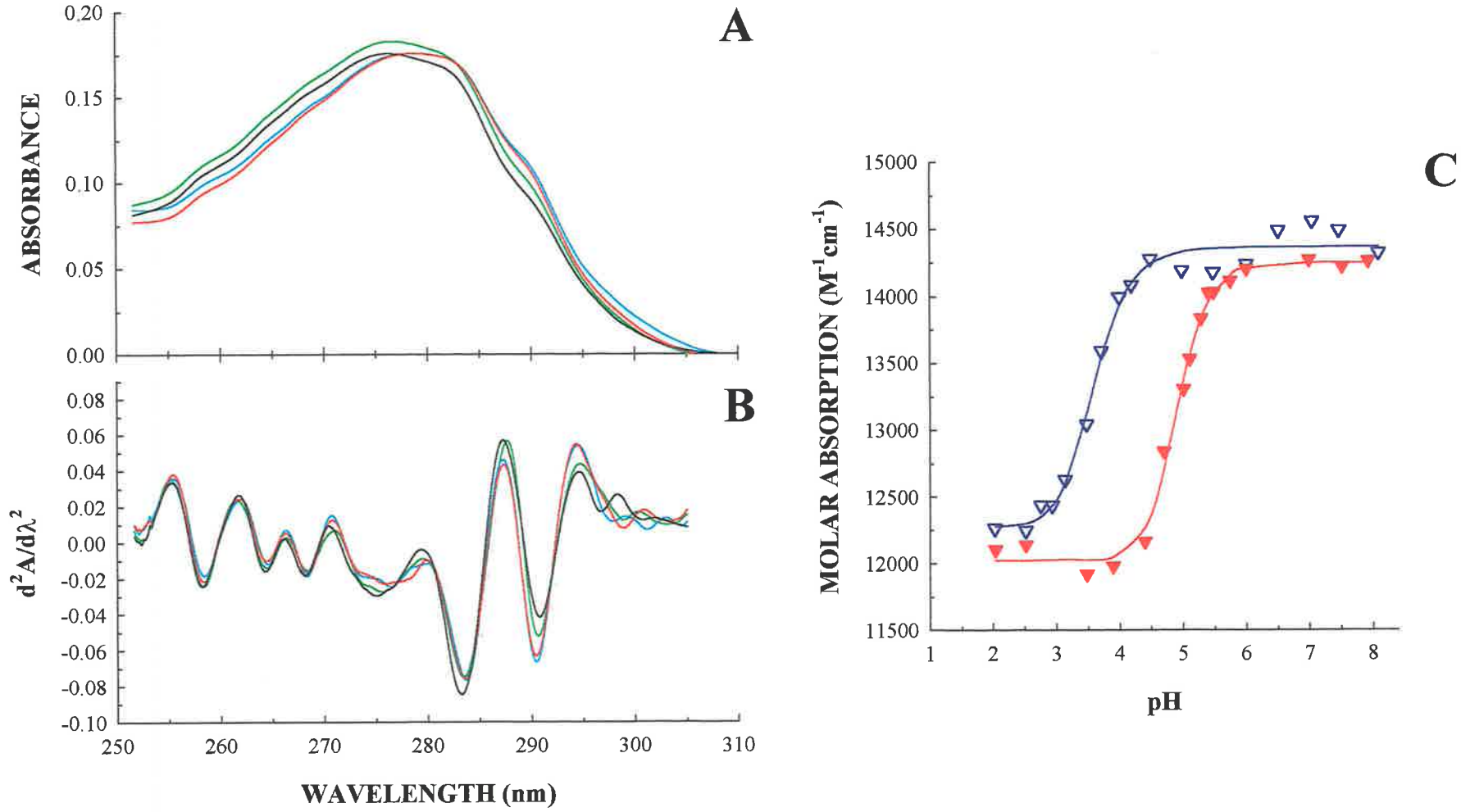

FIGURE 5.8 ACID-INDUCED DENATURATION OF pGH(M8) MONITORED BY UV-ABSORBANCE. UV-absorbance spectra were recorded as described in 2.3.2.3. The protein concentration was 0.22 mg/ml. The data are representative of n = 5 experiments.

A UV-absorbance spectra at: pH 8.0 - urea —— pH 8.0 + urea —— pH 2.0 - urea —— pH 2.0 + urea ——

B computer derived second derivative spectra from the absorbance spectra described above

C the effect of acid on the absorbance at 290 nm (ε_{290}): - urea ▽ + urea ▼

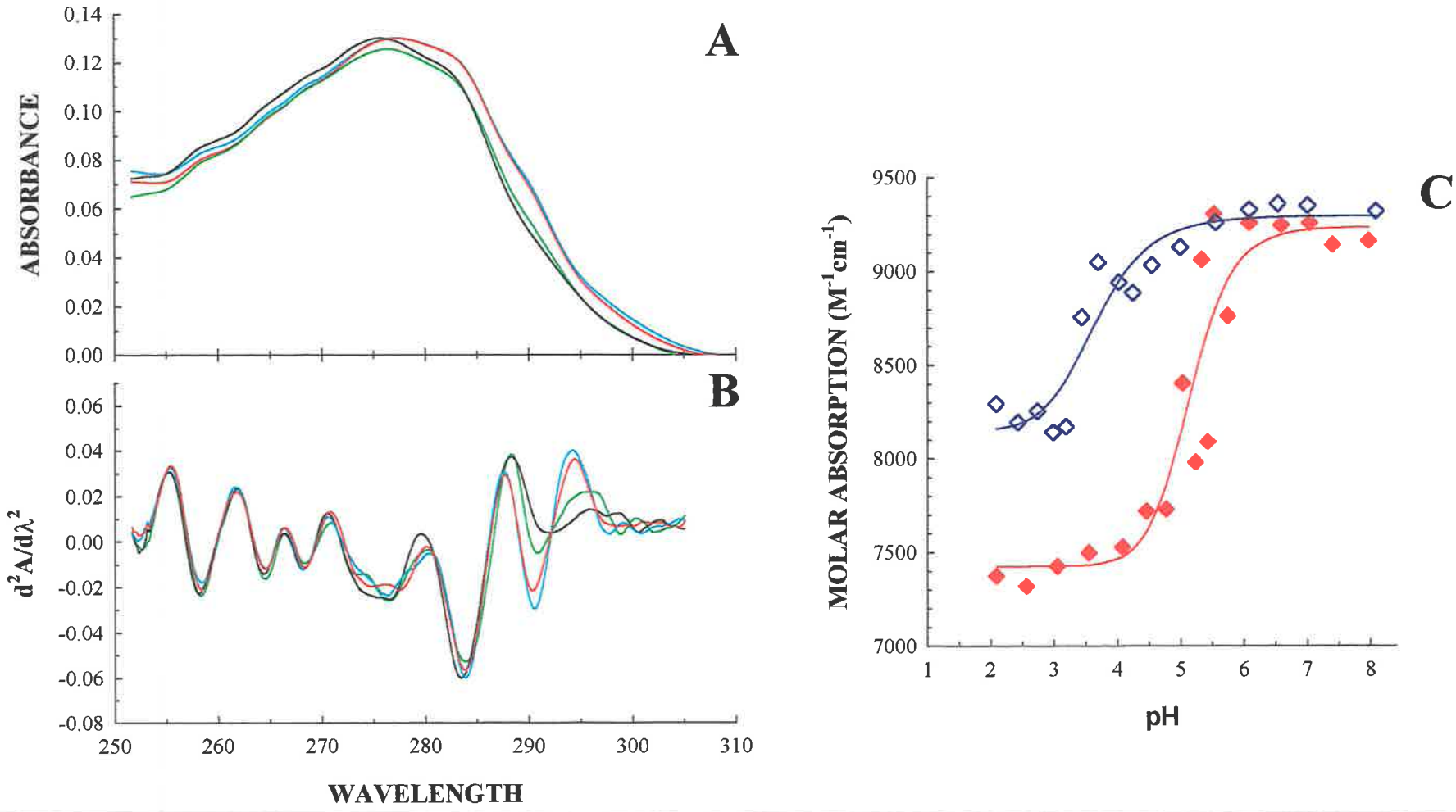

FIGURE 5.9 ACID-INDUCED DENATURATION OF pGH(M17) MONITORED BY UV-ABSORBANCE. UV-absorbance spectra were recorded as described in 2.3.2.3. The protein concentration was 0.22 mg/ml. The data are representative of n = 5 experiments.

A UV-absorbance spectra at: pH 8.0 - urea —— pH 8.0 + urea —— pH 2.0 - urea —— pH 2.0 + urea ——

B computer derived second derivative spectra from the absorbance spectra described above

C the effect of acid on the absorbance at 290 nm (ε_{290}): - urea ◇ + urea ◆

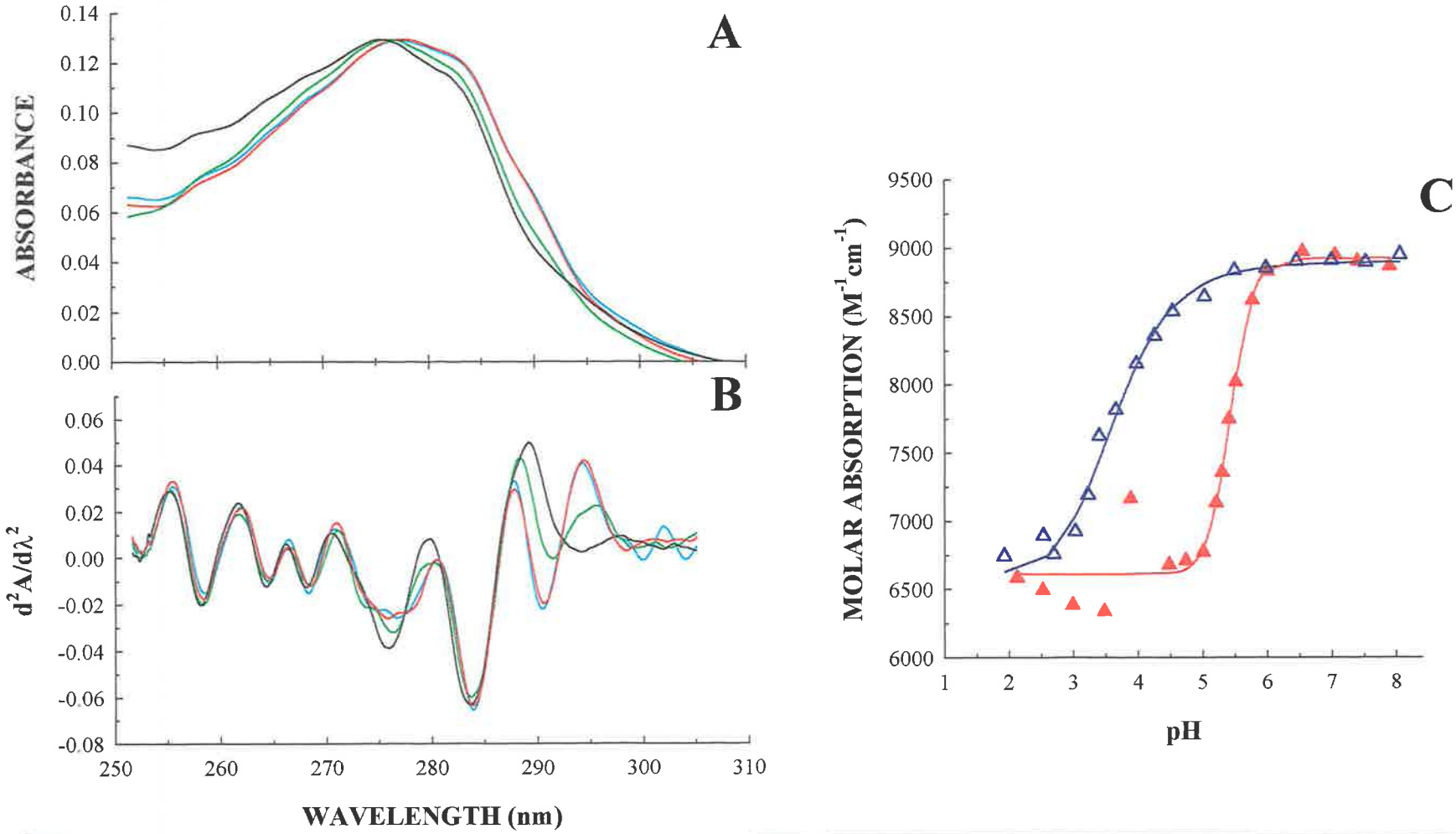

FIGURE 5.10 ACID–INDUCED DENATURATION OF pGH(M31) MONITORED BY UV-ABSORBANCE. UV-absorbance spectra were recorded as described in 2.3.2.3. The protein concentration was 0.22 mg/ml. The data are representative of n = 5 experiments.

A UV-absorbance spectra at: pH 8.0 - urea —— pH 8.0 + urea —— pH 2.0 - urea —— pH 2.0 + urea ——

B computer derived second derivative spectra from the absorbance spectra described above

C the effect of acid on the absorbance at 290 nm (ε_{290}): - urea △ + urea ▲

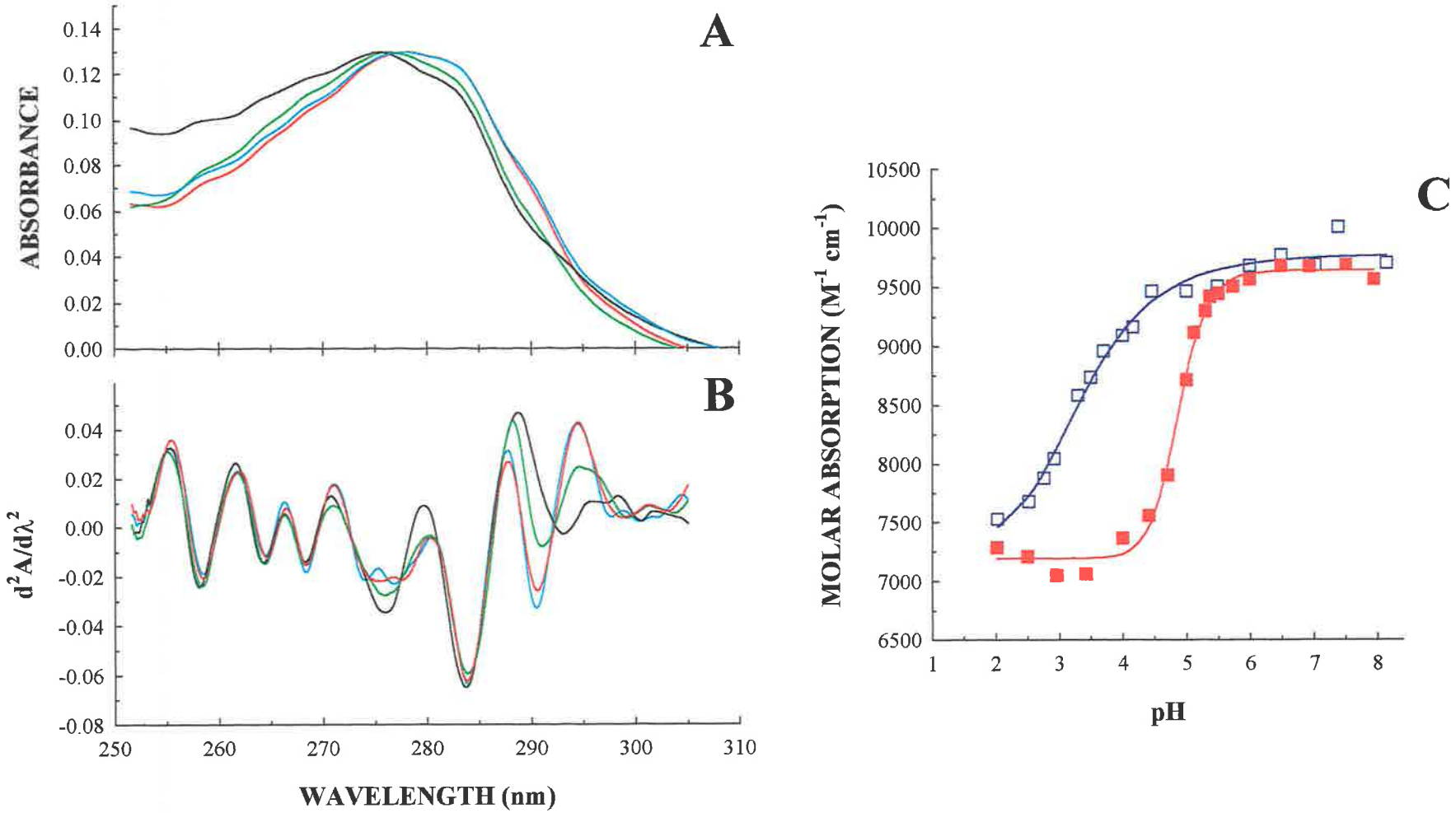

FIGURE 5.11 ACID–INDUCED DENATURATION OF rGH MONITORED BY UV-ABSORBANCE. UV-absorbance spectra were recorded as described in 2.3.2.3. The protein concentration was 0.22 mg/ml. The data are representative of n = 5 experiments.

A UV-absorbance spectra at: pH 8.0 - urea —— pH 8.0 + urea —— pH 2.0 - urea —— pH 2.0 + urea ——

B computer derived second derivative spectra from the absorbance spectra described above

C the effect of acid on the absorbance at 290 nm (ε_{290}): - urea □ + urea ■

pGH ANALOGUE	pH 8.0 MINUS UREA	pH 8.0 PLUS UREA	pH 2.0 MINUS UREA	pH 2.0 MINUS UREA
wild-type pGH	278.00 ± 0.2 nm	278.00 ± 0.2 nm	276.5 ± 0.2 nm	276.20 ± 0.2 nm
pGH(M8)	278.65 ± 0.2 nm	278.35 ± 0.2 nm	277.25 ± 0.2 nm	276.50 ± 0.2 nm
pGH(M17)	277.00 ± 0.2 nm	277.30 ± 0.2 nm	276.40 ± 0.2 nm	275.80 ± 0.2 nm
pGH(M31)	277.60 ± 0.2 nm	277.15 ± 0.2 nm	276.25 ± 0.2 nm	275.65 ± 0.2 nm
rGH	278.55 ± 0.2 nm	278.35 ± 0.2 nm	277.25 ± 0.2 nm	276.50 ± 0.2 nm

TABLE 5.3 SUMMARY OF UV ABSORPTION MAXIMA FOR WILD-TYPE pGH, pGH ANALOGUES AND rGH AT pH 8.0 AND pH 2.0, IN THE ABSENCE AND PRESENCE OF 4 M UREA.

urea produced a general blue shift in all of the spectra (Figures 5.8 A–5.11 A; Table 5.3). The spectra were also red shifted at wavelengths above approximately 293 nm.

The calculated second derivative for each of the zero–order absorption spectra is shown in figures 5.8 B–5.11 B. The wavelength minima attributed to the phenylalanine chromophores in the 250–270 nm region of the spectra did not change for each protein in the four solvent conditions examined. The red shift above 293 nm was similar to that observed for wild-type pGH and attributed to the movement of the Trp^1L_b band. At pH 2.0 without urea, the red shift was small and comparable to wild-type pGH (Table 5.4). A more significant and varied red shift was observed at pH 2.0 with 4 M urea between the proteins (Table 5.4).

A plot of ε_{290} as a function of pH for each protein is shown in Figures 5.8 C–5.11 C. The changes in extinction and the midpoint of each transition are summarised in Table 5.5 and Table 5.2, respectively. For pGH(M8), pGH(M31) and rGH, a smooth sigmoidal transition, with a decrease in extinction of approximately 2000 M^{-1} cm^{-1} and 2500 M^{-1} cm^{-1} in the absence and presence of 4 M urea, respectively was observed. For pGH(M17) smooth transitions were also observed but the loss of extinction was significantly reduced with or without urea (Table 5.5).

5.2.3 ANS Fluorescence

Emission spectra of 100 μM ANS with the various pGH analogues at pH 8.0 and pH 2.0 in the absence and presence of 4 M urea are shown in Figure 5.12. After correcting for the blank (ANS in buffer alone), at pH 8.0 in the absence of urea, the fluorescence emission

pGH ANALOGUE	pH 8.0		pH 2.0	
	minus 4 M urea	plus 4 M urea	minus 4 M urea	plus 4 M urea
wild-type pGH	290.90	290.90	291.50	292.55
pGH(M8)	290.50	290.50	290.65	290.80
pGH(M17)	290.50	290.35	290.80	292.15
pGH(M31)	290.50	290.65	290.80	294.10
rGH	290.50	290.50	290.95	293.65

TABLE 5.4 THE WAVELENGTH POSITION OF THE Trp^1L_b ABSORPTION BAND DETERMINED FROM THE DERIVATIVE OF THE ZERO–ORDER ABSORPTION SPECTRA FOR WILD-TYPE pGH, pGH ANALOGUES AND rGH.

pGH ANALOGUE	DECREASE IN ε_{290} (M^{-1} cm^{-1}) MINUS UREA	DECREASE IN ε_{290} (M^{-1} cm^{-1}) PLUS UREA
wild-type pGH	2100	2500
pGH(M8)	2100	2200
pGH(M17)	1200	1800
pGH(M21)	1500	2200
rGH	2200	2200

TABLE 5.5 SUMMARY OF THE DECREASE IN MOLAR EXTINCTION COEFFICIENT (ε_{290}) AS A FUNCTION OF pH, IN THE ABSENCE AND PRESENCE OF 4 M UREA FOR WILD-TYPE pGH, pGH ANALOGUES AND rGH.

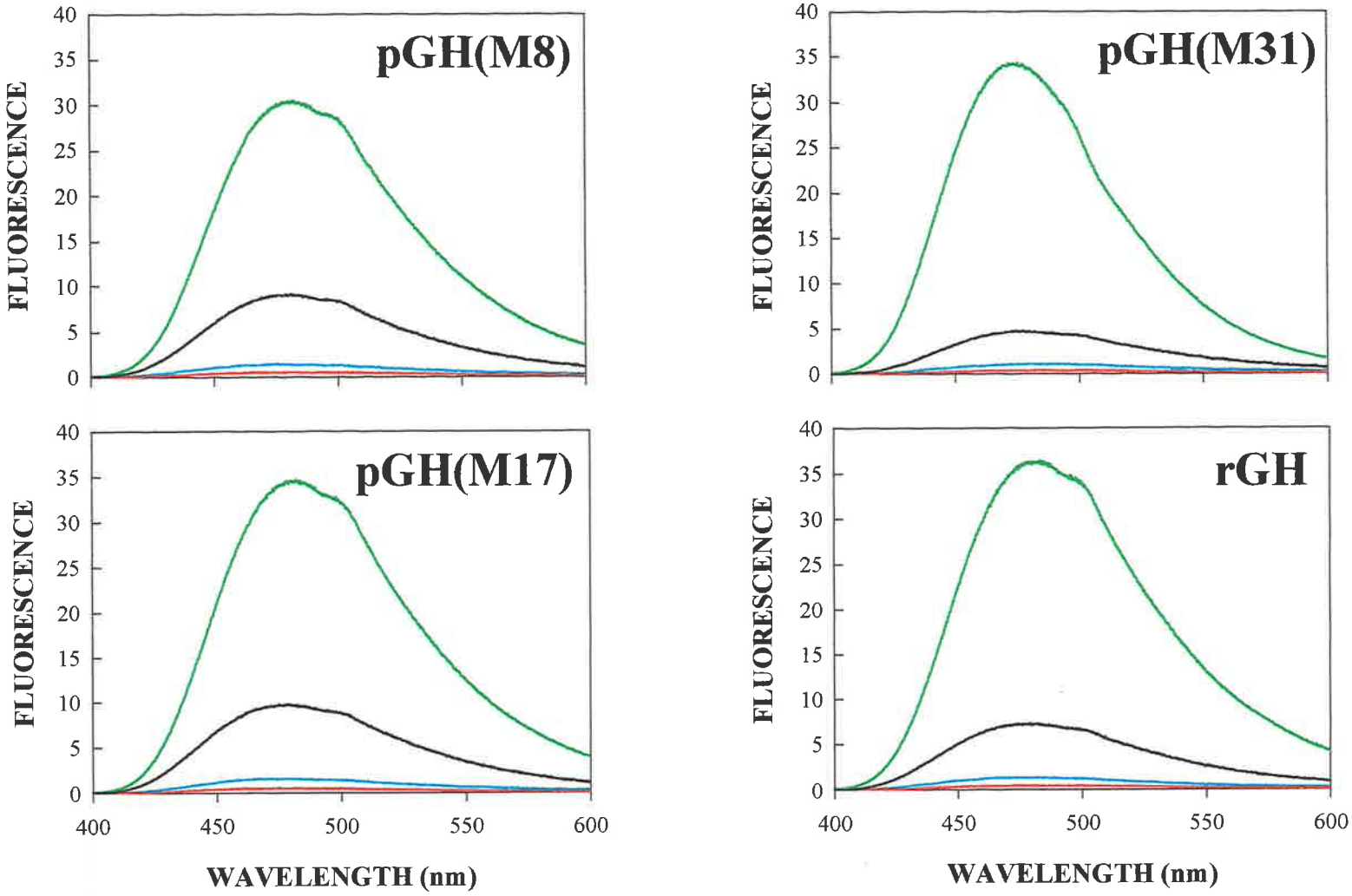

FIGURE 5.12 BINDING OF 1-ANILINONAPTHALENE-8-SULFONATE (ANS) TO pGH(M8), pGH(M17), pGH(M31) and rGH. Fluorescence emission spectra were recorded as described in 2.3.2.3. The ANS concentration was 100 μM and the protein concentration was 0.05 mg/ml (~ 2.5 μM) in all cases.

pH 8.0 - urea —— pH 8.0 + urea —— pH 2.0 - urea —— pH 2.0 + urea ——

was negligible. With the addition of urea, a slight increase in ANS fluorescence with a concomitant blue shift in the λ_{max} was observed.

At pH 2.0 in the absence of 4 M urea, there was an approximately 35-fold increase in fluorescence intensity for all analogues examined. In each spectra a shoulder at approximately 500 nm was seen. This was believed to be caused by a fluorescence artifact known as the "Woods Anomaly", which had not be completely corrected for by the software supplied with the Aminco Bowman fluorescence spectrometer. At pH 2.0 in the presence of urea, the increase in fluorescence intensity was only a fraction of that seen without urea, and ranged from an approximately 5-fold increase for pGH(M31), a 7-fold increase for rGH, to a 9-fold increase for pGH(M8) and pGH(M17).

5.2.4 Size-Exclusion Chromatography

In the absence of urea, similar to wild-type pGH, no protein was recovered from the Superose 12 column between pH 5.0 and pH 2.0. For all analogues, at pH 8.0 a single peak with an elution volume corresponding to an apparent hydrodynamic radius of 18 Å was observed (Figure 5.13). At pH 2.0 for the analogues pGH(M17), pGH(M31) and rGH, the majority of the protein eluted early, with an elution volume corresponding to an apparent hydrodynamic radius of 47 Å. The elution volume and increase in size at pH 2.0 was similar to wild-type pGH at pH 2.0. It was interesting to note that for pGH(M17) and rGH, a smaller peak with a radius comparable to that of the folded state for each analogue was detected. This may be the acid–denatured monomer. The small peak was not observed for pGH(M31). The elution profile for pGH(M8) was quite different. The later eluting peak had a slightly expanded hydrodynamic radius (approximately 22 Å) compared to the radius of 20 Å for the folded state (Bastiras, 1992) at pH 8.0. This was believed to be the partially

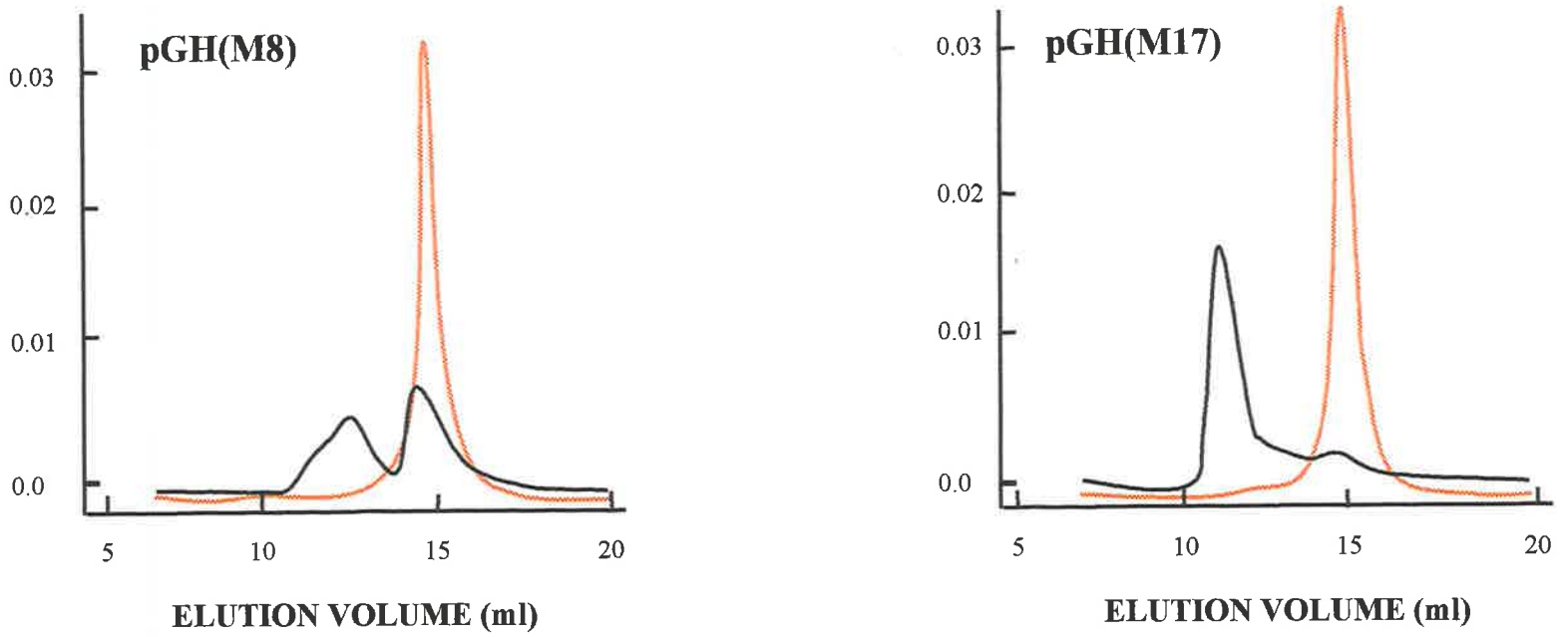

FIGURE 5.13 THE EFFECT OF ACIDIFICATION ON THE ELUTION VOLUME OF pGH(M8) and pGH(M17). The protein concentration was 0.22 mg/ml. Protein elution was followed by the absorbance at 280 nm. Elution profiles in the presence of 4 M urea at:

pH 8.0 ~~~~~~~~ pH 2.0 ————

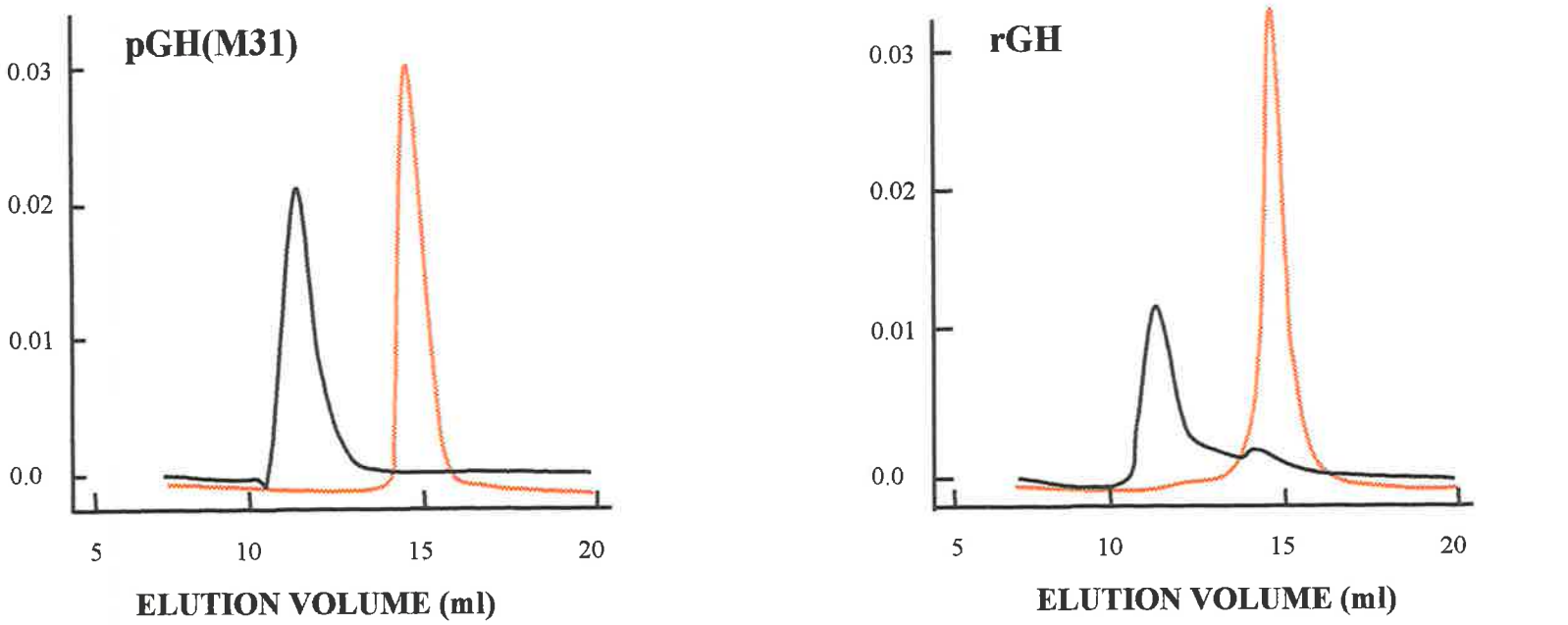

FIGURE 5.13 cont. THE EFFECT OF ACIDIFICATION ON THE ELUTION VOLUME OF pGH(M31) and rGH. The protein concentration was 0.22 mg/ml. Protein elution was followed by the absorbance at 280 nm. Elution profiles in the presence of 4 M urea at:

pH 8.0 ——— pH 2.0 ———

unfolded monomeric intermediate. The broad nature of the early eluting peak suggested the presence of more than one species. The majority of protein in this peak appeared to have a radius of approximately 42 Å. Interestingly, this species was slightly more expanded than that of the Gdn–HCl unfolded state of pGH(M8) (Bastiras, 1992). The shoulder appeared to represent a species with a slightly more expanded radius (approximately 48 Å), similar to the associated species for wild-type pGH.

5.3 DISCUSSION

The aim of this study was to characterise the acid-induced denaturation of 3 pGH analogues and rGH. In terms of acid-mediated partial unfolding, the four proteins in this study, similar to wild-type pGH, fall into category II, with folding intermediates possessing classic characteristics of the molten globule (Fink, 1995).

In the absence and presence of 4 M urea, the properties of the folding intermediates and the pH-dependent transitions that lead to the intermediates, for the 3 pGH analogues and rGH, in most cases, were similar to those observed for wild-type pGH in the same solvent conditions. In general, there was a loss of long range tertiary interactions (as detected by UV absorbance), for all proteins, and Trp86 remained in a hydrophobic environment (as detected by the λ_{max} of intrinsic fluorescence). The retention of Trp86 in a hydrophobic environment suggested that very little secondary structure had been lost. However, there was evidence that the mutations did invoke subtle differences in the UV-absorbance and fluorescence properties of the intermediates, which were dependent on the solvent system employed.

pGH(M8) The decrease in UV-absorbance (hypochromicity) observed upon acidification in the absence of 4 M urea was consistent with the loss of tertiary structure. The increase in the quantum yield of ANS fluorescence at pH 2.0 suggests that pGH(M8) forms a molten globule-like partially folded intermediate. The hydrodynamic properties of this intermediate could not be determined from SEC and to date, no sedimentation equilibrium studies have been performed. The fluorescence properties, particularly within the acid-induced transition were quite different and complex when compared to those observed for wild-type pGH. The complexity of fluorescence is invoked by the presence of two

tryptophan residues, Trp86 and Trp124, both of which contribute to the total fluorescence emission.

In the absence of 4 M urea, despite the initial decrease in fluorescence intensity between pH 8.0 and pH 5.5, there was no appreciable difference in λ_{max} suggesting that the exposure of both tryptophan residues to the aqueous environment had not changed appreciably. The decrease in fluorescence intensity could not be attributed to a loss of protein as the values were corrected for the final protein concentration at each pH. It is highly unlikely that the decrease in fluorescence was due to Trp86, as in wild-type pGH, the fluorescence is already "quenched". An increase in quantum yield of fluorescence and λ_{max}, for the native state of pGH(M8), was previously attributed to the substitution of methionine to tryptophan at position 124 in helix 3 of pGH (Bastiras, 1992). It was suggested that the polar >NH group of Trp124 would be exposed to the surrounding water with the indole ring parallel to the inward facing hydrophobic face of helix 2. Therefore, it is most likely that a change in the local environment of Trp124 is responsible for the decrease in fluorescence intensity observed between pH 8.0 and pH 5.5. As there was not a significant change in λ_{max} it is most likely that the fluorescence decrease was invoked by the rearrangement of nearby residue(s), which have the ability to quench fluorescence. While the λ_{max} continued to blue shift between pH 5.0 and pH 3.0 (Figure 5.4 B), the fluorescence intensity increased (Figure 5.4 A). The significant blue shift suggested the transfer of tryptophan to a more hydrophobic environment, which in this study is believed to be Trp124. The residues Leu77, Leu78, Leu80 and Leu82 on helix 2 and Leu123 and Leu127 on helix 3 could form a pocket near the Trp124. Movement of helix 3 may be sufficient to position Trp124 closer to this hydrophobic pocket. The concomitant rise in fluorescence intensity seen here is speculated to be due to the removal of the quenching

group from Trp86. However, transfer of a tryptophan residue to a hydrophobic environment by virtue of a conformational change or protein association has also correlated with an increase in quantum yield of fluorescence (Ward *et al.*, 1995; Zhang *et al.*, 1997).

The addition of urea, did not significantly change the extent of hypochromicity. However, the fluorescence was different and again complex. For wild-type pGH, at pH 8.0 and 4 M urea, I_{340} was found to increase with a concomitant red shift in λ_{max}. In contrast, for pGH(M8), I_{340} increased while λ_{max} blue shifted. The decrease in λ_{max} is probably due to a change in conformation, which affects Trp124 and masks any effect on Trp86. The rise in I_{340} was most probably due to a change in position of the residue(s) responsible for quenching the fluorescence of Trp86. The continual blue shift in λ_{max} and decrease in I_{340} through the transition from pH 8.0 to pH 2.0, was most likely due to the combinatorial effects of movement of the fluorescence quenching residue(s) and Trp124. Irrespective of these, the value of λ_{max} at pH 2.0 suggested that both Trp86 and Trp124 are each in a relatively hydrophobic environment.

In contrast to wild-type pGH where SEC and sedimentation equilibrium revealed the absence of any monomer, both the partially unfolded monomer and associated state(s) of pGH(M8) were resolved by SEC. Interestingly, the quantum yield of ANS fluorescence paralleled that seen for wild-type pGH, suggesting that the surface hydrophobicity of each species was equivalent. The partially unfolded monomer of pGH(M8) is less transient than the partially unfolded monomer of wild-type pGH. The residues spanning helix 3 of pGH are involved in the association of wild-type pGH at pH 2.0 and 4 M urea. It would appear that the substitution of methionine for tryptophan in pGH might have impeded the ability

to associate. This may in part be due to some structural alteration or steric hindrance brought about by the tryptophan residue.

In summary, under acidic conditions, pGH(M8) forms a partially folded intermediate. The monomeric intermediate is stabilised in the presence of 4 M urea and could be purified and used for further structural studies.

pGH(M17) The fluorescence properties of Trp86 and ANS, suggested that the partially folded intermediates for pGH(M17) were similar to wild-type pGH at pH 2.0 in both the absence and presence of 4 M urea. However, for pGH(M17) the hypochromicity was reduced in both solvent conditions. The double mutation of Lys30 and Arg34 to glutamic acid (Figure 5.1) in pGH(M17), increases the local net charge of the C-terminus of helix 1 from –1 in wild-type pGH to –5 (Bastiras, 1992). A high negative charge at the C-terminus of an α-helix is contrary to the usual situation, where the negative charge due to the helix dipole is stabilised by positively charged residues (Blagdon and Goodman, 1975). Protonation of the glutamaic acid residues by acidification would restore a local nett positive charge at the C-terminus of helix 1, inducing the stabilization of the helix dipole. Moreover, protonation would also increase the hydrophobicity of the helix, as glutamic acid would no longer be involved in hydrogen bond formation with the surrounding aqueous solvent. Tyrosine 29, located on helix 1 of pGH and apparently buried (Figure 3.17; Table 3.4), was postulated to contribute to the change in ε_{290} (see Chapter 3). The increase in helix stability and hydrophobicity most likely inhibits the exposure of Tyr29 to solvent, as suggested in Chapter 3, thus reducing the loss of extinction as observed here.

pGH(M31) In the presence of 4 M urea, replacing the sequence between helix 2 and helix 3 shifted the acid-induced unfolding transitions up by approximately 1.5 pH units compared to 1 unit for wild-type pGH and the other pGH analogues (Table 5.1). Therefore the tertiary structure of pGH(M31), as monitored by the UV and fluorescence probes appears to be less stable than wild-type pGH. In addition, the Trp^1L_b band for pGH(M31) when compared to wild-type pGH was further red shifted by approximately 2 nm to 294 nm (Table 5.4). For wild-type pGH at pH 2.0 and 4 M urea, the shift in the Trp^1L_b band correlated with an intense CD band at 300 nm indicating that Trp86 was in a highly asymmetric environment. It would appear that Trp86 in pGH(M31) is in a slightly more asymmetric environment than in pGH.

In hGH, the polar residue threonine, at positions 98 and 105, is substituted to the non-polar residue alanine. In addition, phenylalanine at position 103 is replaced by a tyrosine (Figure 5.1). It is possible that these substitutions may destabilise loop-helix interactions, which are important for protein stability. From Gdn-HCl-equilibrium denaturation studies, pGH(M31) was shown to form an associated intermediate with similar properties to wild-type pGH. However, the association constant was significantly reduced to 3 nM, compared with 30 μM for wild-type pGH (S. Bastiras, personal communication). In this case the mutations appeared to stabilise the self-associated intermediate perhaps by making helix 3 more available for association by increasing the flexibility of the loop region.

rGH In the absence of urea, the biphasic nature of λ_{max} suggested that at pH 4.0 a conformation was stabilised, whereby the environment of Trp86 was more polar than seen for the other proteins. Further acidification to pH 2.0 resulted in the blue shifting of λ_{max}, consistent with the return of Trp86 to a near native-like hydrophobic environment. At pH

2.0, wild-type pGH was shown to be associated, therefore, the λ_{max} reflected Trp86 in the associated state. With the similarity in λ_{max} at pH 2.0 for the two proteins it is speculated that rGH too, is associated at pH 2.0 and that the partially unfolded monomer is stabilised at pH 4.0. The most significant change between the two proteins is at position 125 in helix 3, where an arginine has been replaced with a glutamine (Figures 5.2 & 5.3). This mutation would result in the removal of a positive charge from the C-terminus of helix 3 destabilising the helix dipole and therefore the helix. For wild-type pGH, helix 3 has been hypothesised to be one of the sites involved in the association process. The destabilised helix 3 in rGH would reduce the protein's ability to associate, stabilising the partially unfolded monomer. Further acidification would expose other sites that were amenable to association. The presence of partially unfolded monomer for rGH at pH 4.0 could be confirmed by sedimentation equilibrium experiments.

In summary, the 3 pGH analogues and rGH all form partially folded intermediates with classic characteristics of a molten globule. These characteristics include substantial loss of tertiary structure, maintenance of a compact shape similar in size to that of the native state, ability to bind ANS and a propensity to aggregate. However, the folding intermediates have distinct properties in different solvent conditions. This study provides further evidence of the great range of structural variability between folding intermediates.

CHAPTER 6

FOLDING KINETICS OF RECOMBINANT PORCINE GROWTH HORMONE AND ANALOGUES

6.1 INTRODUCTION

To gain a complete understanding of the folding mechanism for any one particular protein, it is fundamental to use a combination of equilibrium and kinetic studies. While equilibrium studies provide information of the conformational stability of a protein and can demonstrate the existence of stable folding intermediates, kinetic studies can demonstrate the existence of transient intermediates that may escape detection during equilibrium studies. In many instances, where a denaturation curve has presented a classical two state folding model, subsequent kinetic studies have revealed additional species, including transient intermediates or multiple unfolded forms (Kim and Baldwin, 1982). Therefore, equilibrium and kinetic studies are both complementary and distinct in the insight that they provide (Garvey and Matthews, 1990). In addition to detecting transient intermediates, kinetic studies of mutant proteins can reveal whether changes in stability measured in equilibrium experiments most likely result from changes in the free energy of the native or of the unfolded states.

The equilibrium denaturation of pGH demonstrated the folding pathway to deviate from a two-state folding mechanism, being more consistent with the framework model of folding (Bastiras and Wallace, 1992). A stable intermediate ensemble, with characteristics similar to the molten globule were detected at partially denaturing conditions (Bastiras and Wallace, 1992).

The presence of stable intermediates has been shown for several other members of the growth hormone family, which include bovine, ovine and rat growth hormones (Burger *et al.*, 1966; Holladay *et al.*, 1974). In recent years, from both equilibrium and kinetic folding studies, the folding pathway of bGH has been summarised by the following model:

$$\mathbf{N} \leftrightarrow \boldsymbol{I} \leftrightarrow \mathbf{U}$$
$$\updownarrow$$
$$\boldsymbol{I}_{\mathbf{assoc}}$$

where N, *I*, U and I_{assoc} are the native, monomeric intermediate, unfolded and associated states respectively (Brems *et al.*, 1988). The folding intermediate, *I*, is populated at equilibrium in denaturation studies (Brems *et al.*, 1986) and transiently, during kinetic folding studies (Brems *et al.*, 1987a). Moreover, the structure of *I* has been likened to the molten globule state, having been shown to be largely α-helical with the absence of rigid tertiary structure.

The equilibrium denaturation of pGH is very similar to that of bGH, with the population of a stable equilibrium folding intermediate ensemble under partially denaturing conditions, which possess characteristics akin to the molten globule state. However, very little kinetic examination has been made on the pGH folding process.

The aim of this chapter was to examine the folding kinetics of wild-type pGH using stopped-flow fluorescence spectroscopy. Specifically, the intrinsic tryptophan fluorescence of the single internalised tryptophan at position 86 within helix 2 (Trp86) was used to follow the folding mechanism and address the question: *are there transient intermediates in the folding pathway of pGH that are not detected at equilibrium?* The folding kinetics pGH(M8), pGH(M17), pGH(M31) and rGH was also examined using stopped-flow fluorescence spectroscopy.

6.2 RESULTS

6.2.1 Equilibrium Denaturation of Wild-Type pGH

The amplitude associated with a particular kinetic phase can be calculated in two different ways: (1) the relative amplitude for a specific kinetic phase can be expressed as the fraction of the total kinetically detected amplitude change. (2) the kinetic amplitude can be measured relative to the total equilibrium change and denoted as an absolute amplitude. In this study, the amplitude associated with a kinetic phase is calculated as an absolute amplitude. The determination of the absolute amplitude is useful, as it provides a test of whether all the phases in refolding and unfolding are kinetically resolved within the stopped-flow time range.

To be able to calculate the absolute amplitude associated with a particular kinetic phase, the total equilibrium change at a given Gdn–HCl concentration was determined. The Gdn-HCl-induced equilibrium denaturation profile obtained for wild-type pGH, using the stopped-flow instrument is shown in Figure 6.1. The fluorescence profile was consistent with that previously described for the Gdn–HCl-induced equilibrium denaturation of pGH (Bastiras and Wallace, 1992). The value of the relative fluorescence intensity at each Gdn–HCl concentration was used to determine the total expected equilibrium signal change between different denaturant concentrations.

6.2.2 Folding Kinetics of Wild-Type pGH

A typical kinetic trace obtained for the refolding of wild-type pGH, diluting unfolded protein (protein equilibrated in 5 M Gdn–HCl) to 1.43 M Gdn–HCl, at a final protein concentration of 0.15 mg/ml, is shown in Figure 6.2 A. The kinetic data points were fitted to both a single and double exponential function, with the residuals of the fits presented in

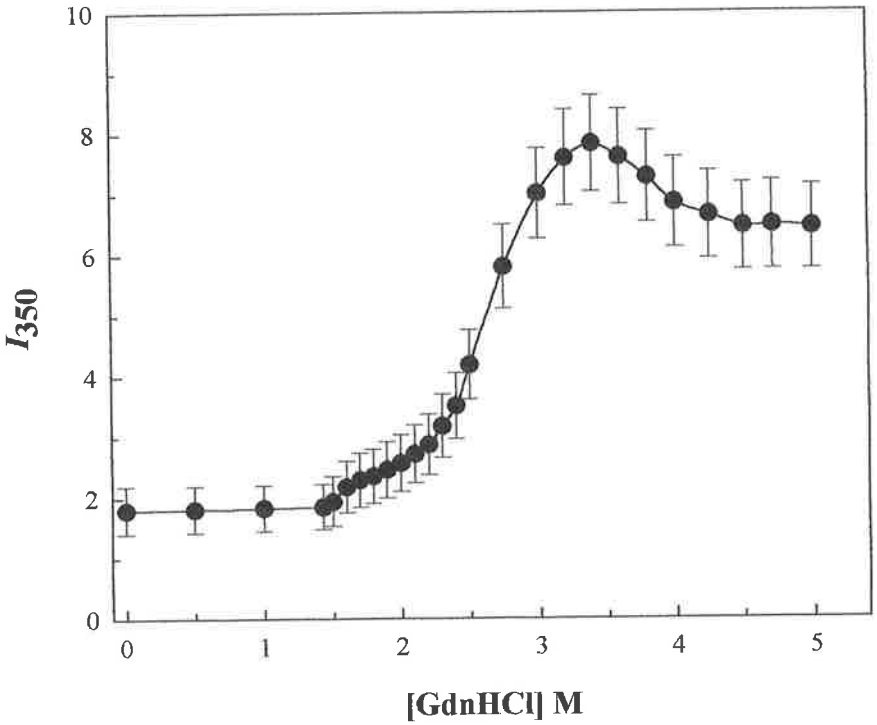

FIGURE 6.1 EQUILIBRIUM DENATURATION OF WILD-TYPE pGH AS MONITORED BY INTRINSIC TRYPTOPHAN FLUORESCENCE. A stock solution of pGH dissolved in 25 mM sodium borate, pH 9.1, was diluted into various concentrations of Gdn-HCl dissolved in 25 mM sodium borate, pH 9.1. The final protein concentration was 0.15 mg/ml. The relative fluorescence intensity at 350 nm was recorded for each sample and plotted as a function of Gdn-HCl concentration. The value of the relative fluorescence intensity at each Gdn-HCl concentration was used to determine the total expected equilibrium signal change between different denaturant concentrations. These values were subsequently used in the determination of absolute amplitudes in the folding kinetics of wild-type pGH. The error bars represent the S.E.M. between repeat experiments (n = 3).

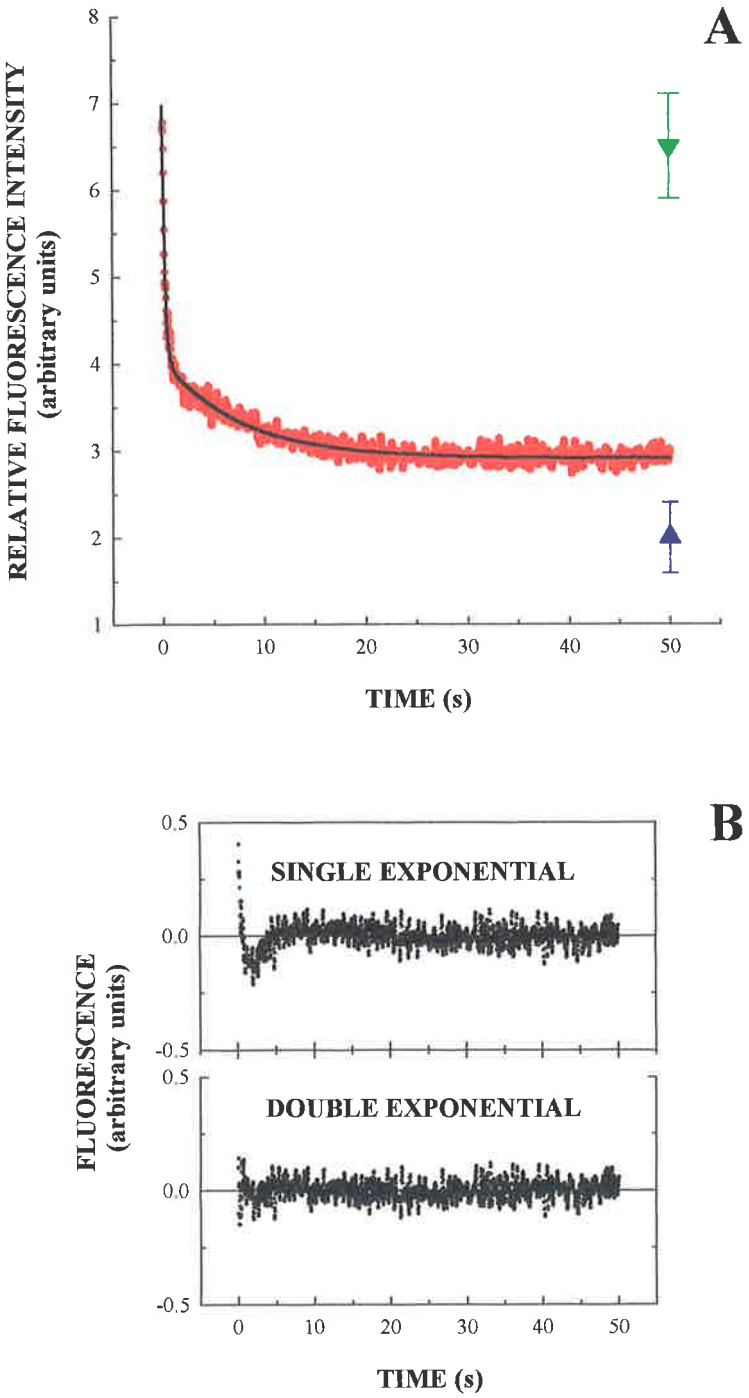

FIGURE 6.2 REFOLDING OF WILD-TYPE pGH. Refolding was initiated by a concentration jump from 5 M to 1.43 M Gdn-HCl. The final protein concentration was 0.15 mg/ml.

A. a representative kinetic trace for the refolding of wild-type pGH. The solid line is the calculated fit for a double exponential function. The relative fluorescence intensity of wild-type pGH at 5 M and 1.43 M Gdn-HCl is shown by the green and blue triangles respectively.

B. the residuals for fitting the refolding kinetics to either a single exponential or double exponential function.

Figure 6.2 B. The residuals returned from the fit to a single exponential were not random, as they clearly resembled the kinetic trace. The single exponential function had apparently not included the change in fluorescence within the first second of the refolding reaction. In contrast, the residuals returned when the data was fit to a double exponential function were both random and even. Refolding was thus characterised by a decrease in fluorescence that was well described by a double exponential function. The two kinetic phases were designated as a fast phase, with a time constant (τ_1) of 1.16 ± 0.05 s that accounted for approximately 55 % of the total expected fluorescence amplitude and a slow phase, with a time constant (τ_2) of 8.11 ± 1 s that accounted for the remaining fluorescence amplitude.

A standard test for the presence of dimeric or oligomeric folding intermediates is to compare the refolding kinetics measured at different protein concentrations. The effect of protein concentration on refolding was examined by dilution of a Gdn–HCl denatured sample from 5 M to 1.43 M, at final protein concentrations ranging from 0.15 mg/ml to 0.4 mg/ml. The results are summarised in Figure 6.3 and Table 6.1. Two kinetic phases that accounted for the total expected fluorescence amplitude were detected at all protein concentrations. The time constant of the fast phase was concentration independent and when averaged over the concentration range returned a value of 1.35 ± 0.26 s. The time constant of the slow phase increased approximately 1.25-fold above 0.24 mg/ml, suggesting a small dependence on the final protein concentration. The relative amplitudes for the rate constants were protein concentration independent and contributed approximately equally to the total expected fluorescence amplitude.

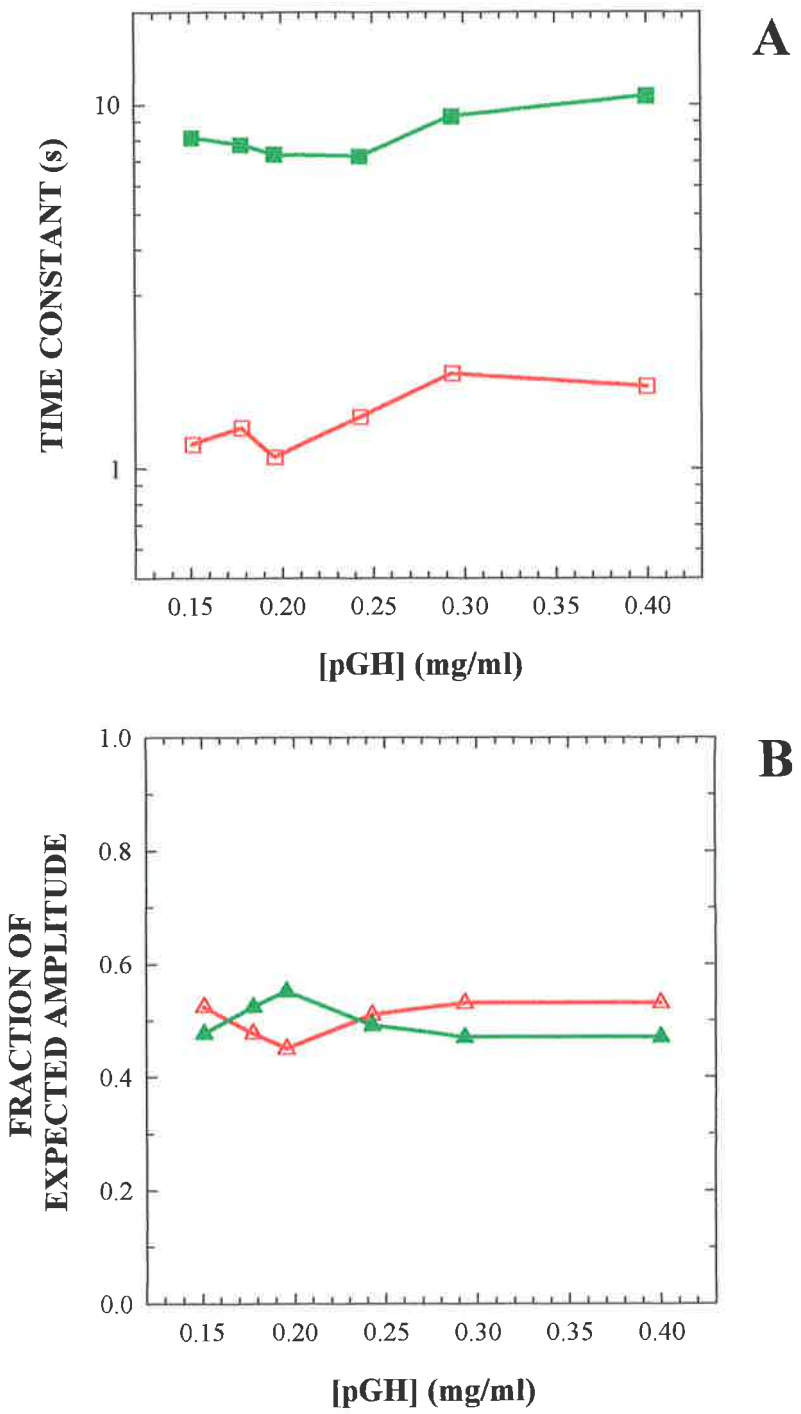

FIGURE 6.3 THE EFFECT OF PROTEIN CONCENTRATION ON THE REFOLDING KINETICS OF WILD-TYPE pGH. Solutions containing varying amounts of wild-type pGH in 5 M Gdn-HCl, 25 mM sodium borate, pH 9.1, were diluted to 1.43 M Gdn-HCl, 25 mM sodium borate, pH 9.1.

A. time constants for the refolding kinetics:

fast phase (τ_1) slow phase (τ_2)

B. amplitudes calculated relative to the total expected amplitude based on equilibrium fluorescence intensities i.e. absolute amplitudes:

fast phase (τ_1) slow phase (τ_2)

FINAL pGH CONCENTRATION (mg/ml)	TIME CONSTANT (s)	
	τ_1	τ_2
0.15	1.16 ± 0.2	8.110 ± 0.001
0.18	1.29 ± 0.2	7.757 ± 0.002
0.20	1.07 ± 0.3	7.304 ± 0.001
0.24	1.39 ± 0.5	7.199 ± 0.007
0.29	1.82 ± 0.4	9.270 ± 0.010
0.40	1.68 ± 0.4	10.560 ± 0.020

TABLE 6.1 EFFECT OF PROTEIN CONCENTRATION ON THE REFOLDING KINETICS OF WILD-TYPE pGH. Solutions containing varying amounts of wild-type pGH in 5 M Gdn–HCl, 25 mM sodium borate, pH 9.1 were diluted to 1.43 M Gdn–HCl, 25 mM sodium borate, pH 9.1. The raw data was fitted to a double exponential function, with the reported values being the mean and standard deviation for the time constants between separate experiments (n = 5).

FINAL pGH CONCENTRATION (mg/ml)	TIME CONSTANT (s)
	τ
0.16	0.92 ± 0.15
0.25	0.83 ± 0.08
0.37	0.66 ± 0.30
0.50	0.73 ± 0.31
0.67	0.71 ± 0.30
0.82	0.63 ± 0.17

TABLE 6.2 EFFECT OF PROTEIN CONCENTRATION ON THE UNFOLDING KINETICS OF WILD-TYPE pGH. Unfolding was initiated by dilution of varying amounts of wild–type pGH in 25 mM sodium borate, pH 9.1 to a final concentration of 4 M Gdn–HCl, 25 mM sodium borate, pH 9.1. The raw data was fitted to a single exponential function, with the reported values being the mean and standard deviation for the time constants between separate experiments (n = 5).

6.2.3 Unfolding Kinetics of Wild-Type pGH

An example of a kinetic trace obtained from the dilution of folded protein into strongly unfolding conditions of Gdn–HCl (4 M), at a final protein concentration of 0.15 mg/ml, is shown in Figure 6.4 A. Unfolding was characterised by an increase in fluorescence that was well fitted by a single exponential function (Figures 6.4 A and 6.4 B), with a rate constant of approximately 0.92 s. However, this kinetic phase accounted for only a fraction of the total expected amplitude. While the final kinetic value of fluorescence was in agreement with the equilibrium value, the initial detectable kinetic fluorescence did not agree with the equilibrium baseline fluorescence. This finding suggested that in the unfolding of wild–type pGH, there was a kinetically unresolved "burst phase", where at least one faster reaction occurred within the dead time of mixing of the stopped-flow instrument (approximately 4 ms).

Unfolding was also examined as a function of protein concentration. Folded protein was diluted into strongly unfolding conditions of Gdn–HCl (4 M), at final protein concentrations ranging from 0.15–0.8 mg/ml. The results are summarised in Figure 6.5 and Table 6.2. A burst phase and a single detectable kinetic phase, which accounted for a fraction of the total expected fluorescence amplitude, was detected at all protein concentrations. The time constant of the detectable phase was independent of protein concentration and when averaged over the concentration range returned a value of 0.75 ± 0.1 s.

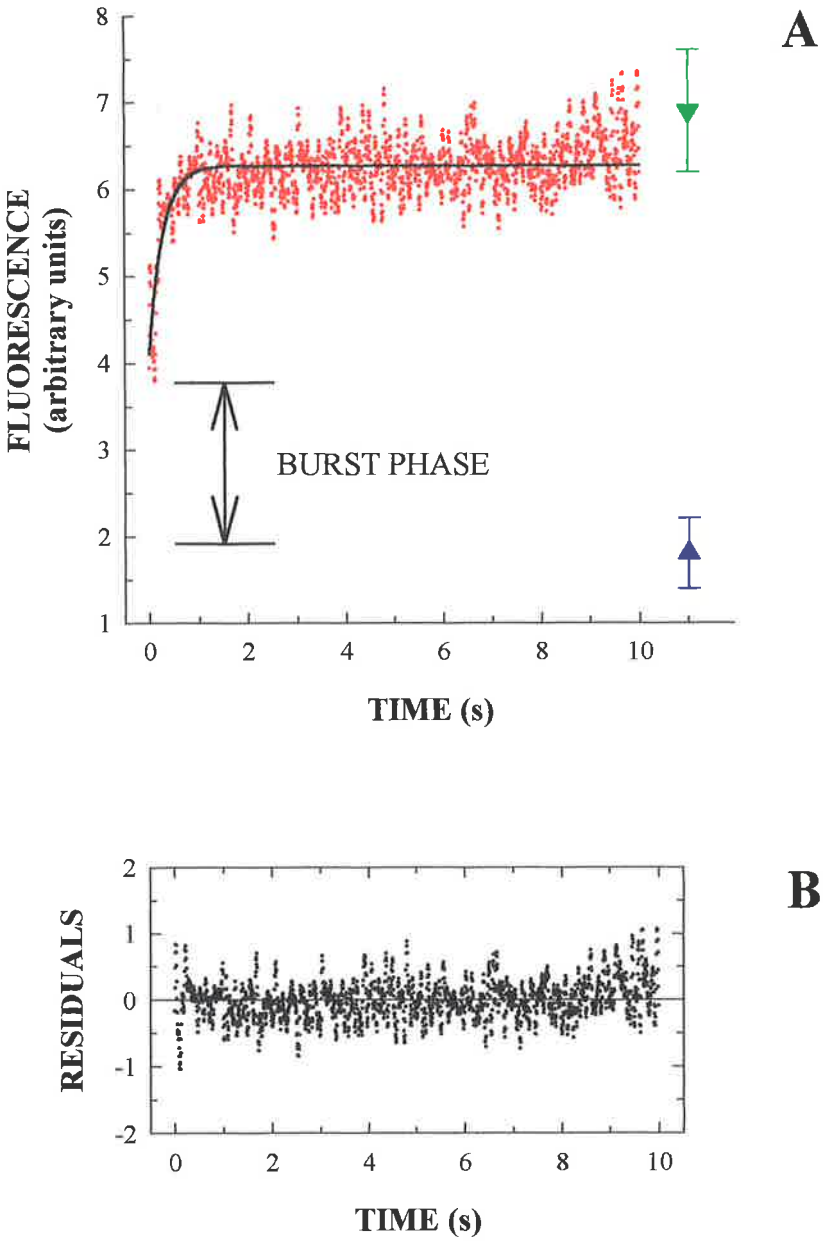

FIGURE 6.4 UNFOLDING KINETICS OF WILD-TYPE pGH. Unfolding was initiated by a concentration jump from 25 mM sodium borate, pH 9.1 to 4 M Gdn–HCl, 25 mM sodium borate, pH 9.1. The final protein concentration was 0.15 mg/ml.

A. a representative kinetic trace for the unfolding of wild-type pGH. The solid line is the calculated fit for a single exponential function. The relative fluorescence intensity of wild-type pGH in 25 mM sodium borate, pH 9.1 and 4 M Gdn-HCl, 25 mM sodium borate, pH 9.1 is shown by the blue and green triangles respectively. The undetectable phase is denoted as a "burst phase".

B. the residuals for fitting the unfolding kinetics to a single exponential function.

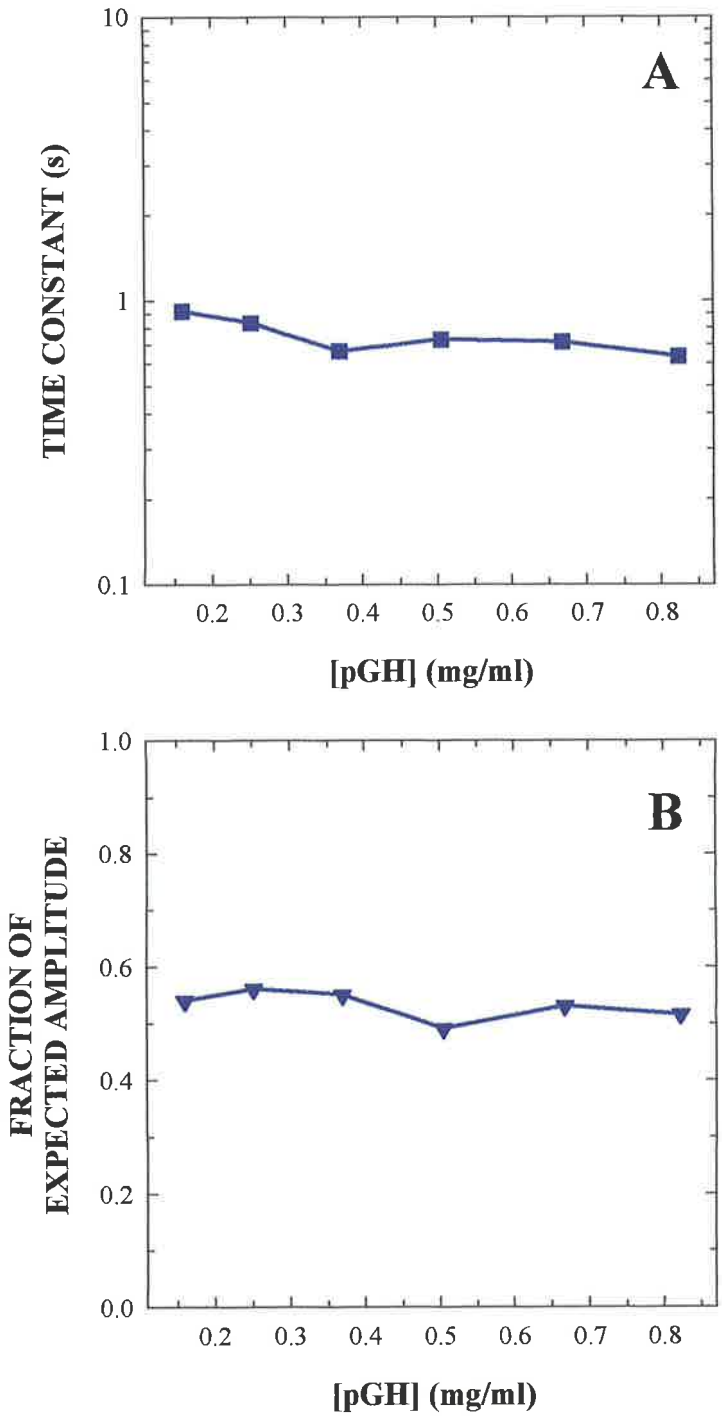

FIGURE 6.5 THE EFFECT OF PROTEIN CONCENTRATION ON THE UNFOLDING KINETICS OF WILD-TYPE pGH. Solutions containing varying amounts of wild-type pGH in 25 mM sodium borate, pH 9.1, were diluted to 4 M Gdn–HCl, 25 mM sodium borate, pH 9.1.

A. time constants for the refolding kinetics: —■—

B. amplitudes calculated relative to the total expected amplitude based on equilibrium fluorescence intensity i.e. absolute amplitudes: —▼—

6.2.4 Refolding and Unfolding Kinetics of Wild-Type pGH as a Function of Final Gdn–HCl Concentration

The refolding kinetics of wild-type pGH as a function of Gdn–HCl concentration are presented in Figure 6.6. All data was obtained by diluting unfolded protein (protein equilibrated in 5 M Gdn–HCl) into various Gdn–HCl concentrations at a final protein concentration of 0.15 mg/ml. At this protein concentration, any contribution from protein self-association is minimal (Bastiras and Wallace, 1992). Two kinetic phases were detected at all concentrations of Gdn–HCl and are designated by τ_1 and τ_2 for the fast and slow phase respectively. The time constant of the fast phase was shown to be independent of Gdn–HCl and when averaged over the entire concentration range returned a value of 1.2 ± 0.05 s. The time constant of the slow phase was also independent in the range 1.43–2 M Gdn–HCl. At concentrations > 2 M, which corresponded to the folding transition region (Bastiras and Wallace, 1992), the time constant appeared to exhibit a small dependence on Gdn–HCl. The fractional amplitudes of each kinetic phase did not vary significantly across the concentration range examined and accounted for the total expected fluorescence amplitude.

Figure 6.6 A illustrates the unfolding kinetics of wild-type pGH as a function of Gdn-HCl concentration, and at a final protein concentration of 0.15 mg/ml. A single kinetic phase was resolved which exhibited a strong dependence on the final Gdn–HCl concentration. The time constant ranged from approximately 0.9 s at 4 M Gdn–HCl to 2 s at 2.5 M Gdn-HCl. Interestingly, Gdn–HCl concentrations between 3 and 4 M coincide with the post transition region of wild-type pGH folding (Bastiras and Wallace, 1992). The amplitude associated with the single phase across the concentration range accounted for only a fraction of the expected amplitude (Figure 6.6 B). The missing amplitude was

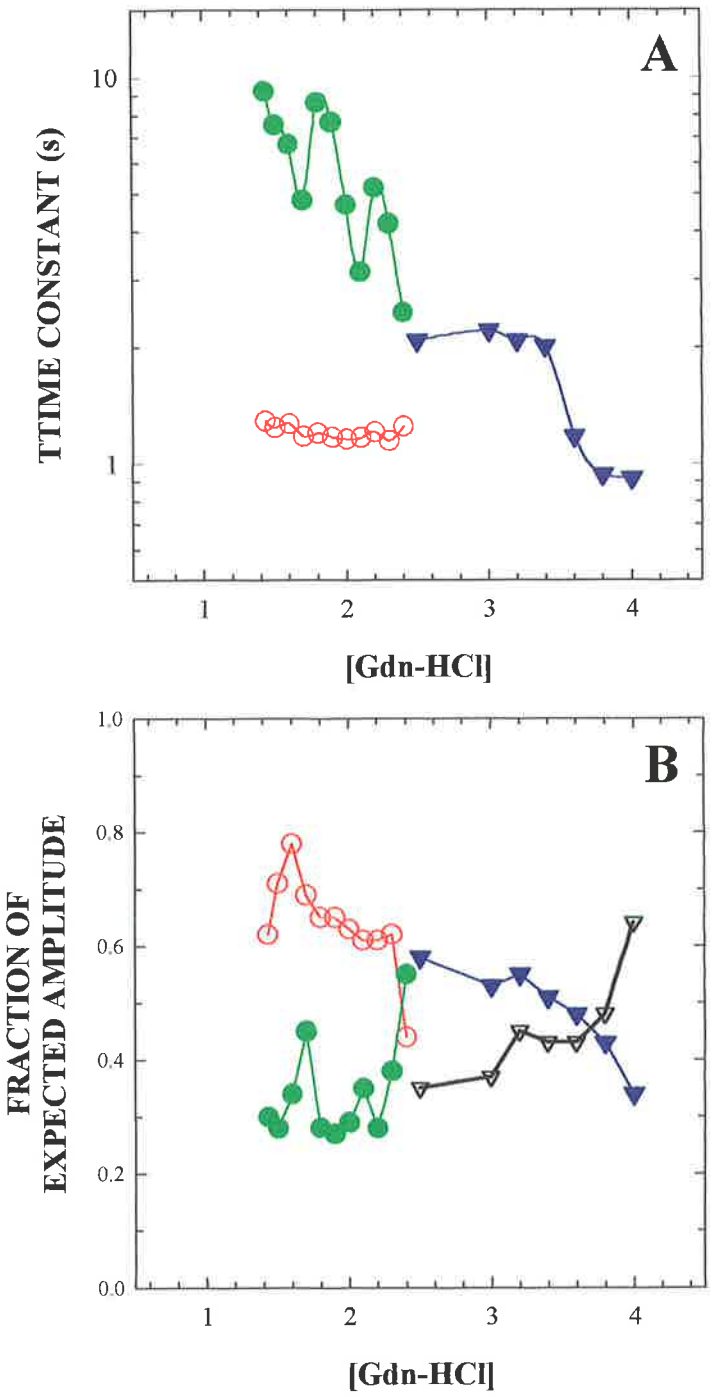

FIGURE 6.6 THE EFFECT OF Gdn-HCl CONCENTRATION ON THE REFOLDING AND UNFOLDING KINETICS OF WILD-TYPE pGH. Refolding was initiated by the dilution of unfolded wild-type pGH in 5 M Gdn-HCl, 25 mM sodium borate, pH 9.1, to the indicated Gdn−HCl concentration, in 25 mM sodium borate, pH 9.1. Unfolding was initiated by dilution of wild-type pGH in 25 mM sodium borate, pH 9.1, to the indicated Gdn−HCl concentration, in 25 mM sodium borate, pH 9.1. The final protein concentration in all cases was 0.15 mg/ml.

A. refolding time constants are represented by ⊖ fast phase (τ_1) and ● slow phase (τ_2). The Unfolding time constant is represented by ▼

B. amplitudes calculated relative to the total expected amplitude based on equilibrium fluorescence intensities i.e. absolute amplitudes. The symbols are the same as in A. The amplitude of the unfolding "burst phase" is represented by ▽

unquestionably due to a burst phase in unfolding. The relative amplitude of the burst phase at each Gdn–HCl concentration was calculated as the difference between the initial protein fluorescence (i.e. fluorescence of wild–type pGH dissolved in buffer without Gdn–HCl), and the initial kinetic fluorescence (Figure 6.6 B), and was found to be strongly dependent on Gdn–HCl.

6.2.5 Folding Kinetics of pGH(M8), pGH(M17), pGH(M31) and rGH

An example of a typical kinetic trace obtained for the refolding of pGH(M8), pGH(M17), pGH(M31) and rGH, when diluted from 5 M to 1.43 M Gdn–HCl, at a final protein concentration of 0.15 mg/ml is illustrated in Figure 6.7.

pGH(M8) The refolding of pGH(M8) was best described by a single exponential function, with an amplitude that accounted for the total expected fluorescence amplitude obtained from Gdn–HCl-induced equilibrium denaturation experiments (data not shown). The time constant for this single kinetic phase was approximately 1.5 s. In contrast to the refolding of wild-type pGH, the refolding of pGH(M8) was characterised by an increase in the relative fluorescence intensity; both the initial and final relative fluorescence values were consistent with those obtained from previous equilibrium denaturation studies performed by Dr. S. Bastiras (personal communication).

pGH(M17, pGH(M31) and rGH The kinetic data for the refolding of pGH(M17), pGH(M31) and rGH was similar to that obtained for wild-type pGH i.e. refolding was characterised by a decrease in fluorescence that was well described by a double exponential function (Figure 6.7), which accounted for all of the expected fluorescence amplitudes obtained from Gdn–HCl-induced equilibrium denaturation experiments (data

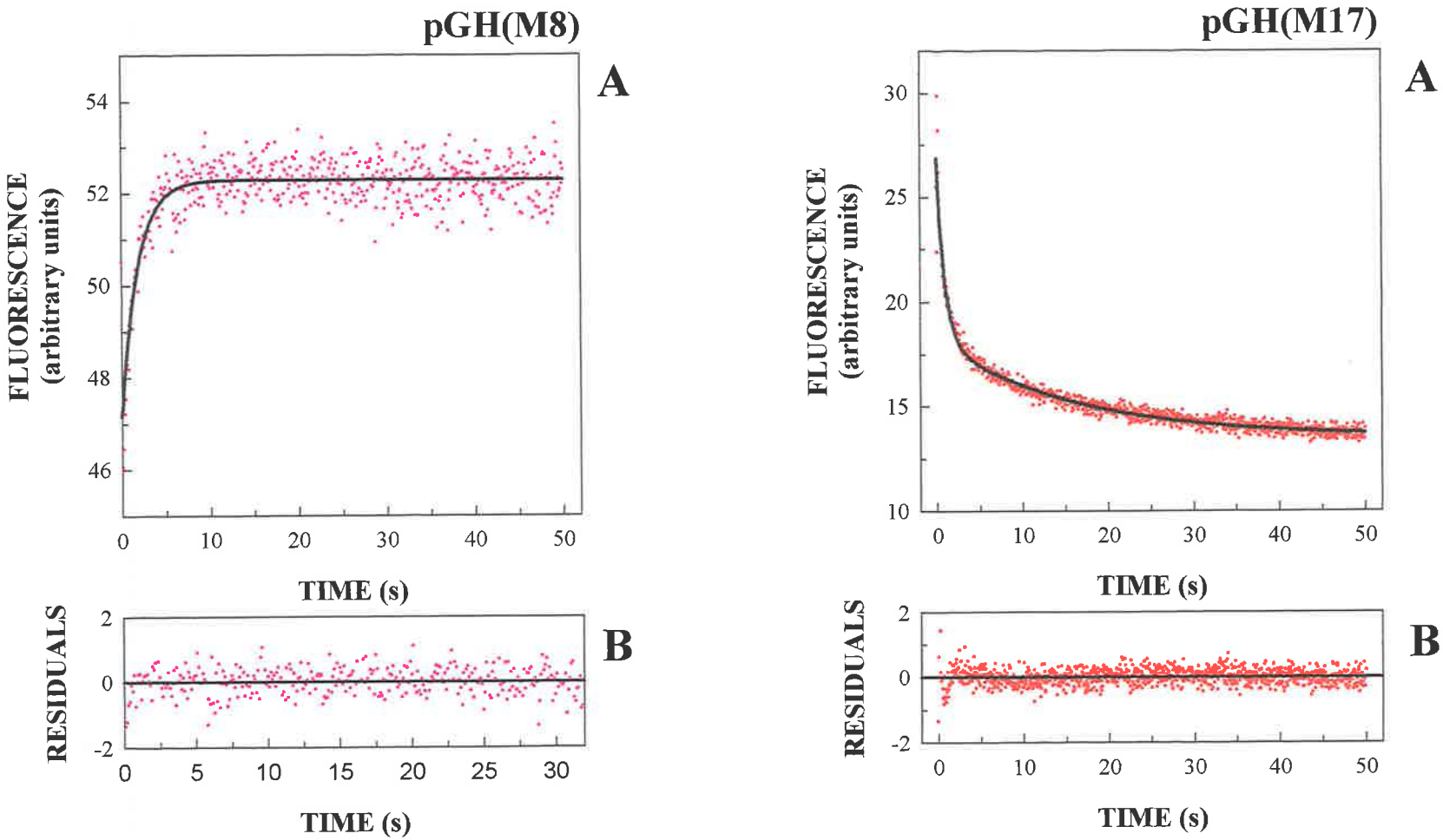

FIGURE 6.7 REFOLDING OF pGH ANALOGUES. Refolding was initiated by the dilution of unfolded protein in 5 M Gdn-HCl, 25 mM sodium borate, pH 9.1, to 1.43 M Gdn-HCl, 25 mM sodium borate, pH 9.1. The final protein concentration in all cases was 0.15 mg/ml.

A. representative kinetic traces for the refolding of pGH(M8) and pGH(M17). The solid line is the calculated fit for a single exponential function (pGH(M8)) and a double exponential function (pGH(M17)).

B. the residuals obtained for fitting the refolding kinetic data.

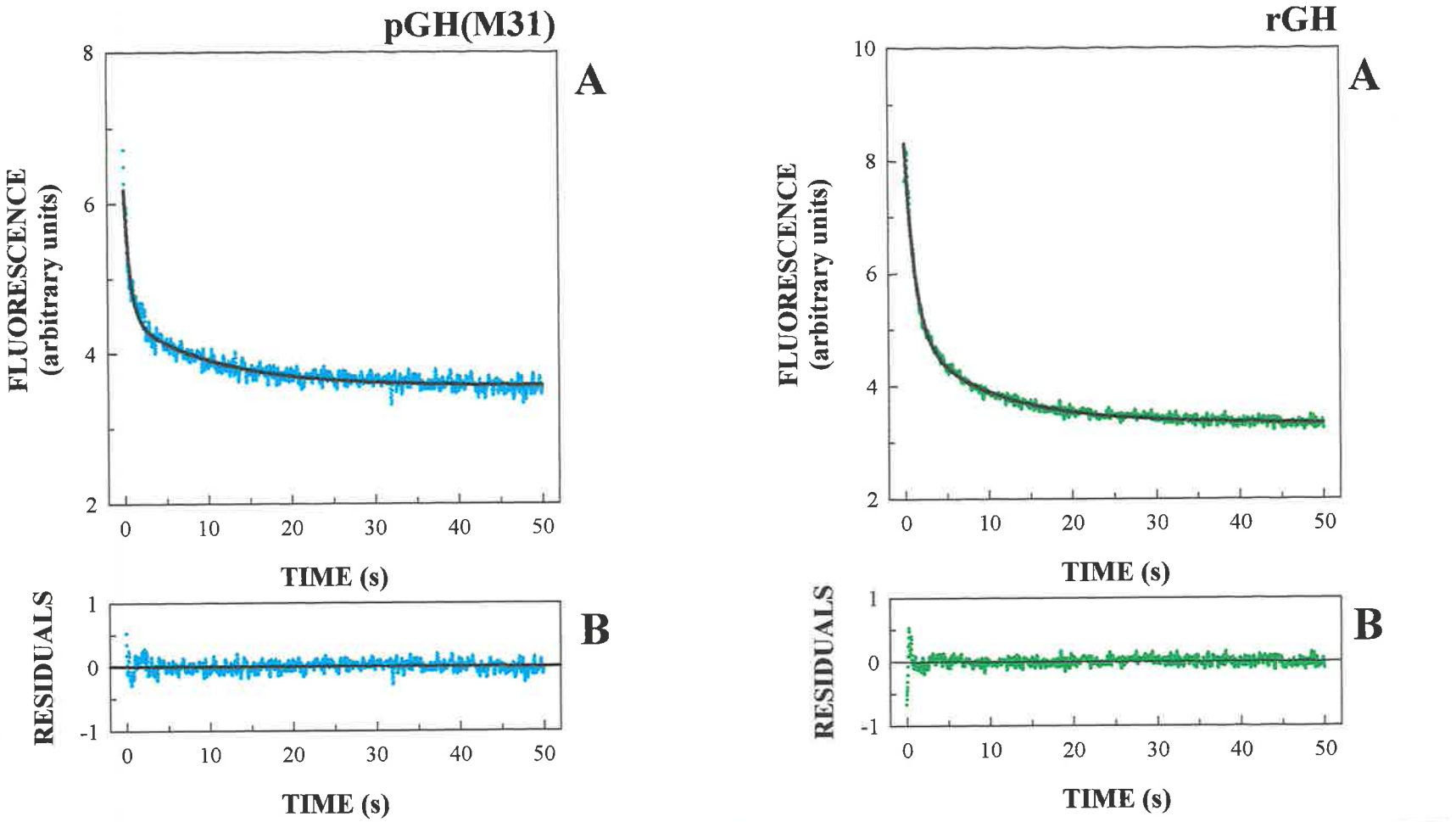

FIGURE 6.7 cont. REFOLDING OF pGH ANALOGUES. Refolding was initiated by the dilution of unfolded protein in 5 M Gdn-HCl, 25 mM sodium borate, pH 9.1, to 1.43 M Gdn-HCl, 25 mM sodium borate, pH 9.1. The final protein concentration in all cases was 0.15 mg/ml.

A. representative kinetic traces for the refolding of pGH(M31) and rGH. The solid line is the calculated fit for a double exponential function.

B. the residuals obtained for fitting the refolding kinetic data.

not shown). The time constant for the fast phase of refolding for each protein was approximately 1 s. The time constant for the slow phase of refolding varied slightly for each protein with a value of 10 ± 2.1 s, 11.1 ± 0.75 s and 15.4 ± 0.2 s for rGH, pGH(M31) and pGH(M17) respectively (Table 6.3).

6.2.6 Unfolding Kinetics of pGH(M8), pGH(M17), pGH(M31) and rGH

Figure 6.8 illustrates an example of a typical kinetic trace obtained for the unfolding of pGH(M8), pGH(M17), pGH(M31) and rGH, when diluted from 0 M to 4 M Gdn–HCl, at a final protein concentration of 0.15 mg/ml. On each plot the initial fluorescence intensity of folded protein (25 mM sodium borate, pH 9.1) and the fluorescence intensity of the protein in 4 M Gdn–HCl at equilibrium are represented.

pGH(M8) For the unfolding of pGH(M8), a single kinetic phase was observed that was well fit by a single exponential function, with an amplitude that accounted for the total expected fluorescence amplitude (Figure 6.8). In contrast to the unfolding of wild-type pGH, the unfolding of pGH(M8) was characterised by a decrease in fluorescence. Similar to the refolding of pGH(M8) as described above, both the initial and final relative fluorescence values were consistent with those obtained from previous equilibrium denaturation studies performed by Dr. S. Bastiras (personal communication).

pGH(M17), pGH(M31) and rGH The unfolding of pGH(M17), and pGH(M31), was characterised by a burst phase and a single measurable kinetic phase. The measurable phase accounted for approximately 35%, and 50% of the total expected fluorescence amplitude change for pGH(M17), and pGH(M31), respectively (Figure 6.8). A single kinetic phase was resolved for the unfolding of rGH, which accounted for the total

pGH ANALOGUE	REFOLDING		UNFOLDING
	τ_1 (s)	τ_2 (s)	τ (s)
wild-type pGH	1.16 ± 0.02	8.11 ± 0.001	0.92 ± 0.15
pGH(M8) (M124W)	1.52 ± 0.12	ND	1.32 ± 0.06
pGH(M17) (K30E; R34E)	1.06 ± 0.03	15.4 ± 0.002	1.13 ± 0.08
pGH(M31) (T98A; F103Y; T105A)	0.73 ± 0.20	11.1 ± 0.75	153 ± 27
rGH	1.28 ± 0.26	10.0 ± 2.1	0.21 ± 0.01

TABLE 6.3 COMPARISON OF THE FOLDING KINETICS FOR WILD-TYPE pGH, pGH(M8), pGH(M17), pGH(M31) AND rGH. Refolding was initiated by diluting protein in 5 M Gdn–HCl, 25 mM sodium borate, pH 9.1 to 1.43 M Gdn–HCl, 25 mM sodium borate, pH 9.1. Unfolding was initiated by diluting protein in 25 mM sodium borate, pH 9.1 to 4 M Gdn–HCl, 25 mM sodium borate, pH 9.1. In all cases, the final protein concentration was 0.15 mg/ml. The reported values are the mean and standard deviation for the time constants between separate experiments (n = 5).
ND; Not Detected

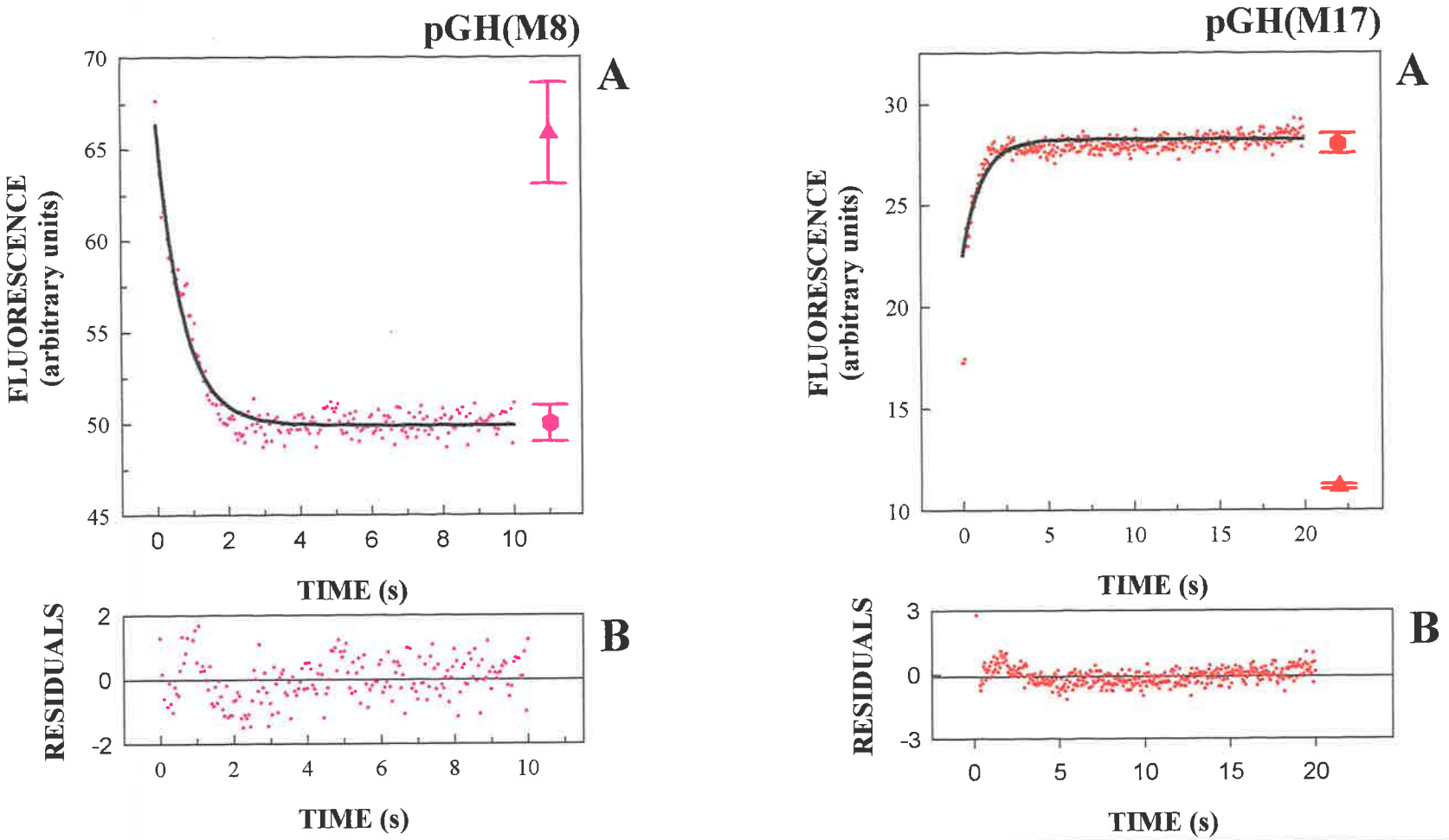

FIGURE 6.8 UNFOLDING OF pGH ANALOGUES. Unfolding was initiated by the dilution of folded protein in 25 mM sodium borate, pH 9.1, to 4 M Gdn-HCl, 25 mM sodium borate, pH 9.1. The final protein concentration in all cases was 0.15 mg/ml.

A. representative kinetic traces for the refolding of pGH(M8) and pGH(M17). The solid line is the calculated fit for a single exponential function. The relative fluorescence intensity of each analogue in 25 mM sodium borate and 4 M Gdn-HCl, pH 9.1 are represented by ▲ ▲ and ● ● respectively.

B. the residuals for fitting the refolding kinetics to a single exponential function.

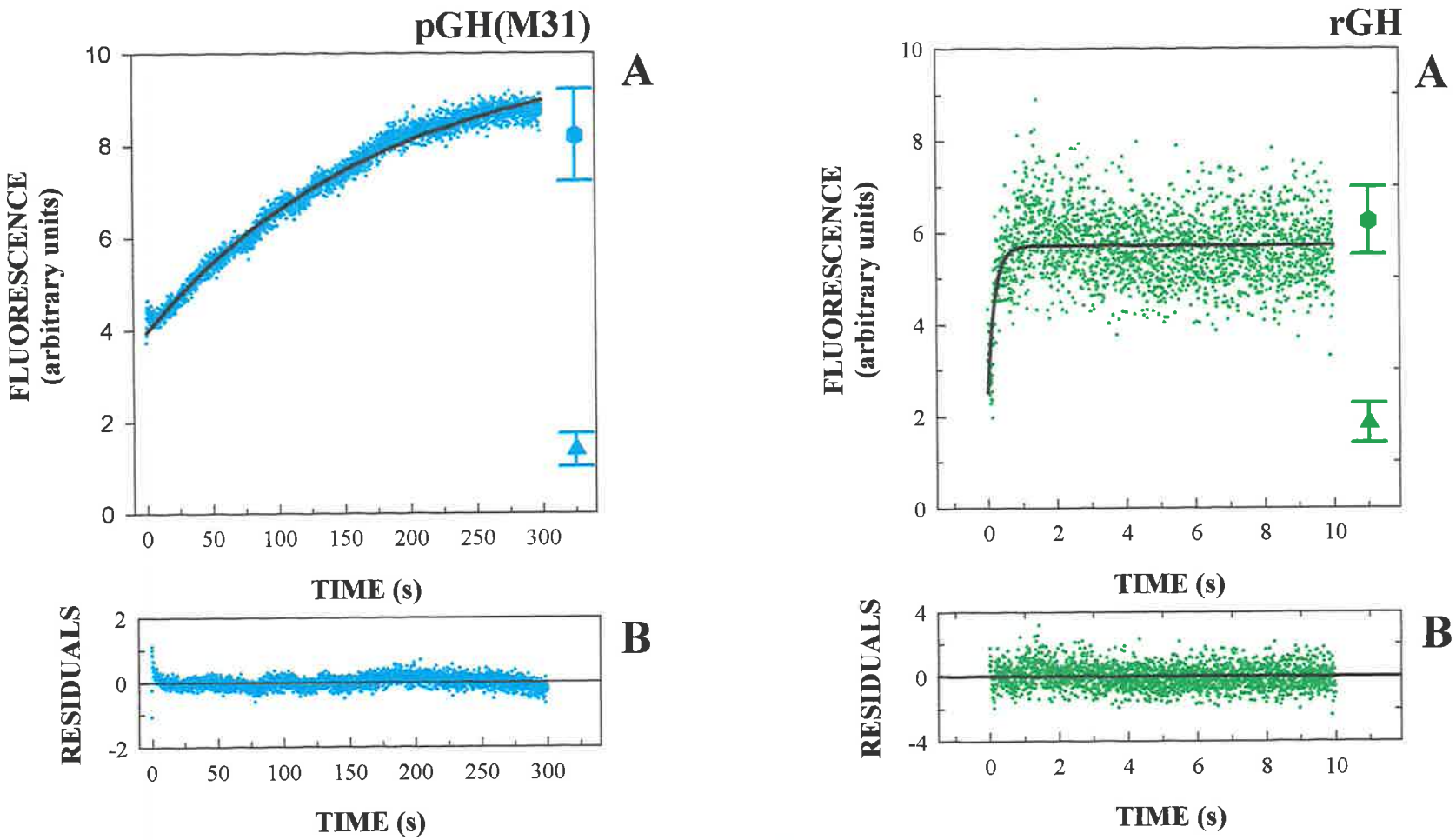

FIGURE 6.8 cont. UNFOLDING OF pGH ANALOGUES. Unfolding was initiated by the dilution of folded protein in 25 mM sodium borate, pH 9.1, to 4 M Gdn–HCl in 25 mM sodium borate, pH 9.1. The final protein concentration in all cases was 0.1 mg/ml.

A representative kinetic traces for the refolding of pGH(M31) and rGH. The solid line is the calculated fit for a single exponential function. The relative fluorescence intensity of each analogue in 25 mM sodium borate and 4 M Gdn-HCl, pH 9.1 are represented by ▲ ▲ and ⬢ ⬢ respectively.

B the residuals for fitting the refolding kinetics to a single exponential function.

expected fluorescence amplitude change (Figure 6.8). The time constant for the measurable kinetic phase for each protein varied, ranging from 0.2 s for rGH to 153 s for pGH(M31) (Table 6.3).

6.3 DISCUSSION

In this study, intrinsic tryptophan fluorescence was used to examine the folding kinetics of wild–type pGH, pGH(M8), pGH(M17), pGH(M31) and rGH. In native wild-type pGH, Trp86 is buried within the well-defined hydrophobic core of the protein and is in close proximity to an intramolecular quenching group, which results in a quenched native state fluorescence. Therefore, a change in the intrinsic fluorescence is a good indicator of the general refolding/unfolding of the molecule; however, it is not necessarily indicative of changes in the secondary structure. The conformational integrity of pGH(M8), pGH(M17), pGH(M31) and rGH has been previously examined by various spectroscopic methods and *in vitro* receptor binding assays (Bastiras, 1992). The mutations did not induce any apparent gross change in conformation or altered Trp86 microenvironment.

Refolding of wild-type pGH

The kinetics of folding and unfolding is a sensitive test for the detection of folding intermediates (Dobson *et. al.*, 1994). If a kinetic folding process is a two-state reaction with no observable intermediates, folding will follow a single exponential time course. The presence of an additional kinetic phase is evidence for the presence of a populated intermediate. Resolution of two kinetic phases for the refolding of wild–type pGH provides evidence for the presence of an intermediate along the kinetic folding pathway. Within the first second of folding the decrease in intrinsic fluorescence suggests that intramolecular quenching of Trp86 is significant, presumably as a consequence of interaction with side chain(s) in a partially collapsed state. In previous kinetic studies of bGH (Brems *et al.*, 1987a) and hGH (Youngman *et al.*, 1995), approximately 70% of the helix structure formed in an unobservable burst phase. With the structural homology between bGH, hGH and pGH, it is most likely that a significant proportion of helix for pGH has formed prior to

the fluorescence changes observed in this study. It is thus envisaged that within the first second of folding the Trp86 containing hydrophobic core has become partially formed creating a loose structure with some long range tertiary interactions.

In the subsequent slow folding phase of approximately 8 s, the final packing of the hydrophobic core and correct alignment of the secondary structure via tertiary interactions takes place, invoking the native interaction between Trp86 and the intramolecular quenching moiety. In a number of small globular proteins, the slow kinetic phases of folding are thought to represent the reversible folding of an intermediate to the native conformation (Kim and Baldwin, 1982). The time constant of the slow phase increased at elevated protein concentrations ($\geq$ 0.3 mg/ml). With evidence for the presence of an intermediate ensemble, the increase in time constant is most likely to be a consequence of competing intermolecular interactions between these intermediates, similar to that observed for bGH (Brems *et al.*, 1987a) and a number of other systems (Utiyama and Baldwin, 1986).

Unfolding of wild-type pGH

The unfolding of wild–type pGH was significantly faster than refolding, with approximately 50% of the reaction occurring within the dead time of the stopped flow instrument (< 5 ms). A burst phase was also observed in the unfolding of bGH as detected by UV-absorbance and only a fraction of the reaction was observable by far-UV CD (Brems et al., 1987a). No explanation was given to the lack of coincidence between the refolding and unfolding kinetics of bGH.

The absence of a significant burst phase in refolding suggests that there is a slow initial step in forming the protein's tertiary structure. In a study of the folding kinetics of the equilibrium folding intermediate of apomyoglobin using tryptophan fluorescence, a similar result was observed (Jamin and Baldwin, 1996). The folding intermediate of apomyoglobin contains the A, G and H helices of myoglobin which form a compact, helical subdomain of myoglobin (Hughson *et al.,* 1990). The authors suggested that the slow folding step might take the form of a nucleation reaction: once a nucleus is formed, folding proceeds extremely rapidly (Jamin and Baldwin, 1996). In a study of the kinetics of unfolding and refolding oligonucleotide $rA_n \bullet rU_n$ double helices, a burst phase in unfolding but not in refolding (Pörschke and Eigen, 1971) was observed. The absence of a burst phase in refolding was explained by the nucleation of the double helix in the first step of refolding: this was a pre-equilibrium step with a highly unfavourable equilibrium constant as measured directly with a special temperature-jump apparatus (Pörschke, 1974). The burst phase in unfolding was caused by the rapid initial unzipping of base pairs at either end of the double helix, which was fast. The folding mechanism of pGH is consistent with the framework model (secondary structure forming independently of tertiary structure). If a significant proportion of the α helical secondary structure of pGH forms within 5 ms of the refolding reaction (as seen for bGH and hGH), this structure may be a "nucleus" or the rate-limiting step required for the subsequent and apparently slow formation of tertiary structure. In contrast, for the unfolding of pGH, the data suggests that there is a very fast concomitant loss of secondary and tertiary structure ("burst phase") with the formation of the intermediate ensemble, which is followed by a final unfolding step. Note that in equilibrium denaturation studies of wild-type pGH, the initial loss of helix upon unfolding was coincident with the disruption of tertiary structure. In native wild-type pGH, Trp86 fluorescence is quenched. The increase in fluorescence in the burst phase may reflect the

removal of this quenching moiety, which is then followed by the complete unfolding of the protein and exposure of Trp86 to the bulk solvent.

The dependence of the detectable unfolding phase on the final protein concentration was negligible. In this study, the change in fluorescence reflects the removal of the moiety responsible for the native-state quenching of Trp86. Previous results have shown that the quenching moiety is removed in the associated intermediate (Bastiras, 1992). Consequently, unfolding monitored by fluorescence would be expected to be concentration-independent because association occurs subsequent to fluorescence-detected denaturation.

Kinetic intermediate for wild–type pGH

The results from this study suggest that a kinetic folding intermediate exists along the folding pathway of wild-type pGH. The refolding and unfolding kinetics determined by intrinsic fluorescence for wild-type pGH are qualitatively similar to the kinetics obtained by UV absorbance at 290 nm for bGH refolding and unfolding (Brems *et al.*, 1987a); the two optical detection techniques being probes of tertiary structure. The increased dependence of the kinetic data for the slower phase of refolding at elevated protein concentrations for wild–type pGH, was also seen in the refolding of bGH and attributed to the formation of a transient associated species (Brems *et al.*, 1987a). Despite the kinetics of secondary structure acquisition remaining unknown for wild-type pGH, by analogy with the homologous protein bGH, it is likely that the features of the kinetic intermediate ensemble detected for pGH are consistent with those of equilibrium molten globule states.

In simplistic terms, the kinetic mechanism, which describes the folding of wild-type pGH can be written as:

$$\mathbf{N} \overset{\text{slow}}{\leftrightarrow} \boldsymbol{I} \overset{\text{fast}}{\leftrightarrow} \mathbf{U}$$
$$\updownarrow$$
$$\boldsymbol{I}_{\mathbf{assoc}}$$

where N, I, I_{assoc} and U correspond to the native, intermediate, associated and unfolded forms respectively.

The transient associated species for bGH was characterised by a strong CD signal at 300 nm [θ_{300}], a unique signal seen for the associated species detected at equilibrium (Havel *et al.*, 1986). For pGH, the associated species detected at equilibrium under partially denaturing conditions (3 M Gdn-HCl, pH 9.1), is also characterised by the same unique CD signal at 300 nm (Bastiras and Wallace, 1992). If the transient kinetic intermediate of pGH is similar to the intermediate detected at equilibrium, it would also have the same unique CD signal [θ_{300}]. Whether this species is similar to that formed near 3 M Gdn–HCl in equilibrium denaturation studies cannot be confirmed from this study. However, with the apparent similarity in the folding behavior of pGH and bGH it seems likely that for wild-type pGH, the equilibrium folding intermediate, *I*, with characteristics of a molten globule (Bastiras and Wallace, 1992) is also populated transiently, during kinetic folding studies.

pGH(M8) The folding kinetics for pGH(M8) were significantly different to the kinetics obtained for wild-type pGH. Both the refolding and unfolding kinetics were monophasic, suggesting that pGH(M8) folds according to a two-state model with no detectable intermediates. For proteins that fold according to a two-state model, the rate of refolding

and unfolding displays a linear dependence on the Gdn–HCl concentration. When plotted together, these rates show a V-shaped dependence (Chevron Plot) on the denaturant concentration with a minimum in the transition region (Matthews *et al.*, 1987). Surprisingly, the rate of refolding and unfolding at different final Gdn–HCl concentrations did not vary (data not shown), which was contrary to what would be expected for a two-state folding system. Therefore, does an intermediate exist on the kinetic folding pathway of pGH(M8)?

The equilibrium denaturation of pGH(M8) as detected by UV-absorbance, intrinsic fluorescence and hydrodynamic properties resulted in very similar transitions, with midpoints of 2.99, 2.97 and 2.96 M Gdn–HCl for UV, fluorescence and hydrodynamic radius, respectively (Bastiras, 1992). The coincidence of the transitions suggested that the denaturation of pGH(M8) approached a two-state folding mechanism. Moreover, an elevated $\Delta G(H_2O)$ for pGH(M8) of 10.19 kcal/mol compared with 7.06 kcal/mol for wild-type pGH predicted that the folding mechanism would more closely approach a two-state mechanism. However, an associated intermediate was populated at elevated protein concentrations, suggesting that a monomeric intermediate does exist albeit transiently (Dr. S. Bastiras, personal communication).

The kinetic traces observed for pGH(M8) were "opposite" to those seen for wild–type pGH For pGH(M8), refolding and unfolding was characterised by an increase and decrease in fluorescence, respectively, whereas for pGH, refolding and unfolding was characterised by a decrease and increase in fluorescence respectively. The ability to identify the presence of intermediate structure depends on both the location and sensitivity of the reporting group. For pGH(M8), the intrinsic fluorescence intensity is the sum of the contributing

emission from both Trp86 and Trp124. In wild-type pGH Trp86 fluorescence is quenched and it is likely that Trp86 fluorescence in pGH(M8) would also be quenched (see Chapter 5). It is therefore proposed that the change in fluorescence properties together with the monophasic kinetics obtained for pGH(M8) reflects changes in the immediate environment of Trp124 rather than the global folding/unfolding of the molecule as interpreted for wild-type pGH. However, it is possible that the folding monitored by fluorescence for Trp86 in pGH(M8) may be different to that for wild–type pGH. Irrespective of this, it is clear that another probe(s) is required to study the folding kinetics of pGH(M8) e.g. UV absorbance spectroscopy or near-UV CD. In addition, the kinetics of secondary structure formation/unfolding may be able to confirm the existence of a folding intermediate.

pGH(M17) The conformational stability of pGH(M17) and wild-type pGH have been previously determined, with a value for $\Delta G(H_2O)$ of 7.57 kcal/mol and 7.06 kcal/mol for pGH(M17) and wild-type pGH respectively (Bastiras, 1992). This suggested that the stability of pGH(M17) is marginally greater than wild-type pGH. The two mutations K30E; R34E have not significantly affected the kinetics of folding of pGH(M17). The fast and slow refolding phases and the observable unfolding phase were similar for pGH(M17) and wild-type pGH. However, the slow folding phase rate for pGH(M17) was decreased. In the proposed mechanism for pGH folding kinetics, the slow phase of refolding corresponds to the I↔N transition. This suggests that the free energy of the intermediate species for pGH(M17) relative to the transition state has changed (Garvey and Matthews, 1990). Interestingly, the rates for refolding and unfolding which correspond to the U↔I transition are in reasonable agreement. Whilst the observable rate of unfolding for pGH(M17) and wild-type pGH were similar, the fraction of observed amplitude was decreased for pGH(M17) (35% of total expected amplitude for pGH(M17) compared to

50% for wild-type pGH). The "burst phase" amplitude is thus larger for pGH(M17) suggesting that the "burst phase" intermediate is stabilised (McGee and Nall, 1998).

pGH(M31) The apparent conformational stability of pGH(M31) and wild-type pGH is similar with a $\Delta G(H_2O)$ of 6.94 kcal/mol and 7.06 kcal/mol for pGH(M31) and wild-type pGH, respectively. However, the mutations were shown to stabilise the self associated intermediate of pGH(M31). At a protein concentration of 2.3 μM, 76% of pGH(M31) was associated, whereas for wild-type pGH association is not apparent until ≥ 10 μM. The three mutations T98A; F103Y; T105A did not affect the kinetics of refolding. In contrast, however, the rate of the observable unfolding phase was significantly reduced when compared to wild-type pGH. For rates of unfolding to be selectively changed, the free energy of the native structure relative to the free energy of the transition state and the intermediate must be altered (Garvey and Matthews, 1990), eminating primarily from alterations in the native structure (Alber *et al.*, 1987). The amino acid changes in pGH(M31) lie within the short omega-loop sequence between helix 2 and helix 3 of pGH. These changes mimic the sequence seen within this region of hGH, which forms a short helix (de Vos *et al.*, 1992). To what extent these mutations would affect the native conformation is unknown. It is possible that an increase in rigidity of the connection between the two helices may affect mobility/stability of the structure.

rGH The refolding kinetics for rGH were very similar to wild-type pGH. The resolution of two kinetic phases for the refolding of rGH provides evidence for the presence of an intermediate along the kinetic folding pathway. In contrast, the unfolding kinetics of rGH was distinctly different to wild-type pGH, with the resolution of a single kinetic phase that accounted for the total expected amplitude change. Like wild-type pGH, the native state

Trp86 fluorescence of rGH is quenched. If we consider the unfolding of wild-type pGH, I have speculated that the burst phase may correspond to the removal of the moiety responsible for quenching. For rGH, although speculative, it would appear that the removal of the quenching moiety and subsequent exposure of Trp86 to bulk solvent upon unfolding is a concomitant process. Such a difference may arise from differences between the native conformation for the two proteins, which would agree with the selective change of the unfolding kinetics of rGH when compared to wild-type pGH. The change in amino acid sequence between rGH and wild-type pGH occur within the loop regions of the protein molecule and are reasonably conservative. However, these changes may be sufficient to induce subtle changes in the packing of the helices which are reflected in the kinetic data. As seen with pGH(M8) fluorescence may not be the ideal probe to study the folding kinetics of rGH.

In summary, wild-type pGH possesses a transient intermediate along the folding pathway. This intermediate is proposed to have similar properties to the stable intermediate detected at equilibrium, possessing characteristics of the molten globule. The kinetics of pGH(M8) folding are complex due to the presence of a second tryptophan and it is clear that other probes are required to study the mechanism. For pGH(M17), the two mutations K30E; R34E have apparently increased the free energy of the intermediate relative to the transition state. The mutations in pGH(M31) reflect changes in the free energy of the native state. The kinetics of rGH folding suggests that the refolding and unfolding mechanisms may be different. Whilst this study has provided some insight into the folding mechanism of the mutants, clearly, further examination using different spectroscopic probes such as near-UV absorbance and far-UV CD will be required to characterise the kinetic folding intermediates and mechanism of folding.

CHAPTER 7

CONCLUDING DISCUSSION

Objectives of this study

It is important to determine the structural characteristics of folding intermediates to gain insight into the folding mechanism of any one particular protein or family of proteins. Previously, it has been shown that the Gdn–HCl-induced equilibrium denaturation of pGH deviates from a two-state mechanism, with the detection of conformations, intermediate to the fully unfolded or native state (Bastiras and Wallace, 1992). These intermediate forms have the characteristics of a molten globule. This study has examined the acid-induced denaturation and folding kinetics of recombinant pGH, to characterise the intermediates in the folding pathway.

Acid-induced denaturation of pGH

Acidification of pGH alone and in the presence of 4 M urea resulted in the formation of intermediate species that possessed characteristics of the molten globule. Both species retained a significant amount of secondary structure and possessed negligible tertiary structure. Differences in the maximum wavelength of emission of Trp86 (which is located in helix 2 and located within the hydrophobic core of the native state molecule), as well as ANS fluorescence and models of self-association show that the conformation of these intermediates is different. However, it is important to note that the monomer of each intermediate was not directly observed, due to stabilisation through self-association, thus the structural characteristics described here for the monomer are inferred from the experimental evidence. The intermediate at low pH is characterised by a native-like tertiary fold (spatial arrangement of the secondary structure elements), with a reasonably tightly packed core of the four α-helices. This proposed conformation is supported by the secondary structure content and the similarity in the maximum wavelength of fluorescence emission for Trp86 in this state and the native state. The intermediate at low pH and 4 M

urea has a reduced amount of helical structure. The core is more loosely packed as evidenced by the reduced hydrophobic environment surrounding Trp86. Interestingly, this less structured intermediate has a reduced hydrophobic surface area and reduced propensity to associate, which is contrary to that seen in other studies (Fink *et al.*, 1998; Uversky *et al.*, 1998). This is likely due to the presence of the self-associated species rather than the monomer. Whether these intermediates represent discrete species along the folding pathway of pGH cannot be determined from this data. This could be confirmed by determining of the stability (ΔG) and the cooperativity (*m*) of each intermediate, a free energy difference between the intermediates would confirm that they are discrete species. Interestingly, the structural characteristics of the intermediate species at low pH and 4 M urea are very similar to the self-associated intermediate detected at equilibrium in moderate Gdn-HCl concentrations (Bastiras and Wallace, 1992). Specifically, they possess a unique CD spectral signal at 300 nm and it is hypothesised that they are indeed the same intermediate.

Acid-induced denaturation of pGH analogues

The acid-induced denaturation of pGH analogues resulted in the formation of intermediate species with characteristics of a molten globule. In comparison to wild-type pGH, the intermediate species of each analogue was shown to have regions of unique structure in terms of fluorescence and ANS binding. However, it is likely that each protein retains a core of native-like α-helical structure. The analogue pGH(M8) may provide a means to study the monomeric intermediate. There was evidence from SEC to suggest that the monomer may be present as a discrete species at low pH, which could be confirmed using sedimentation equilibrium studies. The monomer could be purified and subjected to the advanced NMR techniques, which are providing an insight at atomic resolution as to the

structure of these intermediates. Similarly rGH may be useful. At pH 4, from intrinsic fluorescence, a species, which may be the monomer, was apparently stabilised. If confirmed as a monomer by sedimentation equilibrium this species could also be purified and studied at an atomic level.

Folding kinetics of pGH and pGH analogues

Resolution of two kinetic phases in the unfolding and folding of pGH confirms the presence of an intermediate species along the folding pathway of pGH. Previous kinetic folding studies of bGH and hGH, have shown that a significant amount of secondary structure forms within the dead time of the stopped-flow instrument. With a similar structure for all growth hormones, this would be the same for pGH. Thus the kinetic intermediate species detected for pGH is a molten globule. Is the kinetic molten globule structurally the same as the equilibrium molten globule? The equilibrium molten globule of pGH self-associates, and this self-associated species is characterised by a unique near-UV CD signal at 300nm. The kinetic intermediate was also shown to associate and if shown to possess the same near-UV CD at 300 nm by following the kinetic reaction at 300 nm the similarity between the intermediates could be confirmed. The folding kinetics of the pGH analogues was not grossly changed. Fluorescence detection was shown to be inappropriate for following the folding of pGH(M8), which has an extra tryptophan residue. Thus it would be necessary to use a different optical probe to study the folding kinetics of this protein. For pGH(M17) pGH(M31) and rGH, changes in the unfolding kinetics only, were observed. This suggests that the free energy of the intermediate species relative to the transition-state changes, which emanate primarily from structural alterations in the native structure. These proteins were shown to have similar ΔG values, suggesting that the amino acid changes do not significantly affect the stability of the native state, but as shown here

do affect the kinetics of folding. This highlights the need to examine protein folding both at equilibrium and kinetically.

Concluding remarks

The mechanism of pGH folding has been previously described as being consistent with the framework model of folding (Bastiras and Wallace, 1992), which implies the presence of specific structures along the folding pathway. The new view of folding introduces the funnel concept, where there are ensembles rather than specific structures. The folding of pGH can also be described in terms of a hierarchical model of folding process where two funnels would be present (Arai and Kuwajima, 2000). In funnel 1, the molten globule state forms from the unfolded state and in funnel 2 the native state forms from the molten globule state. The molten globule state of pGH is structurally diverse which is dependent on the solvent conditions. What kind of molten globule state, a structured molten globule state or a less structured one, accumulates during folding will depend where the largest free energy barrier is located along funnel 2 (Arai and Kuwajima, 2000). Recently, the question has been asked, "Is there a unifying mechanism for protein folding" (Daggett and Fersht, 2003). The authors suggest that the framework model of folding can be viewed as an extreme of nucleation-condensation, whereby for a typical domain in which the intrinsic conformational preferences for secondary structure are weak, the formation of the transition state requires a considerable network of tertiary interactions to stabilize it. In domains that have strong conformational preference e.g. engrailed homeodomain, folding appears hierarchical, and some proteins might fall into a trap of a molten globule if hydrophobic interactions are formed too rapidly and strongly. In the more general interpretation, the model describes that heightened stability of secondary structure can shift the mechanism to account not only for the formation of folding intermediates but also for hierarchical models of folding in general. In addition, through combined and experimental

effort a novel mode of secondary structure formation via a tertiary, contact-assisted mechanism was discovered. This mechanism allows for generalization of the nucleation-condensation model and provides a detailed view of the coupling between secondary and tertiary structure.

BIBLIOGRAPHY

Abdel-Meguid, S. S., Shieh, H.-S., Smith, W. W., Dayringer, H. E., Violand, B. N. and Bentle, L. A. (1987) Three dimensional structure of a genetically engineered variant of porcine growth hormone. *Proc. Natl. Acad. Sci.* **84**, 6434-6437

Abildgaard, F., Jorgensen, A. M., Led, J. J., Christensen, T., Jensen, E. B., Junker, F. and Dalboge, H. (1992) Characterization of tertiary interactions in a folded protein by NMR methods: studies of pH-induced structural changes in human growth hormone. *Biochemistry* **31**, 8587-96

Adams, E. T., and Fujita, H. (1963) in *Ultracentrifugal Analysis in Theory and Experiment* (Williams, J. W., Ed.) pp 119-129, Academic Press, New York

Adams, E. T., Tang, L.-H., Sarquis, J. L., Barlow, G. H., and Norman, W. M. (1978) in *Physical Aspects of Protein Interactions* (Catsimpoolas, N., Ed.) pp 1-55, Elsevier/North-Holland, Amsterdam

Agashe, V. R., Shastry, M. C., and Udgaonkar, J. B. (1995) Initial hydrophobic collapse in the folding of barstar. *Nature* **377**, 754-7

Alber, T. (1989) in *Prediction of Protein Structure and the Principles of Protein Conformation* (Fasman, G. D. Ed) pp 161-192, Plenum Press, New York

Alber, T., Sun, D. P., Nye, J. A., Muchmore, D. C., and Matthews, B. W. (1987) Temperature-sensitive mutations of bacteriophage T4 lysozyme occur at sites with low mobility and low solvent accessibility in the folded protein. *Biochemistry* **26**, 3754-3758

Anfinsen, C.B. (1973) Principles that govern the folding of protein chains. *Science* **181**, 223-230

Anfinsen, C. B., and Scheraga, H. A. (1975) Experimental and theoretical aspects of protein folding. *Adv. Protein Chem.* **29**, 205-300.

Arai, M., and Kuwajima, K. (1996) Rapid formation of a molten globule intermediate in refolding of alpha-lactalbumin. *Folding & Design* **1**, 275-287

Arai, M., and Kuwajima, K. (2000) Role of the molten globule state in protein folding. *Adv. Prot. Chem.* **53**, 209-282

Aune, K.C., Salahuddin, A., Zarlenyo, M. H., and Tanford, C. (1967) Evidence for residual structure in acid- and heat-denatured proteins. *J. Mol. Biol.* **242**, 4486-4489

Bailey, J. E., and Ollis, D. F. (1986) in *Biochemical Engineering Fundamentals 2nd Edition*, pp 403-404, MacGraw-Hill, New York

Baker, E. N. and Hubbard, R. E. (1984) Hydrogen bonding in globular proteins. *Prog. Biophys. Mol. Biol.* **44**, 97-179

Baldwin, R. L. (1995) The nature of protein folding pathways: The classical versus the new view. *J. Biomolec. NMR* **5**, 103-109

Barlow, D. J. and Thornton, J. M. (1983) Ion-pairs in proteins. *J. Mol. Biol.* **168**, 867-885

Bastiras, S. (1992) Folding and conformational stability of porcine growth hormone. *Ph.D. Thesis*, Department of Biochemistry, University of Adelaide, South Australia

Bastiras, S. and Wallace, J. C. (1992) Equilibrium denaturation of recombinant porcine growth hormone. *Biochemistry* **31**, 9304-9309

Baum, J., Dobson, C. M., Evans, P. A. and Hanley, C. (1989) Characterization of a partly folded protein by NMR methods: Studies on the molten globule state of guinea pig α-lactalbumin. *Biochemistry* **28**, 7-13

Bello, J. (1978) Tight packing of protein cores and interfaces. Relation to conservative amino acid sequences and stability of protein-protein interaction. *Int. J. Peptide Res.* **12**, 38-41

Bewley, T. A. and Li, C. H. (1970) Human pituitary growth hormone. XXII. Reduction and reoxidation of the hormone. *Arch. Biochem. Biophys.* **138**, 338-346

Bewley, T. A. and Li, C. H. (1984) Conformational comparison of human pituitary growth hormone and human chorionic somatomammotropin (human placental lactogen) by second-order absorption spectroscopy. *Arch. Biochem. Biophys.* **233**, 219-227

Blagdon, D. E., and Goodman, M. (1975) Letter: Mechanisms of protein and polypeptide helix initiation. *Biopolymers* **14**, 241-245

Booth D. R., Sunde, M., Bellotti, V., Robinson, C. V., Hutchinson, W. L., Fraser, P. E., Hawkins, P. N., Dobson, C. M., Radford, S. E., Blake, C. C., and Pepys, M. B. (1997) Instability, unfolding and aggregation of human lysozyme variants underlying amyloid fibrillogenesis. *Nature* **385**, 787-793.

Brand, L. and Witholt, B. (1967) Fluorescence measurements. *Methods Enzymol.* **11**, 776-855

Brandts, J. F., and Hunt, I., (1967) The thermodynamics of protein denaturation. 3. The denaturation of ribonuclease in water and in aqueous urea and aqueous ethanol mixtures. *J. Am. Chem. Soc.* **89**, 4826-4838

Brems, D. N. (1988) Solubility of the folding conformers of bovine growth hormone. *Biochemistry* **27**, 4541-4546

Brems, D. N., Plaisted, S. M., Kauffman, E. W. and Havel, H. A., Kauffman, E. W., Stodola, J. D., Eaton, L. C. and White, R. D. (1985) Equilibrium denaturation of pituitary- and recombinant- derived bovine growth hormone. *Biochemistry* **24**, 7662-7668

Brems, D. N., Plaisted, S. M., Kauffman, E. W. and Havel, H. A. (1986) Characterisation of an associated equilibrium folding intermediate of bovine growth hormone. *Biochemistry* **25**, 6539-6543

Brems, D. N., Plaisted, S. M., Jr. Dougherty, J. J., and Holzman, T. F. (1987a) The kinetics of bovine growth hormone folding are consistent with a framework model. *J. Biol. Chem.* **262**, 2590-2596

Brems, D. N., Plaisted, S. M., Kauffman, E. W. Lund, M. and Lehrman, S. R. (1987b) Helical formation in isolated fragments of bovine growth hormone. *Biochemistry* **26**, 7774-7778

Brems, D. N., Plaisted, S. M., Havel, H. A., and Tomich, C.-S. C. (1988) Stabilization of an associated folding intermediate of bovine growth hormone by site-directed mutagenesis. *Proc. Natl. Acad. Sci. USA.* **85**, 3367-3371

Brems, D. N. and Havel, H. A. (1989) Folding of bovine growth hormone is consistent with the molten globule hypothesis. *Proteins: Struct. Func. Genet.* **5**, 93-95

Brems, D. N., Brown, P. L. and Becker, G. W. (1990) Equilibrium denaturation of human growth hormone and its cysteine modified forms. *J. Biol. Chem.* **265**, 5504-5511

Buck, M. A., Olah, T. A., Weitzman, C. T. and Cooperman, B. S. (1989) Protein estimation by the product of integrated peak area and flow rate. *Anal. Biochem.* **182**, 295-299

Burger, H. G., Edelhoch, H. and Condliffe, P. G. (1966) The properties of bovine growth hormone. I. Behaviour in acid solution. *J. Biol. Chem.* **241**, 449-457

Bychkova, V. E., and Ptitsyn, O. B. (1995) The molten globule state is involved in genetic diseases? *FEBS Lett.* **359**, 6-8

Capaldi, A.P., Shastry, M. C. R., Kleanthous, C., Roder, H. and Radford, S. E. (2001) Ultrarapid mixing experiments reveal that IM7 folds via an on-pathway intermediate. *Nat. Struct. Biol.* **8**, 68-72

Caramelo, J. J., Castro, O. A., Alonso, L. G., de Prat-Gay, G., and Parodi, A. J. (2003) UDP-Glc:glycoprotein glucosyltransferase recognizes structured and solvent accessible hydrophobic patches in molten globule-like folding intermediates. *Proc. Natl. Acad. Sci. USA* **100**, 86-91

Carlacci, L., Chou, K.-C. and Maggiora, G. M. (1991) A heuristic approach to predicting the tertiary structure of bovine somatotropin. *Biochemistry* **30**, 4389-4398

Carra, J. H., Anderson, E. A. and Privalov, P. L. (1994) Thermodynamics of staphylococcal nuclease denaturation II. The A-state. *Protein Sci.* **3**. 952-959

Cleland, W. W. (1967) The statistical analysis of enzyme kinetic data. *Adv. Enzymol. Relat. Areas Mol. Biol.* **21**, 1-32

Colón, W., Elöve, G. A., Wakem, L. P., Sherma, F. and Roder, H (1996) Side chain packing of the N- and C-terminal helices plays a critical role in the kinetics of cytochrome c folding. *Biochemistry* **35**, 5538-5549

Cohn, E. J., and Edsall, J. T. (1943*) Proteins, Amino Acids and Peptides as Ions and Dipolar Ions*, Reinhold, New York

Corbett, RT., and Roche, R. S. (1984) Use of high-speed size-exclusion chromatography for the study of protein folding and stability. *Biochemistry* **23**, 1888-1894

Dabora, J. M., Pelton, J. G., and Marqusee, S (1996) Structure of the acid state of Escherichia coli ribonuclease HI. *Biochemistry* **35**, 11951-11958

Daggett, V., and Fersht, A. R. (2003) Is there a unifying mechanism for protein folding? *TIBS*. **28**, 18-25

DeFelippis, M. R., Alter, L. A., Pekar, A. H., Havel, H. A. and Brems, D. N. (1993) Evidence for a self-associating equilibrium intermediate during folding of human growth hormone. *Biochemistry* **32**, 1555-1562

DeFelippis, M. R., Kilcomons, M. A., Lents, M. P., Youngman, K. M. and Havel H. A. (1995) Acid stabilization of human growth hormone equilibrium folding intermediates. *Biochim. Biophys. Acta.* **1247**, 35-45

De Filippis, V., Polverino de Laureto, P., Toniutti, N., and Fontana, A. (1996) Acid-induced molten globule state of a fully active mutant of human interleukin-6. *Biochemistry* **35**, 11503-11511

de Vos, A. M., Ultsch, M. and Kossiakoff, A. A. (1992) Human growth hormone and extracellular domain of its receptor: crystal structure of its complex. *Science* **255**, 306-312

Dill, K. A. (1990) Dominant forces in protein folding. *Biochemistry* **29**, 7135-7155

Dill, K. A., and Chan, H. S. (1997) From levinthal to pathways to funnels. *Nat. Struct. Biol.* **4**, 10-19

Dobson, C. M. (1991) Characterization of protein folding intermediates. *Curr. Opin. Struct. Biol.* **1**, 22-27

Dobson, C. M. (1995) Finding the right fold. *Nat. Struct. Biol.* **2**, 513-7

Dobson, C. M., Evans, P. A. and Radford, S. E. (1994) Understanding how proteins fold: the lysozyme story so far. *Trends Biochem. Sci.* **19**, 31-7

Dolgikh, D. A., Gilmanshin, R. I., Brazhnikov, E. V., Bychkova, V. E., Semisotnov, G. V., Venyaminov, S. Yu, and Ptitsyn, O. B. (1981) Alpha-Lactalbumin: compact state with fluctuating tertiary structure? *FEBS Lett.* **136**, 311-5

Donovan, J. W. (1973) Spectrophotometric titration of the functional groups of proteins. *Methods Enzymol.* **27**, 525-548

Edelhoch, H. and Burger, H. G. (1966) The properties of bovine growth hormone. II. Effects of urea. *J. Biol. Chem.* **241**, 458-463

Edwards, S. L., and Dubin, P. L. (1993) pH effects on non-ideal protein size-exclusion chromatography on Superose 6. *J. Chromatogr.* **648**, 3-7

Engelhard, M. and Evans, P. A. (1996) Experimental investigation of sidechain interactions in early folding intermediates. *Folding & Design* **1**, R31-R37

Evans, P. A. and Radford, S. E. (1994) Probing the structure of folding intermediates. *Curr. Opin. Strct. Biol.* **4**, 100-106

Ewbank, J.J. and Creighton, T. E. (1991) The molten globule protein conformation probed by disulphide bonds. *Nature* **350**, 518-520

Feng, Y., Sligar, S. G. and Wand A. J. (1994) Solution structure of apocytochrome b562. *Nat. Struct. Biol.* **1**, 30-35

Fink, A. L., Calciano, L. J., Goto, Y., Kurotsu, T. and Palleros, D. R. (1994) Classification of acid denaturation of proteins: intermediates and unfolded states. *Biochemistry* **33**, 12504-12511

Fink, A. L. (1995) Compact Intermediate States in protein folding. *Annu. Rev. Biophys. Biomol. Struct.* **24**, 495-522

Fink, A. L. (1998) Protein aggregation: folding aggregates, inclusion bodies and amyloid. *Folding & Design* **3**, R9-R23

Fink, A. L., Oberg, K. A., and Seshadri, S. (1998) Discrete intermediates versus molten globule models for protein folding: characterization of partially folded intermediates of apomyoglobin. *Folding & Design* **3**, 19-25

Garvey, E. P., and Matthews, C. R. (1990) in *Protein Engineering: Approaches to the Manipulation of Protein Folding* (Narang, S. A., Ed.) pp. 37-63, Butterworths, Toronto

Geierstanger, B., Jamin, M., Volkman, B. F. and Baldwin, R.L. (1998) Protonation behaviour of histidine 24 and histidine 119 in forming the pH 4 folding intermediate of apomyoglobin. *Biochemistry* **37**, 4254-4265

Goldberg, M. E, and Guillou, Y. (1994) Native disulfide bonds greatly accelerate secondary structure formation in the folding of lysozyme. *Protein Sci.* **3**, 883-887

Goto, Y., Calciano, L. J., and Fink, A. L. (1990a) Acid-Induced folding of proteins. *Proc. Natl. Acad. Sci. U.S.A.* **87**, 573-577

Goto, Y., Takahashi, N. and Fink, A. L. (1990b) Mechanism of acid-induced folding of proteins. *Biochemistry* **29**, 3480-3488

Goto, Y.,Hagihara, Y., Homada, D., Hoshino, M. and Nishii, I. (1993) Acid-induced unfolding and refolding of cytochrome *c*: a three state mechanism in H_2O and D_2O *Biochemistry* **32**, 11878-11885

Havel, H. A., Kauffman, E. W., Plaisted, S. M. and Brems, D. N. (1986) Reversible self-association of bovine growth hormone during equilibrium unfolding. *Biochemistry* **25**, 6533-6538

Havel, H. A., Kauffman, E. W. and Elzinga, P. A. (1988) Fluorescence quenching studies of bovine growth hormone in several conformational states. *Biochim. Biophys. Acta.* **955**, 154-163

Havel, H. A. (1996) in *Spectroscopic methods for determining protein structure in solution.* (Havel, H. A., Ed.), pp 62-68

Hayer-Hartl, M. K., Ewbank, J. J., Creighton, T. E., and Hartl, F. U. (1994) Conformational specificity of the chaperonin GroEL for the compact folding intermediates of alpha-lactalbumin. *EMBO J.* **13**, 3192-3202

Holladay, L. A., Hammonds, R. G. and Puett, D. (1974) Growth Hormone conformation and conformational equilibria. *Biochemistry* **13**, 1653-1661

Holzman, T. F., Jr,, Dougherty, J. J., Brems, D. N., and MacKenzie, N. E. (1990) pH-induced conformational states of bovine growth hormone. *Biochemistry* **29**, 1255-1261

Holzman, T. F., Dougherty, J. J. Jr., Brems, D. N. and Mackenzie, N. E. (1990) pH-induced conformational states of bovine growth hormone. *Biochemistry* **29**, 1255-61

Honig, B. and Yang, A-S. (1995) Free energy balance in protein folding. *Adv. Prot. Chem.* **46**, 27-57

Hughson, F. M., Wright, P. E., and Baldwin, R. L. (1990) Structural characterization of a partly folded apomyoglobin intermediate. *Science* **49**, 1544-1548

Hurle, M. R., Helms, L. R., Li, L., Chan, W., and Wetzel, R. (1994) A role for destabilizing amino acid replacements in light-chain amyloidosis. *Proc. Natl. Acad. Sci. USA.* **91**, 5446-5450

Ikeguchi, M., Sugai, S., Fujino, M., Sugawara, T., and Kuwajima, K. (1992) Contribution of the 6-120 disulfide bond of α-lactalbumin to the stabilities of its native and molten globule states. *Biochemistry* **31**, 12695-12700

Jackson, S. E. (1998) How do small single-domain proteins fold? *Folding & Design* **3**, R81-R91

Jacobson, R. H., Matsumura, M., Faber, H. R., and Matthews, B. W. (1992) Structure of a stabilizing disulfide bridge mutant that closes the active-site cleft of T4 lysozyme. *Protein Sci.* **1**, 46-57

Jamin, M., and Baldwin, R.L. (1996) Refolding and unfolding kinetics of the equilibrium folding intermediate of apomyoglobin. *Nat. Struct. Biol.* **3**, 613-618

Jeng, M. F., Englander, S. W., Elöve, G. A., Wand, A. J., and Roder, H. (1990) Structural description of acid-denatured cytochrome *c* by hydrogen exchange and 2D NMR. *Biochemistry* **29**, 10433-10437

Jennings, P. A., and Wright, P. E. (1993) Formation of a molten globule intermediate early in the kinetic folding pathway of apomyoglobin. *Science* **262**, 892-896

Johnson, M. L. and Yphantis, D. A. (1978) Subunit association and heterogeneity of Limulus polyphemus hemocyanin. *Biochemistry* **17**, 1448-55

Kalnin, N. N. and Kuwajima, K. (1995) Kinetic folding and unfolding of staphylococcal nuclease and its six mutants studied by stopped-flow circular dichroism. *Proteins: Struct. Funct. Genet.* **23**, 163-176

Kamtekar, S., Schiffer, J. M., Xiong, H., Babik, J. M. and Hecht, H. H. (1993) Protein design by binary patterning of polar and nonpolar amino acids. *Science* **262**, 1680-1685

Kasimova, M. R., Milstein, S. J. and Freire, E. (1998) The conformational equilibrium of human growth hormone. *J. Mol. Biol.* **277**, 409-418

Kasimova, M. R., Kristensen, S. M., Howe, P. W. A., Christensen, T., Matthiesen, F., Petersen, J., Sorensen, H. H. and Led, J. J. (2002) NMR Studies of the Backbone Flexibility and Structure of Human Growth Hormone: A Comparison of High and Low pH Conformations. *J. Mol. Biol.* **318**, 679-695

Kauffman, E. W., Thamann, T.J. and Havel, H. A. (1989) Ultraviolet resonance raman and fluorescence studies of acid-induced structural alterations in porcine, bovine, and human growth hormone. *J. Am. Chem. Soc.* **111**, 5449-5456

Khorasanizadeh, S., Peters I. D. and Roder, H. (1996) Evidence for a three-state model of protein folding from kinetic analysisi of ubiquitin variants with altered core residues. *Nat. Struct. Biol.* **3**, 193-205

Kiefhaber, T. (1995) Kinetic traps in lysozyme folding. *Proc. Natl. Acad. Sci. USA.* **92**, 9029-9033

Kim, P.S., and Baldwin, R. L. (1982) Specific intermediates in the folding reactions of small proteins and the mechanism of protein folding. *Annu. Rev. Biochem.* **51**, 459-489

Koradi, R., Billeter, M., and Wuthrick, K. (1996) MOLMOL: a program for display and analysis of macromolecular structures. *J. Mol. Graphics* **14**, 51-55

Kuroda, Y., Kidokoro, S., and Wada, A. (1992) Thermodynamic characterization of cytochrome c at low pH. Observation of the molten globule state and of the cold denaturation process. *J. Mol. Biol.* **223**, 1139-1153.

Kuwajima, K., Harushima, Y. S., and Sugai, S. (1986) Influence of Ca2+ binding on the structure and stability of bovine alpha-lactalbumin studied by circular dichroism and nuclear magnetic resonance spectra. *Int. J. Pept. Protein Res.* **27**, 18-27.

Kuwajima, K. (1989) The molten globule state as a clue for understanding the folding and cooperativity of globular-protein structure. *Proteins: Struct. Funct. Genet.* **6**, 87-103

Lakowicz, J. R. (1983) *Principles of Fluorescence Spectroscopy*, Plenum Press.

Laskowski, R. A., Luscombe, N. M., Swindells, M. B. and Thornton, J. M. (1996) Protein clefts in molecular recognition and function. *Protein Sci.* **5**, 2438-2452

Lau, K. F., and Dill, K. A. (1990) Theory for protein mutability and biogenesis. *Proc. Natl. Acad. Sci. USA.* **87**, 638-642

Lazaridis, T. and Karplus, M (1997) 'New view' of protein folding reconciled with the old through multiple unfolding simulations. *Science* **278**, 1928-1931

Lee, R. and Richards, F. M. (1971) The interpretation of protein structures: estimation of static accessibility. *J. Mol. Biol.* **55**, 379-400

Lehrman, S. R., Tuls, J. L. and Lund, M. E. (1990) in *Peptides: Chemistry and Biology* (Rivier, J. E. and Marshall, G. R. Ed.)

Lehrman, S. R., Tuls, J. L., Havel, H. A., Haskell, R. J., Putnam, S. D. and Tomich, C-S. C. (1991) Site-directed mutagenesis to probe protein folding: evidence that the formation and aggregation of a bovine growth hormone folding intermediate are dissociable processes. *Biochemstry* **30**, 5777-5784

Levinthal, C. (1969) How to fold graciously. In *Mossbauer Spectroscopy in Biological Systems* In *Proceedings of a Meeting held at Alberton House* (Monticello, I. L., ed). 22-24, University of Illinois Press

Linderstrom-Lang, K. (1924) The ionization of proteins. *Compt. Rend. Trav. lab. Carlsberg, Ser. chim.* **15**, 29

Luque, I., and Freire, E. (1998) Structure-based prediction of binding affinities and molecular design of peptide ligands. *Methods Enzymol.* **295**, 100-27

Mackenzie, N. E., Plaisted, S. M. and Brems, D. N. (1989) Proton nuclear magnetic resonance study of the histidine residues of pituitary growth hormone. *Biochim. Biophys. Acta.* **994**, 166-171

Manning, M. C., Illangasekare, M. and Woody, R. W. (1988) Circular dichroism studies of distorted alpha-helices, twisted beta-sheets and beta turns. *Biophys. Chem.* **31**, 77-86

Manning, M. C. and Woody, R. W. (1991) Theoretical CD studies of polypeptide helices: examination of important electronic and geometric factors. *Biophysics* **31**, 569-86

Matouschek, A., Kellis, J. T., Jr, Serrano, L., Bycroft, M., and Fersht, A. R. (1990) Transient folding intermediates characterized by protein engineering. *Nature* **346**, 440-445

Matthews, B. W., Nicholson, H., and Becktel, W. J. (1987) Enhanced protein thermostability from site-directed mutations that decrease the entropy of unfolding. *Proc. Natl. Acad. Sci. USA.* **84**, 6663-6667

Matthews, C. R. (1993) Pathways of protein folding. *Annu. Rev. Biochem.* **62**, 653-683

McCutchen, S. L., Lai, Z., Miroy, G. J., Kelly, J. W., and Colon, W. (1995) Comparison of lethal and nonlethal transthyretin variants and their relationship to amyloid disease. *Biochemistry* **34**, 13527-36

McGee, W. A., and Nall, B. T. (1998) Refolding rate of stability-enhanced cytochrome c is independent of thermodynamic driving force. *Protein Sci.* **7**, 1071-1082

McParland, V. J., Kad, N. M., Kalverda, A. P., Brown, A., Kirwin-Jones, P., Hunter, M. G., Sunde, M., and Radford, S. E. (2000) Partially unfolded states of beta(2)-microglobulin and amyloid formation in vitro. *Biochemistry* **39**, 8735-8746

McParland, V. J., Kalverda, A. P., Homans, S. W., and Radford, S. E. (2002) Structural properties of an amyloid precursor of beta(2)-microglobulin. *Nat. Struct. Biol.* **9**, 326-31

Milthorpe, B. K., Jeffrey, P. D., and Nichol, L. W. (1975) The direct analysis of sedimentation equilibrium results obtained with polymerizing systems. *Biophys. Chem.* **3**, 169-76

Mirsky, A. E., and Pauling, L. (1936) On the structure of native, denatured, and coagulated proteins. *Prot. Natl. Acad. Sci. USA* **89**, 439-447

Mitchinson, C., and Wells, J. A. (1989) Protein engineering of disulfide bonds in subtilisin BPN'. *Biochemistry* **28**, 4807-4815

Morris, M. and Ralston, G. B. (1985) Determination of the parameters of self-association by direct fitting of the omega function. *Biophys. Chem.* **23**, 49-61

Milthorpe, B. K., Jeffrey, P. D. and Nichol, L. W. (1975) The direct analysis of sedimentation equilibrium results obtained with polymerizing systems. *Biophys. Chem.* **3**, 169-76

Munk, P. and Cox, D. J. (1972) Sedimentation equilibrium of protein solutions in concentrated guanidinium chloride. Thermodynamic nonideality and protein heterogeneity. *Biochemistry* **11**, 687-697

Myers, J. K., Pace, C. N. and Scholtz, J. M. (1995) Denaturant m values and heat capacity changes: relation to changes in accessible surface areas of protein unfolding. *Protein Sci.* **3**, 2138-2148

Nicholls, A., Sharp, K. A. and Honig, H. (1991) Protein folding and association: Insights from the interfacial and thermodynamic properties of hydrocarbons. *Proteins* **11**, 271-280

Nozaki, Y. (1972) The preparation of guanidine hydrochloride. *Methods Enzymol.* **26**, 43-50

Ohgushi, M. and Wada, A. (1983) 'Molten-globule state': a compact form of globular proteins with mobile side-chains. *FEBS Lett.* **164**, 21-24

Ohlendorf, D. H., Finzel, B. C., Weber, P. C. and Salemme, F. R. (1987) in *Protein Engineering* (Oxender, D. L., and Fox, C. F., Eds.) 165-173, Alan R. Liss, Inc., New York

Oliveberg, M., Vuilleumier, S., and Fersht, A. R. (1994) Thermodynamic study of the acid denaturation of barnase and its dependence on ionic strength: evidence for residual electrostatic interactions in the acid/thermally denatured state. *Biochemistry* **33**, 8826-32

Pace, C. N. (1986) Determination and analysis of urea and guanidine hydrochloride denaturation curves. *Methods Enzymol.* **131**, 266-280

Pace, C. N., Grimsley, G. R., Thomson, J. A., and Barnett, B. J. (1988) Conformational stability and activity of ribonuclease T1 with zero, one, and two intact disulfide bonds. *J. Biol. Chem.* **263**, 11820-11825

Pace, C. N., Laurents, D. V. and Thomson, J. A. (1990) pH dependence of the urea and guanidine hydrochloride denaturation of ribonuclease A and ribonuclease T1. *Biochemistry*, **29** 2564-2572

Pace, C. N., Shirley, B. A., McNutt, M., and Gajiwala, K. (1996) Forces contributing to the conformational stability of proteins. *FASEB J.* **10**, 75-83

Page, G. S., Smith, S., and Goodman, H. M. (1981) DNA sequence of the rat growth hormone gene: location of the 5' terminus of the growth hormone mRNA and identification of an internal transposon-like element. *Nucleic Acids Res.* **9**, 2087-2104

Peng, Z. and Kim, P. S. (1994) A protein dissection study of a molten globule. *Biochemistry* **33**, 2136-2141

Peng, Z., Wu, L. C., and Kim, P. S. (1995) Local structural preferences in the α-lactalbumin molten globule. *Biochemistry* **34**, 3248-3252

Pörschke, D. (1974) A direct measurement of the unzippering rate of a nucleic acid double helix. *Biophys. Chem.* **2**, 97-101

Pörschke, D., and Eigen, M. (1971) Co-operative non-enzymic base recognition. 3. Kinetics of the helix-coil transition of the oligoribouridylic--oligoriboadenylic acid system and of oligoriboadenylic acid alone at acidic pH. *J. Mol. Biol.* **62**, 361-81

Ptitsyn, O. B. (1973) Sequential mechanism of protein folding. *Dokl. Akad. Nauk. SSSR* **210**, 1213-1215

Ptitsyn, O. B., Pain, R. H. Semistonov, G. V., Zerovnik, E. Razgulyaev, O. I. (1990) Evidence for a molten globule state as a general intermediate in protein folding. *FEBS Lett.* **262**, 20-24

Ptitsyn, O. B. (1992) In *"Protein Folding"* (T. E. Creighton, Ed.), 243-300. W. H. Freeman and Company, New York

Ptitsyn, O. B. and Uversky, V.N. (1994) The molten globule is a third thermodynamic state of protein molecules. *FEBS Lett.* **341**, 15-18

Ptitsyn, O. B. (1995) Molten globule and protein folding. *Adv. Prot. Chem.* **47**, 83-229

Ptitsyn, O. B., Bychkova, V. E. and Uversky, V.N. (1995) Kinetic and equilibrium folding intermediates. *Philos. Trans. R. Soc. Lond. (Biol)*

Radford S. E. (2000) Protein folding: progress made and promises ahead. *TIBS.* **25**, 611-618

Ralston, G. B., and Morris, M. B. (1992) in *Analytical Ultracentrifugation in Biochemistry and Polymer Science* (Harding, S. E., Rowe, A. J., and Horton, J. C., Eds) pp 90-125, The Royal Society of Chemistry, Cambridge

Raschke, T. M., and Marqusee, S. (1997) The kinetic folding intermediate of ribonuclease H resembles the acid molten globule and partially unfolded molecules detected under native conditions. *Nat. Struct. Biol.* **4**, 298-304

Rashin, A and Honig, B. (1984) On the environment of ionizable groups in globular proteins. *J. Mol. Biol.* **173**, 515-521

Redfield, C., Smith, R. A. and Dobson, C. M. (1994) Structural characterization of a highly-ordered 'molten globule' at low pH. *Nat. Struct. Biol.* **1**, 23-29

Ribela, M. T. and Bartolini, P. (1988) Stokes radius determination of radioiodinated polypeptide hormones by gel filtration. *Anal. Biochem.* **174**, 693-97

Richards, F. M. (1977) Areas, volumes, packing and protein structure. *Annu. Rev. Biophys. Bioeng.* **6**, 151-176

Richardson., J. S. and Richardson, D. C. (1988) Amino acid preferences for specific locations at the ends of α-helices. *Science* **240**, 1648-1652

Riek, R., Hornemann, S., Wider, G., Billeter, M., Glockshuber, R., Wuthrich, K. (1996) NMR structure of the mouse prion protein domain PrP(121-321). *Nature* **382**, 180-182

Rowlinson, S. W., Barnard, R., Bastiras, S., Robins, A. J., Senn, C., Wells, J. R., Brinkworth, R. and Waters, M. J. (1994) Evidence for the involvement of the carboxy terminus of helix 1 of growth hormone in receptor binding: use of charge reversal mutagenesis to account for calcium dependence of binding and for design of higher affinity analogues. *Biochemistry* **33**, 11724-33

Sanz, J. M., and Fersht, A. R. (1993) Rationally designing the accumulation of a folding intermediate of barnase by protein engineering. *Biochemistry* **32**, 13584-13592

Savitzky, A. and Golay, M. J. E. (1964) Smoothing and differentiation of data by simplified least squares procedures. *Anal. Chem.* **36**, 1627-1639

Scholtz, J. M., Barrick, D., York, E. J., Stewart, J. M. and Baldwin, R. L. (1995) Urea unfolding of peptide helices as a model for interpreting protein unfolding. *Proc. Natl. Acad. Sci. USA* **92**, 185-189

Seeburg, P. H., Sias, S., Adelman, J., de Boer, H. A., Hayflick, J., Jhurani, P., Goeddel, D. V., and Heyneker, H. L. (1983) Efficient bacterial expression of bovine and porcine growth hormones. *DNA* **2**, 37-45

Shaknovich, E. I., and Finkelstein, A. V. (1989) Theory of cooperative transitions in protein molecules. I. Why denaturation of globular protein is a first-order phase transition. *Biopolymers.* **28**, 1667-80.

Shearwin, K. E., and Egan, J. B. (1996) Purification and self-association equilibria of the lysis-lysogeny switch proteins of coliphage 186. *J. Biol. Chem.* **271**, 11525-31

Shortle, D., Chan, H. S., and Dill, K. A. (1992) Modeling the effects of mutations on the denatured states of proteins. *Protein Sci.* **1**, 201-215

Sipe, J. D. (1992) Amyloidosis. *Annu. Rev. Biochem.* **61**, 947-975

Smith, J. S. and Scholtz, J. M. (1996) Guanidine hydrochloride unfolding of peptide helices: separation of denaturant and salt effects. *Biochemistry* **35**, 7292-7297

Sosnick, T. R., Mayne, L., Hiller, R. and Englander, S. W. (1994) The barriers in protein folding. *Nat. Struct. Biol.* **1**, 149-156

Strickland, E. H., Horwitz, J. and Billups, C. (1969) Fine structure in the near-ultraviolet circular dichroism and absorption spectra of tryptophan derivatives and chymotrypsinogen A at 77 degrees K. *Biochemistry* **8**, 3205-13

Strickland, E. H. (1972) Interactions contributing to the tyrosyl circular dichroism bands of ribonuclease S and A. *Biochemistry* **11**, 3465-3474

Strickland, E. H. (1974) Aromatic contributions to circular dichroism spectra of proteins. *C.R.C. Crit. Rev. Biochem.* **2**, 113-175

Tanford, C. (1961) in *Physical Chemistry of Macromolecules*, Chapter 7, Wiley, New York

Tanford, C. (1970) Protein denaturation. C. Theoretical models for the mechanism of denaturation. *Adv. Protein Chem.* **24**, 1-95

Teale, F. W. J. (1960) The ultraviolet fluorescence of proteins in neutral solution. *Biochem. J.* **76**, 381-388

Utiyama, H. and Baldwin, R. L. (1986) Kinetic mechanisms of protein folding. *Methods Enzymol.* **131**, 51-70

Uversky, V.N. and Ptitsyn, O. B. (1994) 'Partly folded' state, a new equilibrium state of protein molecules:four-state guanidinium chloride-induced unfolding of β-lactamase at low temperature. *Biochemistry* **33**, 2782-2791

Uversky, V. N., Karnoup, A. S., Segel, D. J., Seshadri, S., Doniach, S. and Fink, A. L. (1998) Anion-induced folding of *staphylococcal nuclease*: characterization of multiple equilibrium partially folded intermediates. *J. Mol. Biol.* **278**, 879-894

Van der Vies, S. M., Viitanen, P. V., Gatenby, A. A., Lorimer, G. H., and Jaenicke, R. (1992) Conformational states of ribulosebisphosphate carboxylase and their interaction with chaperonin 60. *Biochemistry* **31**, 3635-3644

Van Holde, K. E. (1985) in *Physical Biochemistry*, 2nd ed., Chapter 2, Prentice-Hall, Englewood Cliffs, NJ

Van Snick, J. (1990) Interleukin-6: an overview. *Annu. Rev. Immunol.* **8**, 253-278

Villafranca, J. E., Howell, E. E., Oatley, S. J., Xuong, N., and Kraut, J. (1987) An engineered disulfide bond in dihydrofolate reductase. *Biochemistry* **26**, 2182-2189

Wada, A. (1976) The alpha-helix as an electric macro-dipole. *Adv. Biophys.* **9**, 1-63

Walkenhorst, W. F., Green, S. M., and Roder, H. (1997) Kinetic evidence for folding and unfolding intermediates in staphylococcal nuclease: analysis of peptide fragments. *Folding & Design* **2**, 93-100

Walter, S., Hubner, B., Hahn, U. and Schmid, F. Z. (1995) Destabilization of a protein helix by electrostatic interactions. *J. Mol. Biol.* **252**, 133-143

Ward, L. D., Matthews, J. M., Zhang, J.-G., and Simpson, R. J. (1995) Equilibrium denaturation of recombinant murine interleukin-6: effect of pH, denaturants, and salt on formation of folding intermediates. *Biochemistry.* **34**, 11652-9

Wetlaufer, D. B. (1962) Ultraviolet spectra of proteins and amino acids. *Adv. Protein Chem.* **17**, 303-390

Wetlaufer, D. B., (1973) Nucleation, rapid folding, and globular intrachain regions in proteins. *Proc. Natl. Acad. Sci. USA.* **70**, 697-701

Wetzel, R., Perry, L. J., Baase, W. A., and Becktel, W. J. (1988) Disulfide bonds and thermal stability in T4 lysozyme. *Proc. Natl. Acad. Sci. USA.* **85**, 401-405

Wicar, S., Mulkerrin, M. G., Bathory, G., Khundkar, L. H. and Karger, B. L. (1994) Conformational changes in the reversed phase liquid chromatography of recombinant human growth hormone as a function of organic solvent: the molten globule state. *Anal. Chem.* **66**, 3908-15

Wong, K.-P. and Tanford, C. (1973) Denaturation of bovine carbonic anhydrase B by guanidine hydrochloride. A process involving separable sequential conformational transitions. *J. Biol. Chem.* **248**, 8518-8523

Wu, L. C., and Kim, P. S. (1998) A specific hydrophobic core in the α-lactalbumin molten globule. *J. Mol. Biol.* **280**, 175-182

Yamaski, K., Ogasahara, K., Yutani, K., Oobatake, M., and Kanaya, S. (1995) Folding pathway of Escherichia coli ribonuclease HI: a circular dichroism, fluorescence, and NMR study. *Biochemistry* **34**, 16552-16562

Yamomoto, Y., and Tanaka, J. (1972) Polarized absorption spectra of crystals of indole and its related compound. *Chem. Soc. Jap.* **45**, 1362

Yang, A.-S. and Honig, B. (1992) Electrostatic effects on protein stability. *Curr. Opin. Struct. Biol.* **2**, 40-45

YangA.-S. and Honig, B (1993) On the pH dependence of protein stability. *J. Mol. Biol.* **231**, 459-474

Young, L., Jernigan, R. L. and Covell, D. G. (1994) A role for surface hydrophobicity in protein-protein recognition. *Protein Science* **3**, 717-729

Youngman, K. M., Spencer, D. B., Brems, D. N. and DeFelippis, M. R. (1995) Kinetic analysis of the folding of human growth hormone influence of disulphide bonds. *J. Biol. Chem.* **270**, 19816-19822

Zhang, J. G., Matthews, J. M., Ward, L. D. and Simpson, R. J. (1997) Disruption of the disulfide bonds of recombinant murine interleukin-6 induces formation of a partially unfolded state. *Biochemistry* **36**, 2380-2389